

Nuclear Production of Hydrogen

Second Information
Exchange Meeting
Argonne, Illinois, USA
2-3 October 2003



Nuclear Science

Nuclear Production of Hydrogen

**Second Information Exchange Meeting
Argonne, Illinois, USA
2-3 October 2003**

© OECD 2004
NEA No. 5308

NUCLEAR ENERGY AGENCY
ORGANISATION FOR ECONOMIC CO-OPERATION AND DEVELOPMENT

ORGANISATION FOR ECONOMIC CO-OPERATION AND DEVELOPMENT

Pursuant to Article 1 of the Convention signed in Paris on 14th December 1960, and which came into force on 30th September 1961, the Organisation for Economic Co-operation and Development (OECD) shall promote policies designed:

- to achieve the highest sustainable economic growth and employment and a rising standard of living in member countries, while maintaining financial stability, and thus to contribute to the development of the world economy;
- to contribute to sound economic expansion in member as well as non-member countries in the process of economic development; and
- to contribute to the expansion of world trade on a multilateral, non-discriminatory basis in accordance with international obligations.

The original member countries of the OECD are Austria, Belgium, Canada, Denmark, France, Germany, Greece, Iceland, Ireland, Italy, Luxembourg, the Netherlands, Norway, Portugal, Spain, Sweden, Switzerland, Turkey, the United Kingdom and the United States. The following countries became members subsequently through accession at the dates indicated hereafter: Japan (28th April 1964), Finland (28th January 1969), Australia (7th June 1971), New Zealand (29th May 1973), Mexico (18th May 1994), the Czech Republic (21st December 1995), Hungary (7th May 1996), Poland (22nd November 1996), Korea (12th December 1996) and the Slovak Republic (14 December 2000). The Commission of the European Communities takes part in the work of the OECD (Article 13 of the OECD Convention).

NUCLEAR ENERGY AGENCY

The OECD Nuclear Energy Agency (NEA) was established on 1st February 1958 under the name of the OEEC European Nuclear Energy Agency. It received its present designation on 20th April 1972, when Japan became its first non-European full member. NEA membership today consists of 28 OECD member countries: Australia, Austria, Belgium, Canada, the Czech Republic, Denmark, Finland, France, Germany, Greece, Hungary, Iceland, Ireland, Italy, Japan, Luxembourg, Mexico, the Netherlands, Norway, Portugal, the Republic of Korea, the Slovak Republic, Spain, Sweden, Switzerland, Turkey, the United Kingdom and the United States. The Commission of the European Communities also takes part in the work of the Agency.

The mission of the NEA is:

- to assist its member countries in maintaining and further developing, through international co-operation, the scientific, technological and legal bases required for a safe, environmentally friendly and economical use of nuclear energy for peaceful purposes, as well as
- to provide authoritative assessments and to forge common understandings on key issues, as input to government decisions on nuclear energy policy and to broader OECD policy analyses in areas such as energy and sustainable development.

Specific areas of competence of the NEA include safety and regulation of nuclear activities, radioactive waste management, radiological protection, nuclear science, economic and technical analyses of the nuclear fuel cycle, nuclear law and liability, and public information. The NEA Data Bank provides nuclear data and computer program services for participating countries.

In these and related tasks, the NEA works in close collaboration with the International Atomic Energy Agency in Vienna, with which it has a Co-operation Agreement, as well as with other international organisations in the nuclear field.

© OECD 2004

Permission to reproduce a portion of this work for non-commercial purposes or classroom use should be obtained through the Centre français d'exploitation du droit de copie (CCF), 20, rue des Grands-Augustins, 75006 Paris, France, Tel. (33-1) 44 07 47 70, Fax (33-1) 46 34 67 19, for every country except the United States. In the United States permission should be obtained through the Copyright Clearance Center, Customer Service, (508)750-8400, 222 Rosewood Drive, Danvers, MA 01923, USA, or CCC Online: <http://www.copyright.com/>. All other applications for permission to reproduce or translate all or part of this book should be made to OECD Publications, 2, rue André-Pascal, 75775 Paris Cedex 16, France.

FOREWORD

The use of hydrogen as an ecologically friendly energy carrier has recently received increased interest for industrial applications, including the use of hydrogen fuel cells for transportation (one-third of primary energy consumption) and for distributed stationary electricity production. Anticipating further emissions control limits, major vehicle companies are investing heavily to bring automobiles powered by fuel cells to the market in the early decades of the century. The current high capital cost of hydrogen fuel cells can be expected to decrease as the technology matures.

Other analyses show a trend over the past century and a half towards an increasing use of hydrogen-rich/carbon-poor forms of energy carrier throughout the entire non-electric market, representing about two-thirds of the total energy market. Based on this trend, it is projected that, even while energy demand increases overall, market share for methane, coal and oil will decline, and hydrogen can be expected to hold a major market share of chemical energy carriers (complimentary with electricity) in the future.

Currently, hydrogen is mainly manufactured by reforming fossil fuels; greenhouse gas emission reduction benefits will thus not be significant unless a carbon-free hydrogen manufacturing route is developed. That is the reason for a resurgence of interest to use heat or surplus electricity from nuclear power plants to produce hydrogen through water cracking.

The Nuclear Science Committee of the OECD Nuclear Energy Agency organised its second information exchange meeting on the “Nuclear Production of Hydrogen” at Argonne National Laboratory in the United States on 2-3 October 2003. The main objective of the meeting was to review recent scientific and technical developments in the field since the first meeting held at OECD headquarters in Paris, France in October 2000.

The meeting was attended by 86 participants from seven countries and two international organisations. Papers were presented in the following four sessions:

- I. The Role of Hydrogen in Energy Infrastructures and R&D Planning for Implementation;
- II. Thermochemical Hydrogen Production Technologies;
- III. Electrochemical and Membrane Hydrogen Production Technologies;
- IV. Nuclear Plant Concepts for Hydrogen Production.

At the close of the meeting, the participants noted substantial progress since the previous meeting held three years earlier, especially in the number of papers presenting experimental results. The participants also stressed the need to pursue the use of currently available nuclear reactor types and methods for producing hydrogen (such as electrolysis of LWR-produced electricity), while continuing R&D work on promising new concepts that may become better suited to centralised production.

In light of the rapidly growing interest and R&D activities on the nuclear production of hydrogen, the participants proposed to the NEA Nuclear Science Committee that a new meeting on the same subject be organised no later than 24 months following the present meeting.

TABLE OF CONTENTS

FOREWORD	3
SESSION I: OPENING	9
<i>David Sanborn Scott</i> Back from the future: To plan the best way nuclear can get us there.....	11
<i>Russell A. Brown</i> Critical paths to the post-petroleum age	27
<i>Masanori Tashimo, Atsushi Kurosawa, Kazumi Ikeda</i> Role of nuclear produced hydrogen for global environment and energy	43
<i>Mark D. Paster</i> The US Department of Energy programme on hydrogen production	57
<i>A.D. Henderson, P.S. Pickard, C.V. Park, J.F. Kotek</i> The US Department of Energy's Research and Development plans for the use of nuclear energy for hydrogen production.....	73
SESSION II	83
<i>G. Goldstein, X. Vitart, J.M. Borgard</i> General comments about the efficiency of the iodine-sulphur cycle coupled to a high temperature gas-cooled reactor.....	85
<i>X. Vitart, J.M. Borgard, S. Goldstein, S. Colette</i> Investigation of the I-S cycle for massive hydrogen production	99
<i>Kaoru Onuki, Shinji Kubo, Hayato Nakajima, Shunichi Higashi, Seiji Kasahara</i> <i>Shintaro Ishiyama, Hiroyuki Okuda</i> R&D on thermochemical I-S process at JAERI	111
<i>Richard D. Doctor, Diana T. Matonis, David C. Wade</i> Hydrogen generation using a calcium-bromine thermochemical water-splitting cycle	119

<i>Toshio Nakagiri, Taiji Hoshiya, Kazumi Aoto</i> Investigation on a new hydrogen production process for FBR	131
<i>Michele A. Lewis, Manuela Serban, John K. Basco</i> Hydrogen production at <550°C using a low temperature thermochemical cycle	145
SESSION III	157
<i>Charles Forsberg, Brian Bischoff, Louis K. Mansur and Lee Trowbridge</i> Nuclear thermochemical production of hydrogen with a lower-temperature iodine- Westinghouse-Ispra sulphur process	159
<i>Masao Hori, Kazuaki Matsui, Masanori Tashimo, Isamu Yasuda</i> Synergistic production of hydrogen using fossil fuels and nuclear energy Application of nuclear-heated membrane reformer	171
<i>J. Stephen Herring, Paul Lessing, James E. O'Brien, Carl Stoots, Joseph Hartvigsen, S. Elangovan</i> Hydrogen production through high-temperature electrolysis in a solid oxide cell.....	183
<i>U. (Balu) Balachandran, T.H. Lee, S. Wang, S.E. Dorris</i> Hydrogen production by water dissociation using mixed conducting membranes	201
<i>Matthew B. Richards, Arkal S. Shenoy, Kenneth R. Schultz</i> Coupling the modular helium reactor to hydrogen production processes	203
SESSION IV	217
<i>Samim Anghaie and Blair Smith</i> Hydrogen production with fully integrated fuel cycle gas and vapour core reactors..	219
<i>A.I. Miller, Romney B. Duffey</i> Meeting the near-term demand for hydrogen using nuclear energy in competitive power markets	235
<i>Yoshiyuki Inagaki, Tetsuaki Takeda, Tetsuo Nishihara, Kaoru Onuki, Masuro Ogawa, Shusaku Shiozawa</i> Present status and future plan of HTTR project	249
<i>Masanori Tashimo, Masao Hori, Isamu Yasuda, Yoshinori Shirasaki, Kazuto Kobayashi</i> Advanced design of fast reactor-membrane reformer (FR-MR)	267
<i>Anton Moisseytsev, Diana T. Matonis</i> Integrated heat balance of STAR-H2 system for hydrogen production	277

Per F. Peterson, Charles W. Forsberg, Paul S. Pickard

Advanced CSiC composites for high-temperature nuclear heat transport with helium,
molten salts, and sulphur-iodine thermochemical hydrogen process fluids 289

List of Participants..... 303

SESSION I

OPENING

**BACK FROM THE FUTURE: TO PLAN THE BEST WAY
NUCLEAR CAN GET US THERE***

David Sanborn Scott

Founding Director, Institute for Integrated Energy Systems, Univ. of Victoria, Canada
Vice-President for the Americas, International Association for Hydrogen Energy
Consultant to Argonne National Laboratories through EVENSTAR Inc. Canada

Abstract

We'll start by giving two answers to a single question, "Why hydrogen?" We'll follow this with a brief discussion of the energy system architecture's five-link chain, to emphasize the key role of the central link, energy *currencies*. Then, gluing these two concepts together – (a) systemic architecture and (b) the answer to why hydrogen – we can set out the rationale leading to the premise that our system will ultimately be dominated by the twin currencies, hydrogen and electricity. All this will serve as a foundation for considering the *sources*, *infrastructures* and *service technologies* likely to characterise the deeper future (2100 ~ 2200). Finally, based on this long view (and our sliver of time within it) we can use the perspective to suggest near-term strategies.

* The concepts introduced in this article has been drawn from parts of a forthcoming book by the author, provisionally titled, "Smelling Land: An Odyssey Towards a Cleaner, Richer Hydrogen Age" to be released late 2004.

Introduction

I can't be sure if I'll catch a cold next month. But I'm very confident I won't catch one a century from now. Sometimes, for some things, we can predict the deep future better than tomorrow. Astronomers find most of our galaxy obscured by interstellar dust and, as a consequence, often find it easier to see events in galaxies millions of light-years away than in our backyard Milky Way.

When trying to plan energy system development, "further out" parts the fog of immediacy – allows us to leap the tangles of today's conventional wisdom and wishdom. So to give a different twist to our thinking for this OECD sponsored Information Exchange Meeting on Nuclear Production of Hydrogen, let's jump to a fully developed hydrogen-electricity age to see what we find. What we find is a surprisingly useful platform for developing strategies for what we should be doing today.

Yet before leaping we must set out our premise and it's this: Sometime during the early to mid decades of the 22nd century,

- Sustainable sources dominate energy supply.
- Hydrogen and electricity dominate energy currencies.

Question: What is the justification for this premise? To find the answer we must first have a good feeling for our energy system's architecture – in order to identify those links we can reasonably predict and those we'd be fools to even try. Second, we must also have a concept of the criteria for sustainable development as it applies to energy systems. By answering these two questions in sequence we should solidify our confidence in the premise. Then we'll go on to applying this premise – together with an appreciation of engineering and physical fundamentals – to anticipate the deep future.

About the future, it's good to remember this: While we never know everything, we always know something. And that something can be a platform for strategies. But as promised, let's start by encapsulating the answer to the prime question: why hydrogen?

Why hydrogen?

As we embark upon the 21st century, two specters threaten civilisation. One is the prospect of economic disarray and incitement to war caused by the local depletion and global mal-distribution of high-quality fossil fuels, especially oil. The second is the prospect of almost unimaginable environmental, economic and cultural disruption caused by climate volatility and triggered, primarily, by our energy system's carbon dioxide effluent.

If we remain tethered to fossil fuels it is merely a question of when, not if, one or both specters become reality. Today we're seeing the precursors of both. From the viewpoint of Earth's physiology, climate volatility is much the more critical – which means the global environment, not depletion, is the absolute cap on fossil fuel use. Nevertheless, at any moment, flaring geopolitics could suddenly crash upon us to bring virtual depletion.

Happily, a straightforward pathway can steer us clear of both specters. We must rapidly adopt sustainable energy *sources* that don't emit carbon dioxide, sources like solar, wind and safe, economic next-generation nuclear. Perhaps more critical – since it's less well understood – we must rapidly adopt the twin energy *currencies*, hydrogen and electricity. Alone among currencies, both can be manufactured from any energy source, neither emits carbon dioxide and, together, they can provide the full menu of civilisation's energy services, from flying airplanes to running computers.

These few paragraphs encapsulate both the problems and their solution. Yet before we move on to the main themes of this paper we should explore, just a little deeper, “Why hydrogen?”

First consider depletion and mal-distribution, where a five-step rationale goes like this:

1. Today, transportation fuels are harvested *exclusively* from fossil energy sources.
2. However, because fossil sources are threatened by regional depletion and are a sure cause of international conflict, civilisation must move to sustainable, regionally available, non-fossil sources.
3. This means we must be able to harvest sustainable sources so they can manufacture chemical fuels in general and transportation fuels in particular.
4. Realistically, the only way sustainable sources can manufacture chemical fuels is via hydrogen. (How else can we use the energy from wind, solar or nuclear to fly an airplane?)
5. Therefore, a significant move from fossil to sustainable sources can only begin with the increased use of hydrogen (H_2) in transportation and can only be completed with the supremacy of H_2 among chemical fuels.

Next consider climate volatility, where a parallel logic again takes us to hydrogen:

1. The carbon dioxide (CO_2) effluent from fossil fuel consumption is pushing our planet towards climate destabilisation that, if unabated, will be catastrophic.
2. To eliminate civilisation’s CO_2 emissions we need *both* non-carbon-emitting *sources* and non-carbon *currencies*.
3. Many non-carbon sources are available or can be developed. (Hydraulic power, sunlight, wind, nuclear fission and, later, perhaps fusion are examples.)
4. In contrast, there are only two non-carbon currencies that can, *together*, supply the full menu of civilisation’s energy services. These currencies are electricity and hydrogen.
5. Electricity is already established – but of course electricity can’t fly airplanes. Therefore, anthropogenic CO_2 emissions can only be slowed by the extensive use of hydrogen (H_2) and can only be completed with the supremacy of sustainable-derived H_2 among chemical fuels.

These two five-step rationales must suffice for now. The rest of our discussion will give them background, depth, life and nuance.

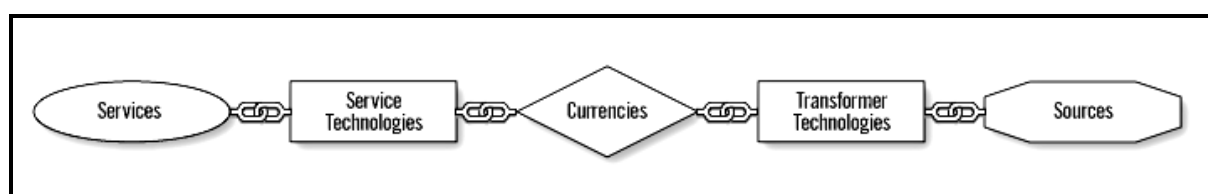
The architecture of the energy system

The strange thing about the energy system is that we almost never think about it as a system. Instead we think about its bits-and-pieces – about electricity networks or oil cartels, airplanes or fax machines – but not about the system. Repeatedly, bits and pieces thinking has caused us to miss opportunity and blunder into misadventure. Funny, because we understand the importance of systemic thinking in many other things.

To understand how our energy system works, we need in front of us, stuck in the mind, a picture of its architecture. We need a vision of how the bits and pieces fit together, what they do for each other, not simply what they do themselves. But when we set out to identify the architecture of any system we run smack into the question: How much detail do we need? Einstein is reported to have once said: “Everything should be made as simple as possible, but not simpler”. [1] That is a profoundly important instruction. Let’s look for an architecture that is as simple as possible but not simpler.

For me an appropriate “as simple as possible but not simpler” architecture is a five-link chain that starts with energy services, moves to technologies that deliver the services, then to energy currencies that feed the service technologies, then transformer technologies that produce the currencies and finally the sources that the transformer technologies harvest. [2] Such a chain is shown in Figure 1.

Figure 1. Energy system architecture



Unfortunately, many people down-select from these five links, to think the energy system is just the three rightmost links. They confuse the energy *system* with what the financial pages of your local newspaper call the energy *sector*. The financial pages amputate the service technologies and services. Once the utility has delivered the electricity, or the oil company the gasoline (petrol) that’s all there is to report. So the financial headlines bleat, “Electricity deregulation” or “Prices at the pump rise on fears of ...” But as we’ve noted, people want energy services. People want to be able to cook a meal, watch the news, talk to grandmother, or keep warm. Energy is a means to an end. Services are the end.

It’s energy services that drive the system, not sources.

For me, this obvious and simple idea took a long time to sink in, a long time to marinate in my head, until it became the *first* thing I thought – not an afterthought I tried to remember. As an engineer I tended to plod through the system, from sources to services, because that is how the energy flows. But energy flow is counter-flow to the way the system works, because it is a cultural system, which translates into an economic system – a demand-supply system. People demand a service, the service demands a service technology, the service technology demands a currency, and so on back to energy sources.

Of course, the energy flow *is* from sources to services. So there are flows both up and down the chain – energy right-to-left, demand left-to-right. That is why I use a chain to connect the links, rather than arrows (as I used to do). I hope to emphasize that direction depends on what you want to consider – energy flow or service delivery.

Since we’re talking about energy use and service delivery, it’s appropriate to mention one more thing.

I’ve often heard it said: “Civilisation has an insatiable desire for energy”. That misses the point. Civilisation may have an insatiable demand for energy *services*, but not energy: people want to get home from work and to cook supper, after which they can listen to a new CD of Mahler’s Second Symphony, or read a book illuminated by an electric lamp. It isn’t that they want the *delivery* of these services to consume large quantities of energy. They want services and, indeed, are pleased if the services require less energy.

This may seem a trivial distinction. But it’s a distinction that will make a huge difference to the future of our planet because, at a fundamental level and for most services, there is almost no limit to

which we can reduce the amount of energy used to supply a service. It is the way we deliver services today, using today's technologies, which requires the energy. *We've been using less energy per unit service since the industrial revolution.* Happily the trend will continue sweeping us into the future – more service for less energy. [3]

Template for sustainability

The idea of sustainability has been described in *Our common future: (report of) the world commission on environment and development* (the Brundtland report) as to "... meet the needs of the present without compromising the ability of future generations to meet their own needs." That works, although I'm uneasy about the word "needs" – because it requires an answer to the ancillary question: by whose criteria? Moreover, it seems to me we should aspire to something more than the mere existence, which "needs" implies. So let's hold the thought but change a few words. Let's try:

Sustainable development improves lifestyles – by bringing cultural and economic growth embedded within environmental gentility – without jeopardising the ability of future generations to live even better.

It's a bit longer than the Brundtland definition, but I prefer the idea of "cultural growth" rather than "needs". Still, I have wondered if "economic" was redundant. Without economic growth, cultural growth is normally foreclosed, although the converse (economic growth without cultural growth) is surely possible – both individually and nationally. In the end, I decided that removing "economic" could be misleading, since it might encourage people to naïvely believe poverty-stricken nations can easily enjoy cultural growth without an underpinning economic growth. That's nonsense. We do well to recall Indira Gandhi's observation, "Poverty is the worst polluter".

No doubt we might find still better "objective statements" for sustainable development. Yet perfection is the ultimate unreality, so for now let's use this statement as our goal for sustainable development. With that settled, we can zoom in to how our statement can be used as a foundation for criteria explicitly designed for energy systems. By focusing on energy systems things become less abstract. We can bore in closer to the core of the matter – pick criteria that reduce "wiggle room".

If we again evoke "keep it as simple as possible but not simpler", I think first rank criteria come down to evaluating:

1. The *quality* of the energy service.
 - ✓ Initially, the service cannot be inferior to an equivalent service provided by established systems.
 - ✓ Soon, the service must be significantly better.
2. The *environmental gentility* of the system chain providing the service.
 - ✓ Inputs and outputs to and from each link of the system chain must minimally intrude upon nature's flows and equilibria.
3. The *economic cost* of the service.
 - ✓ The initial cost of service from new systems may, for a short time, be somewhat greater than the cost from established, competing systems.
 - ✓ Soon, the cost of services must be lower.
4. The *long-term availability* of the energy source.
 - ✓ Energy sources must be available into the foreseeable future (but there is no value in demanding foolishly long timeframes, like thousands of years).

- ✓ The global distribution of the energy source must be relatively uniform, to not aggravate geopolitical tensions that risk wars or economic blackmail.
5. The *surprise resilience* of the system chain providing the service.
 - ✓ As much as possible, the system must be resilient to geopolitical, technological, economic and environmental surprise – or any other surprising surprise.

While all issues must be considered, for the purposes of this conference, let's zoom to the environment. When we analyse the potential for environmental intrusion we must go beyond individual technologies, individual fuels (currencies) – individual anything. We must evaluate the environmental impact of the complete system.

While the need to include the complete system should be obvious, there are nuances. First, environmental intrusion may be exported from one link to other links, either up-system or down-system. [4] Consider a hydrogen-fuelled city bus using a fuelcell power train. The fuel cell bus will improve urban air quality – because it releases only small amounts of clean water vapour, rather than soot, nitrous oxides, carcinogens and tangy-things that find their way into your nose, all of which spew from the diesel bus it likely displaced. But what if the H_2 was produced by electrolysis using electricity generated from a coal-fired station? If the generating station was far from the city, the urban environment will still benefit but the air quality near the generating station will be degraded. Moreover, CO_2 will be dumped into the global commons. By manufacturing the H_2 from coal we push the environmental intrusion down-system – push it from the service technology (buses) in the city, to the transformer technology (coal-sourced H_2 production) on the outskirts. [5]

One way or another, environmental intrusion always involves material. It is material that intrudes upon nature's flows or equilibria – material *taken from* the environment, *diverted within* the environment or *put into* the environment. Knowing that environmental intrusion is always rooted in material, we set out four questions:

1. What is the magnitude of the intrudant material compared to its natural level?
2. What fraction of the global commons does the intrudant occupy?
3. What is the characteristic residence time of the intrudant?
4. Is the disturbed equilibrium fundamentally metastable?

With answers to these questions, it's possible to obtain a first estimate of the environmental impact from almost anything – from PCBs, to mine tailings, to nuclear spent fuel, to river dams, to electromagnetic radiation from overhead power-lines, and so forth. That I included electromagnetic radiation might give you pause because, you could argue, radiation is *not* material. But it's *caused by* material – the oscillatory accelerations of electrons in the power-lines.

Now I'll zoom further: to a specific radiation phenomenon. It's the interaction between material (CO_2) and radiation (infrared) that threatens climate disruption. But in this case it's not the material *making* the radiation that is important. Rather it is the material absorbing it – and thereby choking Earth's export of infrared radiation to the universe. Because it's so damn important, let's remind ourselves of the answers to these four questions when they're applied to atmospheric CO_2 build-up:

1. What is the magnitude of the intrudant material compared to its natural level?
 - ✓ CO_2 made up about 270 parts per million by volume (ppmv) at the beginning of the industrial revolution. By 2000, CO_2 content had risen to more than 370 ppmv. This is a change to about *133% of pre-industrial levels*. All reputable studies have shown that,

even with aggressive mitigation policies, CO₂ atmospheric content will have increased to *200% of its pre-industrial levels* by the turn of the next century.

2. What fraction of the global commons does the intrudant occupy?
 - ✓ Anthropogenic CO₂ is dispersed throughout *Earth's entire atmosphere* and therefore permeates the Earth's entire biosphere.
3. What is the characteristic residence time of the intrudant?
 - ✓ About 200 years in the lower atmosphere, increasing to 400 years or more when it enters the upper atmosphere.
4. Is the disturbed equilibrium fundamentally metastable?
 - ✓ *Climate is metastable.*

Our energy system will always be shaped by many environmental constraints – in part because, today, our energy system is probably the most material-intensive of civilisation's on-going activities. Nevertheless, because atmospheric CO₂ growth is overwhelmingly energy-system sourced, the requirement to reduce (and ultimately eliminate) *CO₂ emissions will become the environmental issue that dominates energy system development.*

Illustrative of the many studies, one is the Greenland ice core data that allowed us to track the global temperature and the atmospheric concentration of CO₂ and CH₄ for some 420 000 years. During this period the planet has gone through periods warmer than today and periods much colder – when *T*, CO₂ and CH₄ tracked each other like three dogs on a short leash. During these more than 240 kilo years, the *highest previous* atmospheric CO₂ concentration was 310 ppmv. Today it's 370 ppmv and growing

Seems to me; the grave risk (to civilisation) of climate instabilities cannot be denied, except by those with a unique immunisation against understanding scientific evidence or with a stunning ability to manipulate it.

A brief return to the premise

Having answered the question “Why hydrogen?”, developed the idea of a five-link systemic architecture and the concept of sustainability as applied to energy systems, we now have more substantive insight into the rationale supporting our premise:

That sometime during the early to mid decades of the 22nd century,

- Sustainable sources dominate energy supply.
- Hydrogen and electricity dominate energy currencies.

So let's now leap ahead to that deep future – a future I'll call a fully developed hydrogen age.

The deep future: A time of a fully developed hydrogen age

Just as it would have been impossible to anticipate cell phones and laptops at the turn of the 20th century, today only a jester would attempt to predict the impossible-to-imagine, hydrogen consumer products of the late 21st or early 22nd centuries. In contrast, I think we can get a good feel for the nature of energy infrastructures, for the dominant energy sources, for energy distribution and delivery systems, and for how hydrogen and electricity will share markets. And while unable to anticipate specific widgets, we should be able to anticipate some features of broad service “domains”, like transportation – or where fuel cells, our “chip of the future”, will be found, and where they won't.

About the future, it's good to remember this: While we never know everything, we always know something.

For energy systems, that “something” can be very useful. That's because it's about the shape of infrastructures – those parts of the energy system that typically take more than half a century to build, or to displace. In this way infrastructures are distinguished from the unimaginables – yet-to-be-dreamt hydrogen age widgets – hydrogen-allowed consumer products that will come along on their own, introduced by clever, innovative people, gobbled up by enthusiastic consumers. Unless, of course – trapped by conventional wisdoms, or foolish fears, or ignorance – we persist with ever more infrastructure “wrong things”. Then there will be no platform for hydrogen age consumer products. But that's not the premise of this article.

First, we'll discuss the deep future from perspective of three middle links in the system chain.

- Service technologies: with a focus on transportation.
- Currencies: with a special examination of distribution and delivery infrastructures.
- Transformer technologies: to examine energy source options in two groupings, “reliables” and what we can call “whimsicals”.

Second, we'll pull back our time horizon to set out strategies for today – strategies building on what we know of the deeper future, to avoid doing all the wrong things before the only thing left is the right thing.

Service technologies

Rather than attempt to cover the full menu of services, it is appropriate that we zoom to free-range transportation.

The reasons for this choice are threefold. First, in transportation H_2 will absolutely dominate electricity as the currency of choice. Second, in terms of quantities, (among service categories) transportation will always be a major energy consumer – probably *the* major consumer. Third, from the vantage of today, it would be foolish to attempt anticipating the H_2 -fuelled “unimaginable” appliances that will shape culture during a fully-developed hydrogen age.

Transportation patterns:

- H_2 will fuel *all* free-range vehicles. Surface vehicle power plants will be fuel cells. Aircraft power plants will remain heat engines, except fuel cells will often fill the auxiliary power unit function. Ocean ships should be classified as surface vehicle and so will most likely be powered by fuel cells. Defence ships (surface and undersea) may remain with heat engines powered by nuclear power plants.
- Fixed route transportation: Some applications (e.g. buses) could mimic free-range vehicles by using hydrogen, but they can also employ electricity (e.g. subways and high-density rail). It might be that H_2 fuel cells power subways – one advantage will be load-levelling.

On board H_2 storage:

- LH_2 will dominate vehicle onboard storage:
- Liquefaction efficiency will be much improved. (Magnetocaloric is but one option.)

- LH_2 has far lowest mass density (weight). LH_2 essential for aircraft, simply better for surface vehicles.

Synergies – the imprimatur:

- The fact that LH_2 contains both thermomechanical and chemical exergy will be the key to important technical synergies. One example is aircraft, where the exergy-of-cold can be used to refrigerate aerodynamic surfaces, that, studies have project, will reduce fuel consumption by 30% and direct operating costs by 20% [6]. To highlight synergies in dual-exergy content currencies, I find it interesting to that, in the case of aircraft, the thermomechanical exergy-of-cold, which constitutes 11% of exergy in LH_2 , provides three times as much “drive” per unit exergy than does the chemical exergy.
- Cryogen exergy recovery systems (CERS) will become *de rigueur*. Various CERS technologies will be employed with fuel cell (and other) vehicles – perhaps the simplest being air-separation for O_2 extraction to give the fuel cell an added acceleration punch. New materials and working fluids will permit “heat engines” to operate by taking heat from the environment and rejecting heat to the cryogen. Sometimes it may be feasible for a CERS to draw its heat from the *liquid* warm water effluent from fuel cells, rather than from the environment. I’ve called such technologies enhanced cryogen recovery systems (ECERS).
- Unlike gaseous H_2 , which contains both chemical and thermomechanical exergy, the ratio of thermomechanical to chemical exergy in LH_2 *remains constant* as the fuel is consumed. This allows CERS and ECERS to operate with constant thermo/chemical exergy ratios throughout the full refuelling cycle. In contrast, if compressed H_2 storage is used, the ratio of thermo/chemical exergy changes over the refuelling cycle – from a maximum (when first refuelled) to zero when (the tank is almost empty).
- The dual-exergy composition of LH_2 is one more feature that means the imprimatur of the hydrogen age will be *technological synergies*.

Energy currencies

Today, the staple modes of transporting bulk energy across continents are via high-voltage alternating-current (hv-ac) electricity networks, oil/gas pipelines and (in the case of coal) railroads. In contrast, during the fully-developed hydrogen age, the primary continental energy transportation will be via gaseous H_2 pipelines. The rationale for this claim is as follows:

- H_2 pipelines will transmit energy with much lower energy losses than can high-voltage direct current electricity (hv-dc). (Hv-dc will be the only competition for gaseous H_2 , not hv-ac, both because – in comparison with hv-ac – high-voltage direct-current (hv-dc) is both less lossy for long distance electricity transmission and is not encumbered by frequency synchronisation.) [7]
- Inherently, H_2 pipelines are wonderful energy storage devices. Therefore, they can both store the product of sources when the demand falls below supply, and also give up energy when demand rises above supply. Thus they inherently load-level for constant-output sources and can always absorb energy from intermittent and unpredictable sources, which I’ve called whimsicals (most of which are renewables).
- Question: Why not LH_2 cryopipelines if the staple onboard storage is LH_2 ? Answer: For distribution/delivery networks, gaseous H_2 is more attractive than LH_2 for pipelines, not

only because the capital cost of a cryopipeline is very high, but because LH_2 is an *incompressible* fluid and, hence, lacks the energy sponge properties of gaseous pipelines.

- In urban settings, we can expect gaseous H_2 pipes will deliver directly to homes, offices, factories – and sometimes community “nodes”. The electricity required for electrical appliances, like computers, will normally be produced on-site from fuel cells. This will be dc electricity – ac will essentially vanish because its prime value in today’s world is for stepping up & down voltages (as the electricity moves from trunk distribution to serving hotel loads such as your TV set). The single other advantage to ac is its inherent ability to keep electric clocks “on time”. But time accuracy can easily be done by many other means – like crystals.
- One niche circumstance when LH_2 cryopipelines might compete with gaseous H_2 pipelines could be special-case short runs. In this circumstance, the LH_2 cryopipelines *might* contain (within the pipe) superconducting electrical transmission lines.
- LH_2 taken from the gaseous H_2 network will be liquefied at high-capacity plants – probably located adjacent to nuclear power plants (NPPs) and distributed by LH_2 road or rail tankers to vehicle refuelling stations. This scenario might be modified if there were significant advances in LH_2 liquefaction processes that improved efficiencies, lowered capital and operation costs, and *also* were not limited by the “economy of scale” that constrains small-capacity liquefaction today. If such advances occurred, liquefaction might be done at the service stations, or even within homes.
- Some remote and/or rural distribution will retain small-capacity electrical grids – because the capital cost of small-capacity H_2 pipelines may push infrastructure cost tradeoffs towards electricity distribution.

Central H_2 storage implications.

- Large-capacity gaseous hydrogen storage will provide continental energy supply security.
- The inherent ease of storing gaseous H_2 will provide access to the full range of energy sources. Isolated locations will be able to generate indigenous hydrogen and use it in (H_2 age) technologies – like farm tractors. Large-scale generating stations will be able to operate with steady outputs, without requiring load management technologies. Intermittent sources – those I call whimsicals – can deliver their energy to the system anytime they choose (*and with no systemic penalty* [8]) where it will be swallowed first by pipelines and then large storage tanks.
- Electricity, of course, is not storable – although, if there were major advances in high temperature superconducting materials, it’s possible that some energy storage nodes might employ superconductor technologies.

Transformer technologies

I think it illuminating to classify energy sources as either reliables or whimsicals.

Reliables are sources, like those that feed most of today’s electricity generation plants (e.g. coal, uranium and hydraulic) that deliver energy whenever called upon, independent of time of day, weather, or other “externalities”. Sometimes, as in the case of electricity generation, this means at almost constant output. At other times, as in the case of the family automobile, it means not only when we want to drive somewhere but also when we want an extra shot of power to accelerate away from the stoplight.

Whimsicals are sources that deliver their power on their own schedule, which may or may not be when it's needed. They are typified by many renewables that deliver energy when the sun shines, or the wind blows, and so on, but not otherwise.

Although both reliables and whimsicals will contribute during the transition to (and within) a fully-developed hydrogen age, reliables will always dominate. And among reliables, nuclear fission will be pre-eminent – at least during the first half-century of the fully-developed hydrogen age. Thereafter, it gets harder to be sure. For example, by 2150 it is conceivable that controlled nuclear fusion might have not only become feasible but might come to dominate energy sources.

Let's first consider the dominant reliable.

- One advantage of nuclear fission, especially during the transition to the fully developed H_2 age, is that its energy product can be *rapidly* swung from producing electricity to producing hydrogen via electrolysis. To facilitate high efficiency production of both currencies during the transition era both ac and dc generators can be mounted on a single shaft. This configuration can continue into a fully-developed H_2 age, because other reliables (for example, HTRs and fusion) will almost certainly be dedicated to H_2 production, and there will always be a need for a fraction of the sources having the capability to quickly “swing” between H_2 and e . [9]
- The capital cost of nuclear fission will have dropped significantly – especially compared with the then-dinosaur technology called coal-fired generation. (Today, the ACRs are projected to cost in the range of \$1 000/kW – about the same as coal-fired capital cost. And since the operating cost of NPP will always be a small fraction of that for a CFPP – the energy currencies from NPP will be lower.) [10] (Note: Today, if you buy a ladder for your home you might pay, \$60 – but the same ladder for a NPP could cost \$600 ~ \$6 000 due to the myriad of “certification” requirements.)

Now to the minor reliables.

- Nuclear Fusion: The fundamental limitations on controlled fusion may prevent its commercialisation for at least another century. [11] If fusion is ultimately commercialised, it is likely to be dedicated to H_2 production – a consequence of its inherently extraordinarily high temperatures (valuable for “direct” thermochemical processes, without intermediate electricity.) The challenge for fusion will be to be competitive with advanced fission – likely a very tough challenge in the 21st century.
- Hydraulic power: In the more developed nations, hydraulic capacity will be saturated long before the 22nd century. Reasons: (a) Available capacity had already been identified and developed *and* (b) Increasingly, hydraulic power will encroach upon *other* renewable needs, like fish, irrigation, etc. In some contrast, within the less developed nations of the late 20th and early, 21st century, new hydraulic capacity will be introduced during the 21st century. Still, by the time of a fully-developed H_2 age, hydraulic resources throughout the world will almost certainly have reached maximum capacity – unless (tragically) today's grossly undeveloped nations have not moved up the economic ladder. Hydraulic power shares with nuclear the ability to rapidly swing output from H_2 to e .
- Natural gas: CH_4 will be used to manufacture H_2 – using “advanced” SMR processes. [12] The heat for SMR will be provided by nuclear, *not* by natural gas. The requirements for sustainability will require sequestering the waste product CO_2 . This means nearby sequestering sites – leak-proof over at least 1 000 y timeframes – must be available. Therefore, while some SMR H_2 may be produced, it will not make a significant contribution

to H_2 markets. (For convenience, the overall process equation for SMR is: $CH_4 + 2H_2O + \text{heat} \rightarrow 4H_2 + CO_2$.) Natural gas will disappear from electricity generation, both because the needs for “grid” electricity will have become trivial and because the requirement for sequestering is much more difficult from gas turbines than from SMR *unless* using pure oxygen is the turbine oxidant.

- Coal and oil: Both will become *illegal* or *irrelevant* or *both* for “fuels” – that is fuels to generate electricity or hydrogen, or as a fuels for transportation vehicles. These 20th century hydrocarbon sources will retain high-value roles for things like medicines, materials, lubricants or, perhaps, foods. This last might startle. But I expect clever people will learn how to make high-quality “simulated” salmon, beef and tomatoes from oil and coal. Moreover, after the initial resistance to these “artificial foods”, succeeding generations (of people) will come to want the “reliability and uniformity” of coal-based tomato soup. (How’s that for something about the future that we, of the early 21st century, can’t possibly imagine welcoming – but early 22nd century people might love?)

Finally to the whimsicals (almost all of which are renewables).

- The rate renewables are harvested must be much less than the replenishing rate– probably less by at least an order of magnitude. This consumption/replenishment ratio too often ignored by today’s renewable proponents – who fail to recognise that the patterns of environmental damage caused by over-harvesting renewables such as fish, fresh water and forests, will carry over to environmental damage wrought by over-harvesting renewable energy.
- The imprimatur of Nature’s mechanisms for delivering renewable energy is low energy density. Nature helps mitigate this limitation in one case, hydraulic, by gathering the energy of diffuse rainfall with her streams, lakes and rivers. But for almost all other renewables, disperse energy delivery dominates. A lightning bolt is one case where Nature deviates from her general pattern of diffuse energy delivery. This exception that proves the rule simultaneously demonstrates a second observation “Nature is kind”. What if all renewable energy came in lightning bolts?
- The magnitude (and location) of harvested whimsical energy is capped by large surface area requirement – whether land or ocean. Moreover, during 22nd century the use of global surface areas for human development will be even more constrained than today.
- The magnitude (and location) of harvested energy will, increasingly, be constrained by the intrusion upon other renewables for which, *unlike* energy sources, there are no alternatives, such as (a) forests, (b) freshwater, (c) wildlife – and (d) food (even if some food comes from coal). Analogous to coal-sourced tomatoes, you might say, “Well, we can always manufacture fresh water (from oceans) using nuclear power”. That is true – at least for potable drinking water. But this becomes increasingly difficult as we move inland from oceanic coasts. Moreover we’re then speaking of “drinking water”. The disruption of the continental fresh water cycle is quite a different matter – and surely a different magnitude.
- Still, with respect to whimsicals (remember these are predominantly renewables) the fully-developed hydrogen age *will* bequeath a major benefit – by releasing one of today’s critical constraints. Coping with intermittency will no longer be an issue, a consequence of gaseous H_2 pipeline networks and gaseous H_2 national storage reservoirs.

The deep future as a platform for energy strategies

Now things become interesting. But we must be prepared re-examine much of today's received wisdom.

Above all, we must avoid intellectual dishonesty born of pandering to special interests – even when some of these are well meaning. These interests fall within two groupings: (a) Large multinational commercial interests (e.g. *some* oil and all coal companies, and *some* automobile manufacturers.) *and* the legislators who lean on financial support of these special interests for re-election. (b) The “self-defined” green saviours-of-the-world – many of whom are immune to numeracy but inoculated with populist political skills (including the ability to draw public “donations” to keep them alive, well-fed and attracting media attention).

We (society) must demand rationality from our leaders – or at least demand they strive for rationality. This is difficult, especially in these times when, rationality is increasingly trumped by faith (in many forms and morphing in different parts of the world). We must remember the wisdom of President John F. Kennedy when, speaking at a Yale convocation, he observed,

“The great enemy of truth is very often not the lie – deliberate, contrived and dishonest – but the myth – persistent, persuasive and unrealistic.”

This is surely a truth without borders – as demonstrated by a very different man, having a very different career, living in quite a different country, thinking in a different language, using different words, when Nietzsche wrote,

Überzeugungen sind gefährlichere Feinde der Wahrheit als Lügen, “Convictions are more dangerous enemies of truth than lies”.

Still, let's set aside the difficulties – legion that they are – to speak to what *should* be done. And can be done only by rational, numerate, intellectually honest, public policies. To keep things organised, we'll consider strategies under two groupings: cultural and institutional.

Cultural

We must make every effort to give the public a more realistic understanding of the pros (which are many) and the cons (which are few) surrounding power from nuclear fission. It seems to me that, among the many misunderstood phenomena, some of the most damaging to public policy include:

- Ionising radiation: First, more people should understand what the adjective “ionising” in front of radiation *means* – and how it differs from the broad term “radiation” – and how “nuclear” radiation is but one form of “ionising” radiation. Second, and even more important, the public should have some appreciation of the hormesis vs. linear no-lower threshold (LNT) models of radiation impact on health. This leads to the startling – to most people – reality that we are almost certainly healthier with full-body dosage up to 20 times “normal” background – a little more ionising radiation than background can be “good for you” – just as one aspirin a day is “good for you” and perhaps, also, a glass of red wine.
- Reprocessing: Legislators and the public must appreciate that reprocessing spent nuclear fuel can massively reduce the amount (by almost 100 times) and toxic longevity of the material that must ultimately be disposed. After that is understood, we should have public policy built upon this reality (even though, as a shareholder in Cameco – with world's largest uranium holdings – the value of my shares may drop).

- Sequestering times: *If* spent fuel is reprocessed, the residual ionising radiation is no higher than natural U in the ground after timeframes of ~ 300 years. (This is same order – yet probably less – than the characteristic atmospheric residence time of CO_2 , which is often quoted as ~ 400 years.) This ~300 year decay of spent fuel toxicity to its original in-the-ground-before-mining toxicity, is true for enriched uranium fuels that are the international norm. (It’s even shorter for today’s spent fuel from natural U fuelled CANDU reactors. [13]) This is in sharp contrast to the widely held myth that spent fuel is dangerously radioactive for many thousands of years.

The public’s hopes for renewable energy sources must be tempered by reality therapy that includes:

- The problems with (a) intermittency, (b) encroachment upon other renewables (e.g. the fish, forests, freshwater that we’ve already mentioned), (c) high land (surface) area demands, (d) high capital costs and (e) low capacity factors.
- In addition, people must ask: Why this *unexamined acceptance, a priori*, of the fundamental desirability of renewables? Might it be a legacy of the “running out” myth that began with the oil supply disruptions of the 1970s? Or could it be the most preposterous of fuzzy thinking: the perception that “renewables are free”.

Institutional

- We *must* reverse today’s institutional memory loss with respect to nuclear power technologies. It seems a strangely skewed policy that retiring US nuclear *weapons* scientists and engineers undergo an extensive de-briefing to inform next generation weapons scientists and engineers while, in contrast, no such debriefing is being required for retirees from the nuclear *power* industry.
- Nations with nuclear power capabilities should *rapidly* develop next generation “conventional” nuclear power reactors. Moreover, the systems/technologies surrounding these reactors should be designed so the reactor’s energy can efficiently and quickly swing between e and H_2 production. *Note*: When a power plant has a multiple-currency capability, a codicil benefit is that there are lower regret-costs, should the demand projections for either electricity or hydrogen turn out to be in error – as such projections always, in some measure, do.
- Work on advanced reactors, including high-temperature reactors (HTRs) and fast breeder (FB)-HTRs, should be accelerated. But this development must not be at the price of either diminishing (or deprecating) efforts to improve conventional reactor technologies, for these will be the work horses of e and H_2 production during the multi-decade transition to the hydrogen age.
- For both environmental and resource-conservation reasons, public policy should require that new fossil fuel projects integrate fossil and non-fossil energy sources to manufacturing multiple energy currencies. Non-fossils sources can be nuclear and might be hydraulic. Products can be synthetic crude (better yet, gasoline), heat, O_2 , even methanol. This strategy should be *demand*ed of any further development of the Athabasca oil sands (political difficulties aside). A lot of design work has been done on multiple-input, multiple-output, fossil/non-fossil integrated systems (in both Germany, Canada and elsewhere) – so it’s not a matter of starting with a clean sheet of paper in an engineering office, rather it’s a matter of first making accessible the immense work already done – and having the political courage to use it.

- Whenever new natural gas pipelines are planned, engineering should examine the marginal addition costs for assuring that the pipelines are H_2 compatible – in the expectation that they may carry gaseous H_2 before they are decommissioned. Unless the marginal cost is found prohibitive (in my view an unlikely prospect), new pipelines should be built “hydrogen ready”.
- The legislative playing field should encourage the commercial development of H_2 fuelled service technologies, such as fuel cell systems for both small niche, novel-service technologies and larger transportation systems. The US military (and NATO) could play an important role with LH_2 aircraft and infrastructures, in part by building on international space programme experience.
- The private sector should recognise the immense markets to be won with the successful development of advanced, energy efficient, low operating/capital cost liquefaction technologies. Magnetic liquefaction is but one avenue. The development of less costly liquefaction for LH_2 is, perhaps, the most serious of the missing technological links in emerging H_2 infrastructures. It amazes that so few innovators and corporations have recognised the opportunity growing out of this need. More importantly, government departments, like DoE and NRCan haven’t recognised it either.
- Legislation should encourage H_2 -fuelled urban fleets using central refueling depots. (The requirements for new refueling infrastructures are less demanding for urban transportation than for either transcontinental or rural venues.) Candidate fleets include urban buses – and perhaps taxis and couriers. Another so-far-neglected opportunity is commuter rail. The city of Toronto, Canada, with an extensive the commuter train schedule *and* where, at one end of the line, North America’s only urban NPP resides, could be an excellent test case.

Conclusion

The needs are critical. The fundamental ideas, simple. The lack of understanding, stupefying. The dithering, scary. The promise, brilliant.

REFERENCES

- [1] Reported in *Newsweek* magazine, Vol. 93, p. 100, 16 April 1979.
- [2] The next level towards “not so simple” but “somewhat more complete” might be to include a distribution and delivery link.
- [3] We can always identify temporary aberrations that seem to go against this trend. But these result from social aberrations, they are not a consequence of technology losing its ability to continuously provide more service for less energy. One example of such a social aberration is trend for foolishly large personal vehicles to satisfy little-vehicle needs.
- [4] I have avoided the descriptors “upstream” or “downstream”, which can be ambiguous – as upstream/downstream depends on whether we’re watching the flow direction of “energy” or the flow of “demand”. Instead, I’ve used the less common, but I hope by now the clear perspective of this paper, that the system begins with a demand for service and responds by moving “down-system” to sources.
- [5] Historically, a lot of H₂ has been manufactured from coal, but seldom by first making electricity and then, using electrolysis to make hydrogen. Usually we use a process involving a reaction approximated by the equation $C + H_2O + (\text{thermal energy}) \rightarrow H_2 + CO$. Today, the H₂ + CO mixture is called syngas. In earlier times it was “town gas”.
- [6] Brewer, G. Daniel, “Hydrogen Aircraft Technology”, CRC Press, 1991.
- [7] High-voltage direct current electricity=hv-dc. High-voltage alternating current electricity=hv-ac.
- [8] Beyond the low capacity factor penalty suffered by any whimsical source suffers.
- [9] HTR = high temperature reactor.
- [10] ACR = advanced CANDU reactor, NPP = nuclear power plant, CFPP = coal-fired power plant.
- [11] For a somewhat dated, but still (I think) good review of the technical challenges to controlled fusion, it’s good to re-read Lawrence M. Lidsky’s “The Trouble with Fusion”, *Technology Review*, 87 (7), p. 32-44. For a later review of the critiques of Lidsky’s paper, you could refer to Chapter 12 of Robert Herman’s book *Fusion: The Search for Endless Energy*, Cambridge U. Press.
- [12] SMR = steam methane reformation.
- [13] CANDU = CANadian Deuterium (natural) Uranium reactor. (Deuterium refers to heavy water, D₂O moderator and coolant.

CRITICAL PATHS TO THE POST-PETROLEUM AGE

Russell A. Brown

Argonne National Laboratory, USA

Abstract

World petroleum production cannot be sustained, and will begin to decline during the next ten to fifteen years. Petroleum represents 39% of US primary energy and 97% of its transportation energy. Hundred year time profiles for per capita supply were calculated for 108 possible combinations of peak production rates, peak years, field depletion rates, and population growth. An optimistic subset of assumptions produced per capita supply reductions of 17% and 45% in 2025 and 2050, respectively; a median subset increased those reductions to 31% and 64%. The energy capacity required for replacement of petroleum-based transportation energy is 312 GW_e. 515 GW_e would be required for hydrogen production, distribution, storage, and transfer. It could be produced by 515 1 000-MW nuclear reactors or 1.72 million 1-MW wind turbines. Subsequent replacement of natural gas would increase total energy demand to 798 GW_e. Hydrogen storage as either a pressurised gas, liquid at 20K, or metallic hydride is technically feasible; however, all three pose significant practical difficulties. The impending loss of a major fraction of primary energy and essentially all transportation energy creates time- and resource-critical problems for the US and world economies. Major impacts on industry, agriculture, personal and mass transportation, and standard of living must be anticipated. Immediate action at both the national and international levels is necessary to mitigate potential effects.

Petroleum

The prosperity of the modern world is based on inherited energy. Coal, petroleum, and natural gas were created by a combination of solar energy, biological conditions, geological conditions, and time. Most of the world's petroleum was formed over a period of 100-300 million years, extending from the late Paleozoic to the early Cenozoic Era. [1, 2, 3, 4, 5]

The majority of the world's petroleum resources will be consumed in less than 200 years. We are consuming it about a million times more rapidly than the rate at which it was produced. US crude oil production peaked at 9.6 million barrels/day (mmb/d) in 1970; current production is about 5.8 mmb/d, a decline of 40%. The world discovery rate was almost four times the consumption rate in the 1960's. In the 1990's, consumption was almost four times the discovery rate. [6, 7, 8]

Zittel's paper, "Future World Oil Supply", described the life cycle of a typical oil region, shown for Norway in Figure 1 [9]:

- "The largest and most productive oilfields are brought on stream first."
- "As soon as the larger oilfields of a region have passed production maximum, an ever-increasing number of new smaller fields have to be developed."
- "At some point... the production decline in the already producing fields gets so steep that it can no longer be compensated by the development of new fields. This is the time when the production of the whole region starts to enter the decline phase."

Figure 2 illustrates the combined profiles for the countries that have passed their production peaks, excluding the FSU and the majority of OPEC nations [9]. Those listed on the on the right side of the graph could increase production. Their combined production, about 35 mmb/d, represents about 45% of world production. As world demand increases, an increasing demand will be made on the OPEC nations, thus accelerating the depletion of their fields.

Eighteen of the top twenty-eight oil-producing nations have already passed their peak production rates. Five of the remaining ten should reach their peaks during this decade. [10] The historical pattern of the United States and Norway production is matched by the combined production profiles illustrated in Figure 2. World production should follow a similar pattern.

Petroleum is a finite resource. Estimates of the upper limit of world reserves, EUR (estimated ultimately recoverable) generally fall in the range between 2 000-3 000 billion barrels. World peak production should occur in the 2010-2020 period. [11] The majority of peak production estimates fall within the 80-90 million barrels per day (mmb/d) range.

The International Energy Agency postulated a maximum production of 115 mmb/d in 2030. [12] The US Energy Information Agency based its estimate of 119 mmb/d by 2025 on a recent USGS reference case. [13] Both are based on significant increases in known reserves and on large undiscovered oil fields.

Figure 1. Norway: Crude oil production, including the individual fields [9]

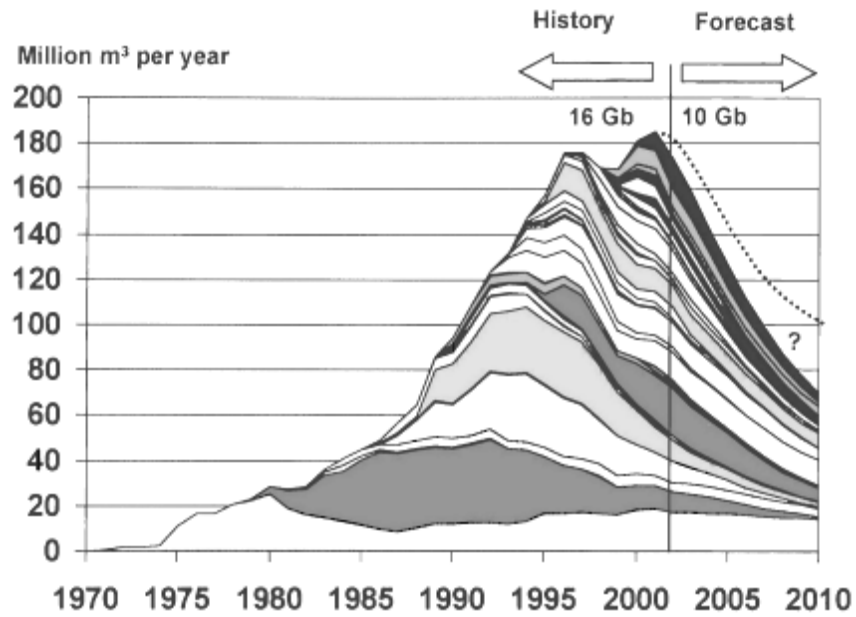
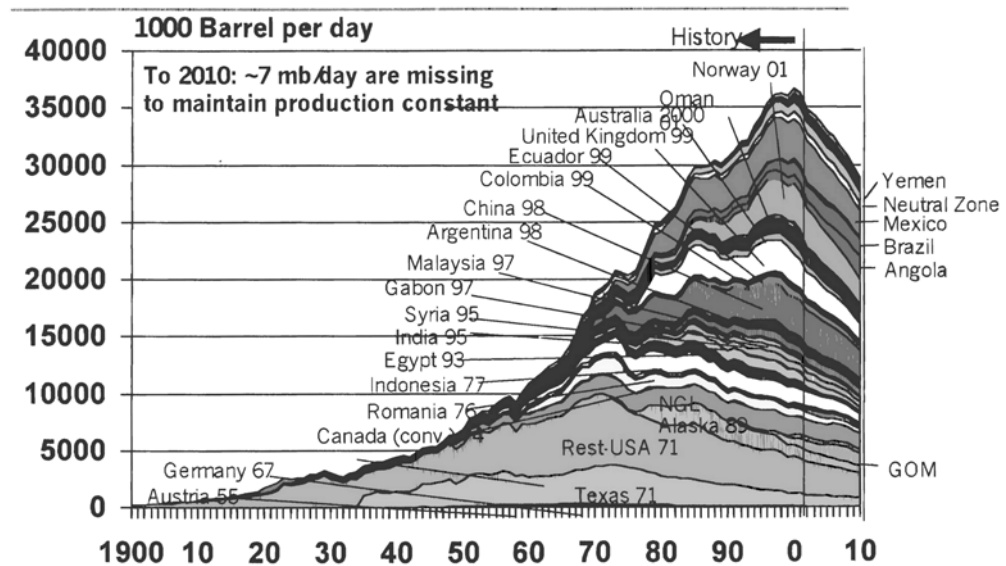


Figure 2. Aggregated production for nations that have passed their production peaks [9]



Additional exploration and improved recovery technology can increase recoverable reserves. The discovery history of the last twenty years suggests that such increases would be relatively small. Drilling deeper wells offers little promise. The majority of the world's oil was formed at depths ranging from 2-4 kilometres, at temperatures of 50-150°C and at pressures up to 1 500 atmospheres. At lower depths and pressures, little petroleum is produced; at greater depths and pressures, the predominant product is natural gas. [14, 15, 16, 17]

Unconventional sources such as the tar sands of western Canada, the heavy deposits of Venezuela, and the oil shale region of Wyoming, Colorado, and Utah have been included in projections of future hydrocarbon production. Deffeyes [14] described oil shale as an “unborn oil field” and tar sand as a “dead oil” field. Extraction of “heavy oil” requires heat, often steam or hot water; production of two barrels requires the energy of one barrel of oil. [18] Shale oil is a waxy substance, an oil precursor called kerogen. Conversion to a bunker oil product requires mining, crushing, and heating the shale to 480°C to liquefy the kerogen, which must then be treated with water to provide hydrogen. Water supply, energy demands, and disposal of the toxic waste by-product led to the failure of all previous operations. [19]

Petroleum represents 39% of US primary energy [20], and more than 97% of its transportation energy. [21] The majority of all fertilizers are based on petrochemicals [14]. There are no adequate substitutes for the transportation capabilities of petroleum. Replacement of raw material uses, where possible, by derivatives of coal and natural gas would accelerate the decline of those resources. The impending decline and eventual disappearance of petroleum resources could create catastrophic transportation, food production, and related economic effects.

Post-peak production estimates

In 2002, world oil production, including natural gas liquids (NGL), was 77.6 mmb/d; EIA projected production for 2003 is 78.7 mmb/d. [22] The International Energy Agency reported the world supply was 78.64 mmb/d in July, 2003. [23] OPEC expected that demand in 2004 would be 79.3 mmb/d. [24]

The path of the production decline after reaching a peak is critical information. Within a reasonable range of uncertainty, that knowledge will define the priorities for future technology development and implementation. It would also provide the basis for estimates of the social, environmental, and economic impacts of the thermodynamic penalties that must be paid for production of energy and the synthesis of substitutes for the raw materials previously provided by vanishing hydrocarbon resources.

Hundred year time profiles for US per capita petroleum supply were calculated for 108 combinations of:

- World peak production rates of 80, 85, and 90 mmb/d, assuming that US share remains at 26%.
- Three peak production years for each peak production rate:
 - 2005, 2010, and 2015 for 80 mmb/d.
 - 2010, 2015, and 2020 for 85 mmb/d.
 - 2015, 2020, and 2025 for 90 mmb/d.

- Field depletion rate constants, k_d of 0.015, 0.020, and 0.025 A $k_d=0.020$ provided an excellent fit for US post-peak field depletion rates for the lower 48 states. Zittel [25] reported that a 2% annual depletion rate after the maximum was “most realistic”.
- Four US population growth rates, producing 2050 populations of 350E6, 375E6, 400E6, and 440E6 respectively; 440E6 was based on the average growth rate for the 1999-2003 period. [26]

Per capita values were based on the assumed peak production and the US population for the peak year. The current value of ~0.0707 bbl per person-day (11.2 liters per person-day) was used as the basis for calculation of percentage profiles (0.0495 would be equivalent to 70% of the basis value).

Per capita values were sensitive to k_d , with differences of 14-15% between the high and low settings. Increased peak production rate and peak year values were neutralised by the effects of population growth rates. Within 25 years of the peak, percentage changes in per capita supply were similar.

Population growth is a major driving force in the calculation. It is the only parameter in the above-described model that could be controlled. The Census Bureau’s mid-range population projection estimated that 63% of US population growth over the next 50 years will be attributable to immigration. [27] The negative population growth organisation estimated an 88.5 million reduction in the projected 2050 population without immigration. [28]

Three examples, each based on the mean of two similar parameter sets, illustrate a representative “worst”, “median”, and “best” set of results. All three sets used a $k_d=0.020$ and a US consumption of 26% of world production.

- Best: 90 mmb/d peak supply in 2015, with populations of 350E6 and 375E6 by 2050.
- Median: 85 mmb/d peak supply in 2010, with populations of 375E6 and 400E6 by 2050.
- Worst: 80 mmb/d peak supply in 2005, with populations of 400E6 and 440E6 by 2050.

Table 1. World petroleum supply
per cent of 2005 per capita level

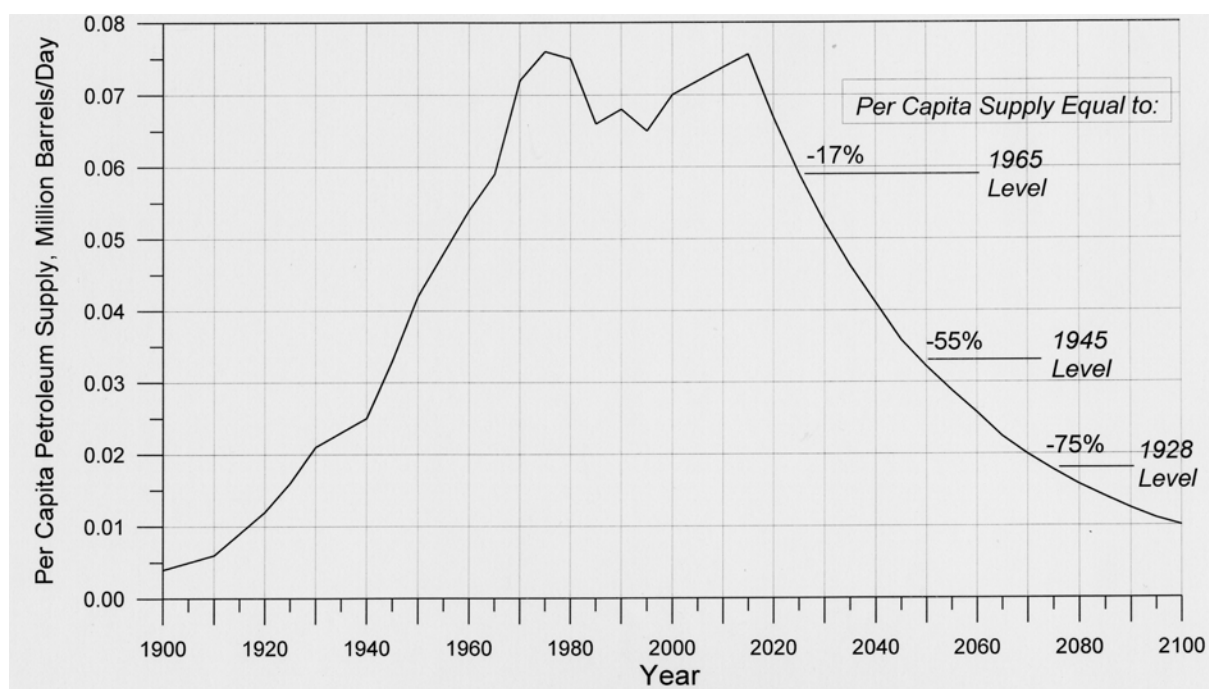
Year	Best	Median	Worst
2025	83%	69%	57%
2050	45%	36%	29%
2075	25%	19%	14%
2100	14%	11%	8%

The Best case assumes a world production increase of more than 12 mmb/d during the next 13 years, a peak in 2015, and populations that are unrealistic without the institution of draconian controls on both legal and illegal immigration. Despite these optimistic parameter values, the calculation yields a reduction of 55% in per capita supply. The median and worst case values for 2050 show reductions of 64% and 71%, respectively.

Figure 3 combines US supply data for 1900-2000 and the Best case projection for 2015-2100. The 17%, 55%, and 75% reductions in per capita supply from the peak level are equivalent to a return

to the oil supply for 1965, 1945, and 1928, respectively. The effect of such declines in primary energy would be serious. A return to the transportation energy equivalent of the early 20th century would produce radical changes in any economy.

Figure 3. A 200 year per capita supply profile for the United States



Hydrogen and energy production requirements

The current US share of world oil production, 26%, will become inadequate to meet transportation requirements before 2050. Ninety-seven percent of US transportation energy is provided by petroleum. The median case (Table 1) projects a 31% reduction in current supply levels by 2025.

Both vehicular and air travel could be severely limited, with concomitant impacts on the economy, when supply is reduced by 20%.

Table 2 illustrates that vulnerability. US oil consumption and imports are the highest in the world, and per capita use is highest among the major consuming nations. Canada has comparable per capita consumption, but is not dependent on imports.

Complete replacement of US transportation-related petroleum consumption establishes an upper bound for the requisite additional electrical energy, hydrogen production, and hydrogen storage capacity. Current primary energy is used as the basis for a baseline estimate; these preliminary values can be corrected to reflect actual growth as it occurs. The EIA reported that 2001 total consumption of vehicle fuels was 1.704E11 gallons, or 6.45E11 liters. [30]

Table 2. The major petroleum-consuming nations [29]

	Consumption, mmb/d	Barrels per person-day	Imports, mmb/d	Rail density, km/km²
United States	19.70 [1]	0.0702 [4]	10.40 [1]	0.020
Japan	5.40 [2]	0.0425 [13]	5.30 [2]	0.061
China	4.90 [3]	0.0038 [50]	1.60 [6]	0.008
Germany	2.71 [4]	0.0326 [19]	2.60 [3]	0.127
Russia	2.38 [5]	0.0164 [29]		0.005
Brazil	2.20 [6]	0.0125 [33]		0.004
Canada	2.00 [7]	0.0627 [5]		0.007
India	2.00 [8]	0.0019 [58]	1.20 [8]	0.019
France	1.96 [9]	0.0328 [18]	1.85 [4]	0.060
Mexico	1.93 [10]	0.0187 [26]		0.010
Italy	1.87 [11]	0.0324 [20]	1.69 [5]	0.065
United Kingdom	1.70 [12]	0.0284 [21]		0.079
Spain	1.50 [13]	0.0374 [15]	1.50 [7]	0.028
Saudi Arabia	1.36 [14]	0.0578 [6]		0.001
Indonesia	1.02 [15]	0.0044 [47]		0.003

Hydrogen properties:

- Molecular weight ▪ 2.016
- Specific gravity ▪ 0.089 g/L as a gas at STP
 ▪ 0.07 g/cc as a liquid at -253°C (20K)
- Volume at STP ▪ 22.428 liters per gram-mole [31]
- HHV ▪ -33.89 kcal/g (high heating value)
- LHV ▪ -28.67 kcal/g (low heating value)

Gasoline (2,2,4-trimethylpentane) properties:

- Molecular weight ▪ 114.23
- Specific gravity ▪ 0.692
- HHV ▪ -1 307.5 kcal/gm-mole (11.45 kcal/g)
- LHV ▪ -1 212.9 kcal/gm-mole (10.62 kcal/g)

Petroleum energy: $6.454E14 * 0.692 * 10.62 = 4.74E15$ kcal

Weight of hydrogen equivalent: $4.74E15/28.67 = 1.65E14$ grams

Petroleum consumption for transportation was 25.61 Quads in 2001. [32] Nuclear power produced 8.028 Quads at a capacity of 97.86 GW_e. [33] Replacement of petroleum energy would require $25.61 * 97.86/8.028$ or 312 GW_e.

Bossel and Eliasson [34] analysed the energy efficiency of electrolysis, packaging, distribution, storage, and transfer of hydrogen. Energy input factors in terms of energy input per HHV of hydrogen were estimated for each element of several possible technology paths. Based on production by electrolysis, the summations were:

- Pressurised gas at 200 bar: 1.65
- Pressurised gas at 800 bar: ~ 1.70 (inferred)
- Liquid hydrogen: 2.12
- Metal hydride: 1.95

Weindorf *et al* [35] of L-B-Systemtechnik GmbH published an extensive critique of the Bossel-Eliasson work, taking issue with both the assumptions and efficiency estimates of “Energy and the Hydrogen Economy” and a final report, issued in April 2003. [36] While some of the Bossel-Eliasson conclusions vis-à-vis a hydrogen economy and one based on synthesized methanol may be speculative, their estimates of system efficiency provide a basis for a preliminary estimate of post-petroleum energy demands. The consequences of overestimates of, for example, 10-20% in energy requirements in 2020-2040 would be less serious than those associated with underestimates.

Application of the Bossel-Eliasson factor for pressurised gas to the 312-gigawatt value for transportation energy produces a demand of $312 * 1.65 = 515$ GW_e.

Replacement of the transportation energy of the US share of a 80 mmb/d petroleum economy would require 515 1 000-MW_e nuclear plants or 1 717 000 1-MW wind turbines with an assumed capacity factor of 30%. The typical range of capacity factors for wind turbines is 20-35%. [37, 38] Eventual replacement of the equivalent energy of natural gas would increase the demand to 798 GW_e, with a proportional increase of the wind turbine requirement to 2 660 000 1-MW units.

Hydrogen storage

Hydrogen may be stored as a gas, a liquid, or a solid hydride. Hydrogen has 2.7-3.0 times the energy per unit mass of gasoline (for the LHV and HHV, respectively).

The volume of hydrogen (compensated for compressibility factors at elevated pressures) required to replace the energy of one liter of gasoline is: [39, 40].

That volume is: $V_{H_2} = 2.04 + 42.007 / \text{Pressure (psi)}$.

- 2 880 liters at STP (0°C and 14.7 psi)
- 23.1 liters at 2 000 psi (138 bar)
- 10.4 liters at 5 000 psi (345 bar)
- 6.3 liters at 10 000 psi (690 bar)
- 3.7 liters at 20 degrees Kelvin (-253°C)
- 2.1 liters in a metal hydride form

Table 3 provides a volume and mass comparison of the four energy sources. [39, 40] Liquid hydrogen has about four times the volume and triple the mass of gasoline on an energy basis. Metal hydride storage would require double the volume of gasoline, and twelve times the mass.

Table 3. Comparison of normalised volume and mass attributes of stored energy forms

	Gasoline	Gas at 5 000 psi	Liquid H₂	Metal hydride
Volume	1	10	4	2
Mass	1	6	3	12

All three storage forms are technically feasible, but may be difficult to implement at the consumer level. Transfer of pressurised hydrogen, liquid hydrogen, or metal hydrides to passenger vehicles 15 000 000 times per day should pose major logistical and statistical challenges. [41] If the transfer error probability were 0.00001, the frequency of hydrogen-related accidents would be 150 per day.

The additional energy costs of liquefying hydrogen and keeping it below 20 degrees Kelvin may become prohibitive in an energy-poor future. Raw material problems could pose major limitations for any of the technologies.

Conclusions and recommendations

World petroleum production will begin to decline during the next decade. The majority of the petroleum-producing nations have already passed their production peaks. US per capita supply could decrease by 20-30% from current levels during the 2020-2030 decade.

Eventually, the behaviour of any general system must mirror the behaviour of its components. The United States has compensated for its production decline by importing oil. The planet does not have that option.

The wealth of the modern world has been driven by ever-growing production and consumption of fossil energy. The liquid form and energy content of petroleum has been the critical component in agriculture, industrial production, and transportation. The peak of world petroleum production will mark a cusp between a long era of growth and prosperity, and one in which the primary energy loss will be exacerbated by the thermodynamic penalties for replacing it with less useful forms. In 1993, Sir Crispin Tickell stated, "We have done remarkably little to reduce our dependence on fuel (oil) which is a limited resource, and for which there is no comprehensive substitute in prospect". [42]

A hydrogen-based transportation economy appears to be the only long-term alternative to our current system. While all three storage forms are technically feasible, none will offer the range, convenience, or cost of the current system. At 5 000 psi, pressurised hydrogen requires ten times the volume per unit energy of gasoline. Liquid hydrogen would occupy about four times the volume per unit energy and would need a capability to maintain the fuel at 20 degrees Kelvin. Both would impose significant weight penalties. Materiel requirements for US demands alone appear to make solid storage forms impractical.

Improved fuel efficiency would mitigate the fuel storage and range limitations. Mazda, Ford, and BMW have recently announced hydrogen-powered internal combustion engines (ICE) for passenger vehicles. The Ford system also incorporates an electric motor in the hybrid power train. [43] BMW's objective is 50% engine efficiency. [44] The Mazda system is based on the rotary engine RX-8 model, with an estimated cost of \$34 000. A comparable fuel-cell vehicle could cost more than ten times that much; Mazda's estimate for a "newly developed prototype" was \$1.7-2.6 million. [45]

A hydrogen-based transportation system would require 515 gigawatts (GW_e) of additional nuclear power capacity to provide the energy for electrolysis, compression or liquefaction, distribution, and transfer. Eventual replacement of natural gas resources would increase that energy demand to 798 GW_e. Wind power capacity would then increase to 2 660 000 1-MW wind turbines.

The critical path structure for meeting the complex and demanding analysis, decision, and implementation processes should include:

- Form national and international task groups immediately. They should be directed by the best technical talent in each nation. The Manhattan Project provides a good example, and the names of Fermi, Oppenheimer, and Feynman come to mind vis-à-vis the quality of leadership. The task groups would direct the preliminary analysis and decision processes. Ideally, they would be independent of political, government, and corporate structures and influences. Initial analyses should be completed by the end of 2006.
- Technology development and testing programmes should concentrate on proven science and technology. Failure in this time/resource-critical factor space could mean never having enough financial, material, and energy resources to complete the necessary tasks. Advanced technology development programmes for nuclear power, hydrogen generation, and vehicles would be included; successful developments could be incorporated in the long-range construction programmes.
- Replacement energy-generation technologies: A stable, long-term nuclear economy must include a breeder reactor cycle, fuel reprocessing and waste management components.

Evaluation of alternative technologies such as wind and solar should include sitting and large-scale field testing in real-world demand environments.

- Development, construction and field-testing of the chosen production, storage, distribution, and delivery technologies for hydrogen.
- Development, construction, and field-testing of candidate hydrogen-powered vehicles. Evaluation of a minimalist design, i.e. with a range of 125 miles, should be included. Hydrogen storage limitations could preclude performance comparable to contemporary personal vehicles.
- Analysis and planning for a transition phase from a petroleum-based to a hydrogen-based transportation system. An assessment of alternative transcontinental and intercontinental transportation concepts should be included, including:
 - Construction of a transcontinental and regional railroad system to replace both personal vehicle travel and air travel. This would be critical for large countries such as the United States and Canada. Both have low rail densities in comparison to the nations of the European Union (the UK rail density, km railway/square kilometre, is 3 times that of the US and 18 times that of Canada).
- Conversion of the current interstate highway system to road bed for a national rail system.
- Recommendations for immediate changes in immigration laws and government subsidy programmes. The long-term impacts of immigration on per capita energy supplies and other resources must be evaluated. Tax laws, agricultural subsidies, and similar policies should be assessed in terms of energy consumption. Existing statutes and policies that encourage either direct or indirect energy consumption should be modified.
- Concurrent risk, economic, and environmental impact analyses should be completed for all technologies and proposed actions for the transition to a post-petroleum economy. The potential risk of delays and technology development failures must be included.
- An international working group should be established to evaluate the potential impacts of prospective changes on the developing nations.

Summary

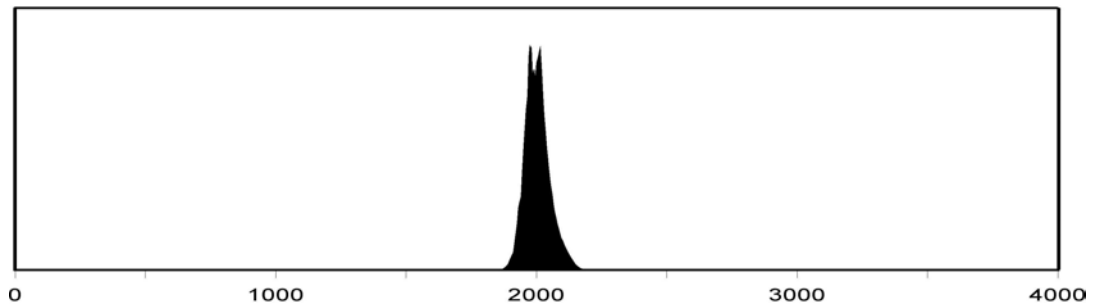
The United States and the world face an energy problem that goes far beyond the need for developing new technologies or building more power plants. As world petroleum production declines, the thermodynamic penalties associated with producing hydrogen or other energy carriers multiply the loss of primary energy.

Each downward step on the primary energy slope has a multiplicative effect. When petroleum supply ends, the effective reduction of US primary energy will be about 56%.

Preparation for both these changes and their effects must begin immediately. If done well, a hydrogen-based transportation system would provide limited personal mobility, decreased agricultural productivity, and increased costs of goods and services. If done either poorly or late, the results could be disastrous.

Figure 4, based on the US supply profile shown in Figure 3, offers a historical perspective on the brief petroleum era on a time-scale of 4 000 years. It is applicable to all developed nations. Until the late 19th century, biomass and animate labour supported human life.

Figure 4. Historical perspective on the age of petroleum



The hydrogen economy will define the state of the world beyond the middle of the 21st century.

REFERENCES

- [1] The Mesozoic World”, www.geo.wvu.edu/~kammer/g3%5Clect13Text.html
- [2] “What is Crude Oil?”, www.chevron.com/learning_center/crude/
- [3] “Geologic Time”, www.leeric.lsu.edu/bgbb/3/geo_time.edu
- [4] “World Oil and Gas”,
<http://www.wistp.murdoch.edu.au/publications/projects/oilfleay/03worldoilgas.html>
- [5] “Origin”, www.leeric.lsu.edu/bgbb/3/origin.html
- [6] World Petroleum Assessment and Analysis”,
www.energy.er.usgs.gov/products/papers/WPC/14/text.html
- [7] Campbell, C.J., “Peak Oil: An Outlook on Crude Oil Depletion”, October 2000.
- [8] “World Petroleum Discovery and Production”,
www.wistp.murdoch.edu.au/publications/OilFleay/00content.html
- [9] Zittel, Werner and Jörg Schindler, “Future World Oil Supply”, International Summer School Salzburg, July 2002.
- [10] “Conventional Oil Endowment, 2001”, ASPO-ODAC, Newsletter, No. 14, February 2002.
- [11] “Oil Prophets: Looking at the World Oil Studies Over Time”,
www.peakoil.net/iwood2003/paper/AndrewsPaper.doc
- [12] “Energy and Technology Perspectives: Insights from IEA Modelling”,
www.eia.doe.gov/oiaf/aeo/conf/unander/unander.ppt
- [13] “International Energy Outlook 2003, World Oil Markets”, www.eia.doe.gov/oiaf/ieo/oil.html
- [14] Deffeyes, Kenneth S. “Hubbert’s Peak, The Impending World Oil Shortage”.
- [15] “Formation Processes of Oil and Gas”,
www.earth.rochester.edu/ees201/Conrad/connradk2.html
- [16] North, F.K. “Petroleum Geology”, pp. 56-57 and pp. 470-471, 1985.
- [17] Hunt, John M. “Petroleum Geochemistry and Geology”, pp. 131-136, 1979.
- [18] Attarian, John, “The Coming End of Cheap Oil”, The Social Contract (Summer 2002).
- [19] Youngquist, Walter, “Shale Oil – The Elusive Energy”, Hubbert Center Newsletter #98/4.

- [20] “Energy Consumption in the United States, 1949-2001”, www.eia.doe.gov/emeu/aer/txt/ptb1801b.html
- [21] “Energy Consumption in the United States, 1949-2001”, www.eia.doe.gov/emeu/aer/txt/ptb1801a.html
- [22] “Short-Term Energy Outlook-August 2003”, www.eia.doe.gov/emeu/steo/pub/steo.html
- [23] “Oil Market Report”, International Energy Agency, August 2003.
- [24] “Report: Global Statistics”, July 2003, www.safan.com
- [25] “Kommentar zur EIA-Präsentation: Long-Term World Oil Supply”, www.energiekrise.de/news/forum/iea.html
- [26] “The World Factbook, United States”, 1999, 2000, 2001, 2002, and 2003; www.cia.gov/cia/publications/factbook/us.html
- [27] “Fact Sheet, US Population Growth”, www.audubonpopulation.org/newpop2/pages/facts/uspop.html
- [28] “US Population Projections”, <http://www.npg.org/popfacts.html>
- [29] “Energy Information Administration, DOE; www.nationmaster.com
- [30] “Estimated Consumption of Vehicle Fuels in the United States, 1992-2001”, <http://www.eia.doe.gov/cneaf/alternate/page/datatables/table10.html>
- [31] “Gases.doc”, www.people.ouc.bc.ca/neggers/Chem%20111/Course%20Notes/Gases.doc
- [32] “US Energy Consumption by the Transportation Sector”, www.bts.gov/publications/nts/2002/html/table_04_04.html
- [33] “Country Energy Data Report”, United States, 2001, www.eia.doe.gov/emeu/world/country/cntry_US.html
- [34] “Energy and the Hydrogen Economy, www.hyweb.de/News/Bossel-Eliasson_2003_Hydrogen-Economy.pdf
- [35] Eliasson, Baldur and Ulf Bossel, “Comments on the Paper”, “The Future of the Hydrogen Economy: Bright or Bleak”, www.hyweb.de/News/LBST_Comments-on-Eliasson-Bossel-Papers_July2003_protected.pdf
- [36] “The Future of the Hydrogen Economy: Bright or Bleak”, www.pacificsites.net/~dglaser/h2/General_Articles/hydrogen_economy.pdf
- [37] “Basics: Energy Output of Wind Turbines”, American Wind Energy Association, www.awea.org/faq/basicen.html
- [38] “Wind Energy”, DOE Office of Energy Efficiency and Renewable Energy, www.eere.energy.gov/femp/techassist/wind_energy.html.

- [39] Harris, R., “Hydrogen Storage: A Critical Technology for the Future”, July 2000, www.seef.org.uk/StAndrews/Presentation%20Harris.pdf
- [40] Young, R.C., “Advances of Solid Hydrogen Storage Systems”, March 2003, www.h2fc.com/Newsletter/PDF/Advances%20of%20Solid%20Hydrogen%20Storage%20Systems.pdf
- [41] “Total Daily Trips and Total Miles Traveled in Daily Trips”, http://www.bts.gov/products/national_household_travel_survey/highlights_of_the_2001/html/table_02.html
- [42] Sir Crispin Tickell, “The Future and its Consequences”, The British Association Lectures, The Geological Society, 1993.
- [43] “H2RV – Ford Hydrogen Hybrid Research Vehicle”, www.autofan.com/newsdetail.asp?id=364&mn=8&yr=2003
- [44] “BMW Presents Dual-Fuel V12 Hydrogen Engine at IAA Frankfurt Motor Show”, www.h2cars.biz/artman/publish/printer_240.shtml
- [45] “Mazda to Develop Hydrogen Car”, Fuel Cell Today, 13 August 2003.

ROLE OF NUCLEAR PRODUCED HYDROGEN FOR GLOBAL ENVIRONMENT AND ENERGY

Masanori Tashimo

Advanced Reactor Technology Co., Ltd.

Atsushi Kurosawa

The Institute of Applied Energy

Kazumi Ikeda

Mitsubishi Heavy Industries Co., Ltd.

Abstract

Sustainability on economical growth, energy supply and environment are major issues for the 21st century. Within this context, one of the promising concepts is the possibility of nuclear-produced hydrogen. In this study, the effect of nuclear-produced hydrogen on the environment is discussed, based on the output of the computer code “Grape”, which simulates the effects of the energy, environment and economy in 21st century.

Five cases are assumed in this study. The first case is “Business as usual by Internal Combustion Engine (ICE)”, the second “CO₂ limited to 550 ppm by ICE”, the third “CO₂ limited to 550 ppm by Hybrid Car”, the fourth “CO₂ limited to 550 ppm by Fuel Cell Vehicle (FCV) with Hydrogen produced by conventional Steam Methane Reforming (SMR)” and the fifth “CO₂ limited to 550 ppm by FCV with Nuclear Produced-Hydrogen”.

The energy used for transportation is at present about 25% of the total energy consumption in the world and is expected to be the same in the future, if there is no improvement of energy efficiency for transportation. On this point, the hybrid car shows the much better efficiency, about 2 times better than traditional internal combustion engines.

Fuel Cell powered Vehicles are expected to be a key to resolving the combined issue of the environment and energy in this century. The nuclear-produced hydrogen is a better solution than conventional hydrogen production method using steam methane reforming.

Introduction

There are two technical approaches to resolve the energy issues on climate change related global environment. One is the improvement of efficiency (i.e. energy demand conservation) and another is the shift to low- or zero-greenhouse gases (GHGs) emission energy supply.

From this view, we selected the combination of fuel cell vehicle (FCV) and nuclear produced-hydrogen (NPH) as new promising technologies in this century. In this study, it is tentatively assumed that NPH is introduced into the energy market at its maximum potential level, because these two technologies are not commercialised at present.

The purpose of this study is to evaluate the potential impact to the environment and energy system by the introduction of NPH, and to understand the importance of nuclear fuel cycle under the uranium resource constraint in the long run.

1. Method of simulation

a) *Model framework*

The calculation of long-term global energy supply and demand balance is conducted by energy module of GRAPE [1] to assess the effect of the transportation energy demand sensitivity and NPH penetration effects. The model can minimise the discounted sum of global energy cost under the limitation of atmospheric CO₂ concentration at 550 ppm during this century. The details of model framework are shown in [2].

b) *Vehicle type and hydrogen production method*

1. Vehicle type

Three vehicle types are assumed. They are conventional inner combustion engine (ICE), hybrid car (HC) and fuel cell vehicle (FCV).

2. Hydrogen production method

There are many proposed methods to produce H₂ at present, such as electrolysis by conventional and new-renewable generation, by-product from steel plant, chemical plant and so on. But quantitative potential of by-product H₂ is not so large.

At present, steam methane reforming is a most widely used and least expensive method [3].

In this study, four types of H₂ production method are selected as measures of large-scale H₂ production as follows.

a) Non-nuclear

SMR (steam methane reforming)

b) Nuclear heated

LWR – EL (light water reactor – electrolysis)

HTGR – IS (high temperature gas reactor – iodine-sulphur cycle)

FR-MR (fast reactor – membrane reformer) [4]
 The characteristics of these methods are shown in Table 1 and Figure 1.

Figure 1. Concept of options

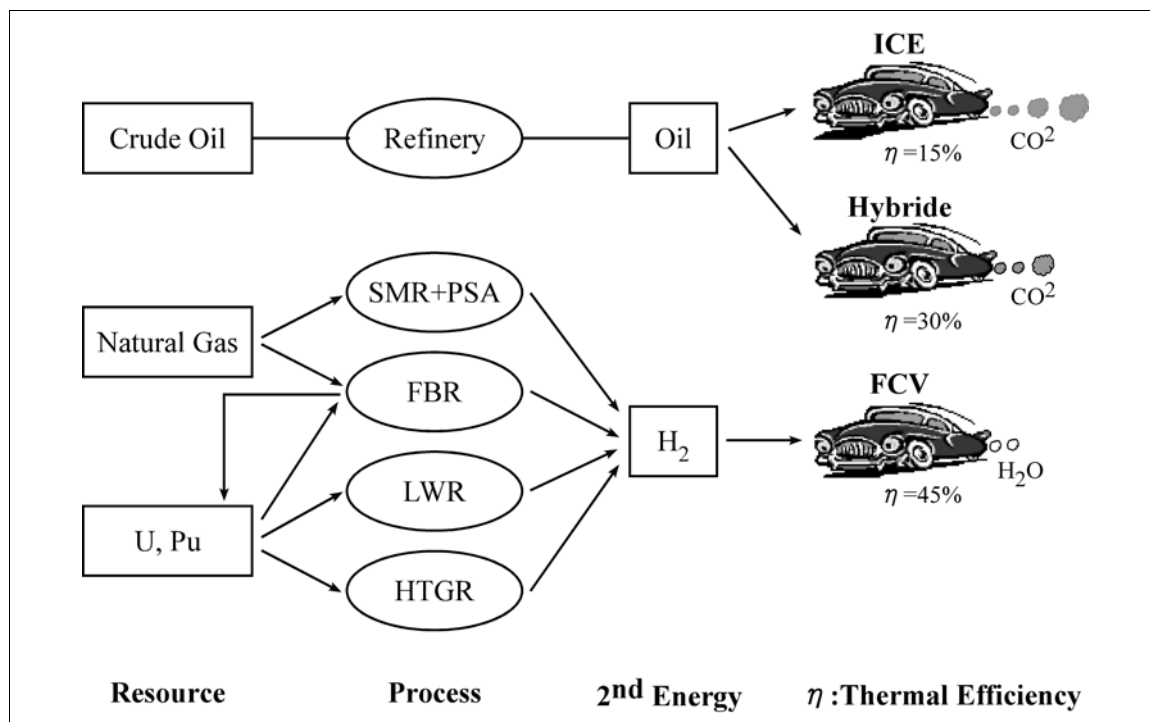


Table 1a. Required energy to product H₂

H ₂ production method	Required energy (Kwh/Nm ³ of H ₂)
SMR	4.1
LWR-EL	13.2
HTGR-IS	6.0
FR-MR	4.1 *

* 1.2^{kwh} (nuclear heat) +2.9^{kwh} (methane)

Table 1b. H₂ Productivity and material balance of nuclear

H ₂ Production method	Productivity ratio per fission	Material balance ton/Gwey
LWR-EL	0.09	-0.4
HTGR-IS	0.20	-0.39
FR-MR	1.00	+0.14~+0.25 *

* Breeding ratio = 1.2~1.35

Table 1c. Natural gas consumption

H ₂ production method	Kcal/Nm ³	With ratio to FR-MR
SMR	~3 600	~1.4
FR-MR	~2 500	1.0

c) *Transportation fuel selection*

The selection of ICE, HC or FCV will be determined by total economy, including the price of vehicle and fuel. In this analysis, we exclude vehicle price effect since low or zero GHG emission vehicles will penetrate into the market by climate policy and/or consumer choice.

As for the fuel cost, it is hard to forecast its uncertainties including:

1. Gasoline price is composed with net production cost, distribution cost and related taxes.

Tax portion is dominant in many developed countries, especially in Europe and Japan (Figure 2).

2. H₂ cost is composed with that of production, distribution and H₂ station (i.e. storage). (Figure 3).

There is great future uncertainty at present. It is assumed that H₂ will be supplied from off-site (i.e. large-scale) H₂ production factory to the market, which is expanded by FCV scenario.

d) *The introduction scenario of FCV*

In spite of there is great uncertainty as discussed above, the introduction scenario of FCV is assumed as follows.

1. In Japan, USA and Western Europe, the introduction of FCV starts from 2030 and dominates the market fully in 2050.
2. The other countries, the introduction of FCV start from 2050 and dominate 100% at 2100.

e) *Transportation energy demand*

The share of vehicle in transportation energy demand is about 80% at present. It is assumed this share will not change in this century. The energy demand for transportation is about 20% in the world at present and is expected to increase in future, because the quality of life in the developing countries will be improved. It is assumed the energy demand for transportation is 23% as is OECD level at present.

The transportation energy is assumed to be 7.2 Gtoe. (WEC-B primary energy 30~35 Gtoe × 0.23 = 6.9~8.0 Gtoe)

Figure 2. Gasoline and tax (1999)

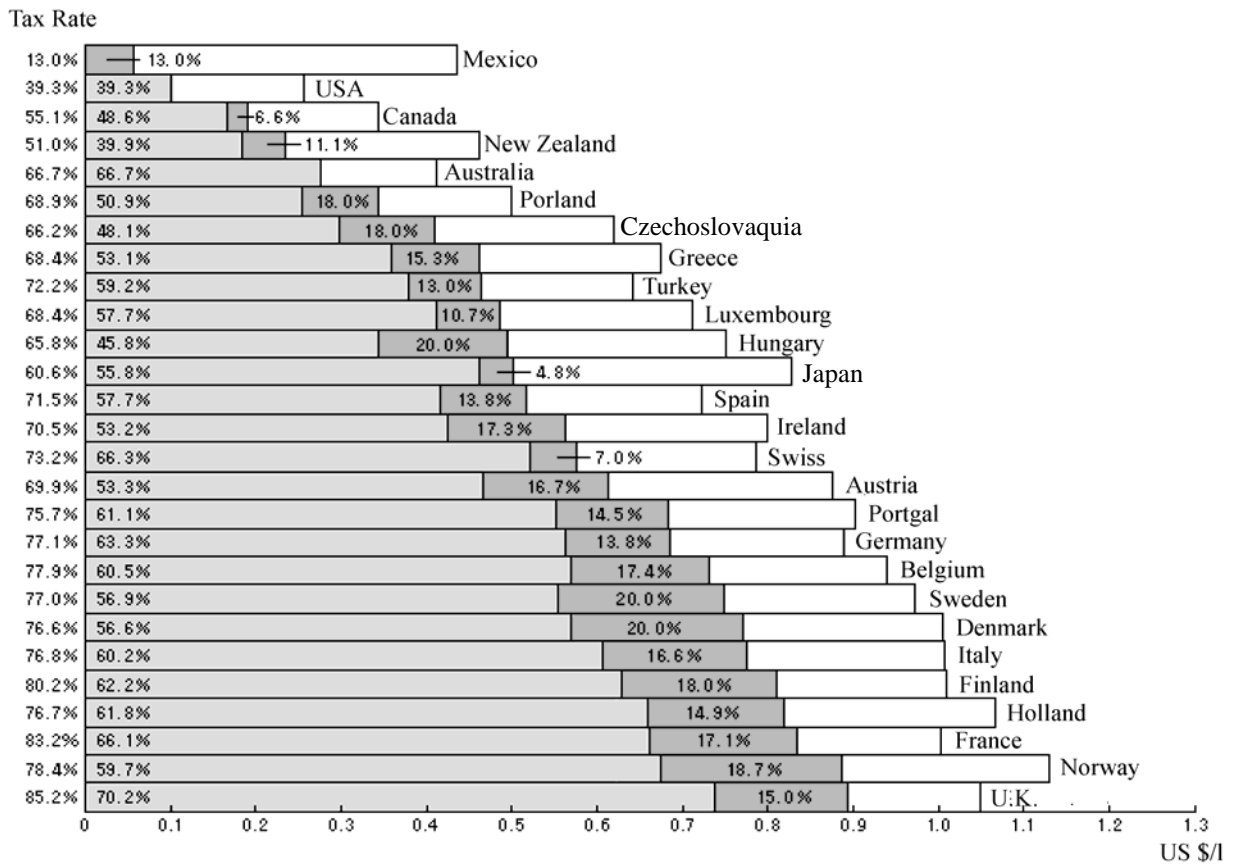
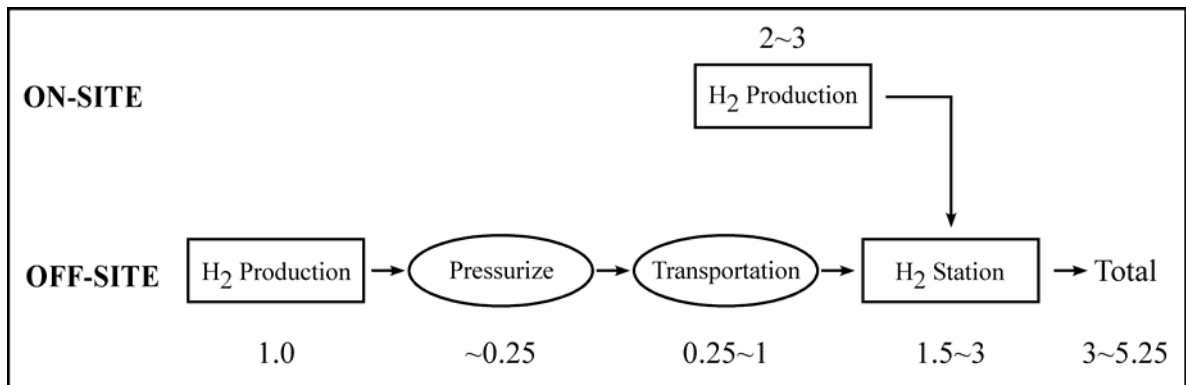


Figure 3. Cost break down of H₂ (from production to station)



* This shows the relative cost ratio to H₂ production.

THE US DEPARTMENT OF ENERGY PROGRAMME ON HYDROGEN PRODUCTION

Mark D. Paster

US Department of Energy, USA

Abstract

Clean forms of energy are needed to support sustainable global economic growth while mitigating greenhouse gas emissions and impacts on air quality. To address these challenges, the U.S. President's *National Energy Policy* and the U.S. Department of Energy's (DOE's) *Strategic Plan* call for expanding the development of diverse domestic energy supplies. Working with industry, the Department developed a national vision for moving toward a hydrogen economy – a solution that holds the potential to provide sustainable clean, safe, secure, affordable, and reliable energy. In February 2003, President George W. Bush announced a new Hydrogen Fuel Initiative to achieve this vision. To realize this vision, the U.S. must develop and demonstrate advanced technologies for hydrogen production, delivery, storage, conversion, and applications. Toward this end, the DOE has worked with public and private organizations to develop a *National Hydrogen Energy Technology Roadmap*. The Roadmap identifies the technological research, development, and demonstration steps required to make a successful transition to a hydrogen economy.

One of the advantages of hydrogen is that it can utilize a variety of feedstocks and a variety of production technologies. Feedstock options include fossil resources such as coal, natural gas, and oil, and non-fossil resources such as biomass and water. Production technologies include thermochemical, biological, electrolytic and photolytic processes. Energy needed for these processes can be supplied through fossil, renewable, or nuclear sources. Hydrogen can be produced in large central facilities and distributed to its point of use or it can be produced in a distributed manner in small volumes at the point of use such as a refueling station or stationary power facility. In the shorter term, distributed production will play an important role in initiating the use of hydrogen due to its lower capital investment. In the longer term, it is likely that centralized production will be more cost effective, but distributed production will still play a role. Utilization of nuclear and renewable technologies inherently addresses greenhouse gas emission directly. The use of fossil fuels requires the development of carbon dioxide sequestration technology to enable a hydrogen economy that also addresses climate change concerns. Ultimately, a spectrum of feedstocks and technologies for hydrogen production will be necessary to address energy security and climate change concerns. The DOE Hydrogen Program will address multiple feedstock and technology options to provide effective and efficient hydrogen production for the short term and the long term. The U. S. DOE Hydrogen Program is contained within the Offices of Nuclear Energy, Fossil Energy, and Energy Efficiency and Renewable Energy that are now working synergistically together to accomplish the overall program goals. The potential benefits of a hydrogen economy are immense. They include increased energy security through the use of domestic and renewable energy feedstocks and a dramatic reduction in green house gas and other criteria air pollutants.

Why hydrogen?

Two key drivers of US energy policy are energy security and the environment. The goals are to reduce our reliance on imported oil, reduce green house gas (GHG) emissions due to climate change concerns, and reduce other air emissions that can result from the production and use of energy. The use of hydrogen, particularly in the transportation sector, is the only currently known approach that can satisfy both of these drivers. Hydrogen can be produced from a variety of plentiful domestic resources with near-zero emissions. It can be utilised with fuel cell-based vehicles (FCVs) to provide emission free transportation.

The US President's *National Energy Policy* and the US Department of Energy's (DOE's) *Strategic Plan* call for expanding the development of diverse domestic energy supplies. Working with industry, the Department developed a national vision [1] for moving toward a hydrogen economy – a solution that holds the potential to provide sustainable, clean, safe, secure, affordable, and reliable energy. In February 2003, President George W. Bush announced a new Hydrogen Fuel Initiative to achieve this vision.

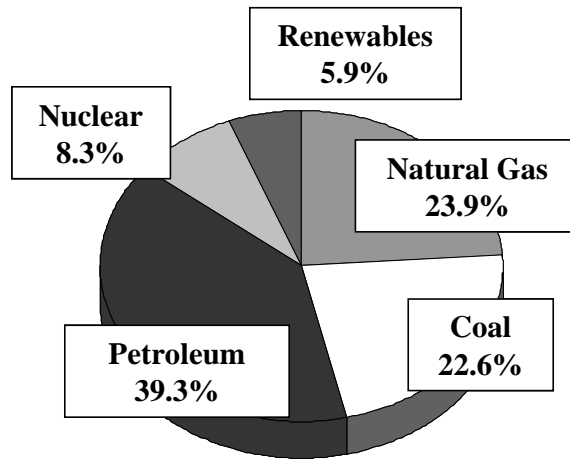
To realise this vision, we must develop and demonstrate advanced technologies for hydrogen production, delivery, storage, conversion, and applications. Toward this end, the DOE has worked with public and private organisations to develop a *National Hydrogen Energy Technology Roadmap* [2]. The Roadmap identifies the technological research, development, and demonstration steps required to make a successful transition to a hydrogen economy.

This spring, Secretary Abraham announced our desire to form an International Partnership for the Hydrogen Economy (IPHE). The US wants to collaborate with major research partners in Japan, the EU and globally in this effort. The US will host the IPHE ministerial meeting in November of this year.

Energy security

Figure 1 shows the sources of energy used in the US petroleum ranks the highest. Figure 2 shows the distribution of energy sources for the major economic sectors. Transportation energy needs are met essentially completely by petroleum. The other sectors use a greater variety of sources for their energy requirements. Figure 3 shows the US petroleum use within the transportation sector along with domestic production. Two-thirds of the 20 million barrels of oil Americans use each day is used for transportation. America imports 55% of the oil it consumes. That is projected to grow to 65% by 2025. This data clearly defines the energy security issue and makes it clear that transportation needs to be the focal point relative to this issue. Replacing petroleum with hydrogen for transportation needs, where the hydrogen is produced from domestic resources, can address this energy security issue.

Figure 1. US energy use [3, 4]



2001 US Energy Use: 97 Quads
Population 284.8 million (July 2001)
341 million Btu/capita

Figure 2. Energy sources for the major economic sectors [5]

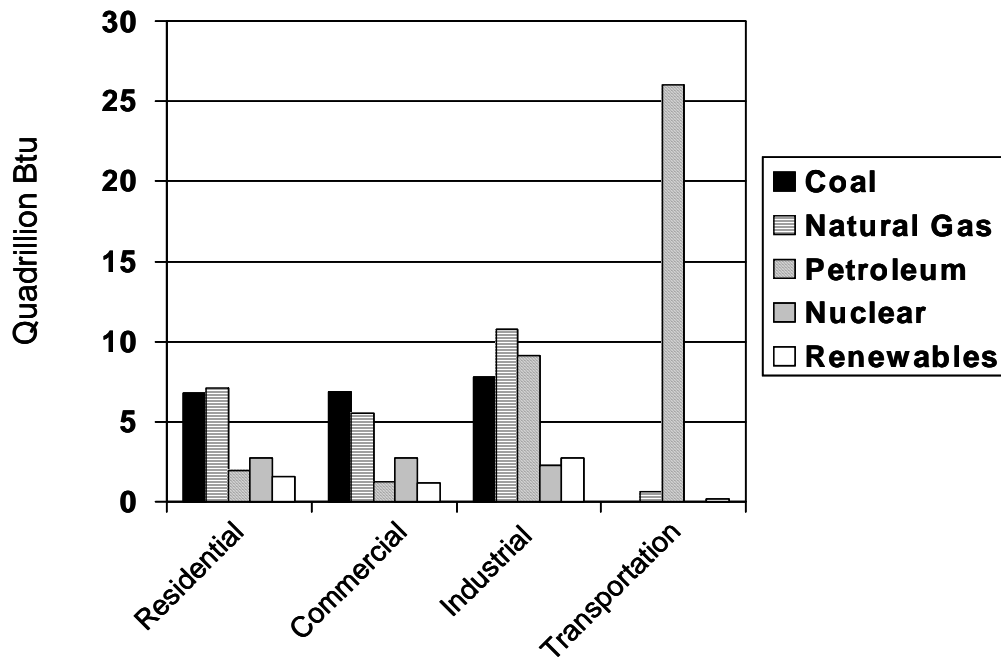
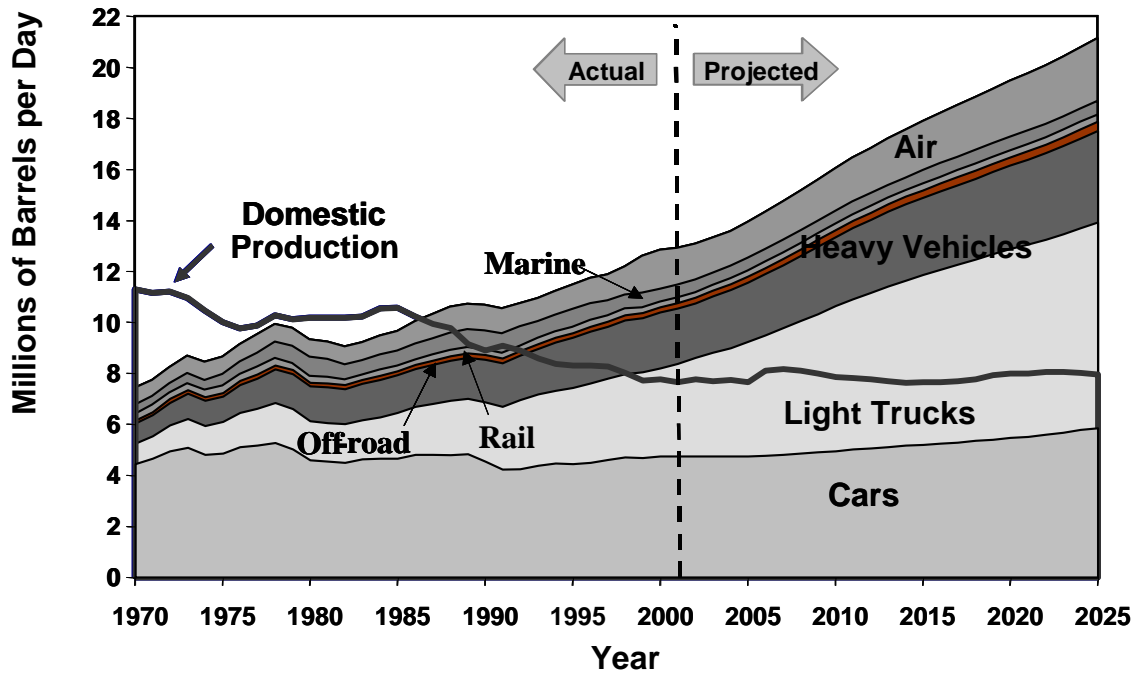


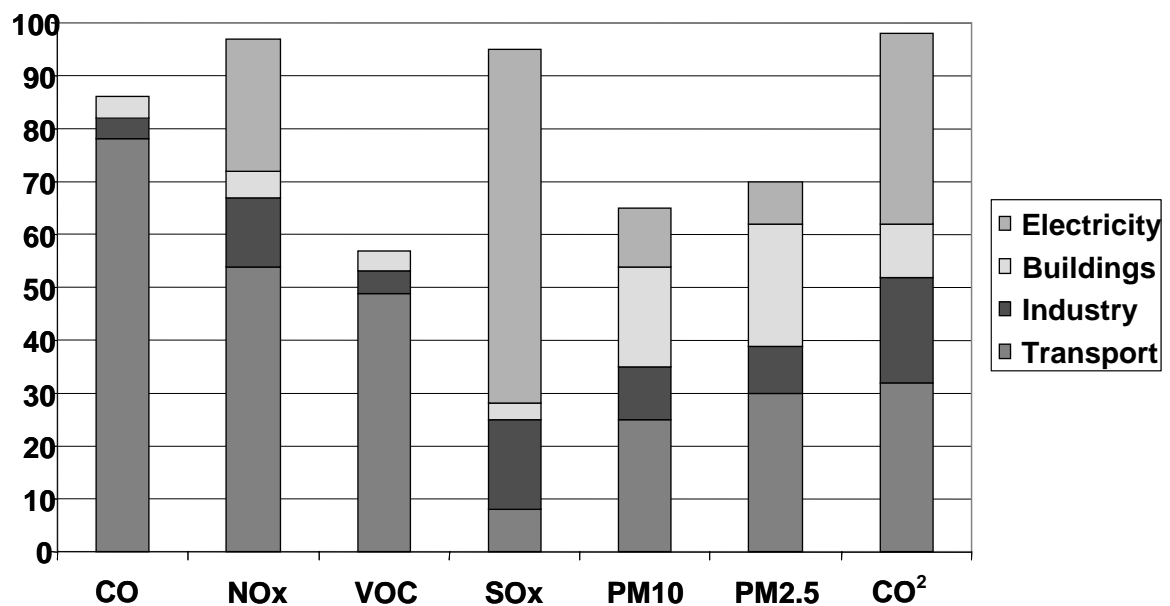
Figure 3. US transportation oil use and production [6, 7]



The environment

Figure 4 shows the major air emissions in the US as a percentage from electricity, buildings, industry and transportation. This data makes it clear that transportation and electricity generation need to be the two focal points relative to climate change concerns and other air emissions. Replacing internal combustion engine vehicles with hydrogen-based FCVs will result in zero harmful emissions from these vehicles. The key is to also produce the hydrogen utilising near-zero emission technology. Air emissions from electricity generation are being addressed through other DOE-sponsored programmes. The use of hydrogen for stationary power can also help in this sector.

Figure 4. US 1998 energy-linked emissions as percentage of total emissions [8]

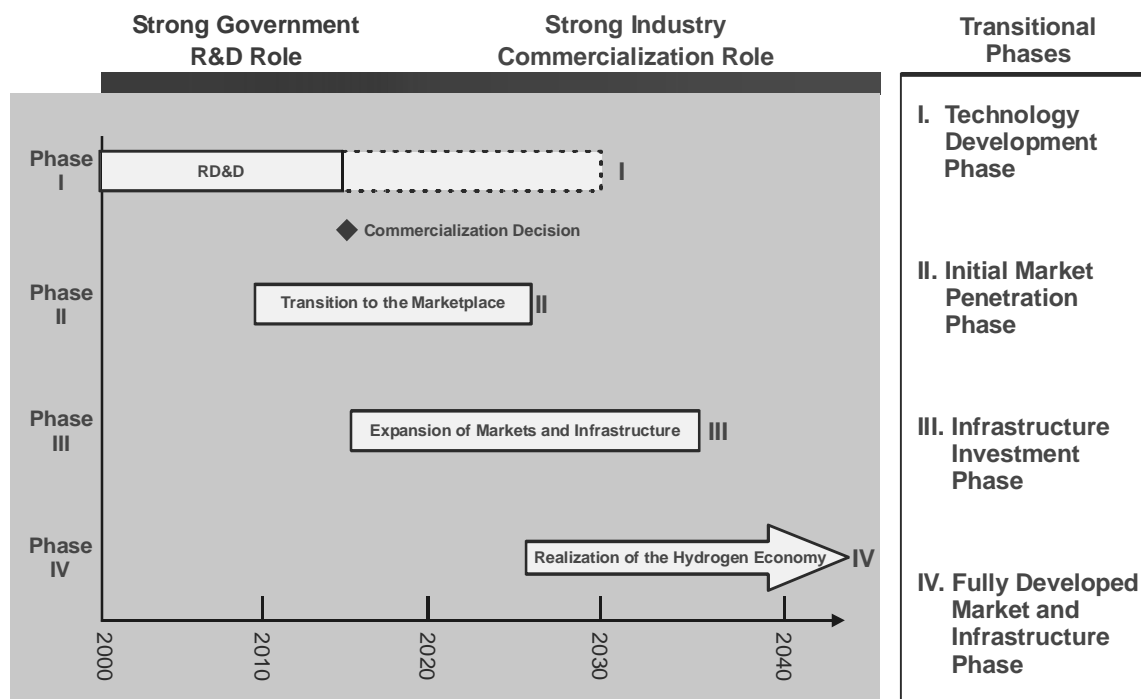


The timeline

Figure 5 shows that a transition to a hydrogen economy will take decades. This is an immense challenge requiring successful high risk research breakthroughs, very large investment in new infrastructure, and a significant change for all of us. The US government has made a firm commitment and will need to play a major role at the outset to help fund the research and to have technologies sufficiently developed and advanced to allow industry to make the decision to proceed to commercialise hydrogen-based FCVs by 2015. The government role will probably not end there. We will likely continue to support R&D advancements just as we are still supporting advancements in today's combustion vehicle technologies such as hybridisation and lighter weight materials.

Fuel cells may start to enter the marketplace before 2015 where the commercial value proposition is high. Portable power is such an application. The first fuel cell powered-cell phones, lap top computers or other such devices may be commercialised as early as 2004 or 2005. Some stationary fuel cell applications may also lead the transportation sector in such applications as back-up emergency power for hospitals or in other high value applications. Mass marketing of hydrogen FCV vehicles is targeted by 2020. Markets and infrastructure will then expand over time. As time proceeds during the transition, the federal role will diminish and industry will take over.

Figure 5. The transition timeline

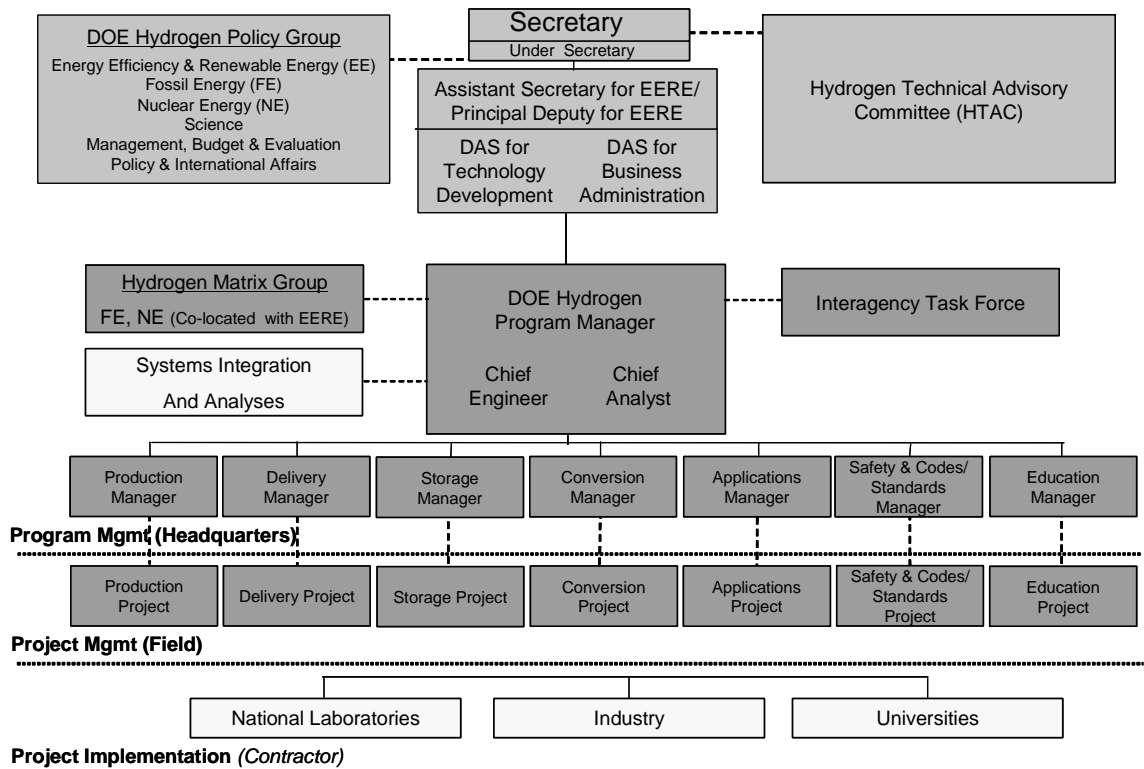


The DOE hydrogen programme organisational structure

Figure 6 shows the proposed DOE organisational structure being put together to help manage this immense challenge. There are a number of Offices within the DOE involved in this effort including; the Office of Hydrogen, Fuel Cells, and Infrastructure Technologies (OHFCIT) within Energy Efficiency and Renewable Energy, Fossil Energy (FE), Nuclear Energy Science and Technology (NE), and the Office of Science (OS). The Secretary of Energy will be counselled by a DOE Hydrogen Policy Group. The programme is supported by an Interagency Task Force, and, when appropriate, externally by the Hydrogen Technical Advisory Committee, the National Academy of Sciences, and stakeholders. The research is conducted through National Laboratories, universities and industry partners selected through competitive solicitations. Most often the project teams are collaborative efforts with industry cost share.

The OHFCIT has the lead DOE coordinating role and has extensive efforts in nearly all aspects of hydrogen and fuel cell development. This includes hydrogen production, hydrogen delivery, storage, fuel cells for transportation and distributed stationary power, safety, codes and standards, education, and technology validation. FE has the responsibility for centralised hydrogen production from coal and natural gas. NE has the responsibility for nuclear energy enabled routes to hydrogen. The Office of Science supports enabling basic research.

Figure 6. Proposed management structure



OHFCIT goals and objectives

Table 1 presents the goals and the key objectives of the various elements of the hydrogen and fuel cell activities in the OHFCIT in DOE. More details can be found in the OHFCIT draft multi-year R&D plan [9]. The overall programme includes all aspects of hydrogen and fuel cell technology development: production, delivery, storage, fuel cells, codes and standards, safety, and education.

Table 1. OHFCIT goals and objectives

Goals	Objectives
<p style="text-align: center;">Production</p> <p>Research and develop low cost, highly efficient hydrogen production technologies from diverse, domestic sources, including fossil, nuclear, and renewable sources.</p>	<ol style="list-style-type: none"> 1. By 2010: Reduce the cost of distributed production of hydrogen from natural gas/or liquid fuels to \$1.50/gallon of gasoline equivalent (\$1.50/kg of hydrogen) delivered, untaxed. 2. Long term, develop renewable based routes to hydrogen at a cost competitive with gasoline.
<p style="text-align: center;">Delivery</p> <p>Develop hydrogen fuel delivery technologies that enable the introduction and long-term viability of hydrogen as an energy carrier.</p>	<ol style="list-style-type: none"> 1. By 2006: Define a cost effective and energy efficient hydrogen fuel delivery infrastructure for the introduction and long-term use of hydrogen for transportation and distributed stationary power. 2. By 2015: develop technologies to reduce the cost of hydrogen delivery from the point of production to the point of use in vehicles or distributed stationary power units to <\$1.00/kg.
<p style="text-align: center;">Storage</p> <p>Develop and demonstrate viable hydrogen storage technologies for transportation and stationary power applications.</p>	<ol style="list-style-type: none"> 1. By 2015: On-board vehicle hydrogen storage systems achieving: 3 kWhr/kg (9 wt%), 2.7 kWhr/L and \$2/kWhr. 2. Develop low cost off-board storage systems
<p style="text-align: center;">Fuel cells</p> <p>Develop and demonstrate fuel cell power system technologies for transportation, distributed stationary, and portable applications</p>	<ol style="list-style-type: none"> 1. By 2010: Develop a 60% efficient, durable, direct hydrogen fuel cell system for transportation at a cost of \$45/kW (including hydrogen storage). 2. By 2010: Develop a distributed generation PEM fuel cell system operating on natural gas or propane that achieves 40% electrical efficiency and 40 000 hr. durability at \$750/kW
<p style="text-align: center;">Codes and standards</p> <p>Facilitate the creation and adoption of model building codes and equipment standards for hydrogen systems in commercial, residential, and transportation applications. Provide technical resources to harmonise the development of international standards.</p>	<ol style="list-style-type: none"> 1. By 2006: Complete the adoption of the ISO standards for hydrogen refuelling and storage. 2. By 2010: Complete US adoption of a global technical regulation for hydrogen fuel cell vehicles.

Table 1. OHFCIT goals and objectives (cont'd)

Goals	Objectives
<p style="text-align: center;">Safety</p> <p>Develop and implement the practices and procedures that will ensure safety in the operation, handling, and use of hydrogen and hydrogen systems for all DOE-funded projects.</p>	<ol style="list-style-type: none"> 1. By 2004: Draft a comprehensive safety plan. 2. By 2010: Publish a handbook of Best management practices for hydrogen safety.
<p style="text-align: center;">Education</p> <p>Educate key audiences about fuel cell and hydrogen systems to facilitate commercialisation and market acceptance of these technologies.</p>	<ol style="list-style-type: none"> 1. By 2010: Achieve a fourfold increase in the number of students and teachers who understand the concept of a hydrogen economy and how it may affect them 2. By 2010: Achieve a fourfold increase and twofold increase in the number of state and local government representatives and large scale end users, respectively, who understand the concept of a hydrogen economy and what it means to them. 3. By 2010: Launch a comprehensive and coordinated public education campaign on the hydrogen economy and fuel cell technology.

Hydrogen production options

Table 2 summarises the multitude of options for the production of hydrogen.

Coal is a resource with abundant supply in the US. There are 5 780 quadrillion Btu [10] (Quads) of recoverable reserves. Various cost estimates indicate current central coal gasification technology could produce hydrogen at a cost of \$0.90-\$1.80/kg at the plant gate. Advanced technology being researched including ion transport membranes for oxygen separation and other membrane technology for hydrogen separation could reduce this cost to potentially \$0.50-\$1.10/kg in the future. To meet climate change concerns, technology to sequester the carbon dioxide evolved must be developed and implemented. The current costs projected for this technology would only add 10-20% to the cost of the hydrogen. The key question is if sequestration approaches will be successfully developed and proven. In addition, the hydrogen still needs to be transported and delivered to its point of use, which could cost under \$1.00/kg to as high as \$10/kg or more depending on the technology used, distance, quantity, and advances in delivery technology.

Natural gas (NG) resource availability is quite different from coal. There are 188 Quads [11] of proven reserves in the US and we are currently importing 15% of our needs. The cost of NG is a significant component of the cost of the hydrogen produced from it. NG costs have seen significant fluctuations over the past several years due to supply and demand and its increasing use as a cleaner energy source. Hydrogen can be produced by reforming NG in large central facilities and in a distributed manner at refuelling stations or distributed stationary power sites. Central reforming of NG

is the lowest cost production option with current technology estimated at \$0.60-1.00/kg at the plant gate and projected advances in technology could reduce this to \$.40-\$.90/kg. Delivery costs need to be added to this. Central production from NG gas would also require carbon sequestration, and the associated costs, to fully address climate change concerns.

Distributed reforming of NG is estimated at \$4.00-\$6.00/kg of hydrogen using current technology and building a single unit. Advances in technology and producing hundreds of units per year could result in cost of \$1.50-\$3.00/kg delivered to a vehicle at a refuelling station. Distributed reforming of NG cannot fully address climate change unless cost effective distributed carbon sequestration technology could be developed, which is highly unlikely. However, distributed reforming of NG in combination with FCVs, can reduce GHG emissions by 60% compared with conventional gasoline internal combustion engine vehicles on a well to wheels (WTW) basis. Due to its relatively low cost and small initial capital cost requirements, this is an excellent option for initial implementation of hydrogen FCVs.

Biomass offers a renewable feedstock source for hydrogen production. Biomass resources include crop residues, forest thinning and pulp and paper residues, energy crops such as switchgrass or short rotation woody crops, MSW, landfill gas, and animal wastes. It is estimated that there is currently 6-10 Quads/year of biomass that could be available beyond current food, feed and other current uses in the US [12]. Furthermore, it is believed that this could be increased significantly with crop advancements through breeding and biotechnology. The use of biomass as a feedstock for hydrogen directly addresses climate change in that the net carbon cycle can be near-zero carbon emissions. To produce hydrogen from biomass in large quantities will require new infrastructure for harvest, collection, transport and storage for biomass. This is an area for focus of the Biomass Programme at DOE in collaboration with the US Department of Agriculture for increased use of biomass for fuels, power and chemicals.

Hydrogen can be produced from biomass utilising a variety of technologies that include both central and distributed production approaches. The most advanced route is central gasification. This technology is much like coal gasification. Cost estimates for current technology range from \$2.00-\$4.00/kg with technology advancements projected to reduce this to \$1.00-\$3.00/kg at the plant gate. Anaerobic fermentation of biomass produces methane that could be reformed to hydrogen. Biogas produced this way is currently being utilised to some degree to produce power at landfill sights. The concept could be refined using digesters and extended to MSW and animal wastes to produce much larger quantities of methane, which could be reformed on-site to hydrogen. There is also the possibility of centralised direct production of hydrogen through fermentation utilising micro organisms grown on sugars or other carbon-based substrates. There are a few organisms known that possess this metabolic pathway but they are very inefficient. Biotechnology advancements might result in an efficient direct fermentation route to hydrogen.

Biomass can be converted to a liquid intermediate that could be transported and delivered to a refuelling station or distributed stationary power facility where it could be reformed to hydrogen. This route trades the cost of potentially more expensive hydrogen delivery for the cost of delivering and reforming a liquid hydrogen carrier. There are several options that fall within this scheme. Biomass can be fermented to ethanol. It can be gasified and converted to methanol, or pyrolysed to bio-oil which similar in nature to diesel fuels. Sugars from biomass can be hydrogenated to liquid polyols, which can also be transported and reformed. An example of the latter is glucose hydrogenated to sorbitol. More thorough analyses of costs, energy efficiencies, and GHG emissions need to be developed for all of these options. They potentially offer a way around the possibly high costs of hydrogen delivery by utilising distributed reforming of a liquid carrier, while addressing the climate change issue since the feedstock is biomass.

Water electrolysis is another attractive route to hydrogen. Water is essentially an unlimited resource though it needs to be of high purity for electrolysis, which could add cost to this production option. Both distributed and central electrolysis are possible options. To address climate change, the electricity would need to be produced from non-GHG emitting power sources. This includes; wind, solar, geothermal, hydroelectric, nuclear and fossil with carbon sequestration. If one were to produce hydrogen with electrolysis utilising the current US grid mix of electricity production for FCVs, the GHG emissions would actually be 22% higher than using conventional gasoline internal combustion vehicle technology on a well to wheel (WTW) basis.

The estimated cost of hydrogen from distributed water electrolysis utilising current technology ranges from \$4.00-\$8.00/kg. Possible advances in technology could reduce this to \$2.50-\$4.50/kg. The final cost will always be very dependent on the cost of electricity. This route is still very attractive in that it avoids hydrogen delivery costs.

Water electrolysis could also be used in large central facilities for hydrogen production. This would require hydrogen delivery but has some potential advantages and synergies. It could enable more efficient use of intermittent renewable energy sources. For example, an intermittent renewable electricity resource such as wind could also be used for hydrogen production and use. During times when a wind turbine has more electricity generating capability than that demanded by the electric power grid, it could be used to produce hydrogen through electrolysis. This hydrogen could then be used in fuel cell vehicles or stored for use in a stationary fuel cell, supplying electricity when electric power demand is at its peak. Similarly, the electric grid might be used more efficiently by utilising its excess capacity during off peak periods to produce hydrogen. High temperature steam electrolysis is potentially more efficient than standard electrolysis. However, it would require larger scale central production. The trade-offs between these potential advantages and the added cost of hydrogen delivery need to be better analyzed.

Direct photolytic water splitting is a longer term option for hydrogen production. This could be done using photosynthetic organisms such as algae or using photo electrochemical methods. Both require major technological breakthroughs. The photosynthetic organism approach is best suited to central production. Direct photo electrochemical production could function as a central production or distributed production approach. It uses sunlight and water and would have nearly no moving parts. If durable and cost effective electrochemical materials are discovered for this route, it is extremely attractive.

Thermochemical water splitting offers yet other production routes to hydrogen. There are chemical cycles such as the I-S cycle [13] or Ca-Br cycle [14] that operates in the temperature range of 500-1000°C that split water and recycle all the chemical intermediates. Such cycles could be driven by relatively low cost high temperature heat from advanced nuclear reactors. There are other such chemical cycles that operate at higher temperatures (1 000-2 500°C) that could be driven by concentrated solar energy. Water will thermochemically split into hydrogen and oxygen on its own at temperatures above 2 500°C but there are no known materials that could be utilised to effect the separation of the two gases at these temperatures. There is research being conducted to explore the use of hydrogen separation membranes to drive this reaction at much lower temperatures despite the thermodynamic limitations. Thermochemical water splitting has the potential of providing an essentially unlimited supply of hydrogen with near-zero GHG emissions, but none of these approaches have yet been proven feasible and practical. Some initial cost estimates suggest they could produce hydrogen cost effectively and new research is being initiated.

Table 2. Hydrogen production options

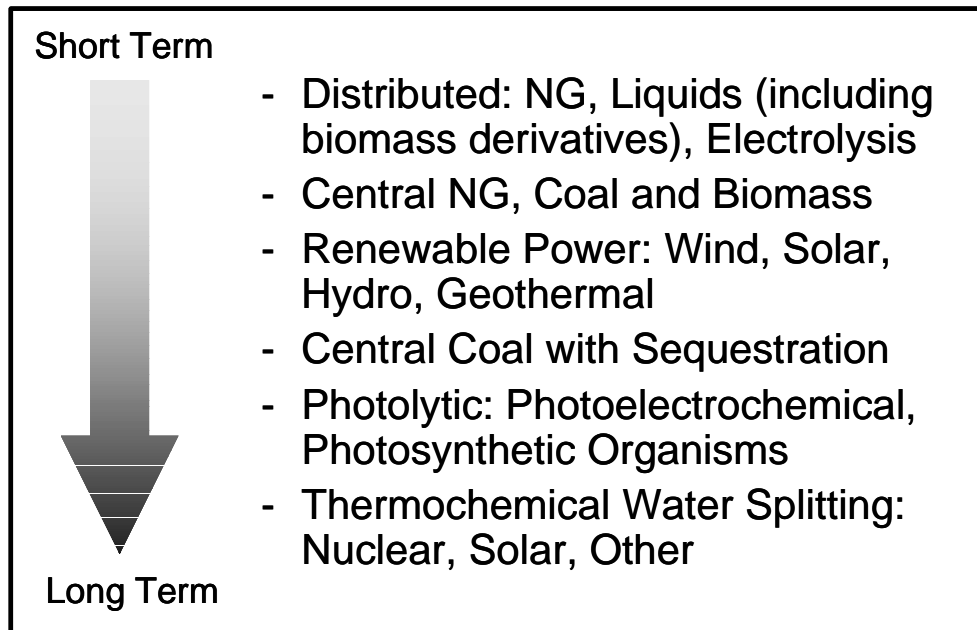
Route	\$/kg Current	\$/kg Projected	%EE WTP [15]	GHG WTW Reduc. [15, 16]
Coal: central gasification	\$0.90-1.80 [17, 18]	\$0.50-1.10 [19]	–	High w/Sequest.
Coal: C/D gasification/reforming	–	–	–	Low-medium
NG: central reforming	\$0.60-1.00 [20, 21]	\$0.40-0.90 [22]	62%	61%
NG: distributed reforming	\$4.00-6.00 [23, 24]	\$1.50-3.00 [25]	60%	High
Biomass: central gasification	\$2.00-4.00 [26]	\$1.00-3.00 [27, 28]	–	High
Biomass: central fermentation	–	–	–	High
Biomass: central fermentation /Methane/Hydrogen	–	–	–	High
Biomass: C/D gasification/methanol or ethanol/hydrogen	–	–	–	High
Biomass: C/D pyrolysis	–	–	–	High
Biomass: C/D fermentation /ethanol/hydrogen	–	<\$3.00	41% Total 92% Fossil	98%
Biomass: C/D sugar hydrogenation/polyols/hydrogen	–	–	–	High
Water: electrolysis: distributed	\$4.00-8.00 [29, 30]	\$2.50-4.50 [31]	28% Grid 68% Renew.	(22%) Grid ~100% Renew.
Water: electrolysis: central	–	–	–	Low: Grid High: Renew.
Water: central photolytic: organisms (e.g., algae)	~\$200	<\$5.00 [32]	–	High
Water: central or distributed photolytic: photo electrochemical	–	<\$3.00 [33]	–	High
Water: central HT splitting chemical cycles	–	<\$2.00 [34]	–	High
Water: central U-HT splitting chemical cycles	–	–	–	High
Water: direct water splitting	–	–	–	High

The path forward

There are many possible scenarios for the production of hydrogen over the short, medium and long term as we drive towards the hydrogen economy. Much will depend on the success and the rate of success of the research now or soon to be underway supported by the DOE and stakeholders. As stated earlier, one of the very attractive features of hydrogen is that it can be produced from a variety of feed stocks with a variety of process technologies, most of which can result in near-zero GHG emissions. Not all of the options discussed will be successful developed to produce hydrogen cost effectively. Some will be developed before others. Efforts on some methods will be terminated in favour of others.

Figure 7 suggests a possible manner in which the technologies discussed might emerge over time. Many factors including the rate of technology development will dictate the final outcome. The DOE is committed to developing a portfolio of cost effective technology options that meet the key drivers for hydrogen.

Figure 7. Potential hydrogen production commercialisation scenarios



REFERENCES

- [1] *A National Vision of America's Transition to A hydrogen Economy-To 2030 and Beyond*; www.eere.doe.gov/hydrogenandfuelcells
- [2] *National Hydrogen Energy Roadmap*; www.eere.doe.gov/hydrogenandfuelcells
- [3] Annual Energy Review, US Department of Energy, Energy Information Administration, 2001.
- [4] National Population Estimates, US Census Bureau, 2001.
- [5] Annual Energy Review, US Department of Energy, Energy Information Administration, 2001.
- [6] Transportation Energy Data Book: Edition 22, September 2002.
- [7] EIA Annual Energy Outlook 2003, January 2003.
- [8] National Air Pollutant Emissions Trends: 1900-1998, US Environmental Protection Agency, March 2000, <http://www.epa.gov/ttn/chief/trends/trends98/index.html>.
- [9] US Department of Energy, Office of Hydrogen, Fuel Cells, and Infrastructure Technologies, www.eere.energy.gov/hydrogenandfuelcells
- [10] US Coal Reserves: 1997 Update, US Department of Energy, Energy Information Administration, February 1999, <http://www.eia.doe.gov/cneaf/coal/reserves/front-1.html>.
- [11] US Crude Oil, Natural Gas, and Natural Gas Liquids Reserves 2001 Annual Report, U.S. Department of Energy, Energy Information Administration, November 2002, http://www.eia.doe.gov/oil_gas/natural_gas/data_publications/crude_oil_natural_gas_reserves/cr.html
- [12] *Aggressive Growth in the Use of Bioderived Energy and Products in the United States by 2010*, Final Report, A.D. Little, Inc. Reference No. 71038, October 2001.
- [13] <http://web.gat.com/pubs-ext/AnnSemiannETC/A23451.pdf>
- [14] <http://web.gat.com/pubs-ext/AnnSemiannETC/A23451.pdf>
- [15] The estimates, except for the distributed water electrolysis case using renewable electricity, are from "Guidance for Transportation Technologies: Fuel Choice for Fuel Cell Vehicles", Final Report prepared by Arthur D. Little for US Department of Energy, February 6, 2002, <http://www-db.research.anl.gov/db1/cartech/document/DDD/192.pdf>. The distributed water electrolysis estimates are from Wang, M., "Fuel Choices for Fuel-Cell Vehicles: Well-to-Wheels Energy and Emissions Impacts", *Journal of Power Sources*, **112(1)**: 307-321, October 2002.
- [16] GHG well-to-wheels reduction is the reduction of GHG emissions as compared to the emissions from standard/today's gasoline ICE.
- [17] Gray, D., Tomlinson, G. "Hydrogen from Coal", Mitretek Technical Paper, No. 2002-31, 2002.

- [18] Simbeck, D.R., and E. Chang. "Hydrogen Supply: Cost Estimate for Hydrogen Pathways – Scoping Analysis", SFA Pacific, Inc., NREL/SR-540-32525, Subcontractor Report, July 2002.
- [19] "Fossil Fuel Processing Plants for Hydrogen Production", presentation at Fossil Fuel Production and Delivery Analysis Subgroup Meeting, Parsons Infrastructure and Technology Group, March 2003.
- [20] Hydrogen Production Facilities Plant Performance and Cost Comparisons, Parsons Infrastructure and Technology Group, Final Report, March 2002.
- [21] Simbeck, D.R., and E. Chang. "Hydrogen Supply: Cost Estimate for Hydrogen Pathways – Scoping Analysis", SFA Pacific, Inc., NREL/SR-540-32525, Subcontractor Report, July 2002.
- [22] Hydrogen Production Facilities Plant Performance and Cost Comparisons, Parsons Infrastructure and Technology Group, Final Report, March 2002.
- [23] Simbeck, D.R., and E. Chang. "Hydrogen Supply Cost Estimate for Hydrogen Pathways – Scoping Analysis", SFA Pacific, Inc., NREL/SR-540-32525, Subcontractor Report, July 2002.
- [24] Ogden, J., *et al.* "Hydrogen Energy Systems Studies", Proceedings of the 1996 US DOE Hydrogen Program Review, Volume 1.
- [25] Mintz, M., *et al.* "Hydrogen: On the Horizon or Just a Mirage?", presented at Future Car Congress, June 2002, Doc. No. 2002-01-1927, <http://www.sae.org>
- [26] Simbeck, D.R., and E. Chang. "Hydrogen Supply: Cost Estimate for Hydrogen Pathways – Scoping Analysis", SFA Pacific, Inc., NREL/SR-540-32525, Subcontractor Report, July 2002.
- [27] Larson, E.D., Katofsky, R.E. "Production of Methanol and Hydrogen from Biomass", The Center for Energy and Environmental Studies, Princeton University, PU/CEES Report No. 217, July 1992.
- [28] Mann, M.K. "Technical and Economic Assessment of Producing Hydrogen by Reforming Syngas from the Battelle Indirectly Heated Biomass Gasifier", NREL/TP-431-8143, 1995.
- [29] Simbeck, D.R., and E. Chang. "Hydrogen Supply: Cost Estimate for Hydrogen Pathways – Scoping Analysis", SFA Pacific, Inc., NREL/SR-540-32525, Subcontractor Report, July 2002.
- [30] Ogden, J., *et al.* "Hydrogen Energy Systems Studies", Proceedings of the 1996 US DOE Hydrogen Program Review, Volume 1.
- [31] Ogden, J., *et al.* "Hydrogen Energy Systems Studies", Proceedings of the 1996 US DOE Hydrogen Program Review, Volume 1.
- [32] Benemann, J.R., Consultant, Process Analysis and Economics of Biophotolysis of Water, IEA Report, March 1998.
- [33] Gray, D., Tomlinson, G. "Hydrogen from Coal," Mitretek Technical Paper, No. 2002-31, 2002.
- [34] *High Temperature Gas-Cooled Reactors for the Production of Hydrogen: An Assessment in Support of the Hydrogen Economy*, EPRI, Palo Alto, CA. Report No. 1007802, 2003.

**THE US DEPARTMENT OF ENERGY'S RESEARCH AND DEVELOPMENT PLANS FOR
THE USE OF NUCLEAR ENERGY FOR HYDROGEN PRODUCTION**

A.D. Henderson

US Department of Energy
Office of Nuclear Energy, Science and Technology
Germantown, MD, USA

P.S. Pickard

Sandia National Laboratories
Albuquerque, NM, USA

C.V. Park

Idaho National Engineering and Environmental Laboratory
Idaho Falls, ID, USA

J.F. Kotek

US Department of Energy, Idaho Operations Office
Idaho Falls, ID, USA

Abstract

The potential of hydrogen as a transportation fuel and for stationary power applications has generated significant interest in the United States. President George W. Bush has set the transition to a “hydrogen economy” as one of the Administration’s highest priorities. A key element of an environmentally-conscious transition to hydrogen is the development of hydrogen production technologies that do not emit greenhouse gases or other air pollutants. The Administration is investing in the development of several technologies, including hydrogen production through the use of renewable fuels, fossil fuels with carbon sequestration, and nuclear energy. The US Department of Energy’s Office of Nuclear Energy, Science and Technology initiated the Nuclear Hydrogen Initiative to develop hydrogen production cycles that use nuclear energy.

The Nuclear Hydrogen Initiative has completed a *Nuclear Hydrogen R&D Plan* to identify candidate technologies, assess their viability, and define the R&D required to enable the demonstration of nuclear hydrogen production by 2016. This paper gives a brief overview of the Nuclear Hydrogen Initiative, describes the purposes of *the Nuclear Hydrogen R&D Plan*, explains the methodology followed to prepare the plan, presents the results, and discusses the path forward for the US programme to develop technologies which use nuclear energy to produce hydrogen.

Introduction

Clean forms of energy are needed to support sustainable global economic growth while mitigating greenhouse gas emissions and impacts on air quality. To address these challenges, the President's National Energy Policy and the US Department of Energy's (DOE's) Strategic Plan call for expanding the development of diverse domestic energy supplies. Working with industry, the Department developed a national vision for moving toward a hydrogen economy – a solution that holds the potential to provide sustainable, clean, safe, secure, affordable, and reliable energy. To realise this vision, President George W. Bush announced a new Hydrogen Fuel Initiative in February 2003.

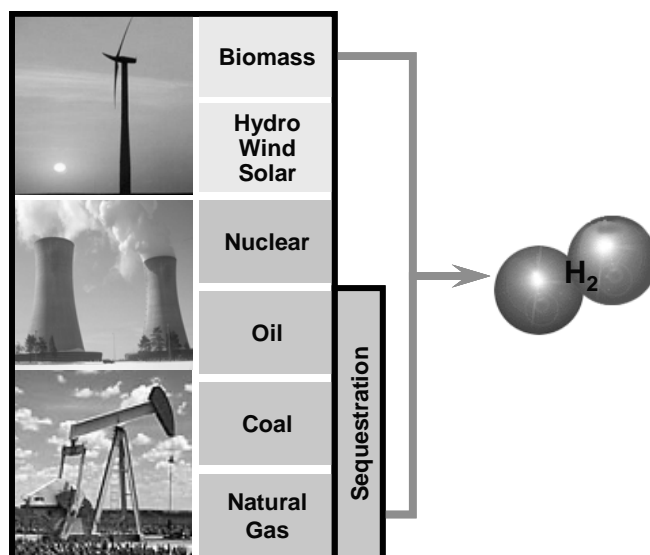
As part of the Hydrogen Fuel Initiative, the DOE has initiated the Nuclear Hydrogen Initiative to develop hydrogen production technologies for use with nuclear energy systems. This programme will develop these systems from the current laboratory-scale research and development to an engineering-scale system driven by nuclear heat by 2016. The *Nuclear Hydrogen R&D Plan* has been developed to guide this new programme and will be released early in Fiscal Year 2004.

Why nuclear?

Domestic energy sources that do not generate greenhouse gases and have the potential to produce hydrogen at costs competitive with gasoline will be essential components of the long-term energy supply. The DOE hydrogen programme is investigating the potential for all of the practical energy sources for hydrogen production, including:

- Fossil sources with carbon sequestration (coal and natural gas).
- Renewable energy sources (biomass, solar, geothermal, wind, and hydroelectric).
- Nuclear energy.

Figure 1. Primary energy sources for hydrogen production

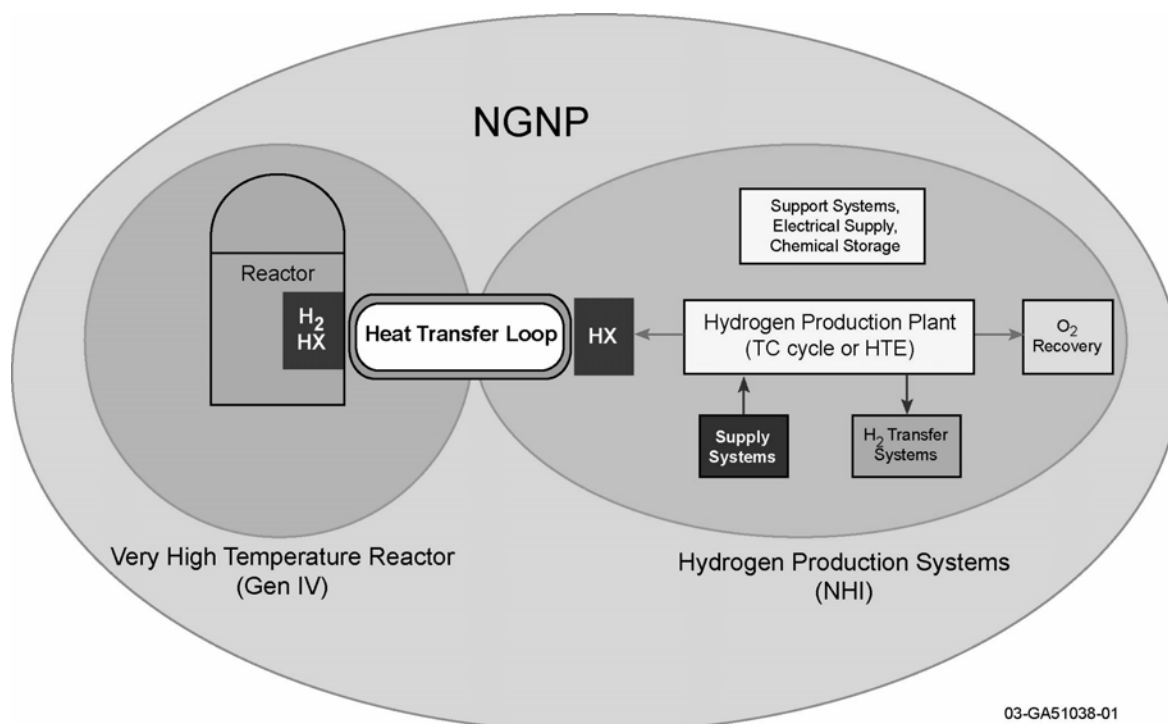


In the long term, economics and policy will determine the mix of energy sources that are implemented, and the technologies initially implemented may differ from those ultimately selected for long-term deployment. In any scenario, domestically-based, emission-free energy sources are the choices for long-term development.

Among these primary energy sources, nuclear energy offers great potential for the large-scale production of hydrogen that is virtually emission-free and based primarily on domestic resources. The production of hydrogen represents a new mission for nuclear energy that is potentially larger than the current mission of emission-free electrical production.

The DOE Office of Nuclear Energy, Science and Technology (NE) has initiated the next-generation nuclear plant (NGNP) project to demonstrate the commercial potential of hydrogen from nuclear energy and to provide a basis for industry investment decisions. The NGNP project will demonstrate the very-high-temperature reactor (VHTR) as a part of the Generation IV Nuclear Energy Systems Initiative in addition to the hydrogen production processes being developed in the Nuclear Hydrogen Initiative (NHI). DOE has set a goal to demonstrate nuclear hydrogen production through the NGNP project by 2016. The NHI and Generation IV programme together provide the capabilities for emission-free transportation fuels from nuclear energy.

Figure 2. The next-generation nuclear plant combines the very-high-temperature reactor with a hydrogen production process



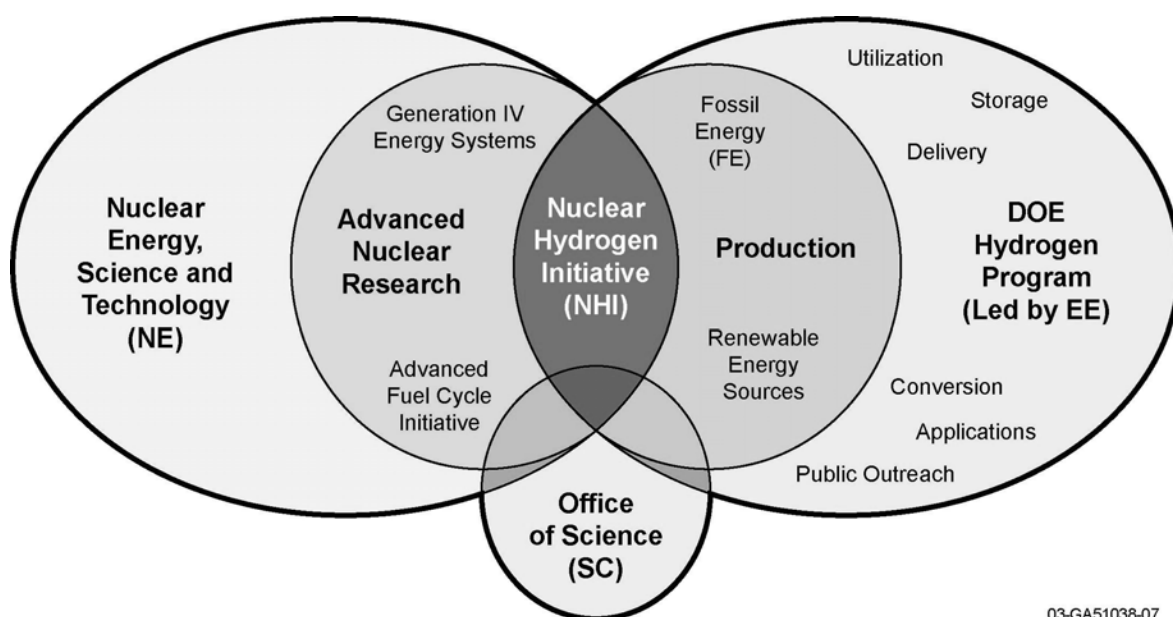
For hydrogen production from nuclear energy to be sustainable, we must also address the technology and policy questions that have limited nuclear energy's contribution to the energy supply. Advanced reactor systems that are safer and more efficient than current reactors, proliferation-resistant, and demonstrably cost effective are essential to the wider public acceptance of the nuclear role. We must also take advantage of more efficient fuel cycles that minimise waste volumes, toxicity, and proliferation concerns. The DOE Advanced Fuel Cycle Initiative (AFCI) has initiated development of advanced fuel, separations, and transmutation technologies to address these issues.

The Nuclear Hydrogen Initiative

The NHI is a new programme in Fiscal Year (FY) 2004 which will develop the necessary technology and demonstrate hydrogen production using nuclear energy through the NGNP project. Although there are already significant quantities of hydrogen produced in the United States, it is primarily produced by steam reforming of natural gas, which is already a high-quality fuel. This reforming of one high-quality fuel to another is economically justified because of the value of hydrogen to the petrochemical industry for use in refining lower-grade crude oil to produce gasoline, and to the agricultural industry for use in fertilizer production.

The NHI will focus on developing efficient production processes for use with advanced high-temperature reactors. The technology being developed for the NHI is also relevant to hydrogen production research being performed by the Offices of Energy Efficiency and Renewable Energy (EE), Fossil Energy (FE), and Science (SC). The NHI research activities on hydrogen production processes for the nuclear option will be closely coordinated with other parts of the overall DOE hydrogen programme. The NHI will collaborate, augment, or complement ongoing DOE research efforts, where appropriate, or initiate needed R&D in nuclear specific areas to accomplish NHI programme goals.

Figure 3. Relationship of the Nuclear Hydrogen Initiative to other DOE programmes

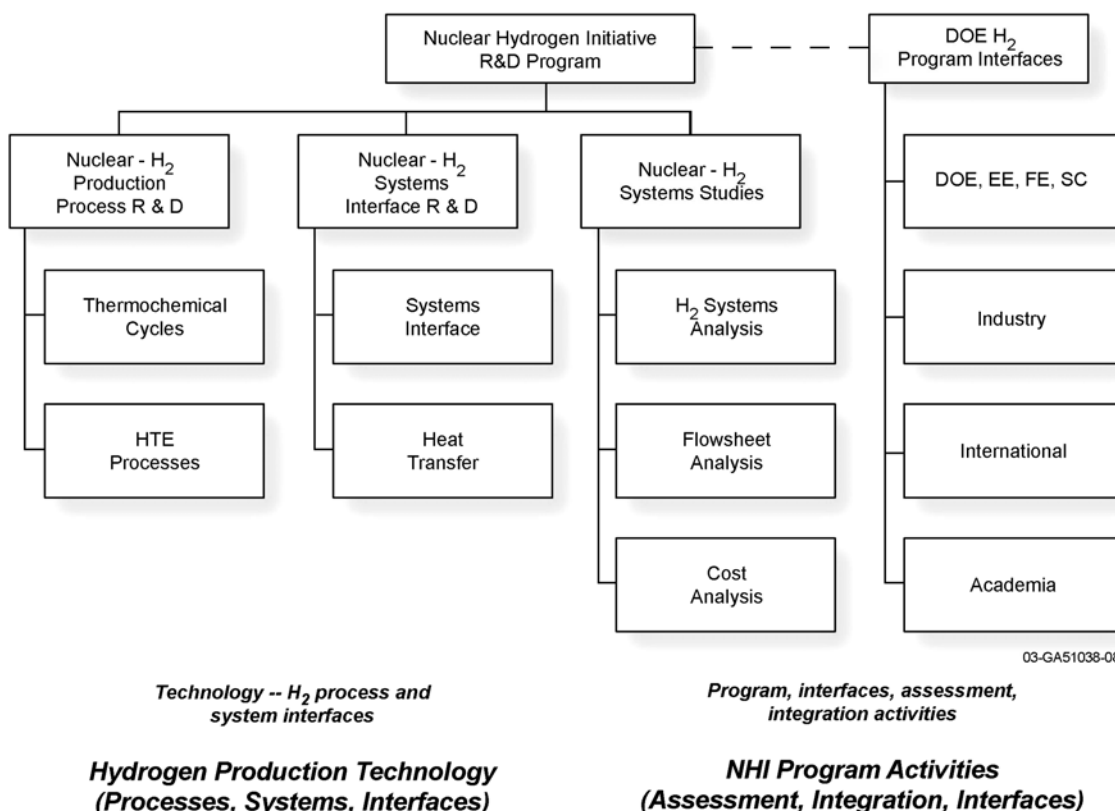


03-GA51038-07

Fossil fuel production options based on coal, such as coal gasification, and the necessary carbon sequestration technologies are being developed by other parts of the DOE hydrogen programme. Although nuclear energy can be used instead of fossil fuel as the heat source in a reforming or gasification process, greenhouse gases are still generated, significantly reducing the environmental benefit of using emission-free nuclear heat. The most attractive hydrogen production options for nuclear energy are those that utilise high-temperature heat or efficient electricity from a high-temperature reactor to produce hydrogen from water.

To successfully demonstrate nuclear hydrogen production by 2016, the NHI will perform research on hydrogen production processes and system interfaces to ensure that production processes efficiently couple to advanced high-temperature reactors. The NHI will also require independent analysis capabilities and programmatic interfaces to support the assessment and evaluation of technology options and scaling decisions, and effective interfaces with other US and international hydrogen research to assure effective collaboration and integration. The selection of chemical processes to produce a hydrogen product includes both technical and commercial factors and should have strong chemical and nuclear industry components.

Figure 4. Nuclear Hydrogen Initiative programmatic and technology development elements



Technology assessment

Although research is being conducted elsewhere on techniques to reduce the temperature required for thermolysis (direct splitting of water using thermal energy) and other possible production approaches, the most promising methods using nuclear energy are based on electrolytic or thermochemical processes. To identify the most promising hydrogen production options, available information on thermochemical cycles, high-temperature electrolysis, and other possible production methods was reviewed, and limited confirmatory analyses were performed. Processes were evaluated using general evaluation criteria based on performance potential and demonstrated technical viability. These criteria are also part of the ongoing systematic re-evaluation of process potential based on R&D results.

Since all nuclear hydrogen production approaches being considered in the NHI avoid the production of greenhouse gases and utilise domestic resources, the primary issue for nuclear hydrogen is the development of systems that produce hydrogen at a cost that is competitive with gasoline. Projecting costs for technologies at this early stage of development is highly uncertain for any of the approaches being considered. The criteria used to evaluate the benefits of the various hydrogen production methods to meet these cost objectives include the system and performance characteristics that drive costs, and the uncertainty of the projected costs.

- *Costs* – Capital costs are considered the dominant component of nuclear hydrogen costs. The most direct indicator of process costs is process efficiency since higher efficiency processes leverage both hydrogen and nuclear plant capital costs. Processes with potential for efficiencies in the range of 50% were considered promising. Other factors considered as cost indicators were process complexity (number of reactions, separations), materials (high-temperature compatibility requirements, corrosion, toxicity), level of industrial safety concern, and operational modes and flexibility.
- *Uncertainty/risk* – Assessing the probability that a particular hydrogen production option will meet expectations for performance and cost involves significant uncertainty at this stage of development. Processes demonstrated at a laboratory-scale allow more reliable estimates of performance and cost. Promising processes that have not been demonstrated may still deserve further evaluation, but not as a near-term priority until additional confirmatory analyses are available. To be considered as a baseline process, all individual chemical reactions or physical process steps should have been demonstrated in laboratory experiments.

Implementation strategy

Performance and viability information on candidate hydrogen production processes will be needed by 2007 to provide the basis for pilot plant decisions. Integrated laboratory-scale experiments on those cycles under consideration must be sufficiently complete by that time to assess performance and cost implications. To ensure that the necessary information is available for critical scale-up decisions, it is essential to establish a prioritisation process that ensures that information on the high-priority processes is available for this decision, while not overlooking potentially higher performance alternatives. The NHI will pursue a two-tiered approach as described below.

Processes identified as having the highest probability of achieving programme goals in the planned schedule and budget will have the highest priority. The goal of the R&D for these “baseline” processes will be to complete an integrated, laboratory-scale experiment by 2007 to provide a basis for pilot plant process selection. Initial process priorities will be systematically re-evaluated as R&D

progresses. At the same time, however, it is recognised that “alternative” processes, those posing higher risk but with potentially higher gain, should also be evaluated further to ensure that potentially important options are not overlooked. These analyses will be lower priority but in parallel with baseline process development. This demonstration strategy is designed to ensure that the 2016 objective is fully supported while minimising risk and allowing flexibility by exploring potentially more efficient, yet currently immature, processes.

Baseline processes

Two families of thermochemical processes, sulphur cycles and calcium-bromine cycles, were identified as baseline methods. These processes have potential for high efficiencies (~50%), have process steps that have been demonstrated to show feasibility, and can be developed by 2016. High-temperature electrolysis was also identified as a baseline process. Cost uncertainties remain, but preliminary projections were available to support the potential for making hydrogen at a cost competitive with gasoline.

Alternative processes

In addition to the baseline processes which have been developed and demonstrated at some small scale, several other thermochemical cycles show significant promise, but are not sufficiently mature to proceed at the same scale of development. These cycles, which include various copper and iron cycles, require a consistent, systematic evaluation to verify their performance potential before any laboratory-scale R&D is conducted.

Three-phased scaling approach

In order to move from the current status of the production technologies to a suitable scale to demonstrate their commercial viability, a three-phased scaling approach will be taken. Baseline processes will be demonstrated on a laboratory, pilot, and engineering scale. However, if an alternative process proves to have higher performance than the baseline processes, there are opportunities to integrate that process into the scaling sequence as shown in Figure 6.

Initially, the process feasibility will be proven at a laboratory scale. At this scale, the chemical reactions are demonstrated to be viable and to work as anticipated, and the first experimental validation of process performance and cost are obtained. Then the process will be demonstrated on a pilot plant scale (500 kilowatts to 1 megawatt) to confirm the engineering approach and system performance. This experimental stage provides a decision basis for the final, engineering-scale demonstration.

Figure 5. Sulphur-based thermochemical cycles

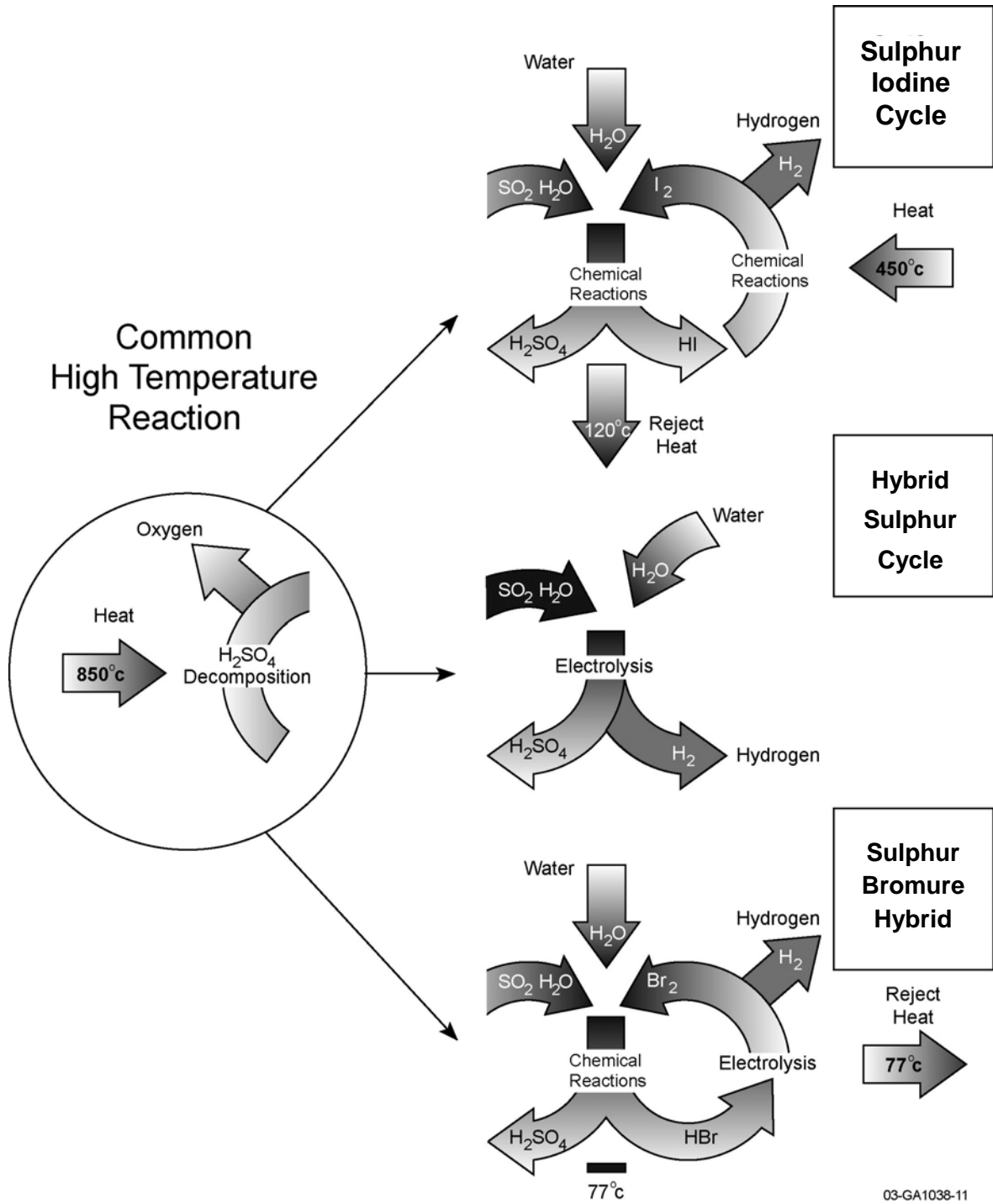
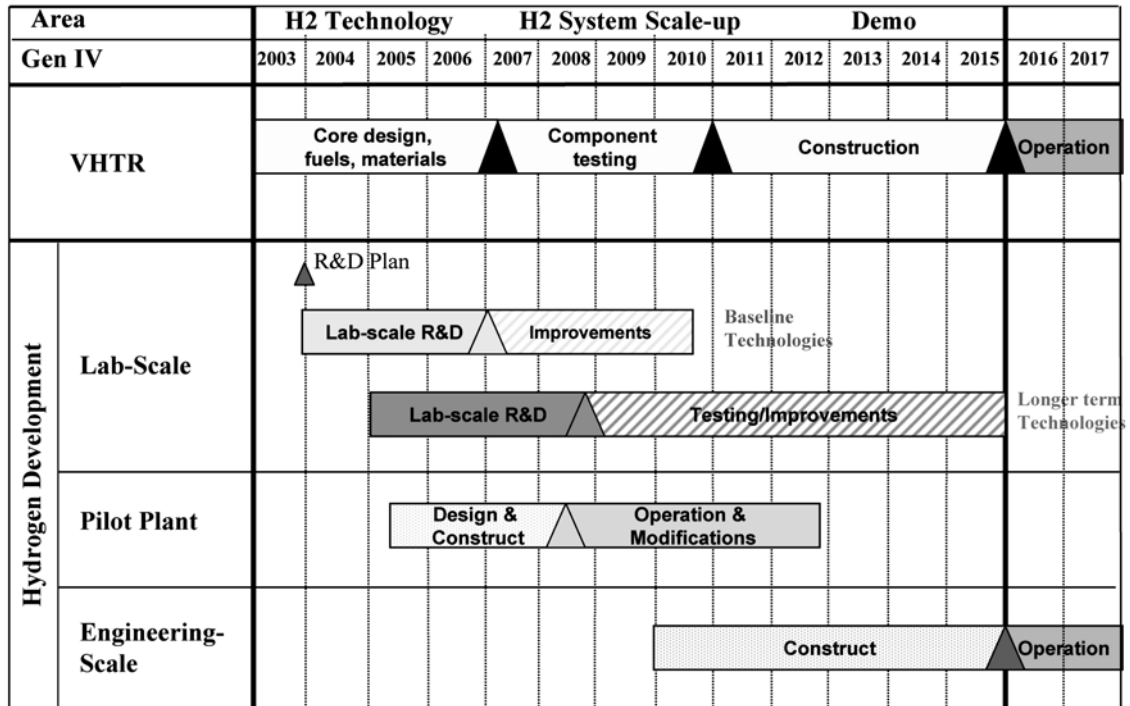


Figure 6. Three-phased scaling approach of Nuclear Hydrogen Initiative



The engineering-scale demonstration will be sufficiently large to confirm the economics and commercial viability of the process. The required scale varies with the production process; the modular nature of a high-temperature electrolysis system allows a smaller scale of demonstration than a more complex thermochemical cycle. This engineering-scale demonstration will be the first demonstration driven by nuclear heat, provided by the NGNP. This demonstration will provide sufficient information to allow an industry decision to deploy the process commercially. To meet this requirement, chemical and nuclear industry involvement will be necessary throughout the three demonstration phases.

International collaboration

In addition to the significant resources that the United States has committed to the transition to a hydrogen economy, several other nations are making similar efforts, specifically in the use of nuclear reactors for hydrogen production. It is recognised that collaborating and leveraging resources will best use limited funding.

The DOE has collaborated with France for the last year through the International Nuclear Energy Research Initiative (I-NERI) on the sulphur-iodine thermochemical process, and other countries have also expressed interest in such collaboration. Some countries have an existing

knowledgebase, while others are interested in beginning an R&D programme. Both groups will be important to the successful development of a nuclear-driven hydrogen production capability.

Conclusion

The NHI has defined the initial path to demonstrate hydrogen production from nuclear energy by 2016. The technical challenges to achieving this goal are significant, but the development of emission-free hydrogen production technologies is essential to the long-term viability of a hydrogen economy. Nuclear energy has the potential to play a major role in assuring a secure and environmentally sound source of transportation fuels. The fundamental challenge is to focus finite research resources on those processes, which have the highest probability of producing hydrogen at costs that are competitive with gasoline. Both thermochemical and high-temperature electrolysis methods were identified that have the potential to achieve this objective.

Initially, a broader research effort involving laboratory-scale demonstrations and analytical evaluations are needed to provide a more consistent and complete assessment on which to base future R&D funding and scaling decisions. Integrated laboratory experiments confirm technical viability, and provide information needed for pilot plant decisions. Pilot plant demonstrations of the selected processes confirm engineering viability and establish a basis for process costs, needed for the selection of production processes for the NGNP. The NHI programme will perform consistent and independent analyses of performance and costs to support the comparative assessments required for technology selection and scaling decisions and establish effective interfaces with industry and international partners. The development of a portfolio of hydrogen production technologies, including nuclear energy technologies, is vital to strengthen the United States' energy, economic, and national security.

SESSION II

GENERAL COMMENTS ABOUT THE EFFICIENCY OF THE IODINE-SULPHUR CYCLE COUPLED TO A HIGH TEMPERATURE GAS-COOLED REACTOR

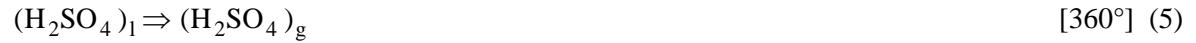
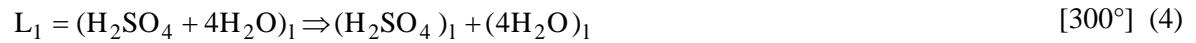
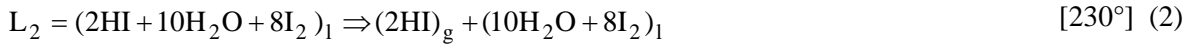
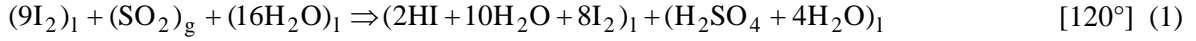
S. Goldstein – X. Vitart – J.M. Borgard
CEA/DEN/DPC-CEN Saclay, 91191 Gif-sur-Yvette

Abstract

Several theoretical papers deal with the efficiency of the thermochemical cycles. In 1966, Funk and Reinstrom established the conditions to fulfill in order that no work is required by the cycle. They investigated a cycle comprised of two reactions and concluded that it was not feasible. In 1974, Abraham and Schreiner found that a minimum of three reactions were required if the maximum temperature is lower than 1 000 °K, and proposed the entropy vs. temperature diagram analysis to evaluate the thermochemical cycles. Finally, in 1975 Estève, Lecoanet and Roncato presented a simplified method to estimate the efficiency of a cycle. Each endothermic reaction is assumed to be achieved at a constant temperature for which $\Delta G=0$. This enables a calculation of the thermal irreversibility due to the exchanges of heat with the intermediate circuit of the reactor. Until now, none of these theories have been applied to the well known Iodine Sulphur (I-S) cycle. The objective of the paper is to put in evidence the conclusions that can be drawn from the application of these theoretical results to the I-S cycle, and in particular what efficiency bounds one can reasonably expect.

I. Introduction

Among the large scale, cost effective and environmentally attractive hydrogen production processes, sulphur iodine (I-S) thermochemical cycle [1] seems to be a quite promising one. This cycle was originally studied in the 80's by General Atomics Co. [2] (GA) and can be split into the following reactions:



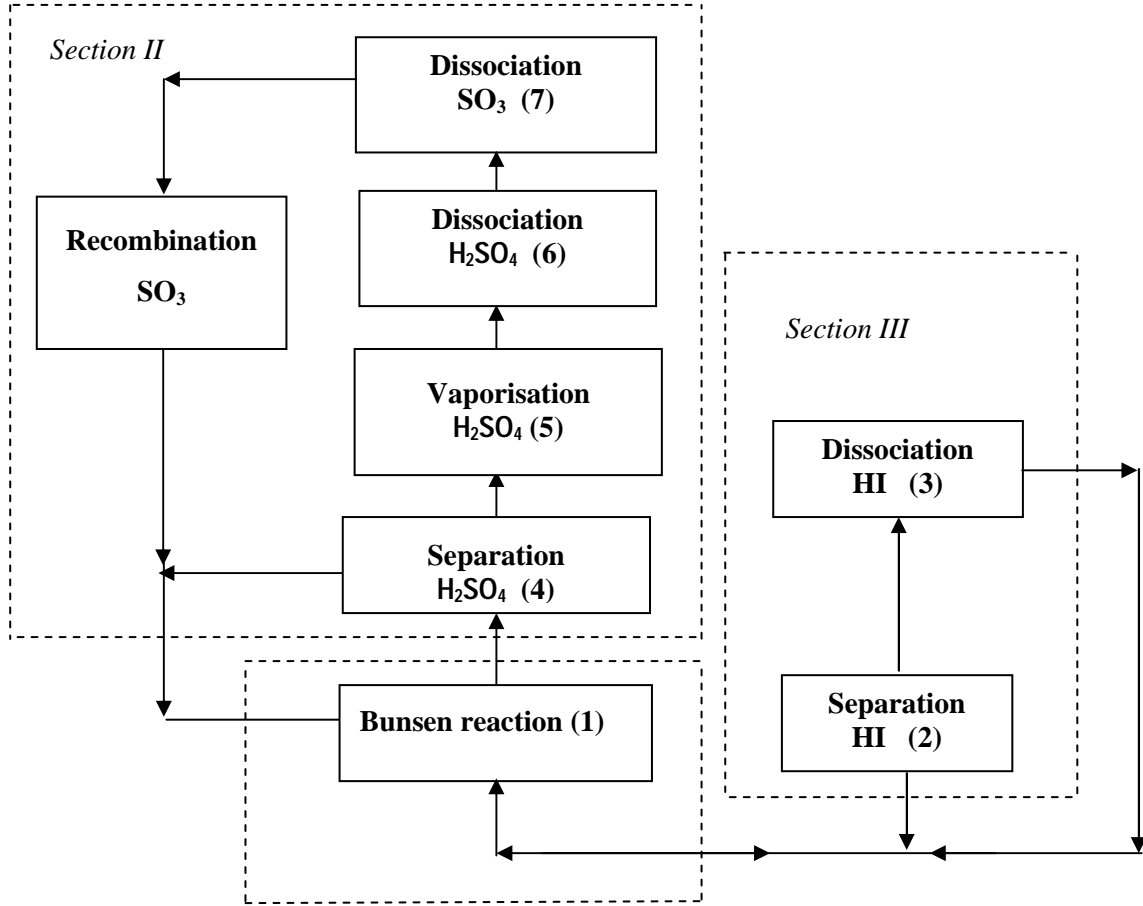
The temperatures between brackets are approximate and depend upon the pressure which is not necessarily uniform in the different parts of the cycle.

The first reaction, called Bunsen reaction, proceeds exothermically in liquid phase and produces two immiscible aqueous acid phases which compositions are indicated between brackets: L_1 phase which is aqueous sulphuric acid and L_2 phase which is a mixture of hydrogen iodide, iodine and water named HI_x . In the second reaction, HI is separated from L_2 . This separation is the most critical phase of the cycle. Several separation processes have been proposed but today, none is demonstrated and much remains to do. Reaction (3) is the thermal decomposition of HI. Knoche [3] proposed to perform reactions (2) and (3) in the same reactive distillation column. Reaction (4) is the separation of L_1 in H_2SO_4 and H_2O . Up to now only distillation has been proposed for this separation. Several distillation flow sheets are found, ranging from the simple column [4] to multi effect arrangements [5, 6, 9]. This step is energy consuming due to the large number of water moles to evaporate. Reactions (5) to (7) proceed in gas phase and produce H_2O , SO_2 and oxygen. These gases are cooled down before to bubble in the Bunsen reactor to separate oxygen from SO_2 and H_2O . Due to the fact that reaction (7) is incomplete, a residual quantity of SO_3 is found in the hot gases at the outlet of reaction (7). This SO_3 is recombined to H_2O in a reactor where the reverse of reaction (6) is performed and the produced diluted H_2SO_4 is recycled in reaction (4). US teams are currently working on ceramic membrane separation as an alternative process to separate oxygen at high temperature. It has the double advantage to shift the SO_3 decomposition reaction and to increase the partial pressure of SO_2 in the Bunsen reactor. Besides it reduces the amount of H_2SO_4 recycled. The whole cycle can be divided into three sections according to the GA nomenclature [1], we shall call section I reaction (1), section II reactions (4) to (7) and section III reactions (2) and (3). A sketch of the cycle is shown Figure 1.

In this paper, we would like first to find an upper bound of the efficiency of this cycle. Therefore, in next paragraph, we assumed that the energy requirement of the reactions (1) to (7) is the minimum energy prescribed by the thermodynamics, and that the decomposition reaction (7) is complete, therefore no H_2SO_4 is recycled. In paragraph III, we review the published efficiency calculations and present our best assessment of section III. A more realistic efficiency of the whole

cycle is then deduced. Finally we conclude with the R&D needs to bring this cycle to an industrial level.

Figure 1. Sketch of the I-S cycle



II. Efficiency bound

We define the thermal efficiency as the ratio of the enthalpy of the hydrogen and oxygen recombination reaction at ambient temperature and pressure $\Delta H_{\text{H}_2\text{O}}^0(T_a) = 286\text{kJ/mole}$ to the total heat requirement of the cycle:

$$\eta_{\text{th}} = \frac{\Delta H_{\text{H}_2\text{O}}^0(T_a)}{Q + \frac{W}{\eta_r}} \quad (1)$$

Q and W are the heat and work requirements and η_r the efficiency of the conversion system. We used for the numerical calculations $\eta_r=0.5$, which corresponds to the efficiency of the GTMHR.

Let ΔH , ΔS and ΔG be the enthalpy, entropy and Gibbs free enthalpy of a chemical reaction at a given temperature T , the heat Q and work W requirements are:

$$Q \leq T \Delta S \quad W \geq \Delta H - T \Delta S = \Delta G \quad W + Q = \Delta H$$

The signs \leq, \geq are replaced by $=$ when the reactions are reversible.

If the turbine which produces W is included in the system, then we must consider the heat Q_a rejected to the ambient temperature T_a . In this case:

$$W = 0 \quad Q\left(1 - \frac{T_a}{T}\right) \geq \Delta H - T_a \Delta S \quad Q - Q_a = \Delta H$$

All the energy input is heat, and in the reversible case, the turbine is supposed to have a Carnot efficiency, which is too optimistic. Consequently we shall use the first formulation.

Hence, the heat requirement is:

$$\frac{\Delta G}{\eta_r} + (\Delta H - \Delta G) \text{ if } \Delta H - \Delta G > 0 \text{ and } \frac{\Delta G}{\eta_r} \text{ if } \Delta H - \Delta G < 0$$

In the latter case, the reaction is exothermic and the heat of reaction is lost, or can be recovered for internal use if T is high enough.

Thermodynamic data of the reactions

The optimum pressures of the three sections of the cycle are not equal due to thermodynamic reasons. The temperature of section I must be higher than the melting point of iodine but not too high to avoid the occurrence of the reverse reaction. Therefore, we assumed that this reaction (1) is performed at 400K and 2 bar. The pressure of section II must be low, due to the fact that the number of gaseous moles is increasing, therefore, the low pressure shifts the reactions towards completion. We have chosen 1 bar for this section. Finally the best pressure for section III is 50 bar. The more the pressure of this section is high, easier is the distillation of HI, because, the position of the azeotrope depends upon the pressure. 50 bar seems a reasonably high value. Of course, pumping power is needed to adjust the pressures. They will be taken into account in the energy balance.

The Bunsen reaction ($T=400K$, $p=2$ bar) can be split into four elementary reactions



(8) and (9) are endothermic and their heats of reaction can be computed with standard thermodynamic tables [7]. (10) and (11) stand for the exothermic dissolutions of H_2SO_4 and HI in water. Their heats of

solution are computed using Engels strong acid model [16]. In (11) iodine is supposed to have no influence on the heat of solution. This assumption is probably wrong because evidence of ion solvation with iodine molecules has been demonstrated in several papers. V. Calabrese [8] for example, shows experimentally that I_3^- ions exist in dilute solutions and theoretically that $\text{I}_2 \cdot \text{H}^+$ should exist as well. Unfortunately, there is no direct measurement of the heat of the Bunsen reaction. We shall then assume that we can add the heats of (4) to (7), which gives -93 kJ/mole.

The data for the other reactions are found for example in [7].

Figure 2. Thermodynamic data for reaction (7) – p=1 bar

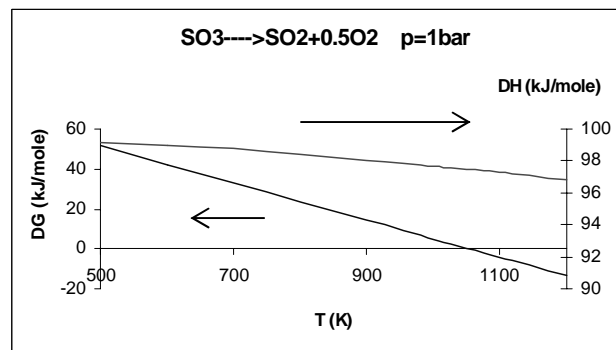
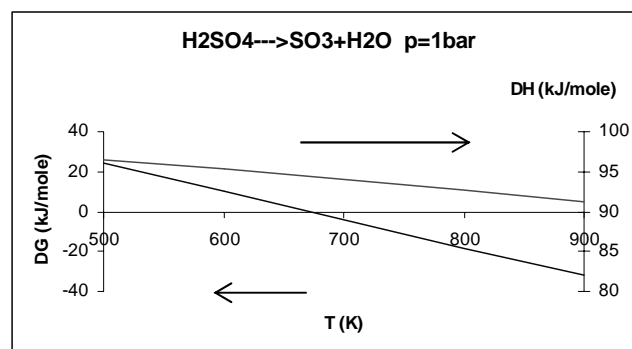


Figure 3. Thermodynamic data for reaction (6) – p=1 bar



Given the fact that the sulphuric acid boils at 612 K at 1 bar and that the heat of vaporisation is 58 kJ/mole, we can draw the Q/T diagram of section II (Figure 5).

We assumed that the maximum helium temperature was 1 144K and the return to the reactor temperature was 760K. The pinch point was taken equal to 17°C.

We have now all the inputs to calculate the total heat request.

Figure 4. Thermodynamic data for reaction (3)

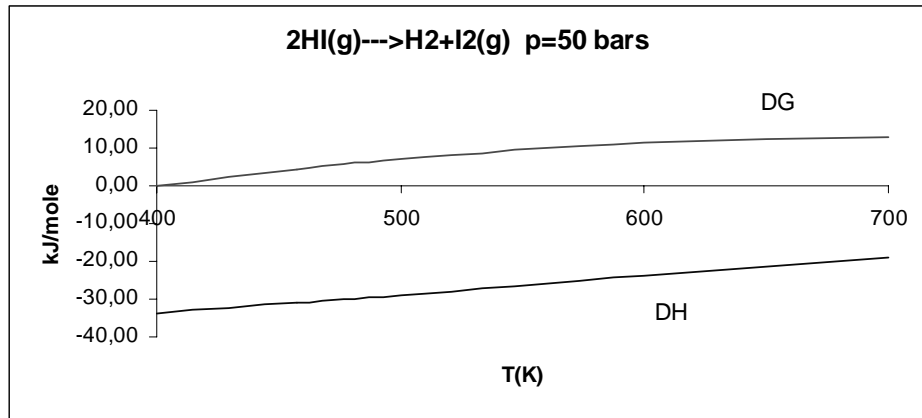
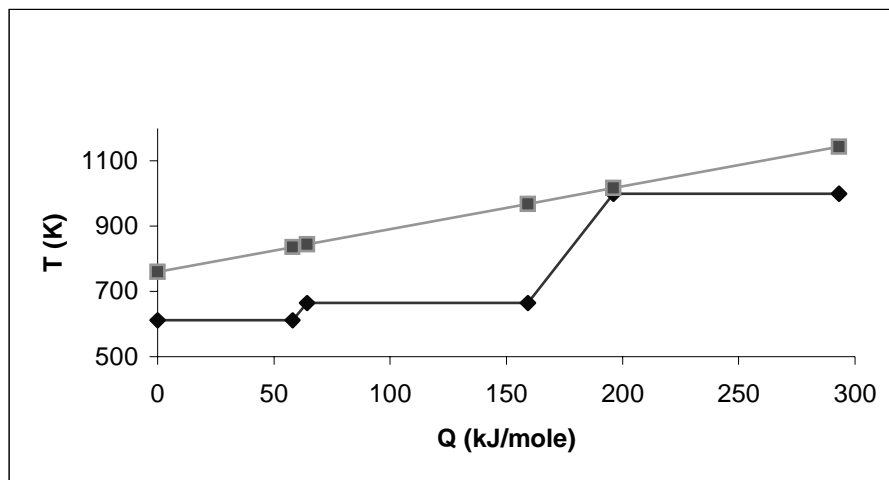


Figure 5. Q-T diagram of section II



Section II

Reaction (4): The temperature has a slight influence on the heat requirement of this reaction. Therefore, we supposed that this reaction is the reverse of reaction (10). Hence, $\Delta H=58$ kJ/mole and $\Delta G=66$ kJ/mole. The reaction can be performed with 66 kJ of mechanical work and releases 8 kJ heat. The heat demand is then: $66/0.5=132$ kJ/mole.

Reaction (5): heat demand: 58 kJ/mole.

Reaction (6): According to Figures 3 and 5, the reaction is performed at $\Delta G=0$, therefore, the heat demand is $T\Delta S=94.3$ kJ/mole.

Reaction (7): Due to the pitch of 17°C , the reaction occurs with a slightly positive ΔG i.e. $\Delta G=4.5$ kJ/mole and $\Delta H=97.6$. The heat request is then: $(97.6-4.5)+4.5/0.5=102$ kJ/mole.

The hot gases at the outlet of reaction (7) are supposed to exchange exactly their heat with the gases at the outlet of the Bunsen reaction. Hence, the total amount of heat request for this section is: $132+58+94.3+102=386$ kJ/mole.

Section III

Reaction (2) is the reverse of reaction (11), but occurs at higher temperature and pressure. At 500K and 50 bar, we have $\Delta H=66$ kJ/mole and $\Delta G=77$ kJ/mole. Due to the fact that the mixing enthalpy depends upon the temperature, we cannot assume that the specific heats of the reactants and products are the same. Therefore we shall take $\Delta H=122$ kJ/mole [opposite of reaction (11)] and $\Delta G=77$ kJ/mole. Hence the heat requirement is: $(122-77)+77/0.5=199$ kJ/mole.

Reaction (3): According to Figure 4, $\Delta G=12$ kJ/mole, $\Delta H=-24$ kJ/mole, therefore the heat is request is $12/0.5=24$ kJ/mole.

The two reactions occurring in the same reactor, we added the ΔG and ΔH , which results in $\Delta G=89$ kJ/mole and $\Delta H=98$ kJ/mole. The heat requirement is then: $89/0.5+98-89=187$ kJ/mole.

Pumping power

The pumping power (mechanical efficiency of 0.75) to raise the pressure of SO_2 from 1 to 2 bar is $\frac{RTL\ln(2)}{0.75} = 3\text{kW}$ and the pumping power of section III (see next paragraph) is 5.3 kW. The additional heat due to the pumping power is then $(3+5.3)/0.5=17$ kW.

According to these figures, an upper bound for the efficiency is:

$$\eta_{\text{th.}} = \frac{286}{386 + 187 + 17} = 0.485$$

III. Best estimate of the efficiency

Many estimations are found in the literature. Either for the whole cycle or for sections II or III taken separately. The first efficiency estimation was published by GA [1] in 1981. H_2SO_4 was separated from water by a constant pressure multi effect distillation and HI was separated from HIx by using phosphoric acid which had to be regenerated. The heat demand of section II was 460 kJ/mole H_2 and of section III, 148 kJ/mole. The total efficiency was then: $286/(421+187)=0.47$. The value for section III seems low.

Other papers deal with the heat demand of section II. In a recent work GA [8] using a more accurate thermodynamic model, estimated the heat demand at 420 kJ/mole. The pressure was decreased from 35 bar to 0.07 bar. The reason of this variation is to recover the maximum heat for internal reuse in the first stages of the distillation. Ozturk [5] proposed a flow sheet where the produced oxygen is used to boil by direct contact the sulphuric acid. The heat demand was

441.5 kJ/mole. In an alternative flow sheet, Schepers [6] proposed an increasing pressure multi effect distillation process. The heat demand could be decreased to 389 kJ/mole. Finally the author [4] found that with a simple distillation column a heat demand was 520 kJ/mole. The conclusion of these results is that there should be a compromise between efficiency and complexity and therefore cost of this section and that the optimum design is not necessarily the one with the minimum heat request. In the following we shall take the GA value of 420 kJ/mole as a best estimate value.

Much less results are available for section III, due to the lack of thermodynamic data of the HIx mixture. Roth and Knoche [10] calculated a reactive distillation column and external circuits and found an overall heat request of 237 kJ/mole. Unfortunately this calculation could not be reproduced due to a mismatch in the liquid and vapour flows in the column. Anyway, this value seems very low. The Japanese teams use electro dialysis to concentrate HI in HIx before to distillate the enriched HIx, but their publications are not yet available.

The calculation of the reactive distillation of section III is very difficult because of the complex behaviour of the vapour-liquid equilibrium of HIx. In the next section we describe briefly the model used and give preliminary results concerning the heat requirement of this section.

Available experimental data

Experimental data are available for the binary systems I₂-H₂O, HI-H₂O and for the ternary HI-I₂-H₂O.

The I₂-H₂O system has been studied by Kracek [11] in 1931. He measured the solubility of iodine in water and put in evidence a miscibility gap lying between the solid-liquid equilibrium point at 112.3°C (very close to the melting point of iodine: 113.7°C) and an upper temperature of approximately 280°C. At 112.3°C, the light aqueous liquid contains a very small amount of iodine (0.05 mole %) and the heavy liquid 98 mole % of iodine.

Total pressures of HI-H₂O mixtures have been measured by Wüster [12] and the mixing enthalpies by Vanderzee [13]. This system exhibits an azeotrope whose precise location depends on temperature and pressure. At ambient temperature, the azeotrope corresponds to a molar fraction of HI of almost 15%. For HI concentrations higher than the azeotrope, the vapour phase is very rich in HI, and for high temperatures (>200°C), HI might be dissociated in the vapour phase in H₂ and I₂. The kinetics of this reaction is in principle very slow but possible catalytic effects or hydrogen production in the liquid phase might appear as discussed by Berndhauser [14]. We shall assume in this paper that the decomposition reaction of HI takes place only in the vapour phase. These experimental results have been used by Engels [5] to fit the binary interaction parameters of his model, using the Wilson model for the calculation of the activity coefficients.

Detailed total pressure measurements for the HI-H₂O-I₂ ternary system for a [HI]/[H₂O] ratio up to 0.19 and various iodine concentrations are found in Neumann [15]. A synthesis of these results has been published by Engels and Knoche [4]. Experimental location of borderlines of the ternary phase diagram is found in [2]. From these results, it appears that the liquid phase exhibits two miscibility gaps which are the extensions in the ternary diagram of those found for the binaries I₂-H₂O and HI-H₂O. The I₂-H₂O miscibility gap tends to disappear rapidly with increasing HI concentration probably because of the formation of polyiodides ions like I₃⁻ or I₂H⁺.

Neumann's thermodynamic model

The thermodynamic model for the H₂O-HI-I₂-H₂ reactive-liquid-liquid-vapor system proposed by Neumann is based on the following assumptions:

- hydrogen is only present in the gas phase;
- the vapour phase is ideal, despite high pressures;
- the following solvation equation is taken into account in the liquid phase (Engels [6]):
 $m \text{H}_2\text{O} + \text{HI} \leftrightarrow \{(m\text{H}_2\text{O}, \text{H}^+) + \text{I}\}$ with $m=5$
- HI decomposition $2 \text{HI} \leftrightarrow \text{H}_2 + \text{I}_2$ takes place in the gas phase only.

The NRTL activity coefficient model is used to take into account the non ideality of the liquid phase and the binary interaction parameters (including solvent-complex) have been estimated by Neumann [15] from the experimental data of Engels and Knoche [4] for the H₂O-HI-I₂-H₂ system. The entire thermodynamical model includes solvation equilibrium, mass balances, HI decomposition equilibrium in vapour phase and vapour-liquid phase equilibria. With such model, the phase diagrams can be calculated with confidence on the left-hand side of the binary azeotropic H₂O-HI or for low iodine content. Uncertainties remain for high iodine contents (>20%) and high temperatures (>270°C).

The main features of this model, have been published in [4]. We recall here the behaviour of the ternary mixture at 22 bar, which is the pressure chosen by Roth and Knoche [3] for their reactive distillation calculation.

Ternary system HI-I₂- H₂O

A fundamental aspect for the reactive distillation design is the influence of I₂ concentration on the maximum bubble temperature of the ternary system H₂O-HI-I₂. The calculated results are presented on Figure 6. Each curve corresponds to the bubble curve of a ternary system H₂O-HI-I₂ with constant I₂ mole fraction varying in the interval: 1 (pure I₂), 0 (binary H₂O-HI). Thus the last curve on the right is the bubble curve of the binary H₂O-HI with a maximum azeotrope at $x_{\text{HI}}=0.133$. The crest line, locus of the maximum bubble points, joins the pure I₂ point (T=359.17°C) to the binary azeotrope H₂O-HI (T=245.13°C).

Figure 7 shows the ternary diagram of the system H₂O-HI-I₂ at 22 bar, limited to the region of interest for the reactive distillation design. We have notably reported:

- The singular points:
 - Pure I₂ (origin) and pure H₂O;
 - The binary azeotrope H₂O-HI;
 - The binary heteroazeotrope H₂O-I₂.
- The distillation frontier that is the projection of the crest showed on Figure 7. Note that a linear approximation of this frontier is not correct.
- The liquid-liquid – vapour domain for low HI content.

This diagram gives information on feasible distillation paths at 22 bar. Thus, as mentioned by Roth and Knoche [18], from the feed composition (HI/H₂O/I₂ = 0.1/0.51/0.39), we could obtain pure

iodine as residue and, by dissociation of HI, a distillate with H₂, the feed point being just on the right of the distillation frontier. The straight line in Figure 6 represents the mass balance and gives the composition of the distillate we could obtain without chemical reaction (HI/H₂O = 0.17/0.83). As a matter of fact we see that the number of water moles to evaporate is significant. Finally, we present in Figure 7 the liquid profile obtained by simulation of a reactive distillation column, with HI dissociation in the vapour phase. This profile follows very closely the distillation frontier. These preliminary simulation and thermodynamics results give the basis for the optimal design of the reactive distillation process (They [17]).

Figure 6. Influence of I₂ on the maximum bubble temperatures

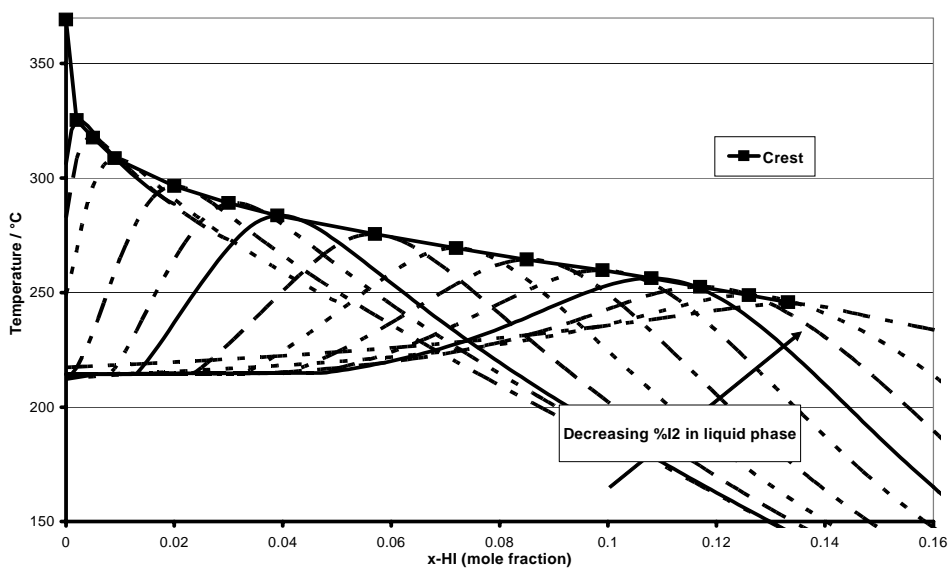
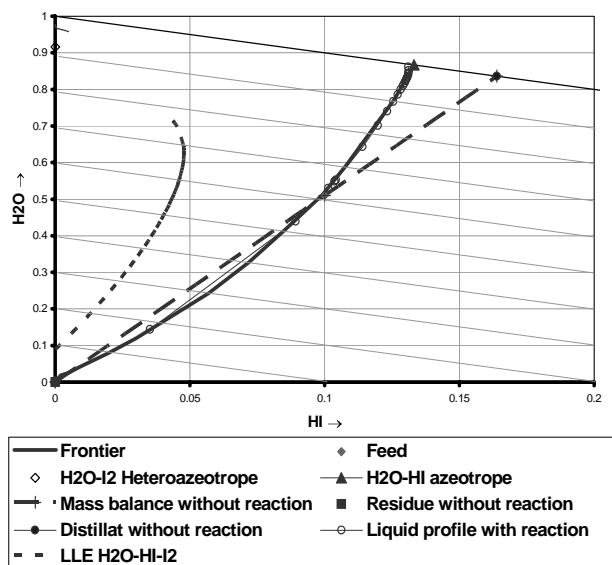
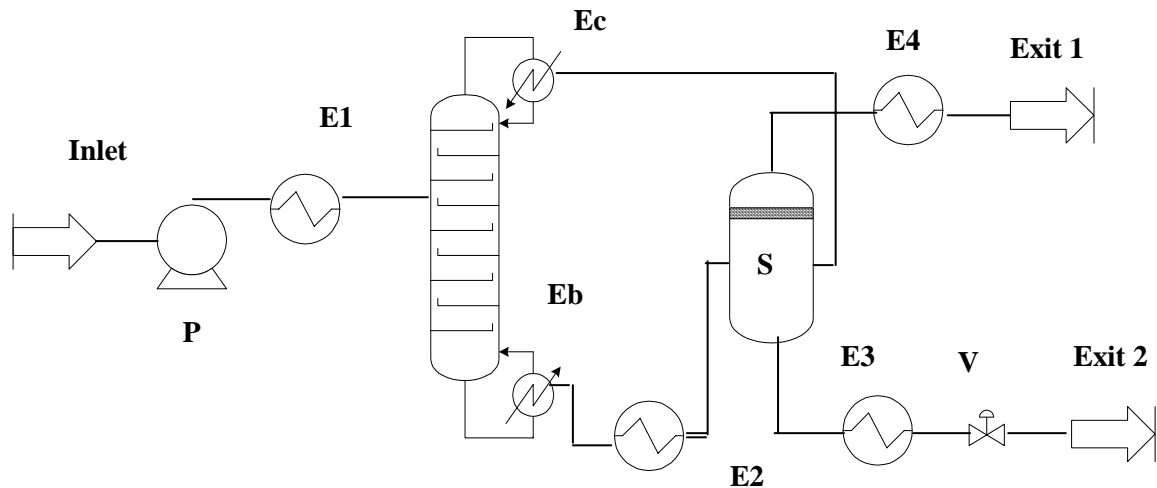


Figure 7. Ternary diagram of the system H₂O-HI-I₂



Reactive distillation of HIx

The above Neumann's model has been implemented in the chemical engineering code PROSIM and we proceeded by trial and error to converge on the following flow sheet:



The pump P raises the pressure at 50 bar and the valve V brings it back to 2 bar. The results of the heat and mass balance calculation are the following:

Inlet: Temperature: 393K, molar flow rate: 20 moles/s ($H_2O/HI/I_2 = 0.51/0.1/0.39$) pressure 2 bar.

Pump P: Electrical power: 5.3 (mechanical efficiency 0.75).

Heat exchanger E1 exit temperature: 575.4K (bubble temperature of the mixture), heat input 482 kW.

The column has 25 stages, feed is at stage 18 (stage N°1 is the upper stage). The condenser Ec is at 548K and the heat output is 82 kW. The boiler is at 580K and the heat input is 111 kW.

The molar flow rate at the outlet of the condenser is 1 mole/s and the composition is: $H_2O/HI/I_2=0.84/0.0186/0.00003/0.14$.

The molar flow rate at the outlet of the boiler is 19 mole/s and the composition is: $H_2O/HI/I_2=9.36/1.70/7.94$.

Heat exchanger E2 cools the residue at the same temperature as the condenser: 548K. Heat output: 76kW.

The liquid vapour separator S condenses part of the water and HI of the distillate. This additional condensation occurs because the composition of the distillate and the residue are different. Heat output: 18kW.

Heat exchanger E3 cools down the residue to 393K to be fed in the Bunsen reactor. Heat output: 402 kW

Heat exchanger E4 cools down the distillate to 393K. Heat output: 11 kW

The compositions and temperatures at the outlets are:

- Exit 1: $T=393\text{K}$, $\text{H}_2\text{O}/\text{HI}/\text{I}_2/\text{H}_2 = 0.19/0.008/0.027/0.141$
- Exit 2: $T=393\text{K}$, $\text{H}_2\text{O}/\text{HI}/\text{I}_2 = 10/1.71/7.91$

The heat released by E2, E3 and S can be used for E1. The amount of heat recovered by E1 depends on the temperature difference assumed between the primary and the secondary circuit. For example, if the temperature difference is 10°C , then the heat can be recovered in E1 from 570K to 393K i.e. $482 \cdot (570-393)/(575-393)=469$ kW. The amount of heat available in E2 and E3 is $76+401=478$ kW which is enough. Consequently, it remains $482-469=13\text{kW}$ to supply at a temperature comprised between 570 and 575K. In a similar way, if the temperature difference is 20°C , the heat to supply becomes 40 kW to be supplied between 560 and 575K.

Due to the fact that the temperature difference between the condenser and the boiler is small (32.5°C), a heat pump can be used to raise the temperature of the heat released at the condenser and to use it for the boiler. We selected water as the working fluid and tabulated the performances of the heat pump as follows.

For one mole of water circulating in the heat pump, the heat request at its boiler (which is the condenser of the column) is:

$$q_b = -0.0868 T_e + 52.44$$

where T_e ($^\circ\text{C}$) is the inlet temperature. The electric power P_c for an ideal compressor is:

$$P_c = (-0.000283 T_e + 0.131) \cdot \Delta T$$

where ΔT is the difference temperature between boiler and condenser. Finally the heat recovered at its condenser (which is the boiler of the column) is:

$$q_c = (0.09325 - 0.000524 \cdot T_e) \cdot \Delta T + 52.9 - 0.0833 \cdot T_e$$

If T_c and T_b are the condenser and boiler temperatures of the column, we assumed a temperature difference of 5°C between primary and secondary circuits. Therefore, $T_e=T_c-5$ and $\Delta T=T_b-T_c+10$.

The separator S being at the same temperature as the condenser, we applied the previous correlations to sum of the heat available at the condenser (82 kW) and at the separator S (18 kW). The application is straightforward: $T_e=270^\circ\text{C}$, $\Delta T=580-548+10=42^\circ\text{C}$, $q_b=29\text{kW}$, $P_c=2.29\text{kW}$, $q_c=28.4\text{kW}$. Therefore if $100/29=3.45$ moles/s circulate in the heat pump they can transfer $28.4 \cdot 3.45=98$ kW to the boiler of the column. Then it remains $111-98=13\text{kW}$ to supply as heat. The work of the ideal

compressor is $2.29 \times 3.45 = 7.9$ kW. If we assume a mechanical efficiency for the compressor of 0.75, the corresponding heat demand is $7.9/0.5/0.75 = 21$ kW. The total heat demand for one mole of H_2 produced is finally: $(21+13+13+5.3/0.5)/0.141 = 408$ kW if the temperature difference is 10°C and $(21+13+40+5.3/0.5)/0.141 = 600$ kW if the temperature difference is 20°C . In both cases the heat content of the gaseous stream at the outlet of the separator S is lost. It amounts 11 kW.

It can be noticed that in this flow sheet, the number of moles/s at the entry is exactly that at the exit of the Bunsen reaction. The H_2 production being only 0.141 moles/s, it means that an important quantity of materials must be recirculated between sections I and III. Typically, $20/0.141 = 142$ moles/s must enter section III. The head losses of such a mass flow rate have not been taken into account.

The best estimate of the efficiency with today's knowledge and a temperature difference of 10°C for the heat recovery between E1 and E2, E3 is then $286/(408+420) = 0.35$. If the temperature difference is 20°C , the efficiency becomes $286/(600+420) = 0.28$.

Conclusion – R&D needs

With the current reactions (1) to (7), widely adopted for the iodine sulphur cycle, we found an upper bound of the efficiency of 0.48. This value has been found by calculating the heat and work requirements of the reactions, assuming that they were reversible. A best estimate could be calculated as well by taking the latest GA value for the heat request of section II together with a reactive distillation calculation of section III. We found a value comprised between 0.28 and 0.34, depending on the temperature difference assumed for the heat recovery between E2+E3 and E1. These values do not take into account the head losses due to the large material circulation.

Many values of the heat requirement of section II are found in the literature. The problem for this section is to design the flow sheet in order to optimise the production cost. Compromises have to be found between the complexity and sizes of the chemical reactors and the efficiency. The main difficulty for section III is the calculation of the reactive distillation column due to the complexity of the thermodynamic model. Anyway, some breakthrough is needed to improve its efficiency. The Japanese are possibly on the right way with the electro dialysis.

Many improvements can be imagined to raise these both figures.

Reduction of the amounts of iodine and water in the Bunsen reaction. We have seen that these excesses of iodine and water burden heavily the heat balances of both sections II and III.

The use of membranes at various steps of the cycle: To separate SO_2 from O_2 , to separate liquid H_2O from H_2SO_4 , to separate HI from HIX (electrodialysis or distillation membranes?) and finally to separate H_2 from $(HI+H_2O)(g)$. Many teams, in particular in Japan, currently work actively on these topics.

Finally the HI_x section still represents a real chemical engineering challenge. Additional thermodynamic measurements are necessary and the best distillation design has to be found. Further experiments are planned, to be performed by the Commissariat à l'Énergie Atomique (CEA), in order to improve the database of the ternary mixture, more specifically at high iodine contents and to measure the vapour partial pressures as well.

REFERENCES

- [1] Funk, J.E., "Thermochemical hydrogen production: past and present", *Int. J. of Hydrogen Energy*, 26, pp. 185-190, 2001.
- [2] Norman, J.H., G.E. Besenbruch, L.C. Brown, D.R. O'Keefe, C.L. Allen, "Thermochemical water splitting cycle. Bench scale investigations and process engineering", DOE/ET/26225, (1981).
- [3] Roth, M., K.F. Knoche, "Thermochemical water splitting through direct HI decomposition from H₂O -HI- I₂ solutions", *Int. J. Hydrogen Energy*, 14, No. 8, 545-549 (1989).
- [4] Goldstein, S., J.M. Borgard, X. Joulia, P. Guittard, "Thermodynamic aspects of the iodine sulphur thermochemical cycle", AIChE Spring National meeting, New Orleans, April 2003.
- [5] Öztürk, I.T. and coll, trans IchemE, Vol. 72, Part A, March 1994.
- [6] Knoche, K.F., H. Schepers, K. Hesselmann, WHEC 1984. [4] H. Engels, K.F. Knoche, "Vapor pressures of the system HI/ H₂O /I₂ and H₂", *Int. J. Hydrogen Energy*, 11, 11, 703-707, (1986)
- [7] Barin, I., O. Knache, "Thermodynamic properties of inorganic substances", Springer Verlag ed.
- [8] Calabrese, V. "Polyiodine and polyiodide Species in an aqueous solution of iodine +KI", Theoretical and experimental studies, *J. Phys. Chem. A* 2000,104, 1287-1292.
- [9] Brown, L.C., and coll. "High efficiency generation of hydrogen fuels using nuclear power", GA-A24285, June 2003.
- [10] Roth, M., K.F. Knoche, *Int J. of Hydrogen Energy*, Vol. 14, No. 8. pp. 545-549, 1989.
- [11] Kracek, F.C., "Solubilities in the system water-iodine to 200°C", *J. Phys. Chem.*, 35, p. 417 (1931).
- [12] Wüster, G., Dissertation, RWTH, Aachen, (1979).
- [13] Vanderzee, C., L. Gier, "The enthalpy of solution of gaseous hydrogen iodide in water, and the relative apparent molar enthalpies of hydriodic acid", *J. Chem. Thermodyn.*, 6:441, 1974.
- [14] Berndhauser, C., K.F. Knoche, "Experimental investigations of thermal HI decomposition from H₂O -HI-I₂ solutions", *Int. J. Hydrogen Energy*, 19, No. 3, pp. 239-244, (1994).
- [15] Neumann, Diplomaufgabe, RWTH Aachen, 28-01, 1987.
- [16] Engels, H., "Phase equilibria and phase diagrams of electrolytes", *Chemistry Data Series*, Dechema ed.
- [17] They, R., "New Methodology for the Feasibility Analysis and the Design of Reactive Distillation Processes", INPT PhD Thesis, 2002.

INVESTIGATION OF THE I-S CYCLE FOR MASSIVE HYDROGEN PRODUCTION

X. Vitart, J.M. Borgard, S. Goldstein, S. Colette
CEA-Saclay, 91191 Gif-sur-Yvette Cedex. France

Abstract

The French Commissariat à l'Énergie Atomique (CEA) has, since mid-2001, performed a preliminary evaluation of different methods to produce hydrogen from nuclear energy. The objective is to compare the hydrogen production costs via high temperature electrolysis or via thermochemical cycles, which are nowadays the two main routes for the long term production of hydrogen without greenhouse effect, both from the technical and economical points of view.

A first comparison of thermochemical cycles has already been done. From this analysis, it appears that, based on known data, the hybrid S process (also call the Westinghouse process) is probably today the most economical friendly, but that possible improvements are limited because of the electrolytic part of the process. However, the integral thermochemical I-S (iodine–sulphur) cycle developed by General Atomics in the 1970s could become much more interesting if some improvements could be done in the flowsheet.

In this paper, we focus on the most critical and pertinent areas which are, from our point of view, R&D efforts in order to reach the goal of the most precise evaluation of the potentialities of the I-S process.

I. Objectives and contract of the French programme

Different institutes mainly in United States and in Japan have been involved for many years in the evaluation of the potentiality of thermo chemical cycles to produce hydrogen, in the perspective of coupling to a nuclear reactor at high temperature (HTR) [1, 2]. The I-S cycle seems the only one to have an international consensus. The objective of this countries seems now to quickly reach the demonstration step, with the construction of significant units, on the basis on known data. In France, however, there has been for a long time a big debate between supporters and opponents of thermo chemical cycles coupled to HTR, everyone arguing on thermodynamic considerations, costs, surety, without any real reliable and pertinent data.

The CEA programme, wanting to keep all possibilities open, consists in a detailed evaluation of the I-S cycle, based on experimental work, enabling to optimise all the three sections of the process with the possibility to evaluate them together.

It consists of the following:

- acquisition of thermodynamic and kinetic missing base data for the reference case of I-S (Bunsen reactor, HI section with a reactive distillation column to produce hydrogen) material behaviour corrosion tests;
- search and tests of advanced technological solutions (membranes, new separation methods, catalysts, booster...);
- R&D efforts structured around a modular experimental loop (production of H₂ of the order of 100 l/h), which enable to easy modify or change, the different component or sections in the term of a logical development plan;
- flow-sheet simulation integrating in real time R&D results (thermodynamical data, technological solutions);
- technico-economical analysis, integrating the R&D results, in comparison with EHT or alkaline electrolysis;
- HT reactor coupling evaluations.

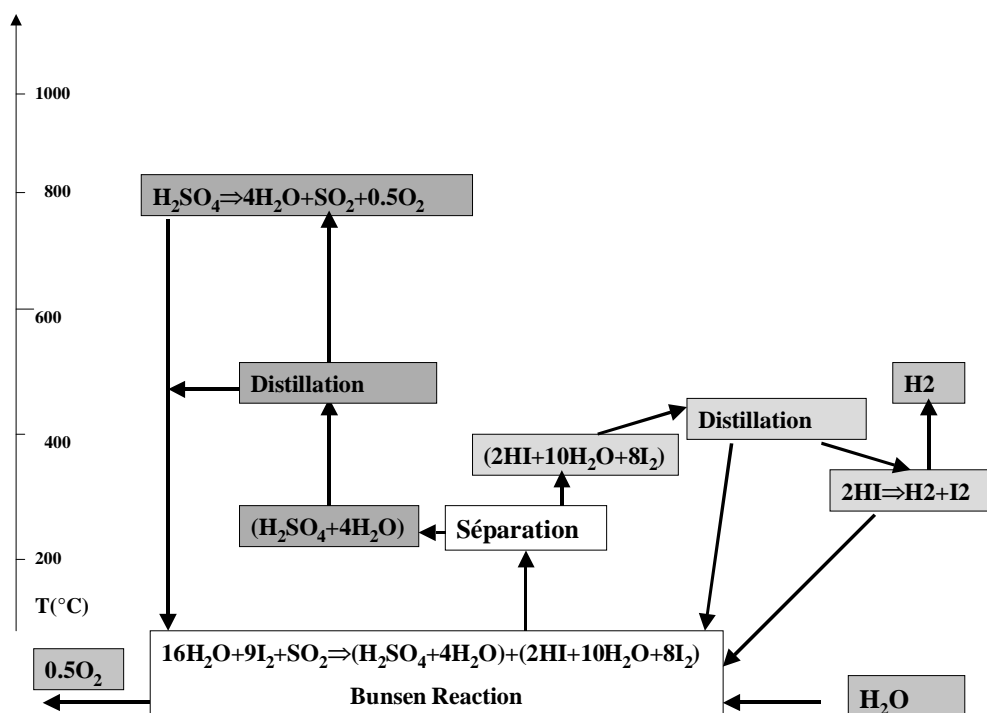
This position of France remains uncommon because it leaves open the options by concentrating his efforts on R&D to optimise the I-S process. It is complementary to the one effected in United States and in Japan.

II. The I-S cycle and it's majors uncertainties

This cycle was originally studied in the 70-80's by General Atomics Co. [2]. Some pertinent improvements were later proposed by Ispra, RWTh Aachen and others in the 80's [4, 5, 6]. It was also studied by the Japanese team of JAERI [3] who built a small demonstration loop in 1999. A demonstration pilot is planed by JAERI for 2008.

The cycle is based on the following reactions (Figure 1).

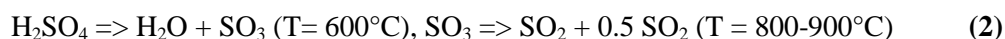
Figure 1. General schema of I-S process



Formation of two acids in two liquid phases in presence of large excess of water and iodine (Bunsen reaction):



Distillation followed by decomposition of sulphuric acid:



Distillation followed by decomposition of iodhydric acid:



As far as we know, a substantial R&D effort is necessary to assess and develop the I-S cycle:

- the purchase of experimental thermodynamic and kinetic data which concern all the chemical reactions that take place in the Bunsen and HI sections, so that the global chemical design of the process may be implemented;
- the search for the best efficiency of the Bunsen section, by optimising the thermodynamic conditions in order to reduce the amount of water involved, and for an efficient way to produce H₂ in the HI section (reactive distillation is the present reference method, but other ways have to be prospected);

- the materials behaviour evaluation.

In this paper, we describe the R&D devoted to those various items, on which we focus today to assess and develop the I-S reference cycle.

III. Flow-sheet considerations

Several simulations of the I-S flow-sheet are done using the PROSIM software and available thermodynamical model.

The main conclusions up to now rise as follow:

1. Dealing with **H₂SO₄** section, for which all main thermodynamical data are known, simulation shows that there should be a compromise between efficiency and complexity and therefore cost of this section. The optimum design is not necessarily the one with the minimum heat request [7]. No real improvement on the thermodynamic of this section can be expected, because a good efficiency is achieved. The use of selective membrane to separate O₂ from SO₂ and SO₃ at high temperature [8] may be an improvement: some US team are currently working on it. It has the double advantage to shift the SO₃ decomposition reaction and to increase the partial pressure of SO₂ in the Bunsen reactor.
2. Scarce experimental data are available to deal with the **Bunsen** reactor and it seems that G.A. best point leads to an important (around 100 kJ/mol) ΔG of this section, which considerably lower the maximum efficiency of the cycle [9]. A large database of the Bunsen reaction is needed, for different pressures of SO₂ (Figure 2). A new design of Bunsen reactor is under consideration too. We intend to react the HIx product of the Bunsen with the incoming SO₂, generating a new small Bunsen reaction so as to lower the part of water in the HIx product. In term of chemical engineering this will act as a counter-current column for the generation of HIx product. The former design of G.A. [2] could be compared to a co-current column. So we can expect, if parasite reactions could be handled, a better product, easing the HIx section. Therefore, a database of reaction of HIx with SO₂ must be constructed as well.

The HIx section is identified as the most problematic section of the process, in terms of feasibility and efficiency [2], [3], [6], [7] on the one hand, because the first, thermodynamical data are incomplete to characterise the Vapour-liquid equilibrium of HIx mixture; on the other hand, because it is difficult to find an efficient way to produce H₂. Direct decomposition at P=1atm and 900K is not an option, because of the too large flow of HIx to be heated. Use of phosphoric acid, as proposed by the G.A team [2] is cost intensive, introduce a new element in the cycle, and has poor efficiency. An elegant solution could be the reactive distillation-decomposition process as proposed by RWTh Aachen [3]. The main idea is to have very low iodine content at the bottom of the column, in order to shift the decomposition rate of HI to higher rates than equilibrium in the last stages.

Figure 2. Bunsen reaction study

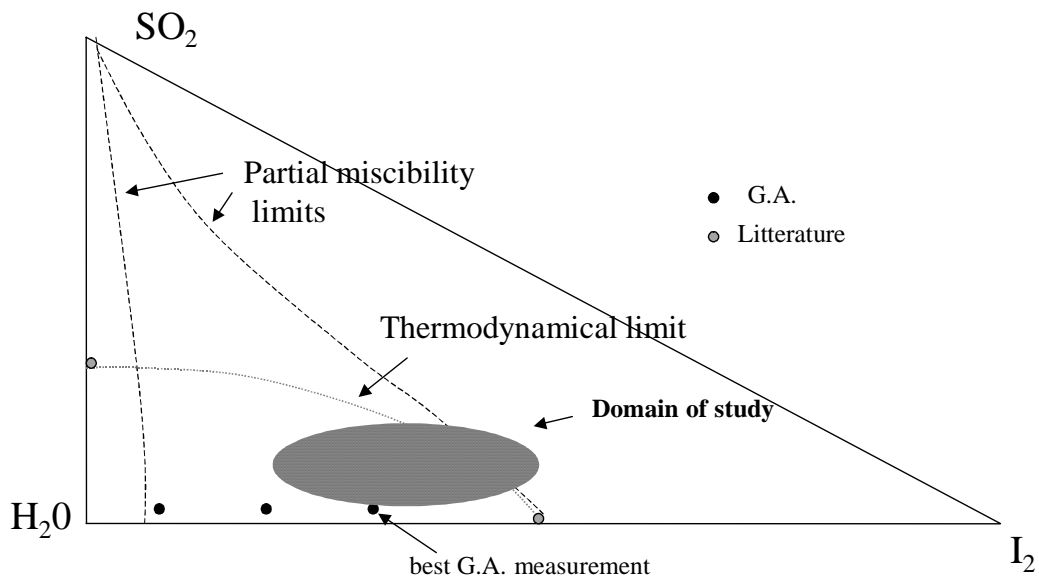
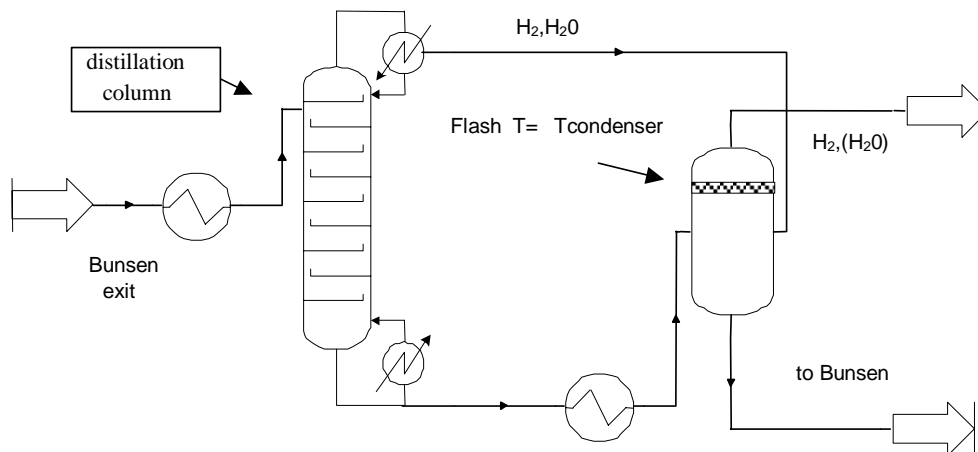


Figure 3. Distillation process scheme simulated by PROSIM software



First calculations [9], using Neumann's thermodynamical model [10] for the HIx mixture, are in the range of 250-350 kJ/mol for an operating pressure of 50 bar but are very dependant of exchanger losses, effective decomposition of HI into hydrogen and iodine and of the HIx thermodynamical model used. So it appears that:

- partial vapour pressure as stated above must be clearly measured to confirm the thermodynamical model;

- exchanger losses between liquid flow of HIx mixture must be clearly stated and included in the economical analysis;
- to improve the result, it is possible to use a very H₂ perm-selective membrane in combination with the column. Some investigations have already begun in Japan with interesting results and similar studies are planned in CEA Saclay.

IV. Experimental programme on vapour equilibrium of HIx mixture

Many published data exist on HIx mixture liquid and on vapour-liquid equilibria, but they are not sufficient to characterise a distillation column. The Figure 4 compares the calculated azeotropic line of HI by a model made by Neumann [11] of the mixture and a similar model done by the CEA.

Real pertinent data available until now are total pressure data but only for a ratio [HI]/[H₂O] lower than 18% [10]. We intend to increase this database to larger [HI]/[H₂O] ratios and measure partial vapour pressure as well. Necessary data acquisition leads to difficulties from both analytical and technological points of view, especially in-situ measurements because of the opacity of the vapour due to the presence of large amounts of iodine and because of high corrosion. The programme is scheduled around three steps, and we try to perform direct pressure and optical measurements as we believe that it is the best way to maintain the original species (in addition, samplings will give complementary information).

- measurements of the total pressure of the ternary mixture named HIx, up to 50 bar and 300°C, so as to determine the azeotropic concentrations versus temperature and [I₂]/[H₂O] ratio, using a micro pressure vessel, made of Tantalum like the piezoelectric pressure gauge coating;
- measurements of the partial pressures around the ambient pressure, by means of optical spectroscopy (IR and UV-visible), so as to avoid sampling and to measure the species “in-situ” above the free surface. Fine tuning of those methods will be achieved using well known binary mixtures; according to the first experiments, we think that UV-visible fits the requirements for iodine measurements, and on the other hand we showed that Fourier-Transform IR is a suitable method for H₂O and HI, so we will use a dedicated commercial or prototypical apparatus, and a glass reactor with a quartz window;
- measurements of the partial pressures up to 50 bar: this is a rather difficult measurement, insofar as we have to control a high temperature and pressure mixture, and as it is essential that we find the spectroscopic IR and UV-visible methods suitable for the actual process conditions (such concentrated phases may induce prohibitive absorption characteristics); nevertheless, we identified two Raman diffusion methods that may be interesting routes for highly concentrated media.

Figure 4. Azeotropic lines at T=180°C

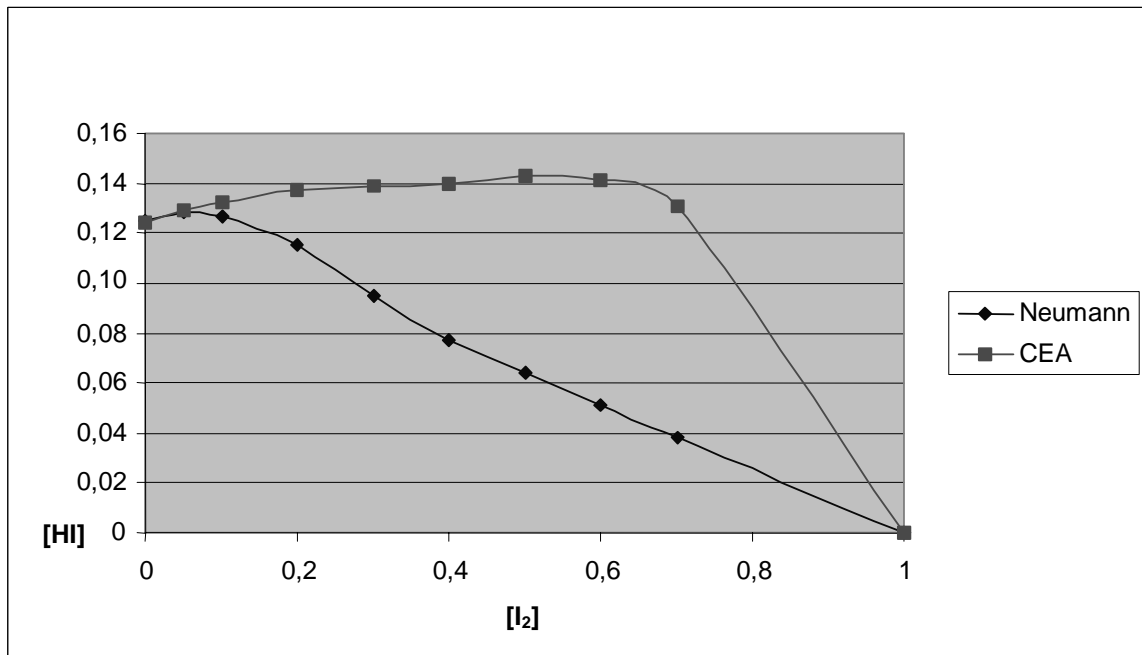
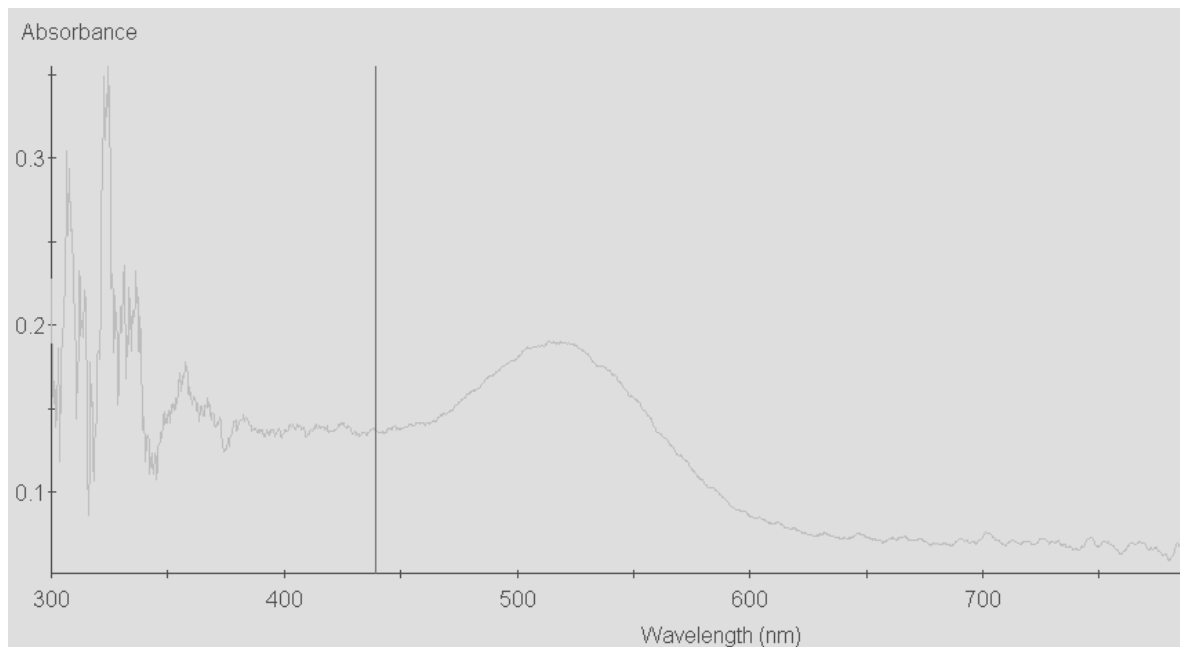


Figure 5. Preliminary results for iodine absorption (spectrum at 20°C)



From our point of view, measurements of the total pressure of the ternary mixture up to 50 bar and 300°C and a good knowledge of the partial pressures around the ambient pressure will form a crucial data source for model improvement while waiting for the (difficult) experiments on the real ternary mixture.

V. Experimental programme dealing with the Bunsen reactor

Experimental studies are devoted to acquire kinetic and thermodynamic data for all the reactions involved in the Bunsen reaction in order to optimise the whole process. The development plan includes three parts:

- Design of analytical methods allowing to measure in each liquid phase the total amount of iodine, by using potentiometry and UV-visible spectrophotometry, sulphur, with ICP-AES and UV-visible spectrophotometry, H^+ ions by acido-basic titration with NaOH.
- Thermodynamic optimisation of liquid phase separation from the mixture of the final products of Bunsen reaction: HI, I_2 , H_2O and H_2SO_4 . A glass reactor has been especially designed. It allows to warm the medium up to about 100°C (the higher limit being fixed by a maximal pressure of 1.5 bar) while limiting cold area likely to condense iodine.
- Optimisation of operating conditions of Bunsen reactor and process design, i.e. thermodynamic and kinetic study performed from the mixture of initial reagents (water, iodine and sulphur dioxide), in a fully instrumented reactor, operating in true temperature and pressure conditions.

First results obtained in a thermostated reactor are in agreement with those reported by JAERI in similar conditions [12] (phase separation, species in each phase).

Figure 6. Molar fraction

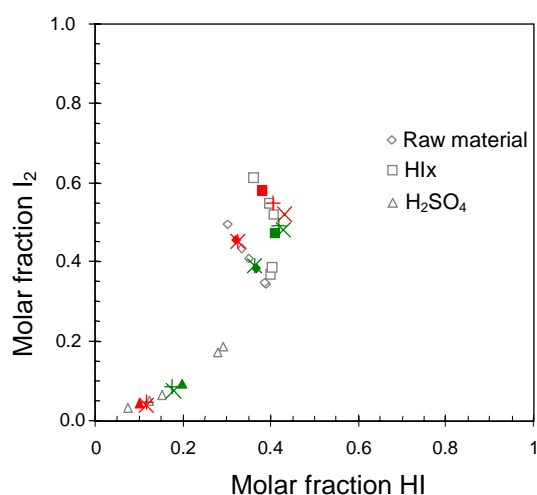
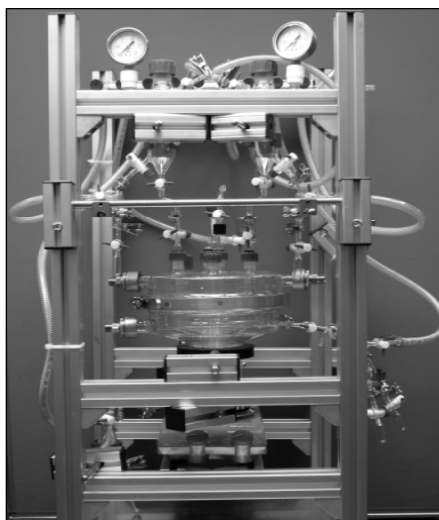


Figure 7. Apparatus for thermodynamic optimisation



VI. Material study

First economic evaluation indicates that that cost of high temperature exchanger are the main costs investment for the thermo-chemical plant to be coupled to the HTR.

Most data exist for adequate material to handle sulphuric acid. However, as iodhydric acid is seldom employed, data are scarce and only available in G.A., Ispra and JAERI studies. A large of material have been proposed for the three different section but they have to be tested on long period for validation [13].

Best efforts are achieved on the Bunsen section. The temperature of the section is low (95-125°C), but it is difficult to find an adequate material for both acids.

From literature review, some materials have a good behaviour:

- metallic materials like tantalum, zirconium, alloy Ni-Mo;
- non-metallic materials like fluorocarbon plastics and glass-lined steel as well as SIC.

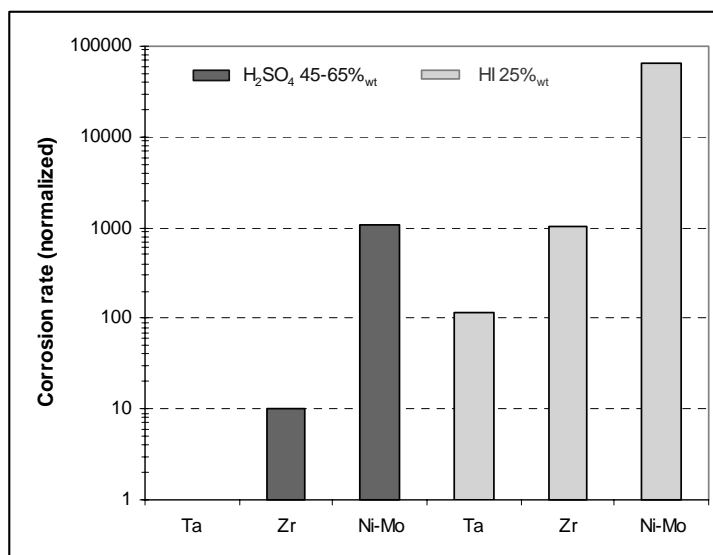
From electrochemical tests, three metallic materials have been tested in sulphuric acid and iodhydric acid media: tantalum, zirconium and Ni-Mo alloy (Hastelloy B3).

First results have shown the iodhydric acid media is most corrosive (factor 100 between acids).

Tantalum is the only metallic material totally resistant. Zirconium corrosion is low in sulphuric acid whatever the concentration and is significant in iodhydric acid even at low concentration. The corrosion behaviour of Ni-Mo alloy is worst. This material must be prohibited, specially in iodhydric acid media.

These electrochemical tests will be completed by immersion tests. Moreover, long term tests including metallic (tantalum) and ceramic coatings are planned.

Figure 8. Corrosion rate



Conclusion

Large R&D efforts are dedicated to the study of the I-S process. An important experimental effort is needed to achieve the assessment and the optimisation of the possible flow-sheets and solutions with dedicated apparatus; a precise and complete diagnosis evaluation is necessary and still remains a major difficulty.

REFERENCES

- [1] Funk, J.E., *Thermochemical hydrogen production: past and present*, Int. J. of Hydrogen Energy, 26, pp. 185-190, 2001.
- [2] Norman, J.H., G.E. Besenbruch, L.C. Brown, D.R. O'Keefe, C.L. Allen, *Thermochemical water splitting cycle. Bench scale investigations and process engineering*, DOE/ET/26225, (1981).
- [3] Miyamoto, Y. and all. "R&D programme on hydrogen production system with high temperature cooled reactor", Proc. Int. Hydrogen Energy Forum 2000, Munich, Germany, Vol. 2 pp. 271-278, September 2000.
- [4] Roth, M., K.F. Knoche, *Thermochemical water splitting through direct HI decomposition from H₂O-HI-I₂ solutions*, Int. J. Hydrogen Energy, 14, No. 8, 545-549 (1989).
- [5] Öztürk, I.T. and coll, trans IChemE, Vol. 72, Part A, March 1994.
- [6] Beghi, G., *A decade of research on thermochemical hydrogen at the joint research centre, Ispra*, Int. J. of Hydrogen Energy, Vol. 11, No. 12, pp.761-771.
- [7] Goldstein, S., J.M. Borgard, X. Joulia, P. Guittard, *Thermodynamic aspects of the iodine_sulphur thermochemical cycle*, AIChE, Spring National meeting, New Orleans, April 2003.
- [8] Brown, L.C., and coll., *High efficiency generation of hydrogen fuels using nuclear power*, GA-A24285, June 2003.
- [9] Borgard, J.M., S. Colette, A. le Duigou, S. Goldstein, *Thermodynamic assessment of IS cycle*, EHEC, 2003.
- [10] Neumann, *Diplomaufgabe*, RWTH Aachen, 28-01-1987.
- [11] Engels, H., K.F. Knoche, *Vapor pressures of the system HI/H₂O/I₂ and H₂*, Int. J. Hydrogen Energy, 11, 11, 703-707, (1986).
- [12] Sakurai, Nakajma and all., Int J. of Hydrogen Energy, Vol. 25, pp. 605-611, 2000.
- [13] Kubo, and all., *Corrosion tests on structural material for iodine-sulphur thermochemical water-splitting cycle*.

R&D ON THERMOCHEMICAL I-S PROCESS AT JAERI

**Kaoru Onuki, Shinji Kubo, Hayato Nakajima, Shunichi Higashi,
Seiji Kasahara, Shintaro Ishiyama, Hiroyuki Okuda**

Department of Advanced Nuclear Heat Technology, Oarai Research Establishment
Japan Atomic Energy Research Institute (JAERI), Japan

Abstract

The Japan Atomic Energy Research Institute (JAERI) has conducted a study on the thermochemical water-splitting process of the iodine-sulfur family (IS process). In the IS process, water will react with iodine and sulfur dioxide to produce hydrogen iodide and sulfuric acid, which are then decomposed thermally to produce hydrogen and oxygen. High temperature nuclear heat, mainly supplied by a High Temperature Gas-cooled Reactor (HTGR), is used to drive the endothermic decomposition of sulfuric acid. JAERI has demonstrated the feasibility of the water-splitting hydrogen production process by carrying out laboratory-scale experiments in which combined operation of fundamental reactions and separations using the IS process was performed continuously. At present, the hydrogen production test is continuing, using a scaled-up glass apparatus. Corrosion-resistant materials for constructing a large-scale plant and process improvements by introducing advanced separation techniques, such as membrane separation, are under study. Future R&D items are discussed based on the present activities.

KEYWORDS: HTGR, Hydrogen production, Thermochemical water-splitting process, IS process, Construction materials

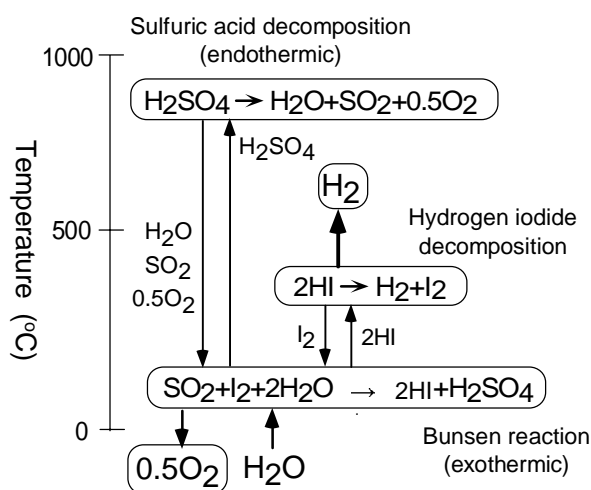
1. Introduction

Japan Atomic Energy Research Institute (JAERI) has been conducting a study on thermochemical water-splitting process of iodine-sulphur family (I-S process, Figure 1). In I-S process, raw material, water, is to react with iodine and sulphur dioxide to produce hydrogen iodide and sulphuric acid, which then are decomposed thermally to produce hydrogen and oxygen. High temperature nuclear heat supplied by HTGR will mainly be used to drive the endothermic thermal decomposition of sulphuric acid.

We are now studying the I-S process from the following three points of view. The first one concerns the process control technique for continuous hydrogen production. The second one aims to improve the performance of unit operations to realise the efficient hydrogen production in terms of thermal efficiency, the most important of which is an innovative separation method of HI from the product solution of the Bunsen reaction. The third one is on corrosion-resistant materials for constructing large-scale plants.

Present status of study is briefly described in this paper.

Figure 1. I-S process



2. Hydrogen production test

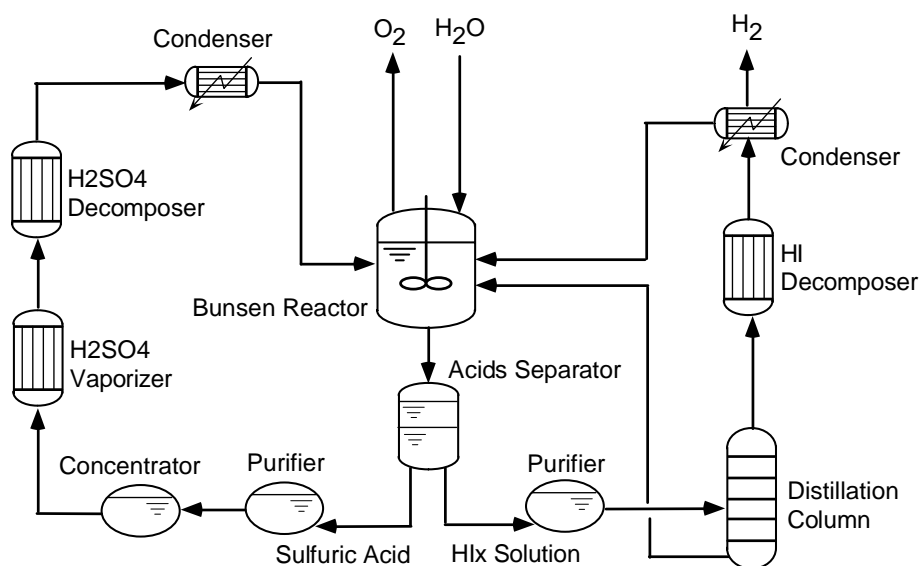
The continuous hydrogen production by I-S process has been examined using small loop apparatuses in order to develop the operation technique of connecting the three chemical reactions and accompanying product separations while using reactants cyclically.

Figure 2 shows schematic flow sheet of the experimental apparatuses. It includes the essential unit operations of I-S process that employs the liquid-liquid phase separation phenomenon for the separation of sulphuric acid and hydrogen iodide produced by the Bunsen reaction. The chemistry of sulphuric acid decomposition section and that of hydrogen iodide decomposition section are rather straightforward in terms of reaction and separation. On the contrary, in the Bunsen reaction section, possible occurrence of side reactions forming sulphur or hydrogen sulphide must be suppressed. Also, line plugging caused by possible iodine precipitation and outflow of unabsorbed sulphur dioxide gas

along with the product oxygen should be suppressed to maintain the stable operation. The objective of the hydrogen production tests is to develop the process control method to avoid these undesirable phenomena that might occur due to the fluctuation of temperature, flow rates and composition of process fluids.

Figure 2. Schematic flow sheet of laboratory-scale test apparatuses

Here, the separation of HI from HIx solution (HI-I₂-H₂O mixture) is carried out by distillation. Two types of apparatus were set up in JAERI lab, both of which were made of glass. Nominal hydrogen production capacity of the first one was 1 NL/hr and that of the second is 50 NL/hr.

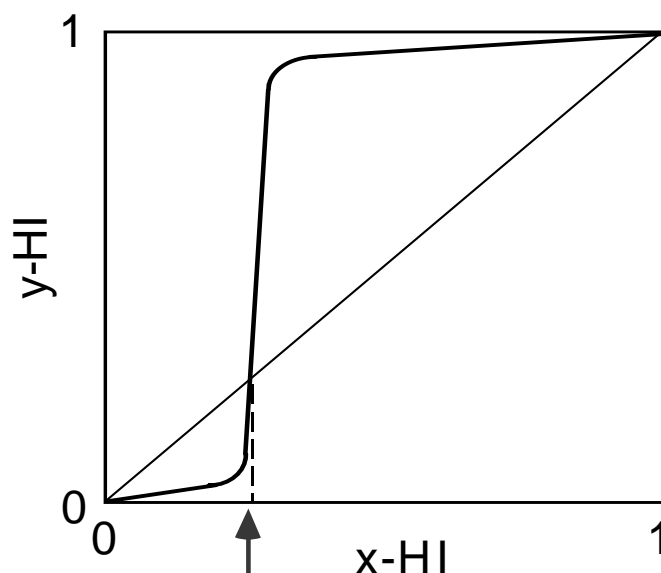


The initial experiments were carried out with a small apparatus made of glass with hydrogen production capacity of 1 NL/h. After successful continuous operation test of about 48 hrs, a scaled-up glass apparatus was setup and the test operation was undertaken. The scaled-up apparatus enables to handle the phase-separated solution of higher iodine concentration than the solubility at ambient temperature and is also equipped with sensors for monitoring density of process solution, liquid-level, etc. Recently, first trial of continuous loop operation was successfully carried out for 6 hrs with hydrogen production rate of 35 NL/h.

3. Improvement of the unit operations

Figure 3 shows schematic VLE of HIx solution (HI-I₂-H₂O mixture) at constant I₂ fraction [1]. Since the composition of HIx solution obtained in the Bunsen reaction section is located near the quasi-azeotropic one where the molar ratio of HI and H₂O is same in both the vapour- and liquid-phase, it is impossible to separate HI and H₂O by equilibrium controlled separation techniques alone such as conventional distillation. On this problem, we have been studying to apply kinetic-controlled separation techniques such as membrane process. By increasing HI molality of the HIx solution using such processes to over-quasi-azeotropic molality, since the volatility of HI is very high in the solution of higher HI molality than the quasi-azeotropic one, pure HI can be separated from the concentrated HIx solution by simple distillation.

Figure 3. Vapour-liquid equilibrium (VLE) of HIx solution at constant fraction of I_2
The ordinate and the abscissa denote molar ratio of $[HI]/[HI+H_2O]$ in vapour and in liquid, respectively. The arrow indicates the composition of HIx solution obtained in the Bunsen reaction section



Electro-electrodialysis (EED) process has been examined for this purpose. The principle of EED is shown in Figure 4. HIx solution is fed to the EED cell that is equipped with a cation-exchange membrane. By applying DC current, redox reaction of I/I^- occurs at both electrodes. Owing to the selective permeation of proton through the membrane, HI molality of the HIx solution increases in the catholyte and decreases in the anolyte. Recently, it was successfully demonstrated to increase the HI molality by about 50% with relatively low energy consumption [2].

A preliminary evaluation of the heat/mass balance was carried out of a flow sheet that adopted the EED and an HI decomposer equipped with hydrogen perm-selective membranes, as well. The results were reported elsewhere [3]. Briefly, Figure 5 shows an estimated effect of the final HI molality in the concentration by EED on the thermal efficiency of hydrogen production. Here, heat/mass balance of HI section was calculated assuming intensive heat recovery, and those of Bunsen section and sulphuric acid sections were taken from the literature [4, 5]. The ideal efficiency was estimated to be close to 60%.

Figure 4. Concentration of HIx solution by EED

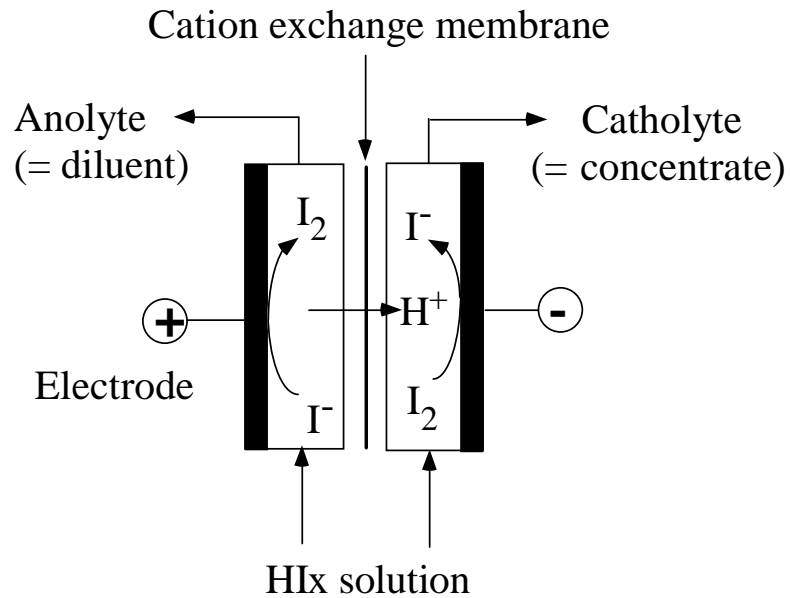
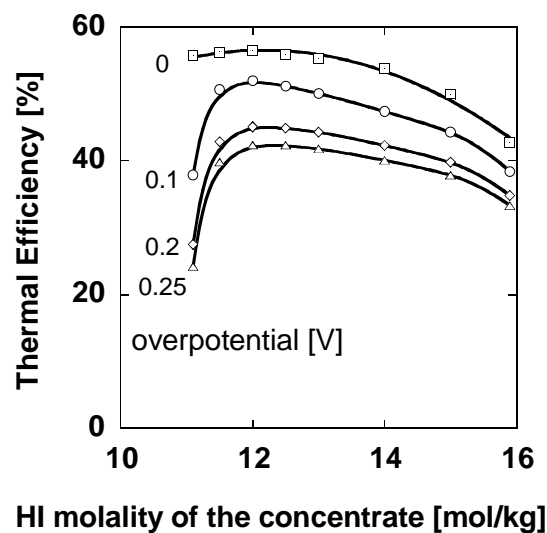


Figure 5. Estimated effects of final HI molality and of over potential in EED on the thermal efficiency

Heat/mass balance of HI processing section was calculated assuming intensive heat recovery, ΔT_{min} (in heat exchanger)=0, etc. As for Bunsen section and sulphuric acid section, reported heat/mass balances were used [4, 5].

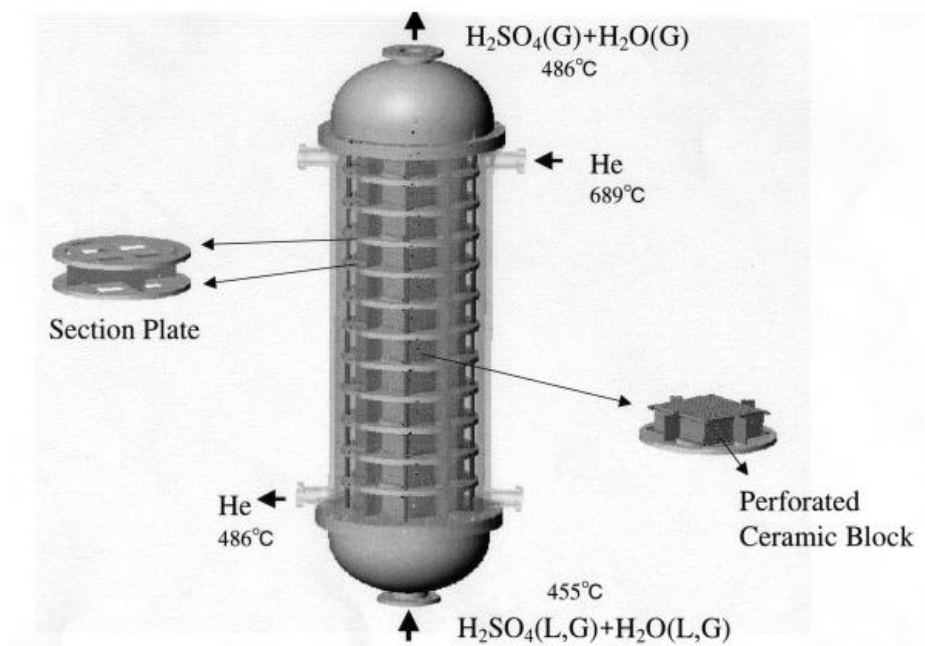


4. Corrosion resistant materials of construction

As for the materials of construction, top priority of selection at this stage of process development is the corrosion resistance and the corrosion data has been accumulated in the representative process conditions. Our recent examination in this field was done with the sulphuric acid of 75wt%, 85wt% and 95wt% at temperatures close to their boiling ones under 2 MPa. Exposure tests in the environments for 100-1 000 hrs revealed the excellent corrosion resistance of silicone-containing ceramics [6].

In addition to the corrosion tests, JAERI started the conceptual design work of key components. Figure 6 shows a concept of sulphuric acid vaporiser in which heat-exchanging columns made of ceramics is utilised.

Figure 6. Sulphuric acid vaporiser featuring ceramic blocks



5. Remarks

Present activity on I-S process at JAERI was briefly described. These works will be completed in FY2004. As the next R&D, a pilot-scale test is under planning.

Acknowledgements

The hydrogen production test of 50 NL/h and part of the conceptual design work has been carried out under the contract of research between JAERI and the Ministry of Education, Culture, Sports, Science and Technology of Japan.

REFERENCES

- [1] Neumann, D., "Phasengleichgewichte von $H_2/H_2O/I_2$ -Loesungen", *Diplomarbeit, RWTH Aachen*, 1987.
- [2] Hwang, G.-J., *et al.*, "Improvement of the thermochemical water-splitting I-S process by electro-electrodialysis", *J. Membr. Sci.*, 220, 129-136, (2003).
- [3] Kasahara, S., *et al.*, "Effects of process parameters of the I-S process on total thermal efficiency to produce hydrogen from water", *J. Chem. Eng. Jpn.*, 36, pp. 887-899, (2003).
- [4] Norman, J.H., *et al.*, "Thermochemical Water-Splitting Cycle, Bench-Scale Investigations and Process Engineering", *GA-A 16713*, 1982.
- [5] Knoche, K.F., *et al.* "Second law and cost analysis of the oxygen generation step of the General Atomic Sulphur-Iodine cycle", *Proc. 5th World hydrogen Energy Conf.*, Toronto, Vol. 2, pp. 487-502, July 1984.
- [6] Kubo, S., *et al.*, "Corrosion test on structural materials for Iodine-Sulphur thermochemical water-splitting cycle", *Proceedings of the 2nd Topical Conference on Fuel Cell Technology, AIChE 2003 Spring National Meeting*, New Orleans, Louisiana, American Institute of Chemical Engineers, New York, 30 March-3 April, 2003.

HYDROGEN GENERATION USING A CALCIUM-BROMINE THERMOCHEMICAL WATER-SPLITTING CYCLE*

Richard D. Doctor, Diana T. Matonis, David C. Wade
Argonne National Laboratory, USA

Abstract

The Secure Transportable Autonomous (STAR-H2) project is part of the US Department of Energy's (DOE's) Nuclear Energy Research Initiative (NERI) to develop Generation IV (Gen IV) nuclear reactors that will supply high-temperature (over 1 100K; 800°C) heat. The goal of NERI is to develop an economical, proliferation-resistant, sustainable, nuclear-based energy supply system based on a modular-sized fast reactor that is passively safe and cooled with heavy liquid metal. STAR-H2 consists of the following:

- A 400-MW_{Thermal} reactor with Pb as the primary coolant;
- Exchange of primary Pb coolant for a salt heat transfer pipe;
- Exchange of salt for steam;
- A combined thermochemical water-splitting cycle to generate hydrogen;
- A CO₂ Brayton cycle to generate electricity ($\eta = 47\%$), and
- An optional capability to produce potable water from brackish or salt water.

Here we review the thermodynamic basis for a three-stage calcium-bromine (Ca-Br) water-splitting cycle. The research builds upon pioneering work on the four-stage University of Tokyo Cycle #3 (UT--3) process, but employs a plasma-chemical stage for the recovery of HBr as H₂ and Br₂ as a substitute for the final two stages of UT-3. A detailed process design, developed by using the ASPEN model, suggests that the practical efficiency is 39-45% for the STAR-H2 Ca-Br cycle. For each tonne of H₂ produced hourly (1 000 kg/h), the demand for electricity for the plasma-chemical stage (13.5 MW_e) is much lower than the demand (28.5 MW_e) for a steam-electrolysis system. At current power grid heat-to-electricity efficiencies ($\eta = 33\%$), there is a clear benefit for using the STAR-H2 Ca-Br cycle. Anticipating Brayton cycle performance ($\eta = 47\%$), H₂ production will demand a total power of 74 MW_{Thermal} per tonne of H₂ from the Gen IV reactor. It is important to recognise that there are capital and operating cost tradeoffs that will depend on the market value of low-carbon electricity in the future. Steam-electrolysis is a far less complex cycle than Ca-Br, but that simplicity comes at a high – and potentially uneconomical – cost for electric power.

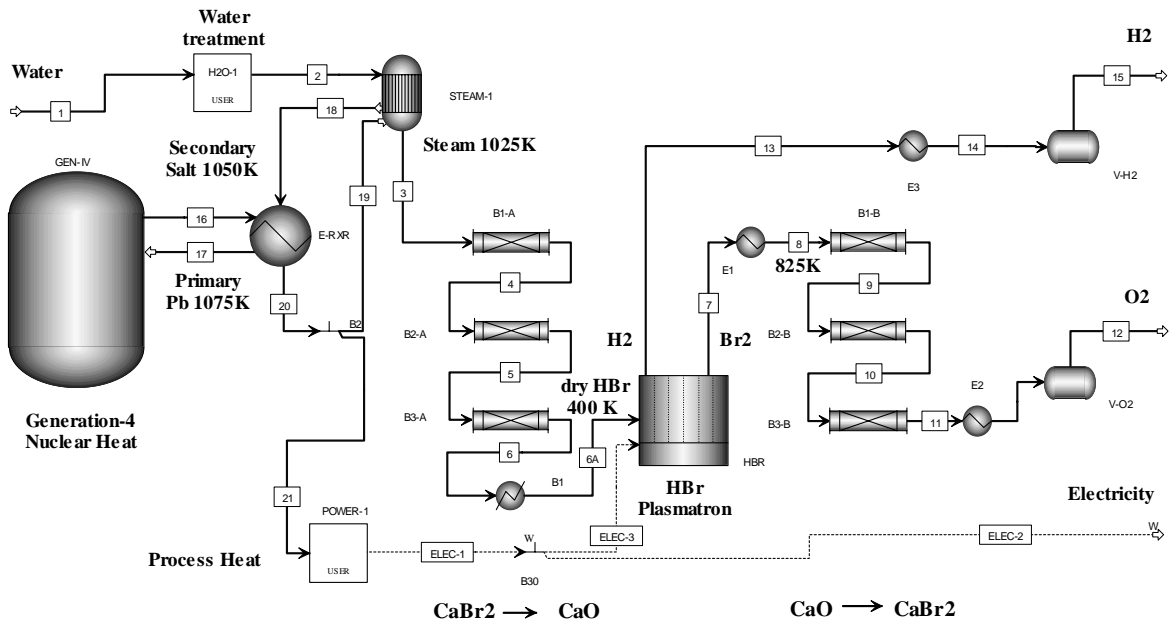
* This manuscript has been created by the University of Chicago as Operator of Argonne National Laboratory ("Argonne") under Contract No. W-31-109-Eng-38 with the US Department of Energy. The US Government retains for itself, and others acting on its behalf, a paid-up, nonexclusive, irrevocable worldwide license of said article to reproduce, prepare derivative works, distribute copies to the public, and perform publicly and display publicly, by or on behalf of the Government.

1. The calcium-bromine (UT-3) cycle

Among the thermochemical hydrogen production cycles that have the highest commercial potential, a recent screening study identified the two leading candidate cycles as sulphur-iodine and UT-3. [1] The UT-3 cycle was investigated by the Japan Atomic Energy Research Institute (JAERI) and has been considered in detailed technical reviews. [2] At Argonne National Laboratory, we are investigating a variation of this cycle that offers some advantages over the original cycle. [3] It is called the “calcium-bromine cycle or Ca-Br cycle”, to avoid confusing it with the excellent efforts on the UT-3 cycle. A simplified diagram for the Ca-Br cycle is provided in Figure 1. The following pages briefly describe the process.

The primary Pb coolant from the Gen IV reactor transfers heat to a lithium fluoride salt heat carrier that, in turn, raises the temperature of the steam to 1025K. In the first stage of the thermochemical cycle, this steam feed reacts with CaBr_2 to form HBr gas as it passes through a series of plug-flow reactors.

Figure 1. Simplified diagram showing principle streams of Ca-Br water-splitting cycle
Products shown are H_2 , O_2 , and electricity. Desalination is not shown.



To dissociate the HBr to H_2 and Br_2 , we are investigating a “plasmatron” system. As the name suggests, this system employs plasma-chemical reactions; it operates at low temperatures and pressures to produce H_2 in a mix of HBr. The entire cycle has a reduced electric power demand compared to H_2O electrolysis. Following plasma-chemical reactions, the original CaBr_2 reagent is regenerated during the production of oxygen. Heat is recovered from the oxygen production stage to produce electricity.

A staged plug-flow operation is employed to minimise the loss of Br₂ from the process. The use of gas-solid reactions for the two stages in the proposed process will simplify separations compared with cycles based on gas/gas separations. However, thermodynamic feasibility and ease of reaction product separations are only some of the factors that must be considered for successful economic development of a commercial water cracking process. We have explored the primary and secondary reactions, the kinds and amounts of by-products that may be generated during the secondary reactions, and strategies to address these by-products. We believe that, as long as operations remain in the specified temperature ranges, by-products such as bromine oxides (Br₂O; BrO₂), hypobromous acids (HBrO), and calcium hydroxide Ca(OH)₂ should not form – so by-products should not offset the significant advantages of this cycle.

2. Water splitting with HBr formation

Steam is reacted with CaBr₂ to crack the water and form two moles of HBr for every mole of water. The developers of the UT-3 process have observed that, in this series of reactions, the "...hydrolysis of CaBr₂ is the slowest reaction". [4] This reaction presents the greatest challenge to the practicality of this cycle. Water splitting with HBr formation takes place at a temperature of 1 030K in a solid-gas reaction where ($\Delta G_T = +50.34$ kcal/gm-mole = +1.93 eV):



What is not shown in this equation is that the calcium is supported on 75 wt.% that CaTiO₃ cycles between CaBr₂ and CaO. This stage is carried out in four plug-flow operations, and a dry HBr product is delivered to H₂ production. A typical counter current flow employing four beds is used, consequently, the reaction progressively demands more cycle heat as it moves through the beds that contain higher and higher concentrations of CaBr₂. The first bed contacted is low in CaBr₂, while the last is nearly pure CaBr₂. As a process optimisation, the beds may be rebalanced so that they have more consistent heat duties. This is an endothermic reaction that requires heat input directly into each of the plug flow reactor beds. Because the reaction products are gaseous, they occupy twice the volume of the reagent steam, which means that for a standard bed, the heat transfer will need to be set so that performance in the last bed can be maintained.

3. Oxygen recovery

Oxygen recovery and the regeneration of the initial CaBr₂ reagent is an exothermic process at 850K, again in a solid-gas reaction where ($\Delta G_T = -18.56$ kcal/gm-mole = -0.71 eV):



An inspection of the simplified reaction scheme (Figure 1) shows that this stage follows the plasmatron. A review of this system of reactions reveals an inherent difficulty in the first and second stages (Equations 1 and 2). This difficulty is linked to the significant physical change in dimensions as the calcium cycles between bromide and oxide. The CaO has a cubic structure (a=4.81 Å) that must undergo a dimensional change to accommodate the CaBr₂ orthorhombic structure (a=6.58 Å; b=6.87 Å; c=4.34 Å). This process must then be reversed. As the calcium reactant undergoes this change in dimensions, sintering will occur unless the calcium is carefully dispersed on a suitable support. Recent efforts by Sakurai et al. have considered pellets with the CaO supported on CaTiO₃ at CaO:CaTiO₃ ratios between 0.5 and 2. [5] Sakurai and his colleagues reported plugging of pore volumes as the cycle is reversed and the CaBr₂ is regenerated. We intend to investigate suitable support structures for the calcium that will tolerate this cycling. We envision two stages of plug-flow operation for CaBr₂ regeneration with the liberation of oxygen.

Oxygen recovery rejects heat at 850K. The practical use of this heat is addressed in a companion paper by Moisseytsev and Matonis that explores the system heat balance – including calculated temperature and pressure distribution of the working fluids inside the reactor, the intermediate molten salt loop, the hydrogen production plant, and the desalination plant – and discusses the opportunities for a Brayton cycle to produce electric power at $\eta = 47\%$.

4. Hydrogen from HBr dissociation

We propose to employ a single-stage, rather than a two-stage, HBr-dissociation step. So our approach represents a *modified* UT-3 cycle in which hydrogen formation will involve either HBr electrolysis ($\Delta G_T = +27.32$ kcal/gm-mole = +1.05 eV) or the use of a plasma chemistry technique operating near ambient conditions.

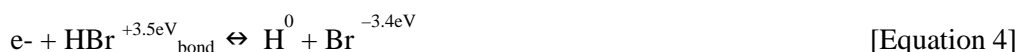
Several approaches to the electrolysis of HBr have been reported in the literature. Aqueous phase decomposition from concentrated HBr solutions has been mentioned in the literature. Kondo investigated a gas-phase graphite electrode proton-transport membrane for HBr electrolysis. [6] The inlet gas requires a wet feed, as is needed for steam electrolysis cells. Complete conversion of the HBr may not prove economical; hence, the resulting product will likely contain H₂O, HBr, and Br₂ which must be separated. A hydrogen and bromine recovery system could be engineered around this approach.

The efforts by Wauters, again in the gas phase looked at bromine transport membranes in HBr service that involved a molten-salt saturated electrode. [7] For the bromine transport cell, the preliminary economics were reported as encouraging.

However, we intend to study decomposition of HBr to H₂ and Br₂ using electrolysis and plasma-chemistry dissociation. Process conditions for the plasma-chemical approach are 400K (~100°C) in a gas phase reaction where ($\Delta G_T = +19.78$ kcal/gm-mole = +0.76 eV): [8]



The following reaction is also significant:



Losing the electron to the bromine is economically unacceptable, so efforts that began By Rusanov at the Kurchatov Institute (Moscow, Russia) during the 1980s address this problem. These efforts focused on designing plasma-chemical systems so that the products of the plasma-chemical dissociation do not recombine. Advances in this technique employing “reverse-vortex flow” have been reported recently. [9, 10] Applying this technique will result in a small draw on the electric power from the system to produce a cold plasma-chemical reaction.

The products of decomposition – H₂ and Br₂ – are in different states at standard conditions, H₂ is a gas and Br₂ is a liquid. Additionally, the main gases involved in the process (H₂, HBr, and Br₂) have very different physical properties. Because of these differences, we can expect the direct separation of components if a plasma chemical reactor is employed. Secondly, the enthalpy of HBr decomposition ($\Delta H = \sim 0.5$ eV/molecule) is quite small – comparable to that of the H₂S decomposition ($\Delta H = \sim 0.2$ eV/molecule) which has shown success in applying this technique. This similarity allows us to anticipate a similar decomposition process in both cases; the Gibbs free energy of HBr dissociation ($\Delta G = \sim 0.3$ eV/molecule) is smaller than its enthalpy ($\Delta H = 0.5$ eV/molecule), which suggests the practicality of carrying out this process in non-equilibrium chemical plasma.

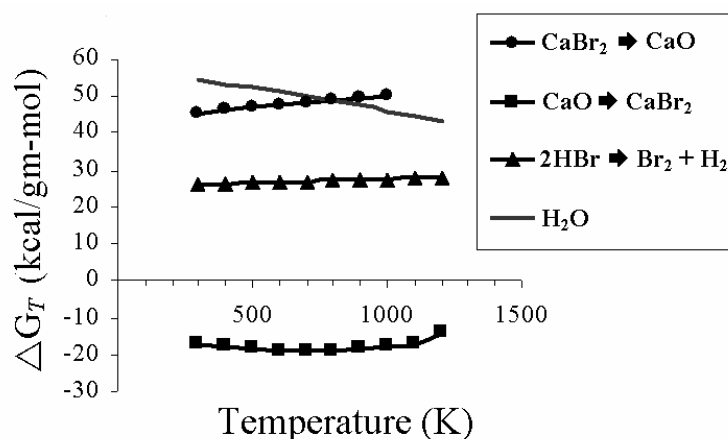
Thermodynamic equilibrium calculations show the significant dissociation of HBr that would be expected as temperatures rise above 1 500K. This temperature is much lower than the characteristic temperature of thermal plasma (~10 000K). So, it is reasonable to use non-equilibrium low-temperature plasma.

A high-efficiency H₂S decomposition (energy cost about 0.7 eV/mol) was achieved by employing a physical mechanism. The gas was introduced into the plasma cavity using a rotational flow pattern at near-sonic speeds, creating a centrifugal separation of hydrogen products from sulphur condensate at the periphery of the rotating flow. Because the atomic mass of bromine (80 g/mol) is higher than that of sulphur (32 g/mol), we would expect the centrifugal separation of bromine from HBr to be as effective as it is in the case of sulphur from H₂S. In addition, this process operates at low temperatures and low pressures, making the recovery of the H₂ straightforward using conventional technology. At the same time, there is a disadvantage to the low-pressure aspect of this approach. Five stages of compression (with the attendant capital and operating penalties) are required to bring H₂ to operating conditions for pressure swing absorption (PSA), a standard H₂ purification technique. Following purification delivery of product to the H₂ pipeline completes the process.

5. Summary of chemical cycle

The thermodynamics for the Ca-Br reaction system are favourable; Figure 2 provides a diagram of the Gibbs free energies for a simplified reaction network. It should be noted that the HBr dissociation does not presume plasma chemistry. We assume here that commercial HBr electrolysis will could used for HBr dissociation with hydrogen formation.

Figure 2. ΔG vs. temperature (K) for the Ca-Br three-stage cycle contrasted with water electrolysis



6. Process design for the calcium-bromine cycle

AspenPlus 11.1 was used for the evaluation of the thermochemical process. The feed rates for the steam were chosen so that the STAR-H₂ system would produce H₂ at 7 500 kg/h. In addition to the major reagents and products (steam, H₂, O₂, Br₂, CaBr₂, CaO, and HBr), the mass and heat balance results of the simulations include carrying the heat from the CaTiO₃ through the temperature cycling between 1 050K and 850K. These practical issues will reduce the efficiency of the cycle.

A counter current plug flow employing four beds is used and the reaction progressively demands more cycle heat as it progresses through the beds that contain higher and higher concentrations of CaBr_2 . Although the solids will not actually flow, a flow of solids is required by the Aspen model to simulate solid packing in a reactor. The final solids stream, containing CaO and any unreacted CaBr_2 , is cooled to 873K (the required bromination reaction temperature) and 1 atm. The volume occupied by CaO is significantly less than that occupied by CaBr_2 and the estimated impact of this reaction is that the volumetric flow decreases by 48 m^3 each hour. The final vapour stream exiting Stage 1 contains only anhydrous HBr which will go into the plasmatron at a temperature of 350K and 1 atm.

Although HBr dissociation follows in the reaction cycle, the CaBr_2 regeneration and oxygen production streams are integrally linked with the CaBr_2 hydrolysis. Bromine is returned from storage at ambient conditions and vaporised. The vaporous bromine will react with CaO in two stages, because this reaction is much faster than the first reaction – thus requiring half the number of reactors for the reaction to proceed to completion. As stated, the bromination stage of this cycle is exothermic. The heat rejected by the system is recovered by the Brayton cycle part of the STAR-H2 cycle. A heat exchange with CO_2 is performed as shown in Figure 3, which provides the details of the integration of Stages 1 and 3 for the cycle. The temperature of CO_2 is increased from 780K to 829K.

Although the conceptual process diagram in Figure 1 shows a simple unit for the production of H_2 and Br_2 , the process is actually more complicated – as seen by the details in Figure 4.

The major streams involved in the production and purification of H_2 are not simply the anhydrous HBr entering the plasmatron. A conversion efficiency of 50% for the HBr through the plasmatron means that the stream actually contains HBr and H_2 . Although the bromine is separated within the plasmatron, where it is quenched and cooled at the wall, it is simulated in Aspen to be diverted into a separate stream. A rotary blower vacuum pump system is included in the final thermodynamic heat analysis to bring the plasmatron exit stream to the required vacuum pressure of 0.05 bar. The remaining H_2 and HBr go through a series of compressors to bring the mixture to a final pressure of 35 bar (500 psi). After the compressors, the HBr and H_2 mixture will enter a pressure swing adsorption purification section for separation. The final product is a compressed stream of 99.9% H_2 , while any residual HBr will be back fed into the plasmatron for further H_2 production. The exit pressure of the H_2 product stream is chosen as a reasonable pipeline pressure for the transport of H_2 , although it might also be compressed for a storage tank.

7. Heat balance

Table 1 summarises heat and major electricity use for each portion of the Ca-Br cycle. Heat from the Gen IV reactor is of premium value. Although the process has been integrated into an overall balance of facility calculations, we provide a stand alone balance for purposes of clarity. For the warming of streams from ambient conditions, we incorporated opportunities to optimise the heat use within the cycle by exchange against other process fluids. So the anticipated heat required (10.12 $\text{MW}_{\text{Thermal}}$) to heat water from ambient temperature to 1 050K is actually less than 50% of that value (4.8 $\text{MW}_{\text{Thermal}}$). The use of electric power within the plant is minimised, and all compressors and the plasmatron vacuum system are steam driven. For practical reasons, all compressor interstage cooling employs only cooling water, and no attempt at exchange against another working fluid was considered. The demands for Gen IV heat are split nearly evenly between the two flow sheets presented. Approximately 10% of the heat is sent to the Brayton cycle, and the majority of the electricity must be produced from steam. An unanticipated opportunity for power generation comes from the expansion turbine that returns the recycled HBr to the plasmatron.

Figure 3. Integration of Stage 1 (steam to HBr) and Stage 3 (oxygen liberation)

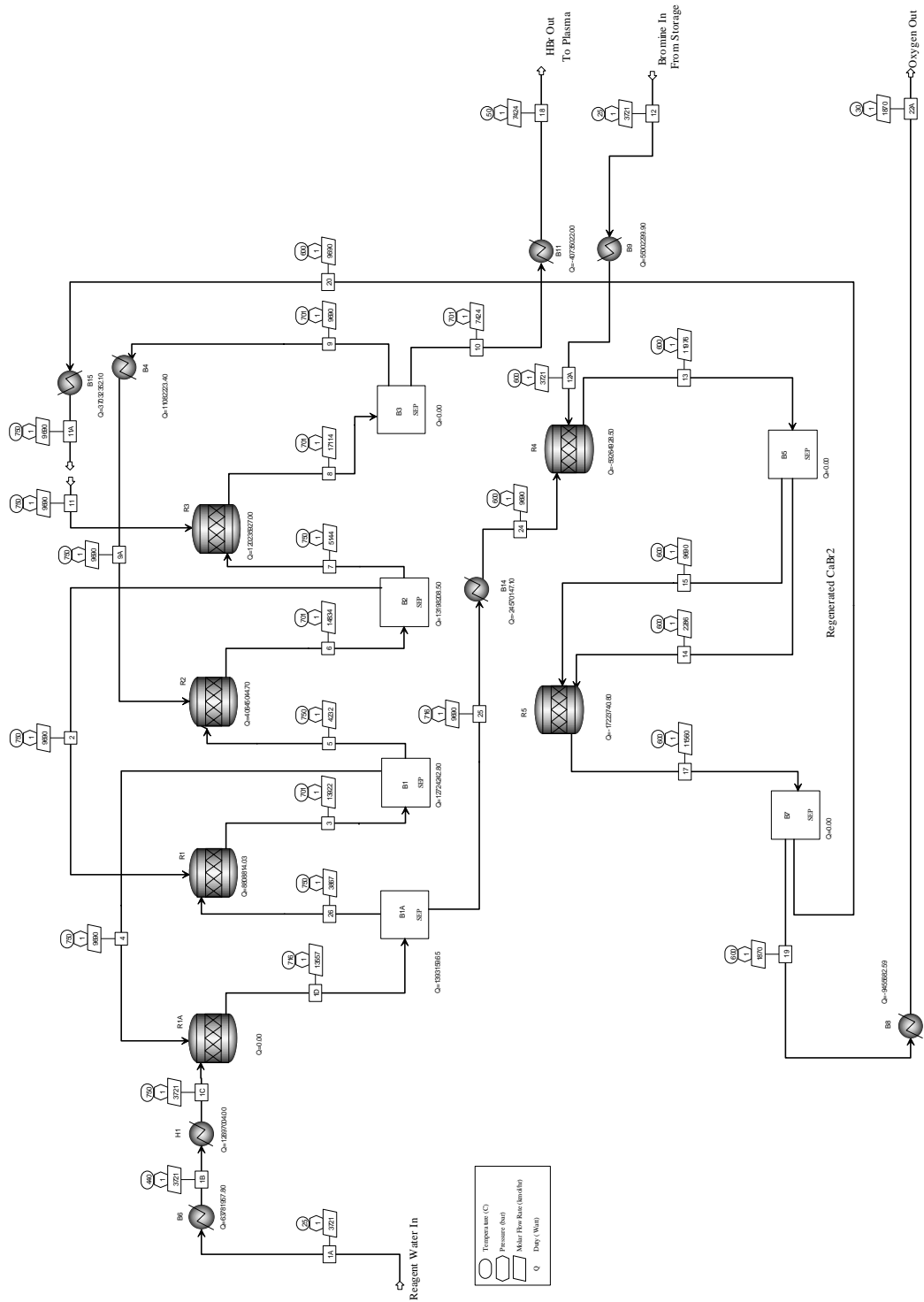


Figure 4. Stage 2 (plasmatron production of H₂) with pressure swing adsorption

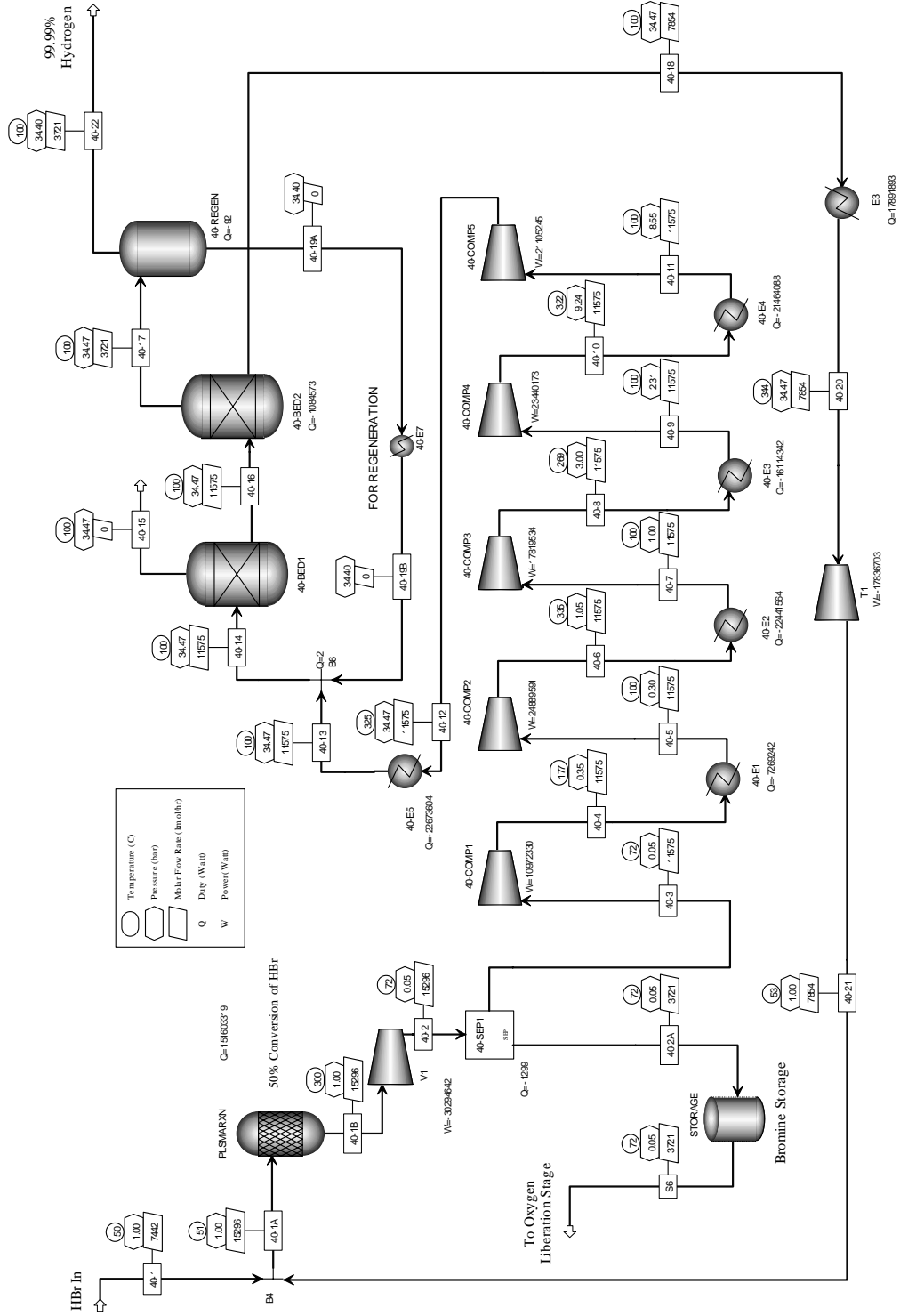


Table 1. Ca-Br water-splitting cycle heat balance

Basis: 1,000 kg/hr H ₂	T _{IN} (K)	T _{OUT} (K)	MW _{Thermal}		Efficiency %	MW _{Electric}
			IN	BRAYTON REJECT		
10 - Reagent Steam	325	1050	4.76			
20 - [1] CaBr ₂ + H ₂ O → CaO + 2HBr	1050	1000	32.68			
30 - [2] CaO + Br ₂ → CaBr ₂ + 1/2O ₂	850	850		-7.90	47.0%	-3.71
40 - [3] 2HBr → Br ₂ + H ₂ (50% conversion)	350	600		-1.68	75.0%	13.47
40 - Compression for Pressure Swing Adsorption	370	330	18.60	-11.07		
50 - Pressure Swing Adsorption - Recovery turbine						-2.26
60 - Electric Power Generation			18.02	-9.55	47.0%	-8.47
70 - Cooling Water	325	340				0.81
80 - Ancillary - controls, services, etc. (1.2%)						0.16
		SUM	74.06	-7.90	-22.31	0.00

Hydrogen Production (Lower Heating Value) = 33.333 MW_{Thermal} Efficiency_{Cycle} = 45.0%

While it currently is not an issue that has come into focus with the community, the use of cooling water and the assumptions that plant designs will continue to standardize on rejecting heat at current ambient conditions needs careful consideration. During the summer of 2003, the unprecedented heat wave led authorities across Europe to either shut down, or curtail by 20% both nuclear and fossil power plant operations. With low river flows and high water temperatures that were considered deleterious to river fauna, power plants across Europe faced shortages of cooling water they needed to operate normally. Further enhancement of the cycle may entail providing ancillary cooling during extremes operating conditions.

8. Materials considerations

From a practical point of view, an additional problem appears to be the choice of materials suitable for these operations. Vessels need to be resistant to corrosion from hydrobromic acid at temperatures of 750°C. Onay and Saito report on the metallurgy for this reaction series and find the greatest success with Fe-20Cr alloys. [11] Smudde et al. report favourably on Hastelloy C22 in HBr service. [12] The development of materials that can withstand the aggressive conditions of water-splitting will be a mandatory programme element.

9. Electric power production

The STAR-H2 Gen IV concept is tailored for energy market conditions predicted for the 2030s and beyond. In the production of multiple products – H₂, electricity, O₂, and fresh water – the plant will meet both its own internal power needs and the needs for delivery of power to the busbar. We plan to target two categories of clients: (1) utility clients in developing countries that are expecting to make *small incremental capacity additions* to their initially spare energy supply infrastructure, and (2) *merchant plant* clients in industrialized countries that wish to enter broadened energy service markets and that are dependent on hydrogen as an energy carrier. Both categories of clients will benefit from the exploitation of shared infrastructure based on grid delivery of electricity, H₂, potable water, and communications *through a common grid of easements* and for *distributed electricity generation architectures in urban settings*. In a distributed power system, the Gen IV based system could allocate process heat so that it would meet both an anticipated regional H₂ demand for transportation fuels and demands for electricity in the same region.

10. Fresh water production

Different types of multiple-effect (ME) desalination plants are possible, depending on the heat-exchange surface orientation, top temperature level, and heat source. In desalination service, ME plants appear to have an advantage over multi-stage flash (MSF) desalination plants. However, the ME arrangement has a major liability: the seawater feed stream enters the first effect at about the source temperature and, because of the multiple effects, the top temperature is usually about 50-70°C higher. To circumvent this problem, we will employ a design referred to as low-temperature multiple-effect (LTME) units. Advantages of the LTME process are less corrosion and the ability to use less-costly materials, such as aluminium tubes and low-carbon epoxy-coated shells. However, the reduced upper/lower temperature does lead to a thermal performance penalty and reduced potable water production. LTME units are the most common ME units in operation today and will serve as the basis for this design effort.

11. Steam electrolysis

Currently, alkaline electrolyzers that convert water to H₂ perform with an efficiency of 70-80%. Practical considerations frequently limit performance to the lower end of this range, with further modest losses from balance-of-plant issues for large-scale systems. For commercially available small production systems, the balance-of-plant issues tend to dominate the process inefficiencies; commercial 1-kg-H₂/h packages may perform at efficiencies as low as 44%, leading to an overall thermal efficiency 15-20% (for electricity produced with an efficiency of 33-47%). The operational simplicity of electrolyser systems represents a tradeoff against this lower performance. Inspection of the declining free energy of water formation as the temperature rises (Figure 2) suggests that steam-electrolysis could significantly improve the efficiency of electrolyzers. This idea has been investigated experimentally with the perspective that the high-temperature steam could be provided by an advanced nuclear cycle. Such cycles are of broader interest to the hydrogen community, and the DOE Office of Hydrogen is currently sponsoring by with the Idaho National Engineering Laboratory, Ceramtec (Salt Lake City, Utah), and Argonne National Laboratory to investigate the practical performance of steam-electrolysis cycles. If experimental efforts prove the practicality of this approach, the performance of these cycles could match that of the Ca-Br cycle (see Table 2).

Table 2. Steam-electrolysis performance if cell H₂O to H₂ conversion rates reach 90%

Basis: 1,000 kg/H ₂		H ₂ O conversion per pass = 90.0%		MW _{Thermal}		Efficiency	Electrolysis	MW _{Electric}
	T _{IN} (K)	T _{OUT} (K)	IN	REJECT	%	%		
10 - Reagent Steam	325	1025	9.374					
20 - Electrolysis Cell	1025	1025	60.722		47.0%	90.0%	28.539	
30 - O ₂ Product	1025	325		-0.122				
40 - H ₂ Product @ 4 bar (wet)	1025	325	1.503	-5.234				
50 - Compression @ 34 bar (dry)	325	325	1.438	-1.429				
70 - Cooling Water	325	340	0.523	0.277	47.0%			0.246
60 - Ancillary - controls, services, etc. (1.2%)			0.344	0.182	47.0%			0.162
		SUM	73.559	-6.785				28.947

$$\text{Hydrogen Production (Lower Heating Value)} = 33.3 \text{ MW}_{\text{Thermal}} \quad \text{Efficiency}_{\text{Cycle}} = 45.3\%$$

At present, conversion rates of H₂O to H₂ per pass are more typically 50% rather than 90%, so considerable development is required to see these higher efficiencies in a practical system. It is important to keep this conversion efficiency distinct from the efficiency with which the electricity supplied to the cell translates into water splitting. These cell efficiencies are typically reported at 90% or higher by the investigating teams.

For each tonne of H₂ produced hourly (1 000 kg/h), the much lower demand for electricity for the plasma-chemical stage (13.5 MW_e) compares favourably with the steam electrolysis power demand (28.5 MW_e). At current power grid heat-to-electricity efficiencies ($\eta = 33\%$), there is a clear benefit for the STAR-H2 Ca-Br cycle. Anticipating Brayton cycle performance ($\eta = 47\%$), H₂ production will demand a total power of 74 MW_{Thermal} per tonne of H₂ from the Gen IV reactor.

It is important to recognise that there are capital and operating cost tradeoffs that will depend on the market value of low-carbon electricity in the future. Steam-electrolysis is a far less complex cycle than Ca-Br, but that simplicity comes at a high – and potentially uneconomical – cost for electric power.

Acknowledgments

This effort was sponsored by the US Department of Energy's (DOE's) Nuclear Energy Research Initiative. The investigations of steam electrolysis are supported by DOE's Energy Efficiency and Renewable Energy (EERE) Office of Hydrogen. Both of the investigations described herein were conducted by Argonne National Laboratory under DOE Contract No. W-31-109-Eng-38.

REFERENCES

- [1] Besenbruch, G.E., *et al.*, “High-Efficiency Generation of Hydrogen Fuels Using Nuclear Power”, The First Information Exchange Meeting on Nuclear Production of Hydrogen, Paris, France, October 2000, Organisation for Economic Cooperation and Development (OECD) (2001).
- [2] Tadokoro, Y. and O. Sato, “Technical Evaluation of Adiabatic UT-3 Thermochemical Hydrogen Production Process for an Industrial-Scale Plant”, *JAERI Review* 98-22; 10.3 (1998).
- [3] Wade, D.C., *et al.*, “A Proposed Modular-Sized, Integrated Nuclear and Hydrogen-Based Energy Supply/Carrier System”, The First Information Exchange Meeting on Nuclear Production of Hydrogen, Paris, France, October 2000, OECD (2001).
- [4] Sakurai, M., *et al.*, “Analysis of a Reaction Mechanism in the UT-3 Thermochemical Hydrogen Production Cycle”, *International Journal of Hydrogen Energy*, Vol. 21, No. 10, pp. 871-875 (1996).
- [5] Sakurai, M., *et al.*, “Improvement of Ca Pellet Reactivity in the UT-3 Thermochemical Hydrogen Production Cycle”, *International Journal of Hydrogen Energy*, Vol. 20, No. 4, pp. 297-301 (April 1995).
- [6] Kondo, W., *et al.*, “Decomposition of Hydrogen Bromide or Iodide by Gas Phase Electrolysis”, *Bulletin of the Chemical Society of Japan*, Vol. 56, No. 8, pp. 2504-2508 (1983).
- [7] Wauters, C.N. and J. Winnick, “Electrolytic Membrane Recovery of Bromine from Waste Hydrogen Bromide Streams”, *American Institute of Chemical Engineering Journal*, Vol. 44, No. 10, pp. 2144-2148 (October 1998).
- [8] Nestor, S.A., B.V. Potapkin, A.A. Levitsky, V.D. Rusanov, B.G. Trysov, A.A. Fridman, Statistical Kinetic Modeling of Chemical Reactions in the Gas Phase [Kinetiko-Statisticheskoye Modelirovanie Chemicheskikh Reactsii v Gasovom Razryade] (in Russian), USSR Atomic Energy Committee, Kurchatov Institute, Moscow, p. 82 (1988).
- [9] Gutsol, A.F. and J.A. Bakken, “A New Vortex Method of Plasma Insulation and Explanation of the Ranque Effect”, *J. Physics D: Applied Physics*, Vol. 31, No. 6, pp. 704–711 (1998).
- [10] Gutsol, A.F. and V.T. Kalinnikov, “Reverse-Flow Swirl Heat Insulation of Plasma and Gas Flame”, *Teplofizika Vysokikh Temperatur*, Vol. 37, No. 2, pp. 194–201, (1999); *High Temperature Physics*, Vol. 37, No. 2, pp. 172–179 (1999).
- [11] Onay, B. and Y. Saito, “Corrosion Behavior of Fe-20Cr and Ni-20Cr Alloys in Ar-H₂O-HBr Gas Mixtures at 1000 K”, *Oxidation Metals*, Vol. 40, pp. 65–83 (1993).
- [12] Smudde, G.H. Jr., *et al.*, “Materials Selection for HBr Service”, *Corrosion Science*, Vol. 37, pp. 1931–1946 (1995).

INVESTIGATION ON A NEW HYDROGEN PRODUCTION PROCESS FOR FBR

Toshio Nakagiri*, **Taiji Hoshiya** and **Kazumi Aoto**
Japan Nuclear Cycle Development Institute
O-Arai, Higashi-Ibaraki, Ibaraki, 311-1393, Japan

Abstract

A new thermochemical and electrolytic hybrid hydrogen production process (thermochemical and electrolytic hybrid hydrogen process in lower temperature range: HHLT) is under investigation to realise the hydrogen production from water by using the heat generation of coolant in fast breeding reactor (FBR). HHLT is based on sulphuric acid (H_2SO_4) synthesis and the decomposition processes developed earlier (Westinghouse process), and sulphur trioxide (SO_3) decomposition process at about 500°C is facilitated by electrolysis with ionic oxygen conductive solid electrolyte which is extensively utilised for high-temperature electrolysis of water.

Decomposition of SO_3 were confirmed with the cell voltage lower than 0.5V at $500\text{-}600^\circ\text{C}$ using 8 mol yttria stabilised zirconia (8 mol YSZ) solid electrolyte and platinum electrode, furthermore, oxygen permeation rate through YSZ into N_2 purge gas agreed well with the calculated permeation rate from measured cell current. Preliminary measured oxygen permeation rate through $\text{La}_{0.9}\text{Sr}_{0.1}\text{Ga}_{0.8}\text{Mg}_{0.2}\text{O}_3$ (LSGM) in air supplied experiments were higher than the rate through 8 mol YSZ. These results show the possibility of development of higher performance electrolytic cell using other solid electrolytes than YSZ. Thermal efficiency of HHLT roughly estimated based on chemical reactions was 47.3% with no heat recovery.

Further investigations are planed on durability of the solid electrolytes and electrodes in SO_3 atmosphere at about 500°C , and on laboratory scale experimental apparatus to substantiate whole process of HHLT.

KEYWORDS: hydrogen, hydrogen production, thermochemical hybrid process, middle temperature range, solid electrolyte, electrolysis, sulphuric acid.

* Corresponding author, Tel. +81-29-267-4141, Fax. +81-29-267-7148, E-mail: naka@oec.jnc.go.jp

I. Introduction

More than 2 000-3 000 thermochemical hydrogen production processes have been proposed to produce hydrogen from water with no exhaust of CO₂ and with thermal efficiency higher than 40%, and application study for high temperature gas cooled reactor (HTGR) have been investigated for some decade [1]. Nevertheless, application study for fast breeder reactor (FBR) have not been performed because high temperature over 800°C was required for thermochemical processes.

A thermochemical and electrolytic hybrid hydrogen production process (thermochemical and electrolytic hybrid hydrogen process in lower temperature range: HHLT) for sodium cooled FBR is proposed by Japan Nuclear Cycle Development Institute (JNC) [2]. HHLT is based on sulphuric acid (H₂SO₄) synthesis and the decomposition processes (named “Westinghouse process”) developed earlier [1, 3], and SO₃ decomposition process is facilitated by electrolysis with ionic oxygen conductive solid electrolyte which is extensively utilised for high-temperature electrolysis of water.

In the present study, electrolytic SO₃ decomposition experiments using yttria stabilised zirconia (YSZ), preliminary experiments on ionic oxygen conductivity measurement of higher performance solid electrolytes and evaluation of thermal efficiency of HHLT based on chemical reactions were performed. Furthermore, advantages and technical problems of HHLT were discussed.

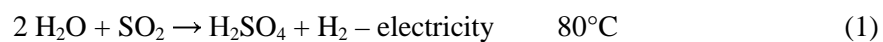
II. Principle and characteristics of HHLT

1. Principle of HHLT

Westinghouse process requires high temperature over 800°C only for SO₃ decomposition reaction, and other reactions can be performed below 500°C. If SO₃ decomposition can be performed in lower temperature than 800°C, hydrogen production using lower temperature heat source such as FBR can be realised, and corrosion problems depending on high temperature and corrosive atmosphere can be reduced.

SO₃ decomposed thermally only 7.8% at 500°C as shown in Figure 1, and also only about 20% in the case membrane reactor technique is used at 500°C. Therefore, some other energy is required to obtain higher decomposition fraction of SO₃.

Electrolysis by ionic oxygen conductive solid electrolyte is applied to increase decomposition fraction of SO₃ in HHLT. HHLT is composed from the reactions shown below.



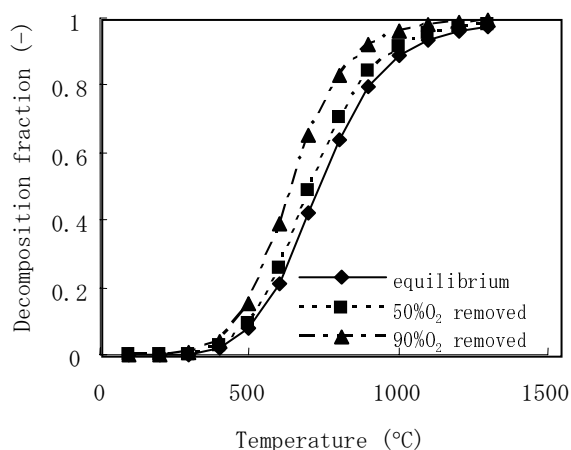
Characteristics of HHLT are shown below.

(1) Low electricity required

Required voltage for reaction (3) is calculated by equation (3) [4, 5]

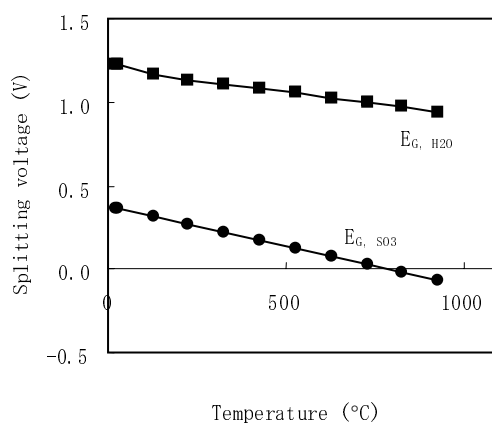
$$E_G = -\Delta G/(nF) \quad (4)$$

Figure 1. Thermal decomposition fraction of SO₃



Calculated splitting voltages of H₂O and SO₃ are shown in Figure 2, and splitting voltage at 500°C is lower than 0.2V. Theoretical voltage of sulphuric synthesis reaction [equation (1)] is 0.17V-0.28V [6, 7], therefore, total theoretical voltage in HHLT is expected to be lower than 0.5V which is about half of the theoretical voltage of direct water splitting, about 1V.

Figure 2. Splitting voltages of H₂O and SO₃



(2) *Simple process flow*

HHLT does not require decomposition and separation processes of HI, HBr and separation of O₂ which are required in I-S process or sulphur-bromide process, therefore, numbers of reactors are

much less than those of I-S process or sulphur-bromide process, and simple process flow can be achieved.

(3) *Decrease in corrosion of structural materials*

Corrosion of structural materials is expected to be suppressed in HHLT rather than I-S process etc. because high corrosive iodine or bromine is not used.

(4) *Higher safety*

In the high temperature on direct electrolysis of water by SOFC (solid oxide fuel cell), hydrogen and oxygen can be mixed at the temperature higher than spontaneous ignition temperature of hydrogen (500 C in air [8]). In the case solid electrolyte ceramics is failed, hydrogen explosion can take place, because the interface between hydrogen and oxygen is broken.

In HHLT, hydrogen is produced in reaction (1) at the temperature lower than 100°C, therefore, possibility of hydrogen explosion is considered to be quite a low.

2. *Technical problems to realise HHLT*

(1) *Proof of SO₃ electrolysis using solid electrolyte*

Electrical SO₃ decomposition reaction [reaction (3)] is the most important part of HHLT, but no experimental data about the reaction has been reported. JNC has performed experiments to confirm SO₃ decomposition using YSZ in the temperature range of 450 to 600°C, and to measure ionic oxygen conductivity in SO₃ atmosphere.

(2) *High performance solid electrolyte*

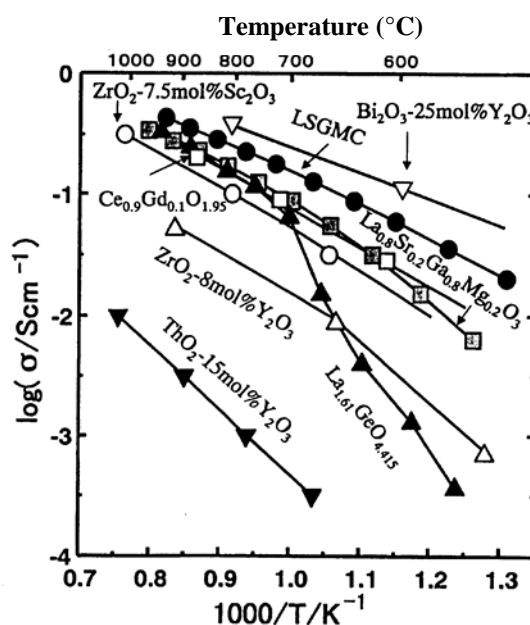
Two kinds of YSZs (3 mol YSZ, 8 mol YSZ) have been utilised in high temperature electrolysis, but ionic oxygen conductivity at about 500°C is not large enough to obtain realistic hydrogen production efficiency in HHLT. To obtain higher hydrogen production efficiency, higher ionic oxygen conductive solid electrolytes are necessary. Some solid electrolyte shown in Figure 3 [9] such as Ce-Sm-O, La-Ga-O, Bi-Y-O have almost equivalent ionic oxygen conductivities in the temperature range between 500°C and 600°C to those in YSZ in 800-1 000°C. Preliminary experiments to measure ionic oxygen conductivities in SO₃ atmosphere were performed using LSGM (La_{0.8}Sr_{0.2}Ga_{0.8}Mg_{0.2}O₃) and ScSZ (10 molSc/CeSZ).

(3) *Investigation of structural material*

Corrosion problem of structural materials in H₂SO₄ boiling environment is considered to be one of the severe issues in I-S process [1]. In HHLT process, this reaction [reaction (2)] can be performed in electrolysis cell which is composed of corrosion-resistant solid electrolyte ceramics, therefore, corrosion problem can be effectively reduced.

But, H₂SO₄ will be high corrosive aqueous solution to obtain higher efficiency in H₂SO₄ synthesis reaction [reaction (1)], so ferrous materials for piping or reactor for the concentration of H₂SO₄ [reaction (2)] must be investigated.

Figure 3. Arrhenius plots of ionic conductivity of oxides [9]



(4) *Development of electrolytic cell for H₂SO₄ synthesis*

Three-component electrolytic cell for H₂SO₄ synthesis has already developed by Struck et al. of KFA. Solid polymer electrolyte such as Nafion125 (DuPont), NEOSEPTA (Tokuyama Soda) were used in this cell. In recent years, higher performance solid polymer electrolytes have been developed, so higher performance electrolytic cell can be developed using these solid polymer electrolytes.

For H₂SO₄ synthesis cell, continuous SO₂ and H₂O supply, and continuous H₂SO₄ extraction with high efficiency, are required for continuous hydrogen production.

(5) *Substantiation of HHLT process*

In addition to the investigations shown above, test apparatus to substantiate whole process of HHLT must be developed. Actual efficiency of HHLT process, durability of structural materials under sulphuric acid, and performance of electrolysis cells, can be evaluated by using this substantiation apparatus.

III. Experiments and thermal efficiency calculation

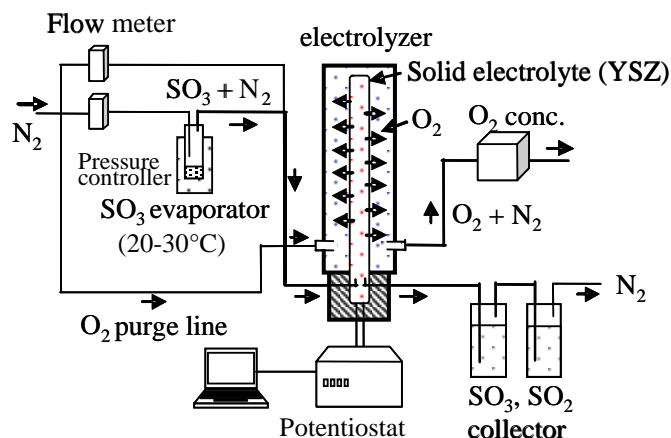
1. *Electrolytic SO₃ decomposition experiment*

(1) *Test apparatus and experimental conditions*

Electrolytic SO₃ decomposition experiments in the temperature range between 450 and 600°C were performed by test apparatus shown in Figure 4. Tubular 8 mol YSZ with a dimension of 2 mm in thickness was used as electrolyte, and Pt electrode was made on both (inner and outer) surfaces of the

tube. N_2 purge gas was supplied to SO_3 evaporator at flow rate of 200 ml/min, and SO_3 vapour was generated from the mixture of dry sulphuric acid and solid SO_3 . Concentration of SO_3 in N_2 gas was about 3%. SO_3 was supplied for about 10 minutes in each experiment. Electrolysis voltage was controlled from 0.0V to 1.0V by potentiostat, and cell current was measured simultaneously. O_2 decomposed from SO_3 was permeated through YSZ from inside to outside, and was carried to oxygen meter by N_2 purge gas (flow rate was 200 ml/min).

Figure 4. Test apparatus of SO_3 splitting experiment



(2) *Measured cell current and oxygen concentration in N_2 purge gas*

Obtained relationship between cell voltage and cell current is shown in Figure 5-a, and relationship between cell voltage and oxygen concentration in N_2 purge gas is shown in Figure 5-b. As shown in these figures, cell current and oxygen concentration in N_2 purge gas increased as cell voltage and cell temperature increased.

Figure 5-a. Relationship between cell voltage and cell current

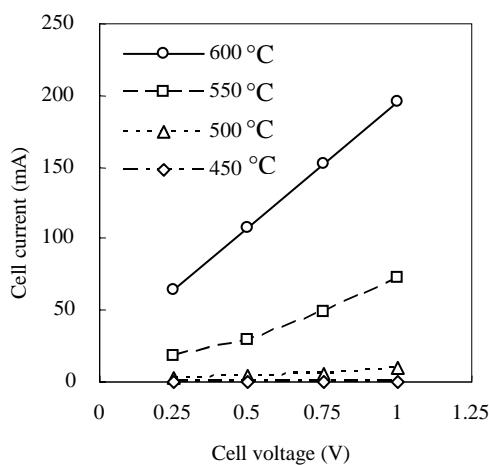
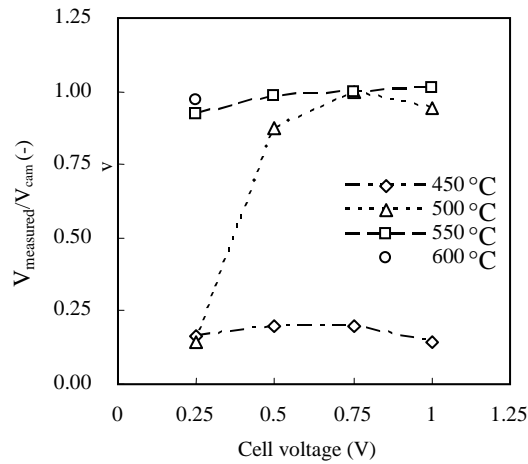


Figure 5-b. Relationship between cell voltage and O₂ concentration in N₂ purge gas

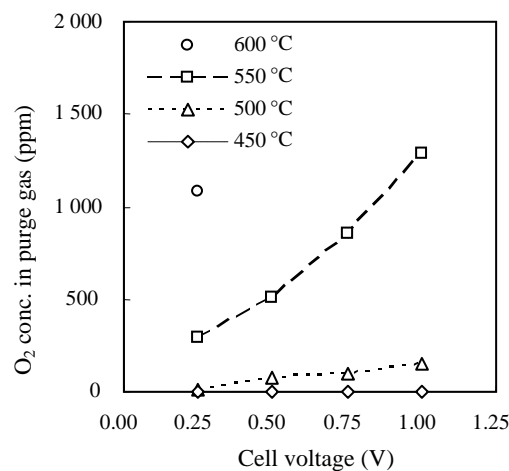


In the case supplied electricity is used only for ionic oxygen conduction, the relationship between cell current and oxygen permeation rate through YSZ into N₂ purge gas is calculated as follows[10].

$$v_{cal} = 0.115 (i/n) \quad (5)$$

The $v_{measured}/v_{cal}$ value calculated from measured oxygen concentration in purge gas and measured cell current are shown in Figure 6 (surface area of solid electrolyte is 158.8 cm²). The ratio is about 1.0 at temperatures higher than 550°C, and at the temperature of even 500°C when the cell voltage was higher than 0.5V, 100% of supplied electricity is considered to be used for ionic oxygen conduction in these cases. The ratio is lower at 500°C when the cell voltage was lower than 0.25V and at 450°C, and it is considered that other mechanisms which are not oxygen conduction consumed electricity.

Figure 6. $v_{measured}/v_{cal}$



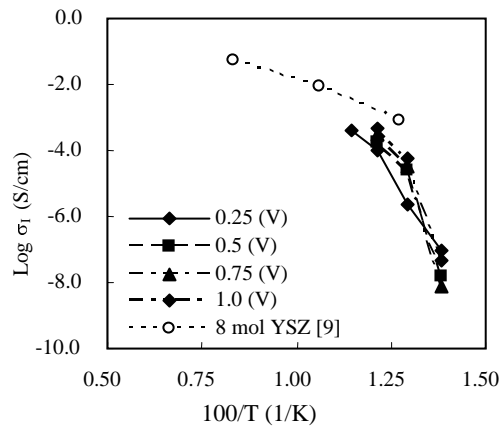
(3) *Oxygen ion conductivity of YSZ*

Oxygen ion conductivity was calculated from oxygen concentration in N₂ purge gas for the experiments at temperatures higher than 500°C by equation (6).

$$\sigma_i = i/E \cdot (v_{\text{measured}}/v_{\text{cal}}) \quad (6)$$

Calculated σ_i are shown in Figure 7 with the σ_i value for 8 mol YSZ [9]. Oxygen ion conductivity of YSZ in 3 mol% SO₃ atmosphere almost agrees with other experimental results.

Figure 7. Ionic oxygen conductivity calculated from oxygen permeation rate into N₂ purge gas



Furthermore, YSZ was used in SO₃ atmosphere for about 3h (about 20 experiments) in the temperature range of 450°C to 600°C in this study, but ionic oxygen conductivity did not decrease as shown in Figure 7.

(4) *Discussions*

From experimental results shown above, it was confirmed that electrolytic SO₃ decomposition using YSZ solid electrolyte is possible in the temperature range of 550°C to 600°C and at cell voltage lower than 0.5V, and in the case of 500°C the cell voltage higher than 0.5V is needed. Furthermore, ionic oxygen conductivity of YSZ in 3% SO₃ atmosphere almost agrees with other experimental results.

Nevertheless, SO₃ concentration in this experiment was only 3% which is much lower than the SO₃ concentration expected in HHLT, and YSZ was in SO₃ atmosphere only for 3h at 450°C to 600°C.

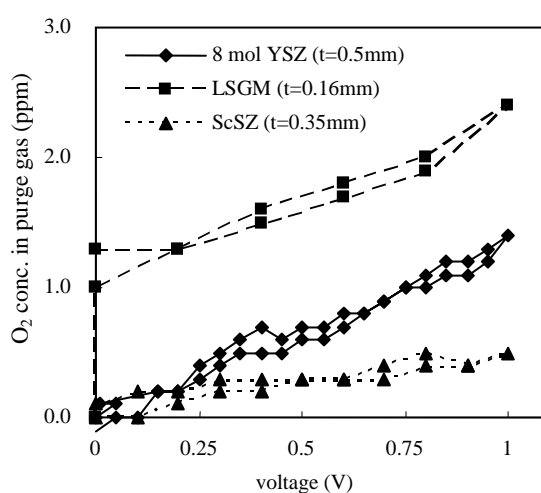
Therefore, experiments in higher SO₃ concentration over 50%, and experiments for more long time should be performed to investigate the degradation of solid electrolyte and electrode.

Furthermore, because of other solid electrolytes which have higher ionic oxygen conductivity must be investigated to obtain higher hydrogen production efficiency.

2. Preliminary experiment on ionic oxygen conductivity of solid electrolytes in SO_3 atmosphere

Preliminary experiments are now performed to obtain ionic oxygen conductivity of four solid electrolytes, 8 mol YSZ, ScSZ (10 mol Sc/SZ) and LSGM ($La_{0.8}Sr_{0.2}Ga_{0.8}Mg_{0.2}O_3$) in SO_3 atmosphere at $500^\circ C$. Test apparatus and instruments for measurement were almost same as electrolytic SO_3 decomposition experiment. Dimensions of the solid electrolyte samples were 17 mm square, and the thickness were 0.5 mm for 8 mol YSZ, 0.35 mm for ScSZ and 0.16 mm for LSGM, respectively. Pt electrodes with area of 0.5 cm^2 were made on both surfaces. Supplied gas was air, and several 100 ppm of SO_3 will be supplied as mixture of SO_3 and N_2 at flow rate of 100 ml/min. Flow rate of N_2 purge gas was 200 ml/min, and cell voltage was of 0.0V to 1.0V.

Figure 8. Measured oxygen concentration in N_2 purge gas



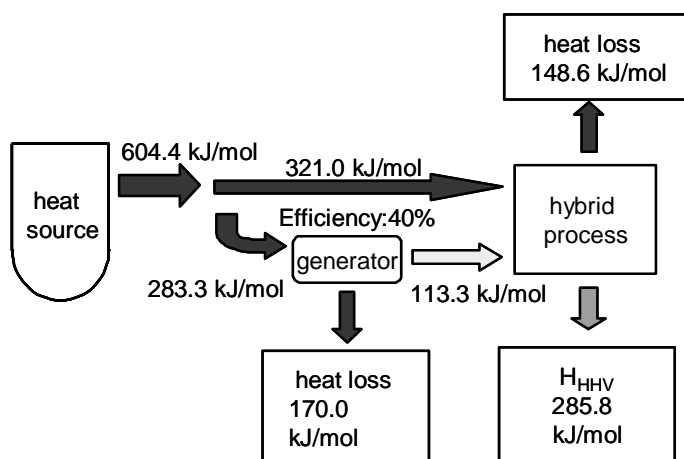
Measured oxygen concentration in N_2 purge gas in air supplied experiments are shown in Figure 8. However the thickness of LSGM sample was thinner about one third of 8 mol YSZ sample, oxygen concentrations in purge gas with LSGM were higher than the oxygen concentration with 8 mol YSZ, therefore, oxygen permeation rate with LSGM were considered to be higher than the rate with 8 mol YSZ in these experiments. These results show the possibility of development of higher performance electrolytic cell using other solid electrolytes than YSZ. Ionic oxygen conductivity and durability in SO_3 atmosphere must be clarified experimentally. Further experiments using new solid electrolytes such as, Ce-Sm-O and Bi-Y-O will be needed.

3. Evaluation of thermal efficiency

Thermal efficiency of HHLT considering chemical reactions [reactions (1)-(3)], latent heat and sensible heat, was evaluated. Electrical and thermal energies ($\Delta_r G$ and $\Delta_r H - \Delta_r G$) required for the reaction are shown in Table 1 and latent heat and sensible heat are shown in Table 2 [11]. Pressure used in the calculation was 1 bar ($=0.987\text{ atm}$). Energy flow from heat source and process flow of HHLT were shown in Figures 9 and 10, respectively. Reaction temperatures of reaction (1) and reaction (3) are $50^\circ C$ and $500^\circ C$, respectively, and reaction temperature of reaction (2) is $372^\circ C$ at which $\Delta_r G$ is 0. Electrical energy $\Delta_r G$ is converted from thermal energy with the efficiency of 40% which is almost the generation efficiency of FBR. Electrical energy and thermal energy required in

HHLT are 113.3 kJ/mol and 321.0 kJ/mol, respectively with no heat recovery in cooling processes C1-C4. Total thermal energy required for heat source is 321.0 kJ/mol+113.3 kJ/mol/0.4=604.4 kJ/mol.

Figure 9. Energy flow from heat source



Generally, thermal efficiency of hydrogen production process (η) is defined in equation (7) [12].

$$\eta = H_{\text{HHV}}/H_{\text{in}} \quad (7)$$

Thermal efficiency of HHLT is evaluated to be 0.473 (=47.3%) using equation (7) with no heat recovery.

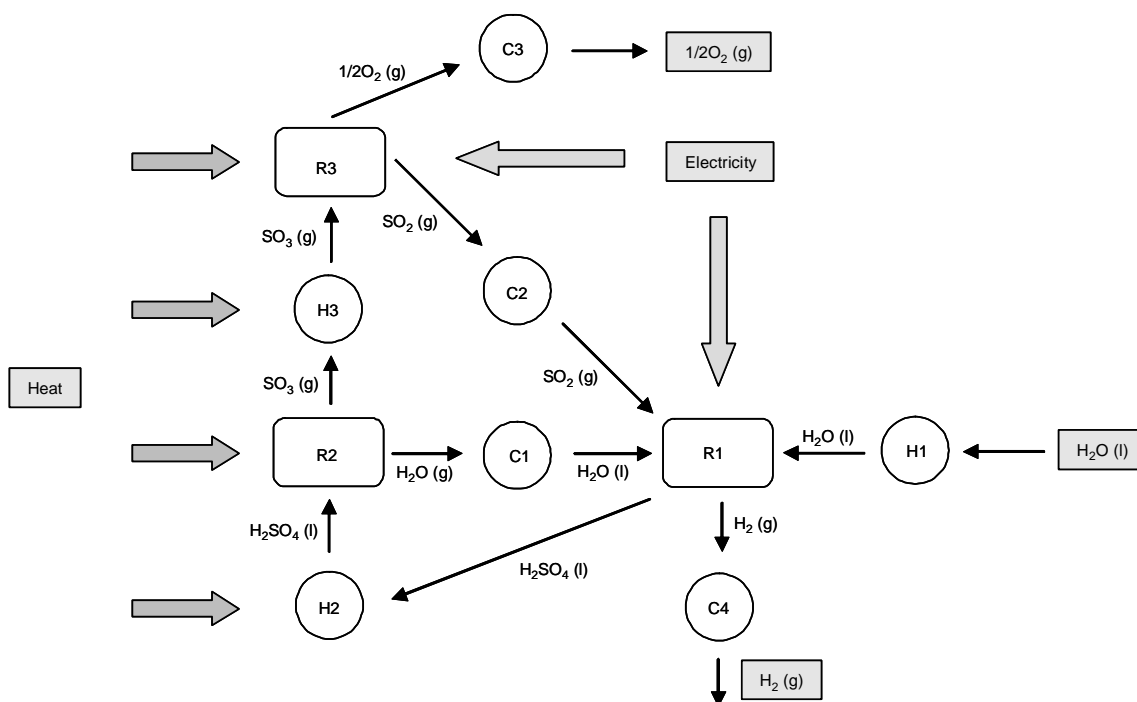
Table 1. Energies and entropy changes of reactions for new hybrid process

No.	Reaction	Reaction temp. (K)	(°C)	$\Delta_r H$ (kJ/mol)	$\Delta_r S$ (J/mol/K)	$\Delta_r G$ (kJ/mol)	T* $\Delta_r S$ (kJ/mol)
R1	$2\text{H}_2\text{O}(l)+\text{SO}_2(g)\rightarrow\text{H}_2\text{SO}_4(l)+\text{H}_2(g)$	323.15	50	54.1	-102.7	87.3	-33.2
R2	$\text{H}_2\text{SO}_4(l)\rightarrow\text{H}_2\text{O}(g)+\text{SO}_3(g)$	645.15	372	149.8	232.2	0.0	149.8
R3	$\text{SO}_3(g)\rightarrow\text{SO}_2(g)+1/2\text{O}_2(g)$	773.15	500	98.5	93.7	26.1	72.4
Total						113.3	189.1

Table 2. Required energies for heating or cooling gases or liquids

No.	Heating, cooling process	Temp. (°C)		Cp (J/mol/K)		Condense heat (kJ/mol)	H (kJ)
		Initial	Final	Initial	Final		
H1	H ₂ O(l) → H ₂ O(l)	25	50	33.59	33.75	–	0.9
H2	H ₂ SO ₄ (l) → H ₂ SO ₄ (l)	50	372	143.40	205.80	–	86.4
H3	SO ₃ (g) → SO ₃ (g)	372	500	68.67	72.12	–	11.5
C1	H ₂ O(g) → H ₂ O(l)	373.2	50	36.85	33.75	-43.0	-55.9
C2	SO ₂ (g) → SO ₂ (g)	500	50	52.04	40.77	–	-27.1
C3	1/2O ₂ (g) → 1/2O ₂ (g)	500	25	33.53	29.53	–	-8.2
C4	H ₂ (g) → H ₂ (g)	50		28.96	28.84	–	-0.4
	Total					–	7.3

Figure 10. Process flow of HHLT



In this evaluation, voltage loss in electrolytic cells, heat loss in heat transmission, energy loss in mass transfer, effect of gas concentration in cells and heat recovery are not included. These effects must be considered in the evaluation of practical efficiency.

IV. Conclusions

A thermochemical hybrid hydrogen production process (HHLT) for sodium cooled FBR is proposed, electrolytic SO₃ decomposition experiments using YSZ and evaluation of thermal efficiency of HHLT were performed taking into consideration of chemical reactions. Furthermore, advantages and technical problems of HHLT were considered and experiments to obtain the ionic oxygen conductivity in SO₃ atmosphere for some solid electrolytes are now performed. Conclusions are summarised as follows.

(1) Electrolytic SO₃ decomposition using 8molYSZ was capable at the voltage lower than 0.5V in the temperatures of 550°C to 600°C and at the voltage higher than 0.5V at 500°C. Therefore, electricity required for HHLT process is expected to be much lower than the electricity for direct water electrolysis. Measured ionic oxygen conductivities in 3% SO₃ almost agree with the values measure in other experiments. Ionic oxygen conductivity of 8 mol YSZ did not decrease after 20 (3h) experiments, and performance of YSZ and Pt electrode were not considered to be degraded.

(2) However the thickness of LSGM sample was thinner about one third of 8 mol YSZ sample, oxygen permeation rate through LSGM in air supplied experiments were higher than the rate through 8 mol YSZ. These results show the possibility of development of higher performance electrolytic cell using other solid electrolytes than YSZ. Ionic oxygen conductivity and durability of solid electrolytes in SO₃ atmosphere must be clarified experimentally.

(3) Evaluated thermal efficiency of HHLT process considering chemical reactions, latent heat and sensible heat was about 47.3% with no heat recovery. Voltage loss in electrolysis, heat transmission loss, concentration of gas in electrolysis cells, heat recovery should be considered in realistic evaluation.

Experiments shown below will be performed in this autumn.

- Experiments to investigate durability of the solid electrolytes and electrodes in SO₃ atmosphere at about 500°C.
- Experiment to substantiate whole process of HHLT in laboratory scale.

Nomenclature

E_G : splitting voltage (V)

ΔG : Gibbs energy change (kJ/mol)

n : number of electron (=2 for 1 oxygen atom)

F : Faraday constant

v_{cal} : calculated oxygen volume flow rate permeating into N₂ purge gas [cm³(STP)/sec/cm²]

i : cell current (A/cm²)

σ_i : ion conductivity (S/cm)

E : cell voltage (V)

η : thermal efficiency (-)

H_{HHV} : higher heat of hydrogen (=285.8 kJ/mol)

H_{in} : heat from heat source (604.4 kJ/mol in this paper)

Acknowledgement

The authors wish to thank Dr. S. Shimizu, Dr. K. Onuki, Dr. M. Nomura of JAERI for their advice and encouragement. Special thanks are due to Messrs. K. Takagi of KAKEN Co. and T. Sasaki of KRI Inc. who performed experimental work.

REFERENCES

- [1] IAEA, "Hydrogen as an energy carrier and its production by nuclear power", IAEA-TECDOC, 1085.
- [2] Kani, Y., "Investigation on hydrogen production by Fast Breeder Reactor (FBR)", Nuclear Viewpoints, Vol. 49, No. 1, 26, (2003), [in Japanese].
- [3] Weirich, W., K.F. Knoche, F. Behr, *et al.*, "Thermochemical processes for water splitting – Status and outlook", Nuclear Engineering and Design 78, (1984).
- [4] Tamura, H. *et al.*, "Hydrogen storage alloys – Fundamentals and Frontier Technologies –", NTS Inc., (1998), [in Japanese].
- [5] Takahashi, M. and N. Mashiko, "(Chemistry of industrial electrolysis)", Agune Inc., (1986), [in Japanese].
- [6] Struck, B.D., R. Junginger, D. Boltersdorf, *et al.*, "The anodic oxidation of sulfur dioxide in the sulphuric acid hybrid cycle", Int. J. Hydrogen energy, Vol. 5, (1980).
- [7] Struck, B.D., R. Junginger, H. Neumeister, *et al.*, "A three-compartment electrolytic cell for anodic oxidation of sulfur dioxide and cathodic production of hydrogen", Int. J. Hydrogen Energy, Vol. 7, No. 1, (1982).
- [8] National Astronomical Observatory, "Rika nenpyo (Chronological Scientific Tables)", Maruzen Co., Ltd, (1996), [in Japanese].
- [9] Ceramics Japan (Bulletin of the Ceramic Society of Japan), 36, No. 7, 483 (2001), [in Japanese].
- [10] Yamamura, H., H. Iwahara, "(Lattice defect and its application in material development)", IPC Inc., (2002), [in Japanese].
- [11] Chase, M.W. Jr., *et al.*, "JANAF Thermochemical tables third edition", American Chemical Society and American Institute of Physics, (1985).
- [12] Nomura, M. *et al.*, "Estimation of thermal efficiency to produce hydrogen from water through IS process", AIChE, (2003).

HYDROGEN PRODUCTION AT <550°C USING A LOW TEMPERATURE THERMOCHEMICAL CYCLE

Michele A. Lewis, Manuela Serban and John K. Basco

Argonne National Laboratory
9700 S. Cass Avenue, Argonne, IL 60439, USA
Email: lewism@cmt.anl.gov

Abstract

A Department of Energy goal is to identify new technologies for producing hydrogen cost effectively without greenhouse gas emissions. Thermochemical cycles are one of the potential options under investigation. Thermochemical cycles consist of a series of reactions in which water is thermally decomposed and all other chemicals are recycled. Only heat and water are consumed. However, most thermochemical cycles require process heat at temperatures of 850-900°C. Argonne National Laboratory is developing low temperature cycles designed for lower temperature heat, 500-550°C, which is more readily available. For this temperature region, copper-chlorine (Cu-Cl) cycles are the most promising cycle. Several Cu-Cl cycles have been examined in the laboratory and the most promising cycle has been identified. Proof-of-principle experiments are nearly complete. A preliminary assessment of cycle efficiency is promising. Details of the experiments and efficiency calculations are discussed.

I. Introduction

More than a hundred thermochemical cycles have been reported in the literature [1, 2]. Most did not survive the initial testing to validate the reactions within the cycle. Of the handful that did, only four have been developed further. Integrated laboratory scale demonstrations were conducted for the sulphur-bromine, the hybrid-sulphur, the sulphur-iodine, and the calcium-bromine or UT-3 cycles in glassware at atmospheric pressure. The corresponding hydrogen production rates in these demonstrations were 120, 100, 1, and 1 L/h., respectively [3, 4, 5, 6]. Further development of these cycles requires a pilot plant demonstration at temperature and pressure. All of the sulphur cycles require heat at 850-900°C for their oxygen generation reaction. This heat is expected to be available from a Gen IV reactor with an outlet temperature of 950°C [2]. Associated engineering and materials issues for this temperature region are challenging. Operating conditions are very aggressive: high temperatures, elevated pressures (up to 35 bars), an oxidising environment, and fuming sulphuric acid in the presence of water vapour. The Ca-Br cycles require slightly lower temperatures. The maximum temperature heat is expected to be 700-750°C [6]. The challenge associated with Ca-Br cycle is the stability of the calcium reagents as they cycle from CaBr_2 to CaO and back again. There is a 76% volume difference in the structures of the two materials. As cycling progresses, fines can form and the particles can sinter. The critical development step for this cycle is the development of supports that stabilise the calcium reagents.

Argonne has recently initiated an exploratory research effort to identify thermochemical cycles that operate with heat at temperatures less than 600°C. These lower temperature cycles can reduce the thermal burden and mitigate demands on materials. During the first phase of the work, we identified the family of Cu-Cl cycles as the most viable for temperatures between 500 and 600°C. Cycle development proceeds through a series of steps and includes the following: (1) evaluating thermodynamic feasibility; (2) establishing proof of principle with off-the-shelf reagents for each reaction and obtaining preliminary kinetic data; and (3) establishing proof of principle with recycled chemicals to determine the importance of competing reactions [1]. These data are used to design an integrated laboratory scale demonstration. Additional information is required for a pilot plant demonstration. The Lecart cycle is the first cycle we investigated [7]. Its maximum temperature is 570°C. Thermodynamic data suggested that the cycle was thermodynamically feasible. The oxygen and hydrogen generation reactions were validated. However, the reactions to close the cycle could not be validated. The combination of competing product formation and the high cost of Ag in the hydrogen production reaction negated further development of the cycle. We are concentrating our development efforts on a second Cu-Cl cycle, which was first identified by Carty et al. [1]. We refer to this cycle as the Argonne Low Temperature Cycle-1 (ALTC-1). ALTC-1 offers several advantages over the Lecart cycle: greater simplicity, lower capital costs, and potentially greater engineering feasibility. The only elements involved in this cycle are copper, chlorine, hydrogen and oxygen instead of the seven elements in the Lecart cycle. Cu metal is used in the hydrogen production reaction instead of Ag. Cu is plentiful and about 160 times cheaper than Ag. The ALTC-1 cycle has fewer reactions and the engineering design is expected to be more standard. One potential disadvantage with the ALTC-1 cycle is that one of the reactions is electrochemical, which imposes a significant energy cost. The ALTC-1 cycle is described in more detail below. The proof-of-principle results are discussed and preliminary estimates of the efficiency obtained.

II. Experimental

Reactor apparatus and materials

Because of the highly corrosive nature of the reactants and products of reaction, the thermal experiments were conducted in ½ by 14 in. Pyrex or quartz vertical microreactors depending on the

maximum desired temperature. All connecting lines and valves are made of Teflon. Anhydrous hydrochloric acid (99.99%) or argon (99.996%), from AGA Gas Central, were fed to the microreactor using Brooks 5850 mass flow controllers connected to appropriate power supply/readout units (Brooks 5876). The HCl mass flow controller is equipped with a corrosion resistant Kalrez[®] inert seal. The volumetric flow rates were varied between 2.5 and 15 cm³/min. HCl or Ar was fed through ¼ in. quartz or Pyrex feeding tubes extending all the way to the bottom of the ½ in. reactor. The temperature was controlled using an Omega CN375-type temperature controller connected to a Lindberg single zone heated furnace. The temperature inside the reactor was monitored with a K-type thermocouple placed adjacent to the reactor. The effluent gas composition was analyzed continuously using a QMS 200 mass spectrometer. The condensable products of reaction, i.e., H₂O and HCl were collected in a NaOH trap placed at the reactor exit. To avoid condensation, the cold zone of the reactor was heat traced using Omega heating tapes. A schematic of the experimental setup is given in Figure 1.

The mass spectrometer was calibrated for H₂, O₂, HCl, and Cl₂ using mixtures of pure gases with Ar over a wide range of compositions. Mass spectrometer analysis was performed at 8 s time intervals, and the amount of gaseous product of reaction detected on the mass spectrometer was quantified using the following formula:

$$V = \frac{A_g}{A_i} \times v_0 \times \tau$$

where: V is the net volume of gaseous product of reaction detected on the mass spectrometer (cm³), A_g is the integrated area of the gaseous product of reaction, A_i is the integrated area of the gaseous reactant or the inert gas signal, v_0 is the gas volumetric flow rate (cm³/min), and τ is the time of the experiment (min).

The weight hourly space velocities, when reported, were calculated according to:

$$WHSV = \frac{v_0 \times \rho}{W} \times 60$$

where: v_0 is the gas volumetric flow rate (cm³/min), ρ is the bulk density of pure or solid mixture (g/cm³), and W is the weight of pure or solid mixture (g).

Reagent grade reactants were used in all reactions. Copper (I) chloride (99.995%), copper (II) chloride hydrate (99+%), copper (II) oxide (99.995%) and dendritic and spheroidal copper (99.7%) were procured from Sigma-Aldrich. Between 0.5 and 2 g of pure or mixtures of solid reactants were loaded in the reactor depending on the experiment requirements.

Materials characterisation

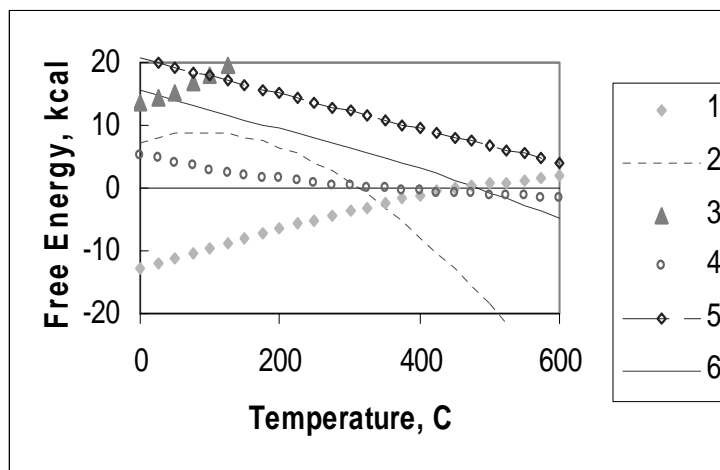
SEM analyses of the copper samples used in the hydrogen generation reaction were performed on a JEOL JSM-6 400 scanning microscope. XRD spectra of solid materials were measured with a Rigaku D/max-2 400V diffractometer using Cu K α radiation.

Table 1. Reactions in ALTC-1

Reaction number	Reaction	Expected temperature, °C	Free energy, kcal	Enthalpy, kcal
1	$2\text{Cu} + 2\text{HCl} = 2\text{CuCl} + \text{H}_2$	450	0.23	-11.200
2	$4\text{CuCl} + 4\text{Cl}^- = 4\text{CuCl}_2^-$	30	8.27	0.062
3	$4\text{CuCl}_2^- = 2\text{CuCl}_2 + 2\text{Cu} + 4\text{Cl}^-$	30	14.50	2.930
4	$2\text{CuCl}_2(\text{aq}) = 2\text{CuCl}_2(\text{s})$	100	6.00	19.900
5	$2\text{CuCl}_2 + \text{H}_2\text{O} = \text{CuO} + \text{CuCl}_2 + 2\text{HCl}$	400	9.50	27.900
6	$\text{CuO} + \text{CuCl}_2 = 2\text{CuCl} + 1/2\text{O}_2$	500	-0.71	30.900

The first step in cycle development is to determine its thermodynamic feasibility. The free energies and the enthalpies for the reactions shown in Table I were obtained from a commercially available thermodynamic database [8]. The free energies are plotted versus temperature in Figure 2. At the temperatures indicated in Table I, based on cycle stoichiometry to produce 1 mol of hydrogen, the free energy change of each reaction step is ± 10 kcal, except for the electrochemical step, which has a ΔG of 14.5 kcal at 25°C. We conclude that all of these reactions are thermodynamically viable based on the values of the free energies and estimated values for efficiency.

Figure 2. Free energy changes associated with reactions 1-6 in Table 1



According to Carty, reactions whose free energy change lies within ± 10 kcal for a given temperature are considered likely candidates for a cyclic process [1]. Small positive free energy changes are acceptable if nonequilibrium reactor configurations can be utilised, such as continuous product removal, reactants in excess, and/or pressure (where there is a smaller number of product

gases than reactant gases). Reactions with a positive free energy change of 10 to 25 kcal can generally be accomplished electrochemically.

An estimate of efficiency, E , suggested by Beghi [3] can be calculated from thermodynamic data, with the following equation:

$$E = \frac{\Delta G_f(H_2O)}{\Sigma Q_i}, \text{ where}$$

$$Q_i = \Sigma q_i + \Sigma W_i / \eta$$

where $\Delta G_f(H_2O)$ (-56.7 kcal/mol) is the free energy of formation of water at standard conditions, the Σq_i refers to the sum of the endothermic enthalpies (heat inputs) and ΣW_i is the sum of work inputs, which are converted to heat inputs by dividing the work inputs by the efficiency for converting heat to electricity, η . This calculation is referred to as the low heating value (LHV) basis. For the electrolytic step, we used an efficiency of converting heat to electricity of 0.33 for current reactors (PWR and BWR) and 0.5 for Gen IV reactors. The corresponding calculated LHV efficiencies for ALTC-1 where the only work input is the free energy for the electrochemical reaction are 46 and 52%, which are equivalent to 0.16 and 0.17 m³ hydrogen per kWt-hr. It is important to note that the energy required for other work inputs, such as compression and separation, any inefficiencies and irreversibility's, have not been included. Nevertheless, these preliminary estimates indicate that further development is justified.

More reliable efficiency values can be obtained after the chemistry of the cycle is well defined, that is, the kinetics and yields are optimised, and the sizes of any recycle streams are minimised. These data are inputs to a process design-modelling programme such as ASPEN™. Efficiencies are then recalculated iteratively as process design engineering is optimised.

After the thermodynamic feasibility study, proof of principle experiments were conducted at the temperatures suggested by thermodynamics to obtain kinetics and to assess the likelihood of side product formation. In the following sections, experimental results are presented for each individual reaction comprising cycle ALTC-1.

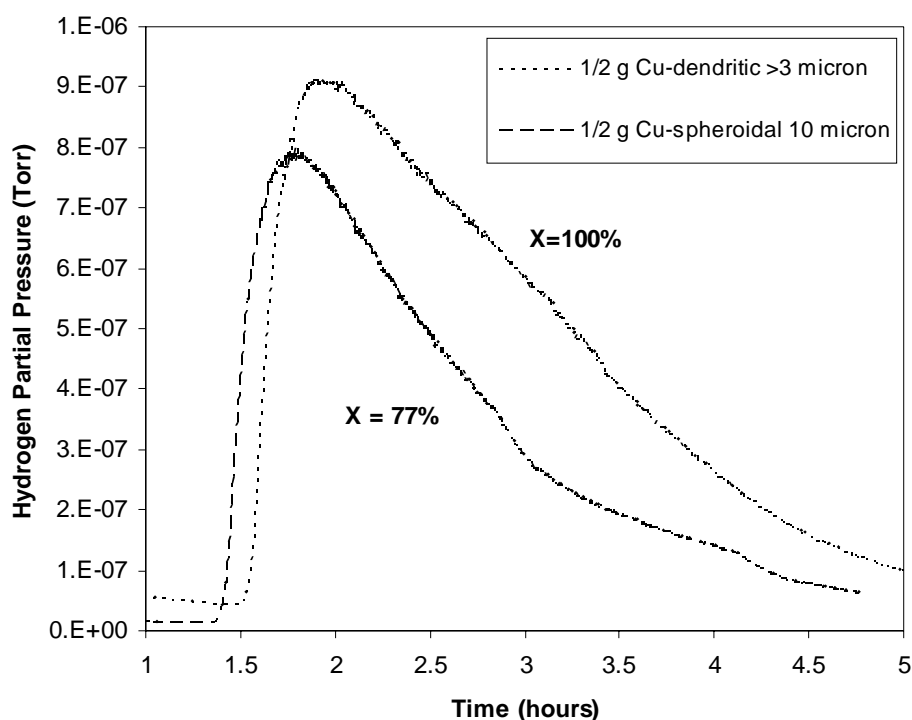
Hydrogen generation reaction



Hydrogen is generated when dry HCl gas is contacted with metallic Cu and the Cu is oxidized to CuCl. In our first experiments in which we monitored hydrogen evolution versus reactor temperature, a very small amount of hydrogen was formed at room temperature and essentially no additional hydrogen until the temperature reached 435°C. These results were surprising. It was reported that the exothermic reaction between Cu and HCl should proceed rapidly at 230°C and 93% of HCl should be decomposed [9]. However, no hydrogen was detected at this temperature, even though the Gibbs free energy change is -5.66 kcal at 230°C. Our experiments indicate that at low temperatures the kinetics of the reaction are very slow. In addition, we believe that CuCl forms a passivating layer on the surface of the Cu particles. At 430-435°C the CuCl starts to melt, facilitating the interaction between HCl and Cu. Similar experiments performed with Ag and HCl indicate the same behaviour [10].

In an attempt to find the best experimental conditions for complete Cu conversion to CuCl, experiments were performed with varying sizes and shapes of Cu particles as well as varying HCl flow rates. The objective is to measure the extent of reaction using well-defined conditions such that the results can be used to design a reactor for virtually complete reaction. Hydrogen evolution with time is shown in Figure 3 for reactions with two types of Cu particles, i.e., 10 micron, spheroidal in shape and >3 microns, dendritic in shape. The experiments were done in the fixed bed reactor with 0.5 g Cu. The corresponding yields were 77 and 100%. Another experiment was completed with 100-micron Cu particles and the yield in this experiment was 57%.

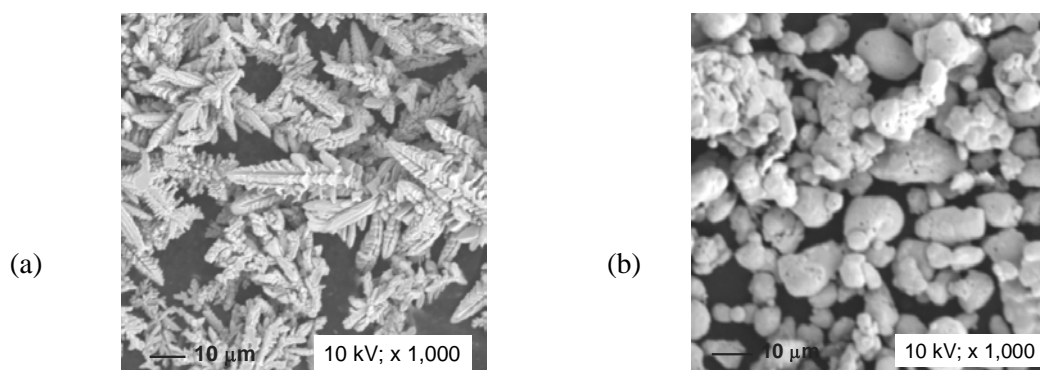
Figure 3. Hydrogen yields as a function of copper (commercial) particle size vs. time



These hydrogen yields were determined by comparing the measured amount of hydrogen produced vs. the stoichiometric amount of hydrogen that would be formed if all of the Cu were oxidized to CuCl. Hydrogen yields decreased with increasing Cu particle size, indicating that high surface areas of contact between HCl and Cu are necessary for high hydrogen yields. Figure 4 shows SEM images of the spheroidal and dendritic Cu particles used in the hydrogen generation reaction.

No gaseous products other than hydrogen and HCl were observed in the effluent stream. XRD examination of the solid product resulting from the reaction showed patterns only for CuCl and Cu. No secondary reactions are favoured in the temperature range studied. Thermodynamic computations indicate that when CuCl(s) is heated to very high temperatures CuCl(g) is formed, which would then spontaneously decompose to Cu and Cl₂ [11]. No Cl₂ was detected on the mass spectrometer at any time, suggesting that the extent of CuCl vaporisation was negligible.

Figure 4. SEM images of commercial Cu (a) dendritic >3 μm , (b) spheroidal 10 μm



To confirm the importance of the contact time between Cu and HCl, comparison experiments were performed with varying HCl flow rates through the bed of Cu metal. Hydrogen yields increased with decreasing flow rates, which is equivalent to increasing the contact time between the HCl and the copper metal as shown in Figure 5.

Figure 5. Hydrogen yields as a function of HCl volumetric flow rates

Reaction conditions: fixed bed reactor, temperature = 450 $^{\circ}\text{C}$, Cu particle size >3 micron dendritic

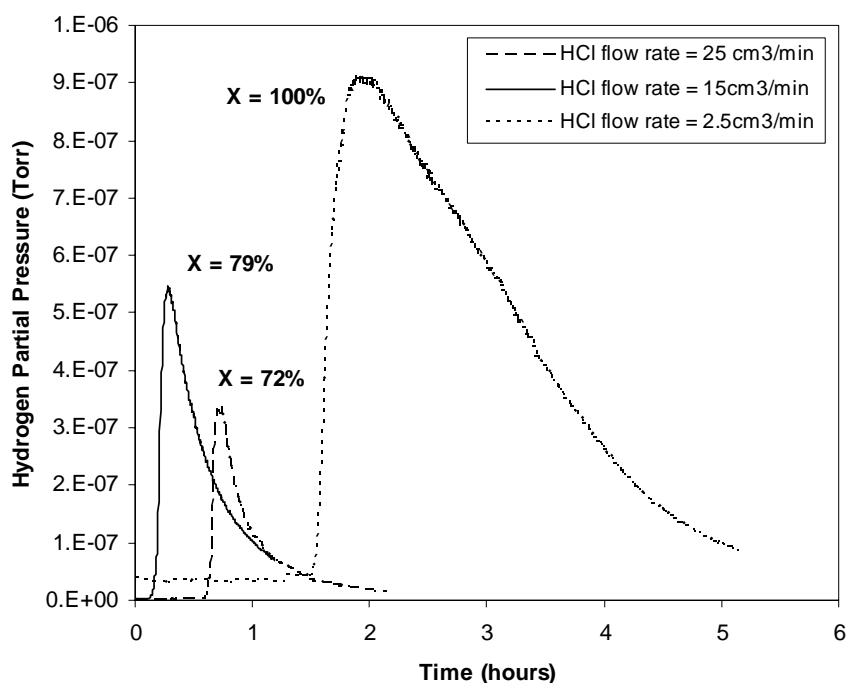
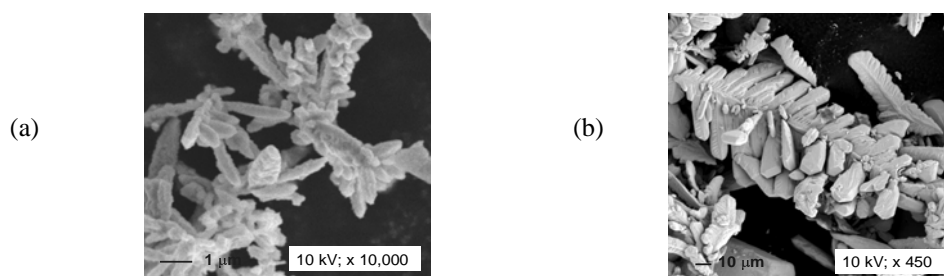


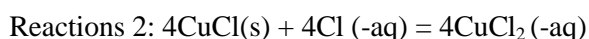
Figure 6. SEM images of electrochemical Cu (a) dendritic >3 μm , (b) >100 μm



The reaction was also performed with copper metal generated in the electrochemical cuprous chloride disproportionation (Reaction 3), described below. The reaction was run at 450°C, with an HCl flow rate of 2.5 cm³/min. The copper generated electrochemically has two different metal particle sizes, i.e., 2-4 and 100-micron particles as shown in Figure 6. The hydrogen yield was 65%, which may be due to the larger average particle size.

Kinetics experiments for the hydrogen generation reaction are currently being performed with dendritic >3 micron commercial Cu particles. The reaction rates are being measured at 4 different temperatures (400, 425, 430 and 450°C, respectively), and different molar ratios of HCl and Ar varied between 0.33 and 0.67. The experimental data will be fitted against proposed rate expressions, and the best kinetic model will be chosen based on the quality of the parity plots. Rate constants and activation energy for the above reaction will be determined.

Cuprous chloride electrolytic disproportionation



CuCl is very sparingly soluble in water but soluble in HCl. Proof of principle experiments for the electrochemical disproportionation of CuCl are therefore being conducted in an HCl aqueous solution. A solution of any soluble chloride salt could be used to form the chloro complex. As shown in Figure 6, the copper formed at the cathode is dendritic. The CuCl₂ formed at the anode is water-soluble and forms a solution whose colour varies with CuCl₂ concentration. A series of experiments in which the concentrations of HCl, CuCl₂, voltage, etc. are varied are on ongoing. These results will be published separately.

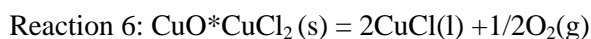
Hydrochloric acid formation



We believe that the sum of the work completed at ANL and GRI is sufficient to conclude that the reaction for forming HCl and CuO·CuCl₂ is proved [1]. For proof of principle experiments at ANL, CuCl₂·2H₂O was heated at 427°C. HCl production was detected by the pH change in the NaOH trap. In another set of experiments, CuCl₂·2H₂O was heated at 125°C in a Teflon[®] vessel for several days. The solids were examined by XRD and some Cu(OH)Cl, a precursor of the CuO, was observed. Work

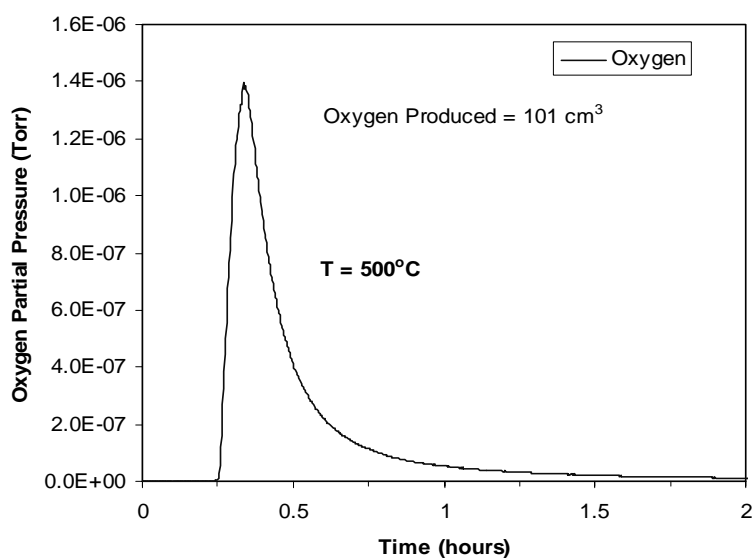
at GRI confirmed that a copper oxychloride was formed and Carty et al. represented this solid as $\text{CuO}\cdot\text{CuCl}_2$. For now, we have chosen to represent the $\text{CuO}\cdot\text{CuCl}_2$ as a simple mixture of CuO and CuCl_2 but this may change when actual material is available for XRD and other structural examinations. Ongoing experiments for reaction 5 include contacting off-the-shelf CuCl_2 with steam at 400-430°C to determine the kinetics of HCl formation and to prepare $\text{CuO}\cdot\text{CuCl}_2$ for further study. We also plan to conduct a series of tests with the CuCl_2 solution obtained from the electrochemical disproportionation reaction to determine optimum concentrations and to determine the effect of HCl carryover. We have included reaction 4 in Tables I and II to be conservative in our estimates of efficiency.

Oxygen generation reaction



A mixture of CuO and CuCl_2 generates O_2 at 500°C. In the experiment, 0.01 moles of CuO (0.8 g) and CuCl_2 (1.34 g) were used. Anhydrous CuCl_2 was obtained from dehydrated CuCl_2 by drying it in air at 175°C. The experiment was run in a flow-through type quartz vertical micro-reactor using off-the-shelf reagents and an Ar flow rate of 15 cm^3/min . With the bulk density of 4.853 g/cm^3 for the mixture CuO and CuCl_2 , the calculated space velocity is 2040 h^{-1} . The reaction was terminated after 45 minutes, and the oxygen yield was 85% (Figure 7). According to the thermodynamic equilibrium curves, at 500°C the reaction is incomplete with only 0.3 moles of O_2 (72 cm^3 O_2 from 0.02 moles of solids) being generated. However, since the reaction was run under non-equilibrium conditions, i.e., by continuously removing the O_2 from the reaction zone, the amount of oxygen generated surpassed the amount predicted by the equilibrium calculations. The only solid products of reaction were CuCl with traces of CuCl_2 as indicated by XRD examination.

Figure 7. Oxygen evolution function of time in reaction 6
*Reaction conditions: fixed bed reactor, temperature = 500 °C,
 0.01 moles CuO and CuCl₂ respectively, Ar flow rate = 15 cm³/min.*



Other reactions

A reaction that is specified in many high-temperature cycles that require chlorine is the reverse Deacon reaction, $\text{Cl}_2(\text{g}) + \text{H}_2\text{O}(\text{g}) = 2\text{HCl}(\text{g}) + 1/2\text{O}_2(\text{g})$ [12]. The nominal temperature for this reaction is 850°C. We are investigating the possibility of using catalysts to lower the temperature for the reverse Deacon reaction so that it is usable in a low temperature cycle. The chlorine would be obtained from the decomposition of CuCl_2 . The advantage of this modification is a slight improvement in overall cycle efficiency. Other reactions are also being examined.

Materials

Materials are an issue for nearly all thermochemical cycles because of the corrosiveness of the acids involved. For that reason, we are starting to identify suitable materials for the various reactions in the Cu-Cl cycle. For reaction 1, a candidate material is Inconel 600, which is reported to be suitable for operations with HCl gas at temperatures up to 525°C [13].

IV. Conclusions

The goals of the present study are to validate thermochemical cycles that operate at temperatures lower than 550°C and to obtain data necessary to design an integrated laboratory scale demonstration of an optimised cycle. Based on thermodynamics and preliminary experimental results we demonstrated the feasibility of the Cu-Cl cycle that was originally suggested by Carty et al. [1] and further refined by Argonne National Laboratory.

Cycle ALTC-1 has important potential advantages over the more mature sulphur and Ca-Br thermochemical cycles. The primary advantage is a lower maximum cycle temperature, which should allow greater flexibility in the heat source and materials. In addition, ALTC-1 has a reasonable thermodynamic efficiency, it does not involve expensive and harmful reagents, and it does not generate unwanted secondary or side reactions.

While each individual reaction comprising cycle ALTC-1 has been demonstrated experimentally, several other alternate reactions for closing the cycle or for generating oxygen are being pursued in parallel so that the most efficient cycle can be used in the integrated laboratory scale demonstration.

Acknowledgments

The work was supported by the US Department of Energy. The authors are grateful to Jay C. Knepper and James L. Willit for their helpful suggestions and stimulating discussions. We would also like to acknowledge Joseph S. Gregar for building the quartz reactors and Ben S. Tani for the XRD analyses. The authors are also grateful for the efforts of Sharon Clark in exemplary literature searching and Virginia Strezo for clerical support.

REFERENCES

- [1] Carty, R.H., M.M. Mazumder, J.D. Schreiber, J.B. Pangborn, *Thermochemical Hydrogen Production*, GRI-80-0023, Institute of Gas Technology, Chicago, IL 60616 (June, 1981).
- [2] Brown, L.C., J.F. Funk, S.K. Showalter, "High Efficiency Generation of Hydrogen Fuels Using Nuclear Power", GA-A23451, San Diego, CA (2001).
- [3] Farbman, H., "The Conceptual Design of an Integrated Nuclear-Hydrogen Production Plant Using the Sulphur Cycle Water Decomposition System", NASA-CR-134976 (1976).
- [4] Beghi, G.E., *Int. J. Hydrogen Energy*, **11**, pp. 761-771 (1986).
- [5] Nakajima, H. *et al.*, "A Study on a Closed-cycle Hydrogen Production by Thermochemical Water-splitting IS Process", Seventh International Conference on Nuclear Engineering (ICONE-7), ICONE-7104 Tokyo, (April 1999).
- [6] Tadokoro, Y., T. Kajiyama, T. Yamaguchi, N. Sakai, K.Yosida, M. Aihara, M. Sakurai, H. Kameyama, T. Sato, R. Amir, "Hydrogen Energy Progress VIII", p. 513 (1990).
- [7] Lecart, B., M. Devalette, J.P. Meunier, P. Hagemuller, *Int. J. Hydrogen Energy*, **4**, pp. 7-11, (1979).
- [8] HSC Thermochemical Database, Outokumpu Research Oy, Pori, Finland.
- [9] Mellor, J.W., *Treatise on Inorganic and Theoretical Chemistry*, Vol. 3, p. 157 (1962).
- [10] Ivashentsev, Y.I., A.I. Ryumin, *Zhurnal Prikladnoi Khimii* (Sankt-Peterburg, Russian Federation), **53**, pp. 2323-4 (1980).
- [11] Gupta, A.K., C.F. Sona, R.Z. Parker, E.J. Bair, R.J. Hanrahan, *Int. J. Hydrogen Energy*, **22**, pp. 591-599 (1997).
- [12] Yalcin, S., *Int. J. Hydrogen Energy*, **14**, pp. 551-556 (1989).
- [13] Kirk-Othmer Encyclopaedia of Chemical Technology, 4th Ed., Ed. M. Howe-Grant, Vol. 13, p. 912, John Wiley & Sons, New York, New York (1993).

SESSION III

NUCLEAR THERMOCHEMICAL PRODUCTION OF HYDROGEN WITH A LOWER-TEMPERATURE IODINE-WESTINGHOUSE-ISPRA SULFUR PROCESS

Charles Forsberg, Brian Bischoff, Louis K. Mansur and Lee Trowbridge

Oak Ridge National Laboratory*
P.O. Box 2008, Oak Ridge, TN 37831, USA
Tel: (1-865) 574-6783, Fax: (1-865) 574-0382
E-mail: forsbergcw@ornl.gov

Abstract

Thermochemical processes are the primary candidates to produce hydrogen (H₂) using high-temperature heat from nuclear reactors. The leading thermochemical processes have the same high-temperature chemical reaction (dissociation of sulphuric acid into H₂O, O₂, and SO₂) and thus all require heat inputs at temperatures of ~850°C. The processes differ in that they have different lower-temperature chemical reactions. The high temperatures are at the upper limits of high-temperature nuclear reactor technology. If peak temperatures can be reduced by 100 to 150°C, existing reactor technology can be used to provide the necessary heat for H₂ production and the H₂ produced using nuclear reactors becomes a much more viable near-term industrial option. If process pressures can be increased, significant reductions in capital cost and improvements in efficiency may be possible.

The use of inorganic separation membranes is proposed to drive the dissociation reaction to completion at lower temperatures and higher pressures. ORNL has developed a variety of inorganic membranes for commercial applications and has initiated a program to develop a membrane to separate SO₃ from its dissociation products. The basis for using such membranes is described herein. A test loop is being constructed, and membrane testing is expected to be initiated before the end of 2003.

* Oak Ridge National Laboratory, managed by UT-Battelle, LLC, for the US Department of Energy under contract DE-AC05-00OR22725. Accordingly, the US Government retains a nonexclusive, royalty-free license to publish or reproduce the published form of this contribution, or allow others to do so, for US Government purposes. Manuscript date: 6 September 2003. File: IS.Membrane.NEA.2003.Paper.

1. Introduction

Three of the four highest-rated H₂ thermochemical processes (hybrid, sulphur-iodine, and Ispra Mark 13) have the same high-temperature step that requires heat input at 850°C at -10 bar. [1] The highly endothermic (heat-absorbing) gas-phase reaction in each of these processes is as follows:



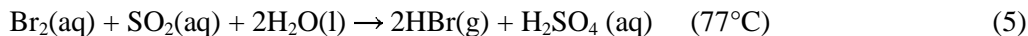
The three processes have different chemistries at lower temperatures. As shown in Figure 1, the “Base Case” high-temperature step on the left (Equation 1) can be coupled with any of the three sets of lower-temperature chemical reactions on the right to produce H₂. The sulphur-iodine process [1] has two other chemical reactions (Equations 2 and 3) that, when combined with Equation 1, (1) yield H₂ and O₂ from water and heat and (2) recycle all other chemical reagents.



The hybrid sulphur process (also known as Westinghouse, GA-22, and Ispra Mark 11) has a single electrochemical step (Equation 4) that completes the cycle. [2]



The Ispra Mark 13 process has one chemical reaction (Equation 5) followed by one electrochemical reaction (Equation 6) that completes the cycle.



In each of these cycles, the high-temperature sulphur trioxide (SO₃) dissociation reaction (Equation 1) is an equilibrium chemical reaction that requires heat and a catalyst. Table I shows this equilibrium [3, 4] as a function of temperature and pressure. *High temperatures and low pressures drive the reaction towards completion.*

Detailed studies have concluded that the peak temperatures need to be very high (850°C) to drive the SO₃ decomposition to near completion. After the high-temperature dissociation reaction, all the chemicals must be cooled to near room temperature, the SO₂ separated out and sent to the next chemical reaction, and the unreacted H₂SO₄ (formed by recombination of SO₃ and H₂O at lower temperatures) reheated back to high temperatures. Unless the chemical reactions go almost to completion, the energy losses in separations and in the heat exchangers to heat and cool all the unreacted reagents (H₂SO₄) result in a very inefficient and uneconomical process. This phenomenon is illustrated in Figure 2, in which the overall efficiency of one variant of the sulphur-iodine process [5] is shown as a function of temperature. In this flow sheet, the process inefficiencies (temperature losses in heat exchangers, etc.) increase so rapidly with decreasing temperature (incomplete SO₃ dissociation) that the process cannot produce H₂ at temperatures below 700°C.

Figure 1. Sulphur family of thermochemical cycles

03-157R

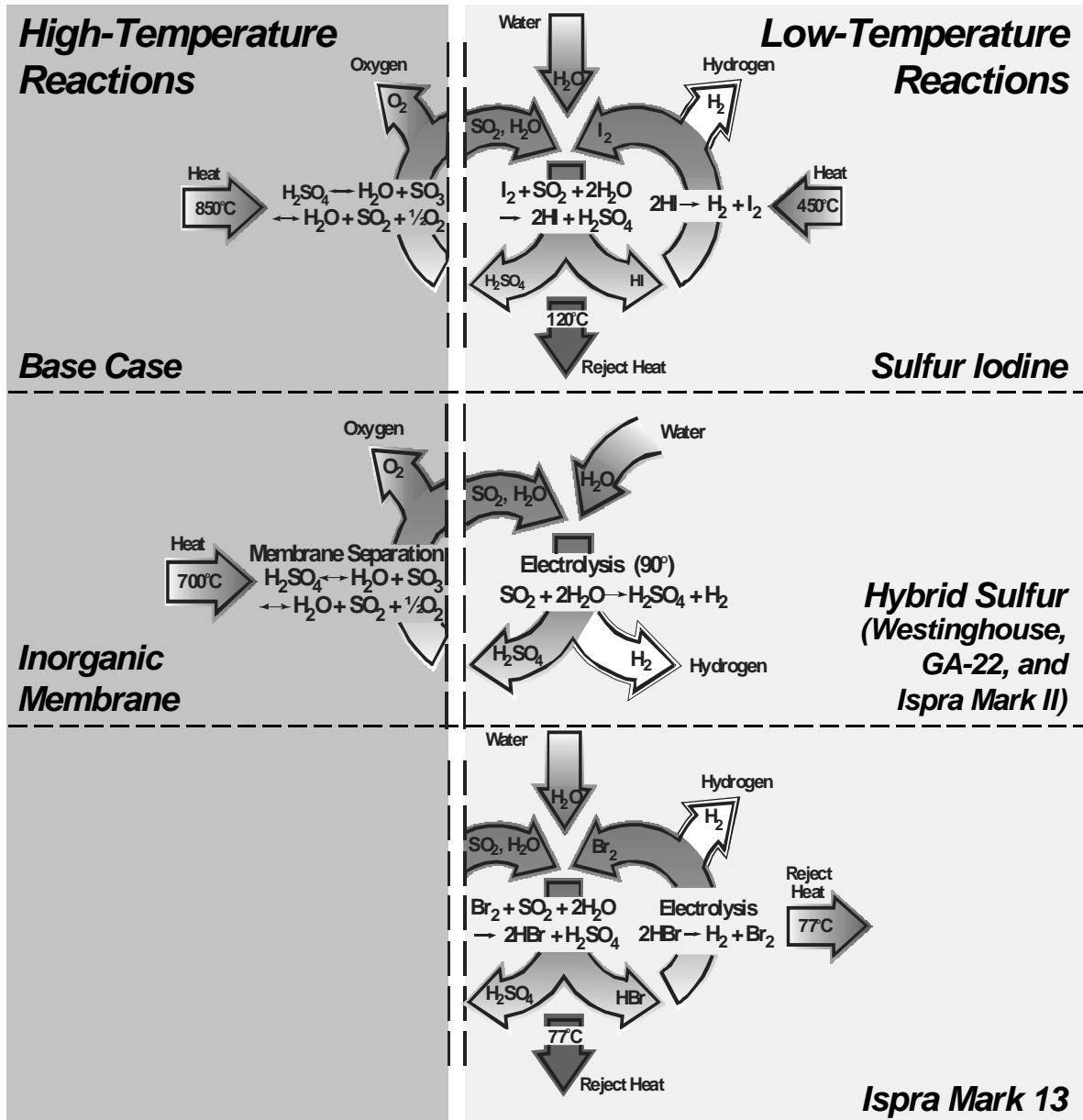
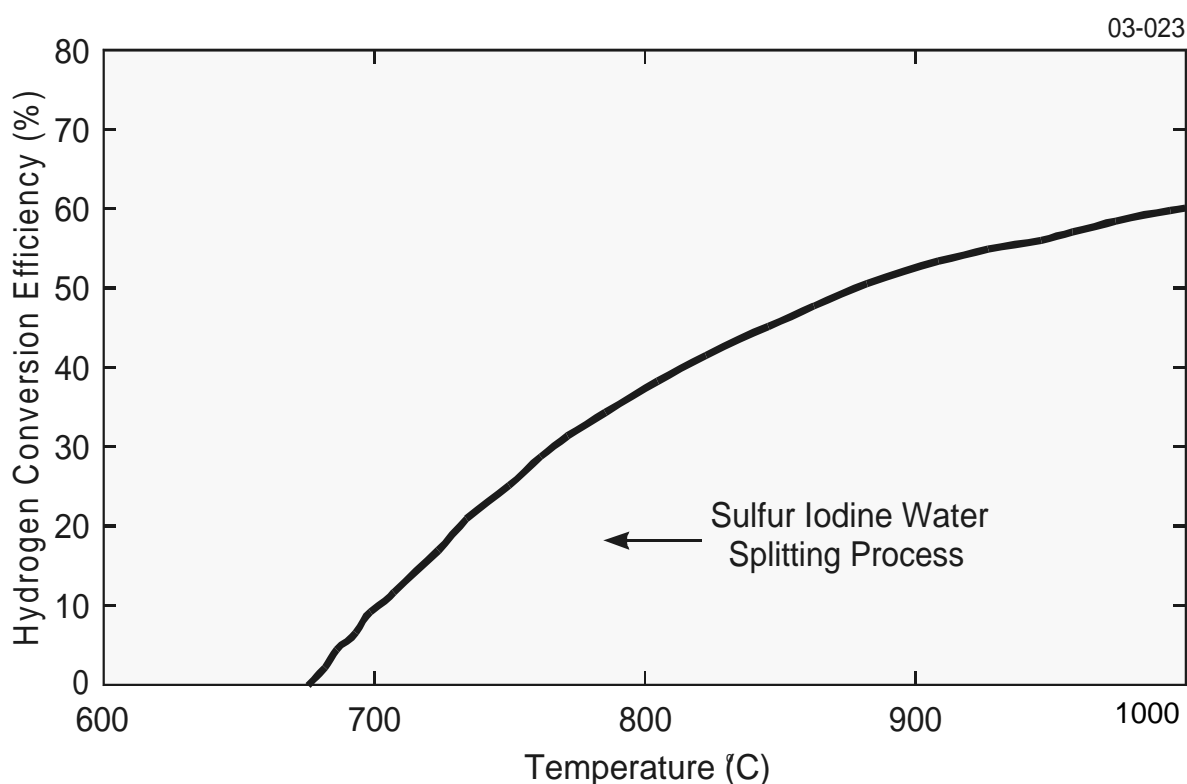


Table 1. Thermodynamic equilibrium for H₂SO₄ decomposition

Pressure (Bar)	Temperature (°C)	Equilibrium fraction of sulphur as		
		% SO ₂ (g)	% SO ₃ (g)	% H ₂ SO ₄ (g)
1	700	54	46	0.100
1	800	76	24	0.020
1	900	88	12	0.004
1	1 000	94	6	0.001
10	700	31	67	1.700
10	800	53	46	0.400
10	900	72	28	0.100
10	1 000	84	16	0.030
100	700	14	69	17.000
100	800	30	64	6.000
100	900	48	50	2.000
100	1 000	64	35	1.000

Figure 2. Efficiency of the iodine-sulphur process vs temperature



There are strong incentives to lower the temperature and increase the pressure at which SO₃ dissociates – the exact opposite of the conditions required by thermodynamic considerations.

1. *Lower temperatures.* A major challenge to thermochemical H₂ production is the high temperature required for efficient H₂ production, which is at the limits of nuclear reactor technology. After the temperature losses in heat exchangers between the reactor coolant and chemical plant are accounted for, the 850°C process temperature implies that the peak nuclear reactor temperature will be significantly higher. If this temperature could be lowered to 700°C, current [6] and advanced [7] designs of high-temperature reactors could be used for H₂ production. Lowering temperatures would also have major benefits in the thermochemical plant by reducing the costs and corrosion challenges in the high-temperature sections of the process.
2. *Higher pressures.* If the thermodynamics of SO₃ dissociation could be overcome, higher-pressure operation would improve economics and process efficiency. Higher pressures would reduce equipment size and gas compression losses. Moreover, higher pressures would improve efficiency for processes such as the hybrid process, in which the product SO₂ is separated from O₂ by sorption in water. At low pressures, the water must be refrigerated to absorb the SO₂. At higher pressures, this absorption occurs above room temperature and no refrigeration plant is required.

We propose to shift the SO₃ dissociation equilibrium to SO₂ and O₂ at lower temperatures and higher pressures by the use of an inorganic separation membrane. [8] The peak temperature may be lowered by up to 150°C. This is accomplished by the separation of SO₂, H₂O, and O₂ from the SO₃ at 650 to 750°C. If these reaction product gases are removed, the remaining SO₃ (with a catalyst and heat) will disassociate into its equilibrium concentrations. If the reaction gases can continue to be selectively removed, the chemical reaction can be driven to completion. The membrane operates with high pressure on one side and a lower pressure on the other side, and this pressure difference drives the separation process.

Inorganic membranes have historically been used to separate uranium isotopes by gaseous diffusion. In recent years, Oak Ridge National Laboratory has developed several inorganic membranes for chemical separations. These membranes are now commercial products. Work has been initiated on inorganic membranes to separate SO₂, H₂O, and O₂ from SO₃. This paper describes the initial analysis and characteristics of these membranes. An experimental test system is under construction to test these alternative membranes.

II. Altering the equilibrium SO₃ dissociation with inorganic separation membranes

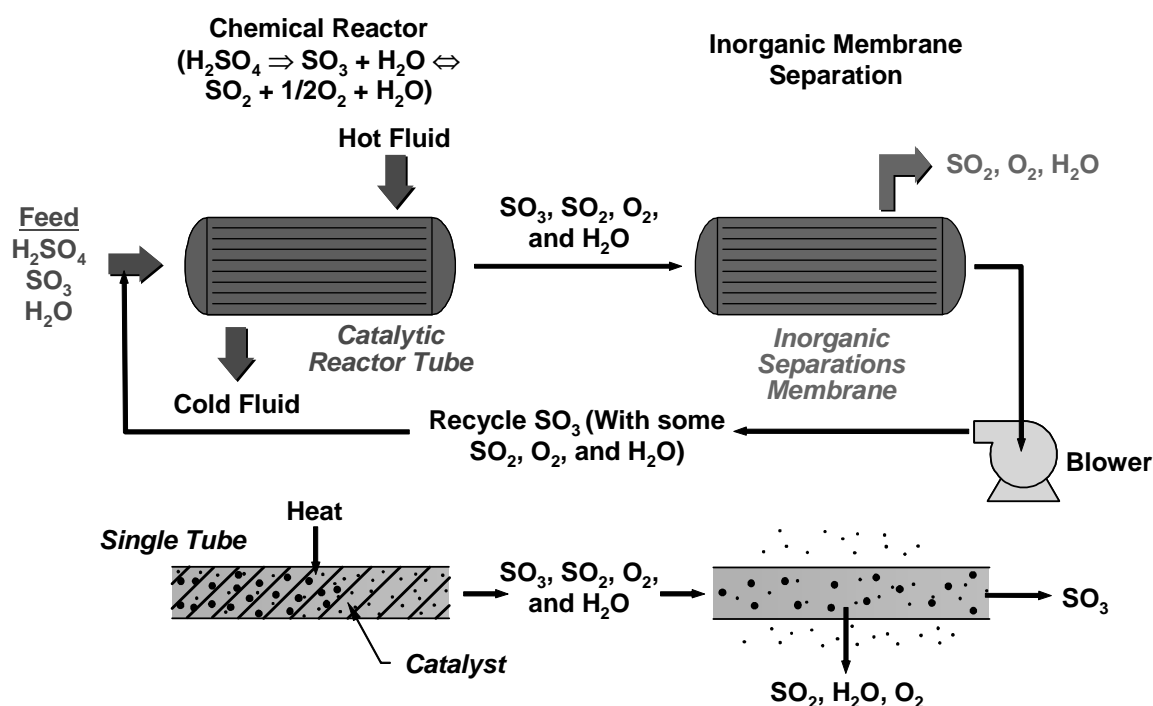
Figure 3 shows a schematic of an idealised high-temperature chemical reactor with inorganic membrane separator. The top of the figure shows the arrangement of equipment while the bottom of the figure shows the reactions within tubes within the main process equipment.

- *Dissociation.* The vaporised mixture of H₂SO₄, SO₃, and H₂O enters the chemical reactor, where the catalyst with added heat dissociates the SO₃ into SO₂ and O₂. (The H₂SO₄ does not require a catalyst to dissociate into SO₃ and H₂O.) The design of the chemical reactor is similar to a heat exchanger where the catalyst is inside the tubes enabling the heat-absorbing chemical dissociation to occur. The hot fluid that transfers heat from the nuclear reactor to the high-temperature chemical reactor will likely be either helium or a molten salt.
- *Membrane separation.* The resulting SO₃, SO₂, O₂, and H₂O mixture from the chemical reactor flows into an inorganic membrane separator. Some fraction of the SO₂, H₂O, and O₂ reaction products flows through the membrane walls into a lower pressure zone and onto the rest of the thermochemical cycle.

- *Recycle of unreacted chemicals.* The gases that did not flow through the membrane walls and exited the ends of the membrane separation tubes (SO_3 with some remaining SO_2 , O_2 , and H_2O) are compressed, mixed fresh feed, and flow back to the chemical reactor, where more of the SO_3 dissociates. Unreacted chemicals are recycled through the system until decomposed and flow through the membrane walls. The pressure drop across the chemical reactor (catalyst bed) and through the membrane separator (but not the membrane wall) is low. With an ideal membrane, the SO_3 can be fully decomposed. With real membranes, some fraction of the SO_3 will flow through the membrane with the SO_2 , H_2O , and O_2 .

Figure 3. Membrane reactor system with recycle of unreacted reagents

03-169



III. Principles of inorganic membrane operations

Membrane separation processes operate by having a higher pressure on one side of the membrane and lower pressure on the other. The relative rates of transport of different molecules through the membrane determine the capability of the membrane to separate different gases. There are multiple gas-transport mechanisms [9]: viscous flow, molecular diffusion, Knudsen diffusion (basis for isotopic separation of uranium isotopes by gaseous diffusion), surface diffusion, capillary condensation, and nanopore diffusion. The precise transport mechanism that is dominant for each gas depends upon a variety of physical factors including temperature (T), pressure (P), molecular mass (m), pore diameter (d_p), molecular size and shape, pore surface composition, pore morphology, and mutual interactions between molecules traversing the membrane.

For high-temperature separations, an inorganic membrane using nanopore diffusion is preferred. This is a term that encompasses several distinct mechanisms that take place in nanometer-diameter pores. For larger molecules, the membrane may function effectively as a molecular sieve, eliminating the transport of molecules through the membrane and giving high separation factors. For smaller

molecules, the transport exhibits thermally activated behaviour – that is, as the temperature is increased, the permeance (membrane throughput per unit area) increases exponentially, rather than decreases as in Knudsen diffusion. One thermally activated mechanism that has been understood is termed “gas translational diffusion”. It is also referred to as “thermally activated Knudsen diffusion”, where again molecules jump between pore walls but with an activation barrier that must be overcome in order to make a diffusion jump. This thermally activated characteristic is similar to the diffusion of defects or atoms in the solid state in the presence of traps, with an activation energy (E_d). Physically this is plausible, since the lower limit on size of a pore must correspond to interatomic spacing in the solid state. In the regime for $d_p \sim 1$ nm, separation factors >100 are possible. For example, Uhlhorn et al. report [10] that a separation factor >200 has been measured for a mixture of H_2 and C_3H_6 gases using a supported amorphous silica membrane with a pore diameter of ~ 1 nm.

Nanopore separations improve with temperature. In contrast, separation processes such as Knudsen diffusion, which decrease with temperature, are not candidates for high-temperature separations because of the low throughput of inorganic membranes. The separation factor for a mixture of two gases is defined as $[y/(1-y)] [(1-x)/x]$. Here, y is the concentration of the fastest-permeating component on the permeate side of the membrane and x is the concentration of the fastest-permeating component on the feed side. The experimentally measured performance for one simple system is shown in Figures 4 and 5. Figure 4 shows how the separation factor for a nanoporous membrane separating helium from SF_6 changes with temperature, while Figure 5 shows the dramatic increases in membrane permeability (throughput) as the temperature of such membranes increases.

IV. Process efficiency

From a thermodynamic perspective, lower temperatures would be expected to reduce the process efficiency because mechanical work is required to provide the pressure difference (a few bar) across the inorganic membrane to drive the separation process. In practice, it is unclear whether the process will be more efficient or less efficient. The irreversible losses in heat exchangers to heat and cool reagents are the primary source of inefficiencies between an ideal process and the real process. Inorganic membranes reduce these inefficiencies by driving the high-temperature reactions to completion and thus reduce the quantities of unreacted chemicals recycled in the process. Ongoing work is under way to quantify these effects.

If higher temperatures become available, a strong incentive remains to use inorganic membranes because the membranes allow the dissociation reaction to proceed at higher pressures (Table 1). Higher pressures reduce equipment size and improve efficiency. Economics drives many chemical processes to operate near 100 bar. Based on these considerations, there are incentives to use inorganic membranes at temperatures to $1\ 000^\circ C$.

Figure 4. Separation factors for the He/SF₆ system vs temperature at different pressures for membrane 2528

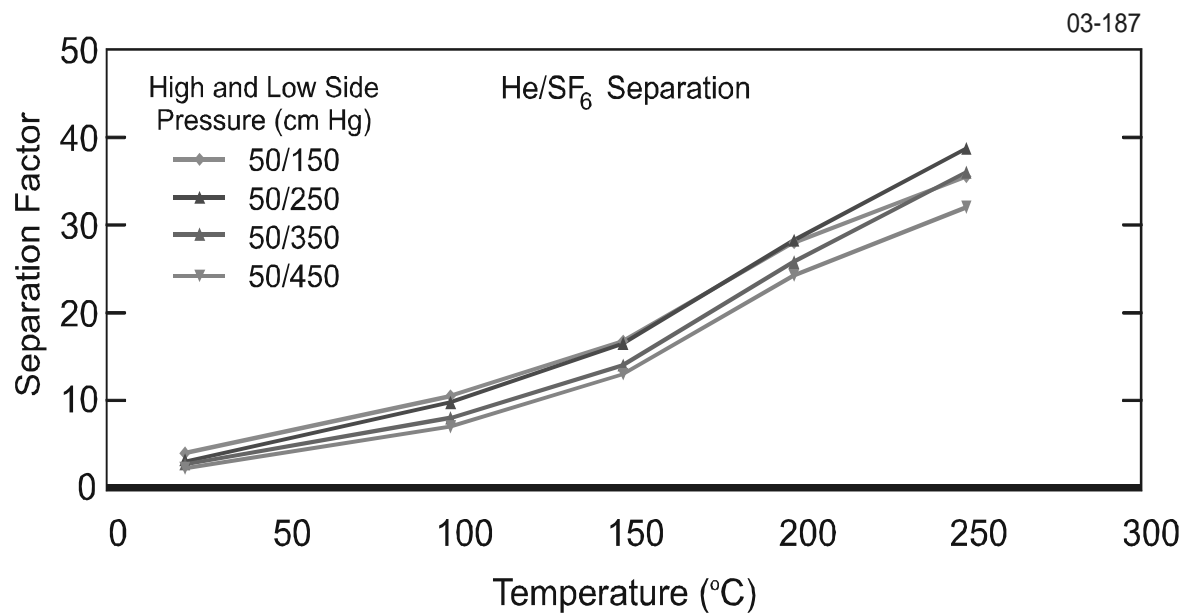
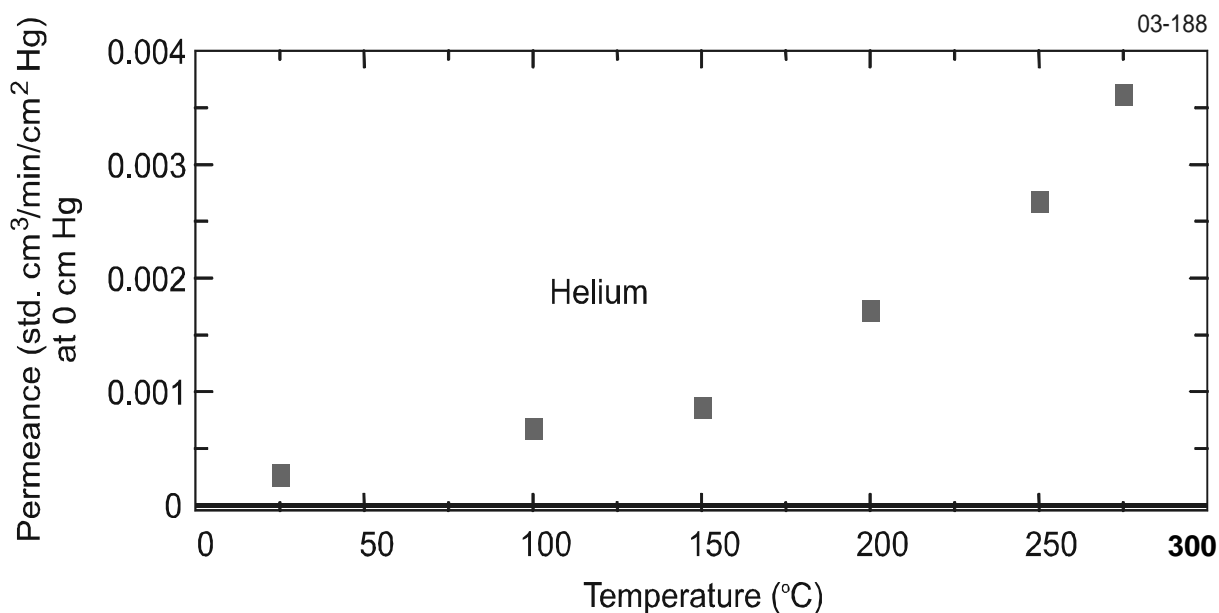


Figure 5. Helium permeance vs temperature for membrane 1230252-8a



V. Experiments

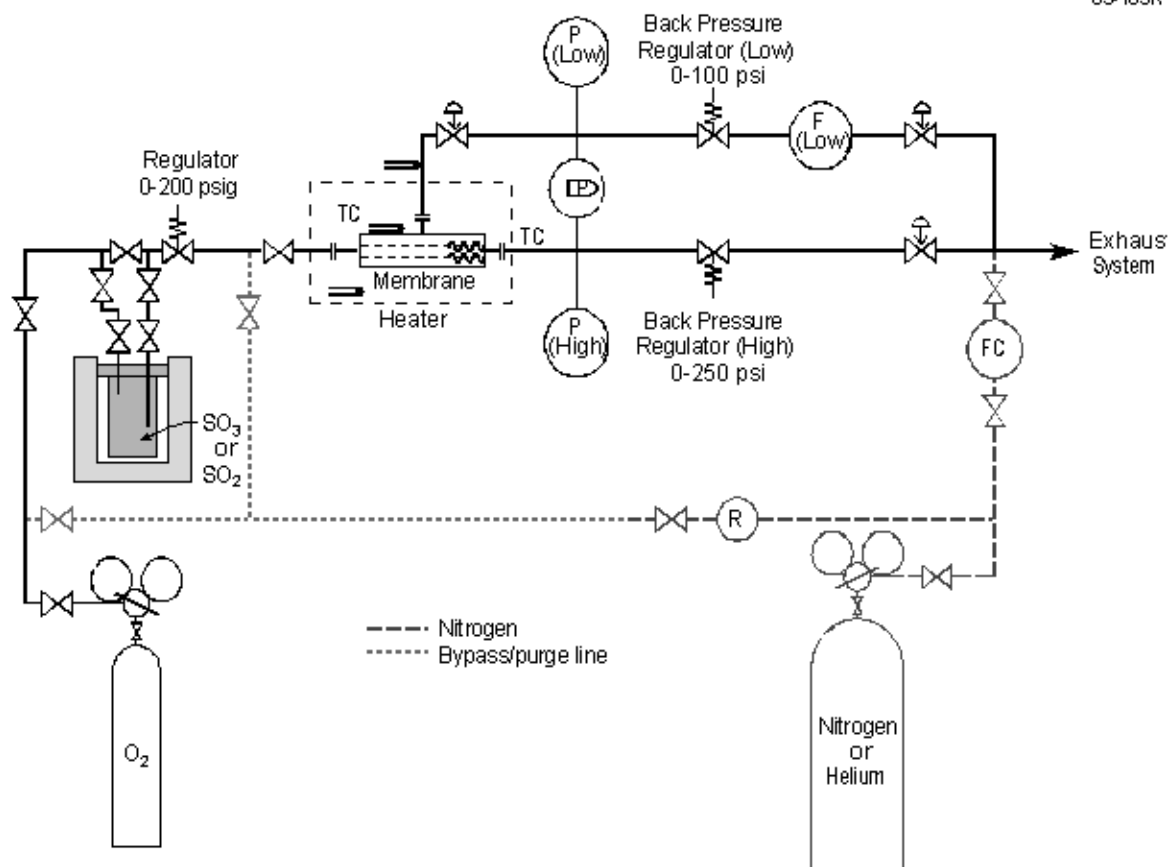
A combination of experiment and theory is used to develop new membranes. Lower-temperature inorganic membranes are commercially used for a variety of applications; however, high-temperature membranes have not yet been commercialised.

Based on theory, a series of existing inorganic membranes have been selected for testing. Most of these membranes have pore sizes on the order of 1 nm. Nanopore diffusion is expected to be the primary separation mechanism. The results of these tests will be combined with theory to develop a custom membrane designed for this specific separation.

The initial testing of these membranes is done by measuring the permeance of pure gases (H_2O , O_2 , SO_2 , and SO_3) as a function of temperature and pressure. The gas flow per unit surface area is measured as a function of pressure drop and temperature. Under most conditions, the interactions between molecules are small. Consequently, the measured permeance of the individual gases can be used to predict the separation performance. The best membranes are then subjected to separation tests using gas mixtures. After the initial selection of the membranes, tests will be conducted on gas mixtures. The test loop for these corrosive materials is under construction and will be operational in the fall of 2003. Initial experimental results will be available in early 2004. Figure 6 shows a simplified schematic of the membrane test loop that is being constructed. It will require several years of work before definitive technical and economic conclusions can be reached regarding the viability of inorganic membranes for this application.

Figure 6. Schematic of the membrane test apparatus

03-185R



REFERENCES

- [1] Brown, L.C., *et al.*, “High Efficiency Generation of Hydrogen Fuels Using Nuclear Power”, Final Technical Report for the Period 1 August 1999 through 30 September 2002, GA-A24285, General Atomics Corporation, La Jolla, California, June 2003.
- [2] Westinghouse Electric Corporation, “The Conceptual Design of an Integrated Nuclear Hydrogen Production Plant Using the Sulphur Cycle Water Decomposition System”, NASA-CR-134976, Contract No. NAS-3-18934, April 1976.
- [3] Trowbridge, L.D. and J.M. Leitnaker, “A Spreadsheet-Coupled SOGAS – A Computerized Thermodynamic Equilibrium Calculation Tool”, K/ETO-140 Rev 1, Lockheed Martin Energy Systems, Oak Ridge, Tennessee, September 1995.
- [4] Chase M.W., *et al.* “JANAF Thermochemical Tables”, 3rd ed., *J. Phys. Chem Ref. Data*, **14** (1), 1 September 1985.
- [5] Brown, L.C., R.D. Lentsch, G.E. Besenbruch and K.R. Schultz, “Alternative Flowsheets for the Sulphur-Iodine Thermochemical Process”, 2nd *Topical Conference on Fuel Cell Technology (Embedded Topical)*, 2003 Spring National Meeting, American Institute of Chemical Engineers, New Orleans, Louisiana, 30 March – 3 April 2003, American Institute of Chemical Engineers, New York.
- [6] LaBar, M.P., “The Gas Turbine–Modular Helium Reactor: A Promising Option for Near Term Deployment”, International Congress on Advanced Nuclear Power Plants, Embedded Topical American Nuclear Society 2002 Annual Meeting, Hollywood, Florida, 9-13 June 2002, GA-A23952, General Atomics Corporation, La Jolla, California.
- [7] Forsberg, C.W., P.S. Pickard and P.F. Peterson, “Molten-Salt-Cooled Advanced High-Temperature Reactor for Production of Hydrogen and Electricity”, *Nuclear Technology* **144** (December 2003).
- [8] Forsberg C.W. *et al.*, “A Lower-Temperature Iodine-Westinghouse-Ispra Sulphur Process for Thermochemical Production of Hydrogen”, *Global 2003, Embedded Topical American Nuclear Society 2003*, Winter Meeting, New Orleans, 16-20 November 2003, American Nuclear Society, La Grange Park, Illinois, 2003.
- [9] Burggraaf A.J. and L. Cot, Eds., *Fundamentals of Inorganic Membrane Science and Technology*, Membrane Science and Technology Series No. 4, Elsevier, Amsterdam, 1996.
- [10] Uhlhorn, R.J.R., K. Keizer and A.J. Burggraaf, “Gas Transport and Separation with Ceramic Membranes, Part I: Multilayer Diffusion and Capillary Condensation, Part II: Synthesis and Separation Properties of Microporous Membranes”, *J. Membr. Sci.* **66**, 259-287 (1992).

**SYNERGISTIC PRODUCTION OF HYDROGEN
USING FOSSIL FUELS AND NUCLEAR ENERGY
APPLICATION OF NUCLEAR-HEATED MEMBRANE REFORMER**

Masao Hori

Nuclear Systems Association, Japan

Kazuaki Matsui

The Institute of Applied Energy, Japan

Masanori Tashimo

Advanced Reactor Technology Co., Japan

Isamu Yasuda

Tokyo Gas Co., Japan

Abstract

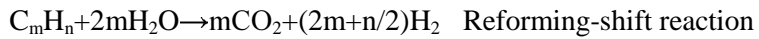
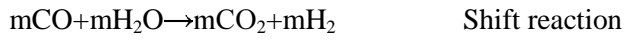
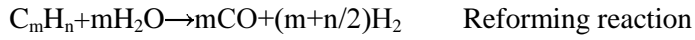
Processes and technologies to produce hydrogen synergistically by the steam reforming reaction using fossil fuels and nuclear heat are reviewed. Formulas of chemical reactions, required heats for reactions, saving of fuel consumption or reduction of carbon dioxide emission, possible processes and other prospects are examined for such fossil fuels as natural gas, petroleum and coal.

The “membrane reformer” steam reforming with recirculation of reaction products in a closed loop configuration is considered to be the most advantageous among various synergistic hydrogen production methods. Typical merits of this method are: nuclear heat supply at medium temperature below 600°C, compact plant size and membrane area for hydrogen production, efficient conversion of feed fuel, appreciable reduction of carbon dioxide emission, high purity hydrogen without any additional process, and ease of separating carbon dioxide for future sequestration requirements.

With all these benefits, the synergistic production of hydrogen by membrane reformer using fossil fuels and nuclear energy can be an effective solution in this century for the world which has to use fossil fuels any way to some extent while reducing carbon dioxide emission. For both the fossil fuels industry and the nuclear industry, which are under constraint of resource, environment and economy, this production method will be a viable symbiosis strategy for the coming hydrogen economy era.

1. General formulas of reforming reaction

Reaction formulas of steam reforming [A] of hydrocarbons are generally expressed by the following equations:

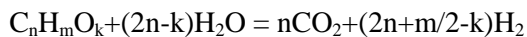


Moles of reactant hydrocarbon and steam and moles of product hydrogen are shown in Table 1 for the steam reforming-shift reactions of representative fossil fuels.

Table 1. Moles of reactant hydrocarbon/steam and of product hydrogen for the steam reforming-shift reactions of representative fossil fuels

Fossil fuel	Name	Representative Component's Molecular Formula	No. of C m	No. of H n	Mole of Steam 2m	Mole of H ₂ 2m+n/2	Mole of H ₂ per No. of C 2+n/2m
Natural gas	City gas	C ₁ H ₄	1	4	2	4	4.00
Petroleum	LPG	C ₄ H ₁₀	4	10	8	13	3.25
	Naphtha	C ₆ H ₁₄	6	14	12	19	3.17
	Kerosene	C ₁₂ H ₂₆	12	26	24	37	3.08
Coal	Coal	C ₁ H ₀₋₁	1	0~1	2	2~2.5	2~2.50

For hydrocarbons that consist of C, H and O, general reaction formulas are expressed by the following equation:



2. Hydrogen production process from various fossil fuels using membrane reformer

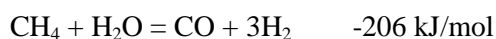
2.1 Natural gas

There have been tendencies in many countries to shift energy from coal and petroleum to natural gas that is environmentally cleaner. In the long-term prospects on energy supply/demand in Japan, natural gas is positioned as the core primary energy by its cleanness and supply stability, and is planned to increase steadily while other fossil fuels are to decrease. The natural gas will become more important as fuels for producing hydrogen for fuel cells and other application in the coming future.

In the following, benefits of supplying heat by nuclear energy to steam reforming of natural gas for hydrogen production are investigated for the case of applying the recirculation-type membrane reformer [B].

Reaction formulas of steam reforming of natural gas (methane) to produce hydrogen are as follows:

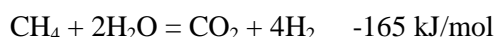
Reforming reaction:



Shift reaction:



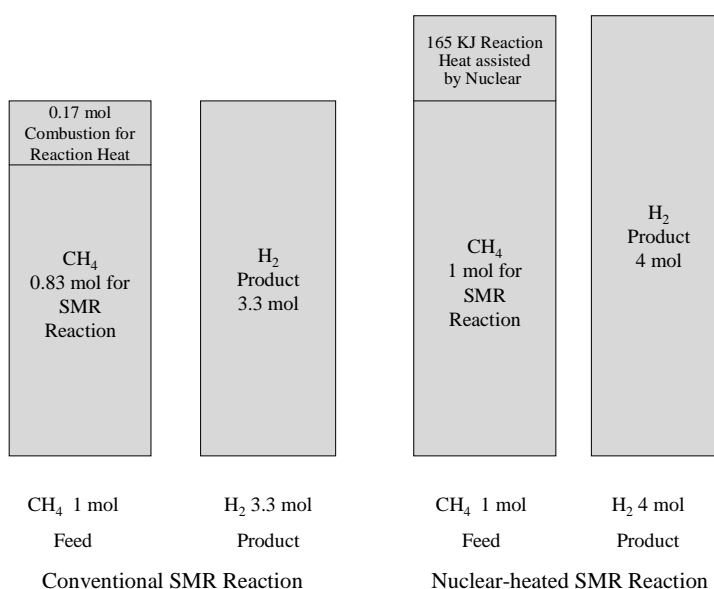
 Reforming-shift reaction:



In a membrane reformer, the reforming reaction and the shift reaction proceed simultaneously in a reaction zone where produced hydrogen is continuously separated by membrane [1]; heat required for endothermic reforming reaction is partly covered by heat generated by the exothermic shift reaction. Thus, the heat balance of reforming-shift reaction is endothermic of 165 kJ/mol, and this heat is supplied by nuclear energy.

As can be seen from Figure 1, even assuming a idealistic [C] case for the conventional SMR reaction, the consumption of methane for the nuclear-heated SMR reaction is 3.3/4=83%, or 17% less, of that of the conventional SMR reaction for producing the same amount of hydrogen.

Figure 1. Advantageous effect of nuclear heat supply to steam methane reforming



In the actual case of conventional SMR reaction, as the heat utilisation and the reaction yield are limited, the efficiency [D] of SMR process will be ~80%, that is ~2.7 mol of hydrogen produced from 1 mol of methane feed. In the case of nuclear-heated recirculation-type, membrane reformer, as no methane is consumed for combustion and the yield of hydrogen is nearly stoichiometric, the nuclear-heated SMR reaction will produce 4 mol of hydrogen from 1 mol of methane. Therefore, the nuclear-heated SMR process will save about 30% natural gas consumption, or reduce about 30% carbon dioxide emission, comparing with the conventional SMR process.

2.2 *Petroleum*

Utilisation of energy will be diversified worldwide, thus the share of petroleum in the primary energy will decrease gradually. However, petroleum will probably keep its leading and exclusive share for transportation demand for the time being, especially in the OECD countries. With that background, it is considered important, from the standpoint of resource and environmental conservation, to produce hydrogen from petroleum for efficient energy utilisation through fuel cells.

In the following, benefits of supplying heat by nuclear energy to steam reforming of petroleum (refinery) products for hydrogen production are investigated for the case of applying the recirculation-type membrane reformer.

In the petroleum products, lighter grade hydrocarbons such as liquefied petroleum gas (LPG), naphtha and kerosene could be reformed by the membrane reformer to produce hydrogen. The reaction formulas, endothermic reaction heat, heat of combustion, ratio of reaction heat to heat of combustion are tabulated for LPG, naphtha and kerosene in Table 2, where values for natural gas which is investigated in the previous section and values for coal which is investigated in the next section are also listed.

The ratio of heat of reaction to heat of combustion of produced hydrogen, which is listed in the rightmost column, shows the percentage contribution of nuclear heat supply to the produced hydrogen heat content. This ratio represents percentage saving of a fossil fuel/hydrocarbon by the nuclear-heated steam reforming reaction as compared to the idealistic [C] case of conventional steam reforming reaction.

As can be seen from the values in the rightmost column, the percentage saving of feed petroleum products or percentage reduction of their carbon dioxide emissions is 15~16%, which is almost in the same magnitude as in the cases of natural gas and coal. In the actual hydrogen production from petroleum products by the conventional steam reforming process, about 70% efficiency is expected in the conversion process due to limited heat utilisation efficiency and reaction yield. In the nuclear-heated recirculation-type membrane reformer, nearly all of the feed hydrocarbons are converted to hydrogen, so more than 30% saving of feed hydrocarbons is considered possible by nuclear heating.

As for the components of heavier than kerosene, direct application of membrane reformer will be difficult because of high temperature requirement of the process. Conventional processes of hydrogen production such as steam reforming or partial oxidation will be used.

Some preliminary tests on the application of membrane reformer to petroleum products have been conducted by Tokyo Gas Company using 1 m³H₂/h scale facility. Propane was used as a petroleum derivative, and its performance was compared with methane. The test condition for both feed fuels was almost the same with average reaction temperature of 580°C. The test results showed very similar characteristics including carbon conversion ratio. Generally, steam reforming of higher

hydrocarbons requires higher steam/carbon ratio by moles (S/C) in order to prevent carbon deposition on catalyst or ‘coking’. In the above tests, S/C ratio of 4 was used for propane while S/C ratio of 3 was used for methane.

Table 2. Ratio of heat of reaction to heat of combustion of produced hydrogen in steam reforming reaction of representative fossil fuels/hydrocarbons

Fossil fuel/hydrocarbon	Representative component's molecular formula	Steam reforming reaction formula	Heat of reaction/mole of hydrocarbon [kJ/mol-HC]	H ₂ heat of combustion/mole of hydrocarbon [kJ/mol-HC]	Heat of reaction/H ₂ heat of combustion [%]
Natural Gas	CH ₄	CH ₄ +2H ₂ O → CO ₂ +4H ₂	165.0	968	17.0
LPG	C ₄ H ₁₀	C ₄ H ₁₀ +8H ₂ O → 4CO ₂ +13H ₂	486.6	3 146	15.5
Naphtha	C ₆ H ₁₄	C ₆ H ₁₄ +12H ₂ O → 6CO ₂ +19H ₂	739.3	4 598	16.1
Kerosene	C ₁₂ H ₂₆	C ₁₂ H ₂₆ +24H ₂ O → 12CO ₂ +37H ₂	1 433.0	8 954	16.0
Coal	C	C+2H ₂ O → CO ₂ +2H ₂	90	484	18.6

In case of applying the membrane reformer to higher hydrocarbons, a pre-reformer zone will be set up in the membrane reformer or a separate pre-reformer will be placed before the membrane reformer. This will convert higher hydrocarbons to methane and the other reaction products (H₂, CO, CO₂) of the steam reforming, so as to prevent coking and to make the reaction zone with membrane more compact.

2.3 Coal

Coal has many advantages as a primary energy over other fossil fuels; abundant resource availability, superior supply stability and excellent cost competitiveness. When coal is liquefied or gasified to be a fluid fuel of liquid or gaseous hydrocarbon, then convenience of its energy utilisation will increase. Further, if hydrogen is produced from coal and is utilised in fuel cells, then efficiency of its energy utilisation will be increased.

In the following, benefits of supplying heat by nuclear energy to steam reforming of coal for hydrogen production are investigated for the case of applying the recirculation-type membrane reformer.

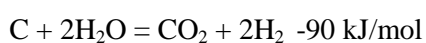
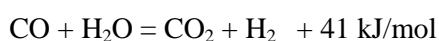
A. Hydrogen production by steam-coal gasification

The steam-coal gasification process has been commonly used for hydrogen production from coal, which is expressed by the following formulas.

Steam-coal gasification reaction:



Shift Reaction:



This steam-coal gasification is a reaction process between solid coal and steam at a high temperature over 800°C. If nuclear reactor is to supply heat to this process, it should be a very high temperature reactor. So this process is out of the condition of membrane reformer that works at a medium temperature lower than 600°C.

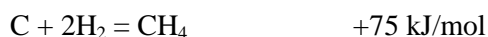
B. Hydrogen production via SNG from coal

Processes to produce SNG (Synthetic or substitute natural gas) from coal have been studied as useful technologies for stable supply of natural gas as high calorie fuel gas. It is considered to produce hydrogen through SNG from coal.

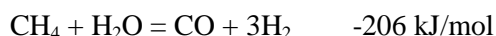
As for the production of SNG from coal, there are methanation process of synthetic gas produced by partial oxidation of coal, and hydro-gasification process by hydrogenation of coal. It is reported that thermal efficiency of the former process is about 65~70%, while that of the latter process is about 75~80%. Moreover, it is not advantageous to produce hydrogen from the SNG by the former process because it is a detour method of producing hydrogen by the steam-coal gasification process described in the previous section. The latter process has higher thermal efficiency to produce SNG and, if the process is combined with nuclear-heated recirculation-type membrane reformer, it can bring certain advantage to reduce carbon dioxide emission associated with hydrogen production.

The process to produce SNG by hydro-gasification of coal, and then produce hydrogen by steam reforming reaction is shown by the following formulas:

Hydro-gasification of coal:

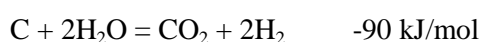


Steam reforming of methane:



Shift reaction:





As the hydro-gasification reaction of coal usually proceeds at high temperature and high pressure, this process is to be conducted outside of nuclear systems.

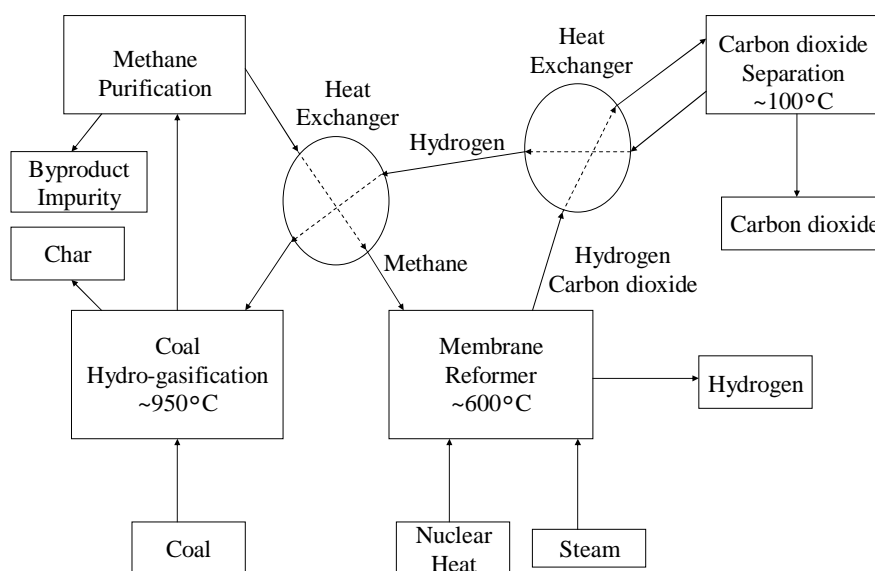
For the steam reforming reaction of methane and the shift reaction, the recirculating-type membrane reformer is to be utilised. In the membrane reformer, both the reforming reaction and the shift reaction occurs simultaneously in the same reaction region, and balance of endothermic and exothermic heats, that is 165 kJ/mol endothermic, are to be supplied by nuclear heat.

Technologies on hydro-gasification of coal for producing SNG (methane) have been developed in various countries. In Japan, the advanced rapid coal hydro-gasification (ARCH) process has been developed with the aim of commercialisation in 2010s [2]. This process is to hydrogenate coal at high temperature and high pressure to produce SNG with char (remains of coal, consisting mostly of carbon and ash, after its volatile components vaporised) and BTX (benzene, toluene and xylene) as by-products. The by-product char is to be used for producing hydrogen by the steam-coal gasification reaction and the shift reaction. This hydrogen is fed into the SNG gasification reactor.

In the ARCH process, three modes of hydro-gasification were developed; maximum thermal efficiency, maximum SNG production and maximum BTX production. For combining with steam reforming process, the maximum SNG production mode will be suitable. In this hydro-gasification mode, under the operating condition of 940°C temperature, 6.9 MPa pressure, 0.38 hydrogen/coal ratio and 10 sec residence time, 62% carbon in coal are converted to gases (52% CH₄, 6% CO, 3.5% BTX).

Hydro-gasification process to produce SNG from coal, of which one of examples is the ARCH process, can be combined with nuclear-heated recirculation-type membrane reformer to produce hydrogen, as shown in Figure 2. The SNG produced in the hydro-gasification process is fed into the membrane reformer where half of hydrogen formed is separated by membrane to output as product and remaining half of hydrogen, after separating carbon dioxide, is fed back to the hydro-gasification process to produce SNG from coal.

Figure 2. Combined process of producing hydrogen from coal – Hydro-gasification process and nuclear-heated recirculation-type membrane reformer –



In the maximum SNG mode of ARCH process, methane and CO of coal converted gases, which is about 58%, can be used for hydrogen production in the membrane reformer. After volatile matters are gasified, about 40% of coal is discharged as solid char. In the combined process of SNG production by ARCH hydro-gasification and hydrogen production by membrane reformer, about 60% conversion of coal to SNG and consequently to hydrogen may be maximum as estimated from the volatile contents of coal. If discharged char has some usages, the overall utilisation factor of coal will be improved.

In the conventional hydrogen production process from coal, such as the steam-coal gasification process, coal gasification efficiency, which is defined as ratio of heat value of produced gas to that of supplied coal, is about 65~70% in case of the TEXACO process. The combined process of hydro-

gasification and nuclear-heated membrane reformer can possibly give about 60% yield of hydrogen from charged coal or about 70% coal gasification efficiency by the above definition.

For producing hydrogen, the efficiency of combined process is almost at the same level as that of steam-coal gasification process. Feature of this combined process is that, because nuclear heat is supplied to the process, it is not necessary to combust coal, therefore to reduce the carbon dioxide emissions in producing hydrogen from coal.

3. Concluding remarks

While expanding expectations towards the hydrogen economy society, is it really possible to produce hydrogen commercially by nuclear energy with no or reduced emission of carbon dioxide? Electrolysis of water by nuclear power go through convenient but precious electricity to produce hydrogen, so it should be appraised by the merit of producing hydrogen by conventional technology on site of demand. Thermo-chemical decomposition of water requires, at present, high temperature, so it is necessary to develop high temperature heat source reactors and thermo-chemical processes, and to solve issues such as temperature transient and pressure limitations in the chemical process side and materials for severe conditions of high temperature and corrosion.

Hydrogen production through nuclear-heated steam reforming of fossil fuels is viewed by many as an intermediate step before any nuclear hydrogen production from water is developed [3]. From the cost estimates of nuclear-heated natural gas membrane reformer, this process is considered to compete economically with conventional hydrogen production methods [4]. Typical merits of this method are: nuclear heat supply at medium temperature below 600°C, compact plant size and membrane area for hydrogen production, efficient conversion of feed fuel, appreciable reduction of carbon dioxide emission, high purity hydrogen without any additional process, and ease of separating carbon dioxide for future sequestration requirements.

In this paper, formulas of chemical reactions, required heats for reactions, saving of fuel consumption or reduction of carbon dioxide emission, possible processes and other prospects are examined for natural gas, petroleum and coal. The ratio of endothermic reaction heat, which is to be supplied by nuclear energy, to heat value of produced hydrogen is less than 20%. That means most of produced hydrogen energy come from chemical energy of carbon. However, saving effect of fossil fuels, and consequently reduction of carbon dioxide emission, of about 30% are obtained when compared with conventional hydrogen production processes for the cases of natural gas and petroleum products. It is shown that this process has similar merits when applied to petroleum and coal as to natural gas.

The foremost feature of nuclear-heated recirculation-type membrane reformer is to reduce consumption of fossil fuels, and consequently emission of carbon dioxide, in producing the same amount of hydrogen. Nuclear energy assists effective use of fossil fuel resources which are valuable as raw materials for the world over the long-term. With all these benefits, the synergistic production of hydrogen by the membrane reformer using fossil fuels and nuclear energy can be an effective solution in this century for the world, which has to use fossil fuels any way, according to various estimates of global energy supply, to some extent while reducing carbon dioxide emission [5]. For both the fossil fuels industry and the nuclear industry, which are under constraint of resource, environment and economy, this production method will be a viable symbiosis strategy for the coming hydrogen economy era.

Notes

- [A] 'Reforming' has generally meant the changing by heat treatment of a high-heating-value hydrocarbons into a gaseous mixture of lower heating value, approximating that commonly used in the local situation, with the resulting increase in volume. (Encyclopaedia of Chemical Technology).
- [B] Outline of the nuclear-heated recirculation-type membrane reformer is described in the Appendix of this paper.
- [C] All the heat generated by combustion of hydrocarbon is assumed to be idealistically used for the heat of endothermic reaction of steam reforming. Also assumed is that the endothermic reaction heat of steam reforming is partly covered by the exothermic reaction heat of shift reaction.
- [D] The efficiency is defined here as ratio of heat value of produced gas to that of supplied fossil fuel, that is $(\text{production rate of hydrogen}) \times (\text{heat value of hydrogen}) / (\text{consumption rate of methane}) \times (\text{heat value of methane})$ for the case of hydrogen production by steam reforming of methane. Another definition includes the electric power consumed by the auxiliary equipment in the denominator.

REFERENCES

- [1] Yasuda, I. *et al.*, "Development of Membrane Reformer for Hydrogen Production from Natural Gas", 14th World Hydrogen Energy Conference, Montreal, 9-13 June 2002.

Shirasaki, Y. *et al.*, "New Concept Hydrogen Production System Based on Membrane Reformer", 2002 Fuel Cell Seminar, Palm Springs, 18-21 November 2002.
- [2] Katsukura, K. "Development of Coal Hydrogasification Technology" (in Japanese), Chemical Engineering (Japan), Vol. 64, No. 4, p. 192-196, (2000).
- [3] American Nuclear Society, "Nuclear Energy for Hydrogen Generation", Position statement 60, June 2003.
- [4] Tashimo, M., *et al.*, "Concept of FR-MR", 11th International Conference on Nuclear Engineering, ICONE-11-36321, Tokyo, 20-23 April 2003.

Tashimo, M., *et al.*, "Advanced Design of Fast Reactor-Membrane Reformer (FR-MR)", To be presented at OECD/NEA First Information Exchange Meeting on Nuclear Production of Hydrogen, Argonne, 2-3 October 2003.
- [5] Hori, M. "Role of Nuclear Energy in the Long-Term Global Energy Perspective", Proceedings of OECD/NEA First Information Exchange Meeting on Nuclear Production of Hydrogen, Paris, France, 2-3 October 2000, p. 25 (2001).

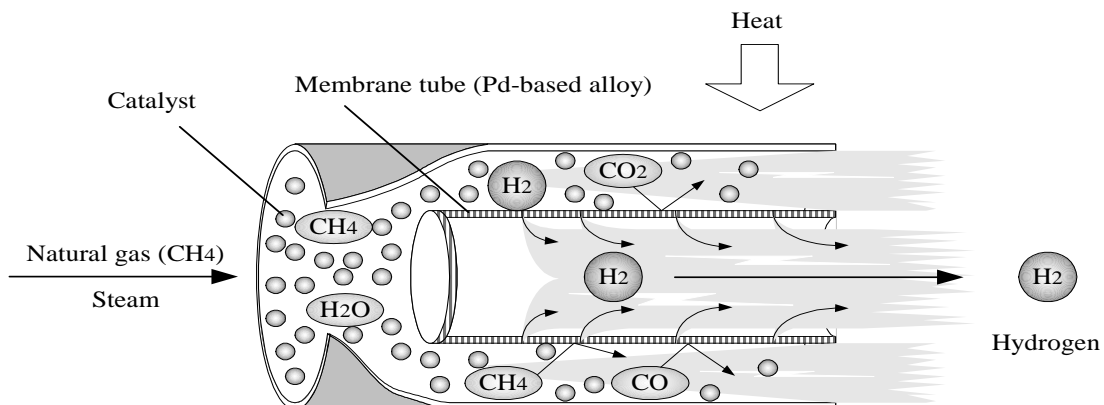
Appendix

OUTLINE OF NUCLEAR-HEATED RECIRCULATION-TYPE MEMBRANE REFORMER

A1. Principles, merits and test results of membrane reformer [1]

The conventional steam methane reforming (SMR) system for hydrogen production is composed of a steam reformer, a shift converter, and a hydrogen purifier based on the pressure swing adsorption (PSA). A mixture of natural gas and steam is introduced into a catalyst bed in the steam reformer, where the steam reforming reaction proceeds on nickel-based catalyst at 700~800°C. Then the reformed gas is supplied to a shift converter, where carbon monoxide is converted into carbon dioxide to produce more hydrogen by the shift reaction. Then the reformed gas is passed to PSA to separate hydrogen.

Figure A1. Principle of membrane reformer



The membrane reformer system is composed of a steam reformer equipped with membrane modules of palladium-based alloy, and nickel-based catalyst, and can perform steam reforming reaction, shift reaction and hydrogen separation process simultaneously, as shown in Figure A1, without a shift converter and PSA. By this simultaneous generation and separation of hydrogen, the membrane reformer system can be much more compact and can provide higher efficiency than the conventional ones. The simultaneous progress of hydrogen generation and separation makes the reaction free from the limitation of chemical equilibrium and thus can lower the reaction temperature down to 500~550°C. This gives benefits of avoiding use of expensive heat-resistant materials and increased long-term durability.

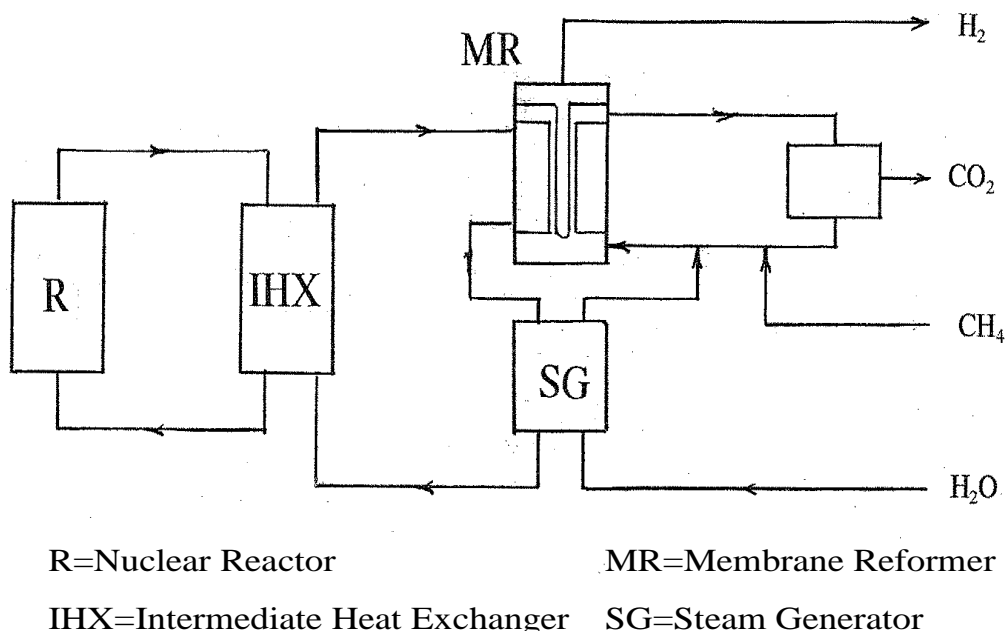
This membrane reformer system has been developed jointly by Tokyo Gas Co. (TGC) and Mitsubishi Heavy Industries (MHI) since 1992. TGC has already established the technical feasibility

of this system by producing pure hydrogen at 15 Nm³/h for about 1 500 hours with 40 start-up and shut-down cycles. Typical operation data of this reformer are: reaction temperature of 550°C, reaction-side pressure of 0.83 MPaG, natural gas conversion of 76.2%, hydrogen production rate of 21.8 Nm³/h, hydrogen purity of 99.999%, hydrogen production efficiency of 73.6% including 3.83 KW auxiliary power. Tests at a 40 Nm³/h facility are scheduled by 2004 to verify system efficiency, long-term durability and reliability, and to establish scale-up technologies.

A2. Merits of nuclear-heated recirculation-type membrane reformer [4]

Combining this membrane reformer technology with a nuclear reactor has been developed jointly by MHI, TGC, Advanced Reactor Technology Co. (ARTECH) and Nuclear Systems Association (NSA). The schematic diagram of nuclear-heated recirculation-type membrane reformer is shown in Figure A2.

Figure A2. Schematic diagram of nuclear-heated recirculation-type membrane reformer



Merits of nuclear-heated recirculation-type membrane reformer, in addition to those for the methane combustion type membrane reformer described above, are as follows:

- Supply of nuclear heat at medium reactor temperature (below 600°C which is in the ordinary temperature range of sodium coolant);
- No combustion of methane for the endothermic heat of reforming reaction, and consequently no combusted carbon dioxide emission (about 30% reduction of overall carbon dioxide emission);

- Ease of separating carbon dioxide for future sequestration requirements (separation of the carbon dioxide reaction product is built into the process);
- Smaller surface area of membrane modules (recirculation of reaction product gases including residual hydrogen in a closed loop configuration makes average driving force for hydrogen diffusion through membrane higher).

Acknowledgement

The authors would like to express their appreciation to the following experts for the valuable comments and discussions; Koji Watanabe (Institute of Applied Energy), Yukuo Katayama (Institute of Applied Energy), Masahiro Hirano (Mitsubishi Heavy Industries) and Yoshinori Shirasaki (Tokyo Gas Co.).

HYDROGEN PRODUCTION THROUGH HIGH-TEMPERATURE ELECTROLYSIS IN A SOLID OXIDE CELL

J. Stephen Herring*, Paul Lessing, James E. O'Brien and Carl Stoots

Idaho National Engineering and Environmental Laboratory
Idaho Falls, Idaho

Joseph Hartvigsen, S. Elangovan,

Ceramatec, Inc.
Salt Lake City, Utah

Abstract

An experimental research programme is being conducted by the INEEL and Ceramatec, Inc., to test the high-temperature, electrolytic production of hydrogen from steam using a solid oxide cell. The research team is designing and testing solid oxide cells for operation in the electrolysis mode, producing hydrogen using a high-temperature heat and electrical energy. The high-temperature heat and the electrical power would be supplied simultaneously by a high-temperature nuclear reactor. Operation at high temperature reduces the electrical energy requirement for electrolysis and also increases the thermal efficiency of the power-generating cycle. The high-temperature electrolysis process will utilise heat from a specialised secondary loop carrying a steam/hydrogen mixture. It is expected that, through the combination of a high-temperature reactor and high-temperature electrolysis, the process will achieve an overall thermal conversion efficiency of 40 to 50% while avoiding the challenging chemistry and corrosion issues associated with the thermochemical processes. Planar solid oxide cell technology is being utilised because it has the best potential for high efficiency due to minimised voltage and current losses. These losses also decrease with increasing temperature.

Initial testing has determined the performance of single "button" cells. Subsequent testing will investigate the performance of multiple-cell stacks operating in the electrolysis mode. Testing is being performed both at Ceramatec and at INEEL. The first cells to be tested were single cells based on existing materials and fabrication technology developed at Ceramatec for production of solid oxide fuel cells. These cells use a relatively thick (~175 μm) electrolyse of yttria- or scandia-stabilised zirconia, with nickel-zirconia cermet anodes and strontium-doped lanthanum manganite cathodes. Additional custom cells with lanthanum gallate electrolyte have been developed and tested. Results to date have shown an area specific resistance (ASR) of 0.45 $\Omega \text{ cm}^2$ at 850°C, and produced 73% H_2 :27% H_2O from a 50:50 input stream. Our most recent results from a six-cell stack show a production of 35 normal liters/hr for a duration of 360 hours. The stack test is continuing. The critical parameters for a 300 MW_{hydrogen} commercial electrolysis plant have been determined, based on these experimental results.

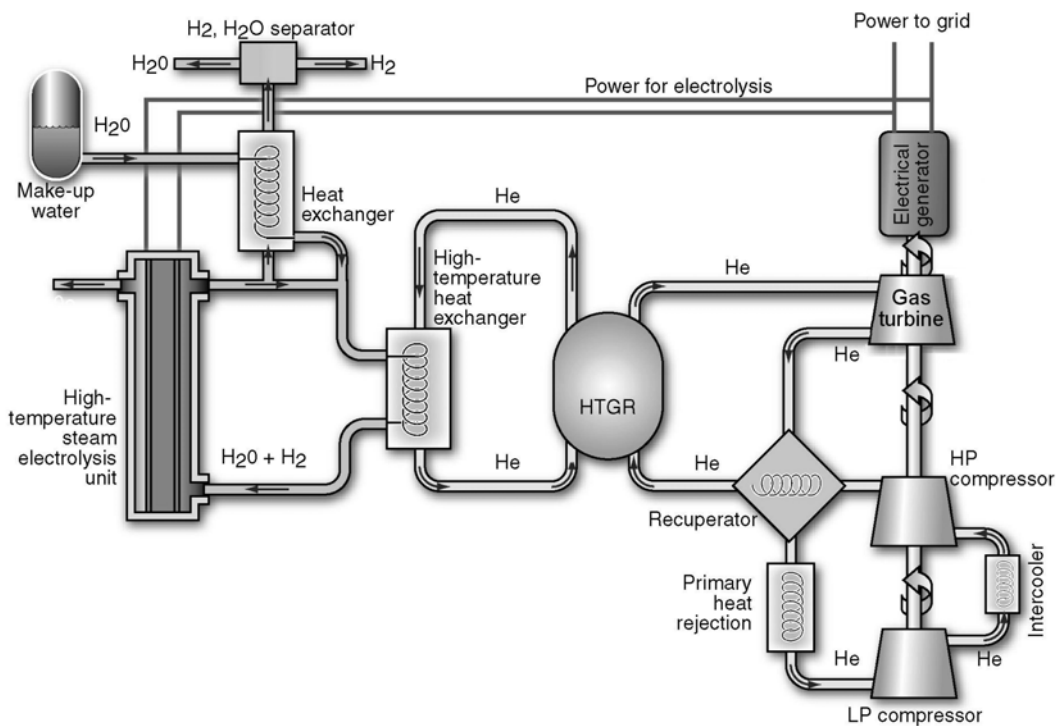
* Contact: 208-526-9497 sth@inel.gov

Introduction

Water splitting through electrolysis can be accomplished using solid-state electrolytes via solid polymer electrolysis (SPE) or via high-temperature electrolysis of steam (HTES) using ceramic membranes [1]. In both laboratory-scale and prototype experiments, the current efficiency of the SPE process is about 85 to 90%; while the laboratory efficiency of the HTES is almost 100%.

The high temperature electrolyser is essentially a solid oxide fuel cell (SOFC) run backwards. The electrolyser makes use of the existing SOFC technology, operating in a less aggressive chemical environment than the S-I or Ca-Br thermochemical processes, and makes use of small, modular components. The higher efficiencies for HTES result from the lower cathodic and anodic overpotentials for the electrolysis cell at high temperatures. In addition, the oxygen ion diffusivity in the electrolyte is much higher (a strongly temperature-activated process) at high temperatures, which reduces electrical power lost to resistance heating of the electrolyte during operation.

Figure 1. High temperature electrolysis using gas-cooled reactor



A schematic of a nuclear hydrogen plant using high temperature electrolysis is shown in Figure 1. The reactor (in this case a high temperature gas-cooled reactor, HTGR) supplies both the electricity and the steam to the electrolytic cell. The steam generator supplies very superheated steam

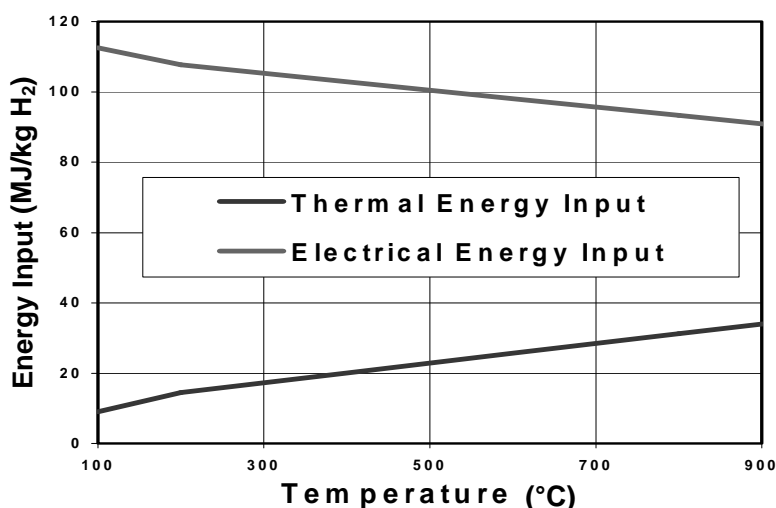
to the cells at a temperature of 750-950°C, and a pressure of 1-5 MPa. The input gas contains both steam and hydrogen in order to maintain reducing conditions at the electrolytic cathode.

High-temperature steam electrolysis units use a thin film of solid-oxide, most commonly yttria-stabilised-zirconia (YSZ), as the electrolyte. When the same configuration is supplied with hydrogen and oxygen, the device can produce electricity, functioning as a solid-oxide fuel cell.

Thermodynamics of high temperature electrolysis

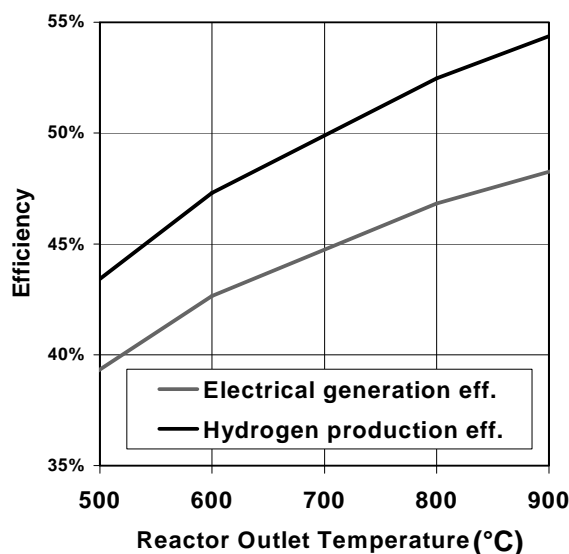
From a Gibbs-free-energy viewpoint, high temperatures reduce the amount of electrical energy required to break the chemical bonds in the water molecules [2]. Therefore, the electrical energy demand, ΔG , for electrolysis decreases strongly with increased temperature. The thermal energy requirement, Q , however, increases with increasing temperature. The ratio of ΔG to ΔH is about 93% at 100°C and about 70% at 1 000°C.

Figure 2. Overall energy requirements for high temperature electrolysis



Higher reactor operating temperatures result in higher thermal efficiencies for electrical power generation, and an overall analysis of the efficiency of hydrogen production with nuclear energy should consider the total thermal energy required per kilogram of hydrogen. If we assume that the power generation cycle efficiency is 65% of the Carnot maximum, then the total thermal energy requirement decreases significantly with temperature.

Figure 3. Efficiencies of electrical and hydrogen production



The respective energy efficiencies of electrical power generation and of hydrogen production (based on the energy content associated with the lower heating value of the product hydrogen) are shown in Figure 3.

Operation of the electrolyser at high temperature is also desirable from the standpoint of kinetics and electrolyte conductivity, both of which improve at higher operating temperatures. Therefore, high temperature electrolysis of steam (HTES) is favoured over solid polymer electrolysis (SPE) from both thermodynamic and kinetic standpoints.

Configuration of a solid-oxide electrolysis cell

High-temperature electrolysis uses a combination of thermal energy and electricity to split water in a device very similar to a solid-oxide fuel cell (SOFC). As seen in Figure 4, the electrolytic cell consists of a solid oxide electrolyte (usually yttria-stabilised zirconia) with conducting electrodes deposited on either side of the electrolyte. Negative charge, either electrons or O^- ions, flow from top to bottom in the figure. In the figure, a 90:10 (volume percent) mixture of steam and hydrogen at 750-950°C is supplied to the anode side of the electrolyte. The oxygen ions are drawn through the electrolyte by the electrical potential and combine to O_2 on the cathode side. The steam-hydrogen mixture exits at about 25:75 volume percent. The water and hydrogen gas mixture is passed through a separator to produce hydrogen. While present experiments and fuel cells operate at pressures near atmospheric, future cells may operate at pressures up to 5 MPa.

Because of shrinkage during sintering in current manufacturing processes, the size of individual cells is limited to about 15 cm square. Therefore, a high-temperature electrolysis plant powered by a reactor would consist of an array of relatively small modules, connected together with the necessary high-temperature gas manifolding, electrical and control connections. Costs for solid oxide fuel cells are currently high (~\$10k/kWe), primarily due to small-scale manufacture. Ongoing SOFC research is investigating approaches to reduce both materials and manufacturing costs. Current estimates are that large-scale manufacturing could potentially reduce costs by an order of magnitude or more.

Figure 4. Components of a high temperature electrolysis cell

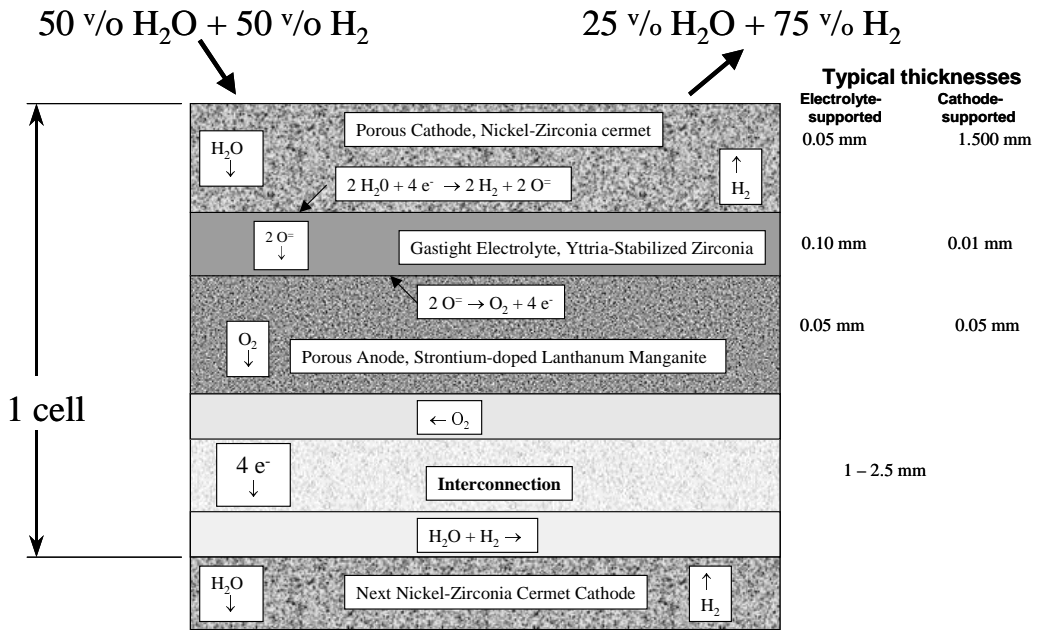
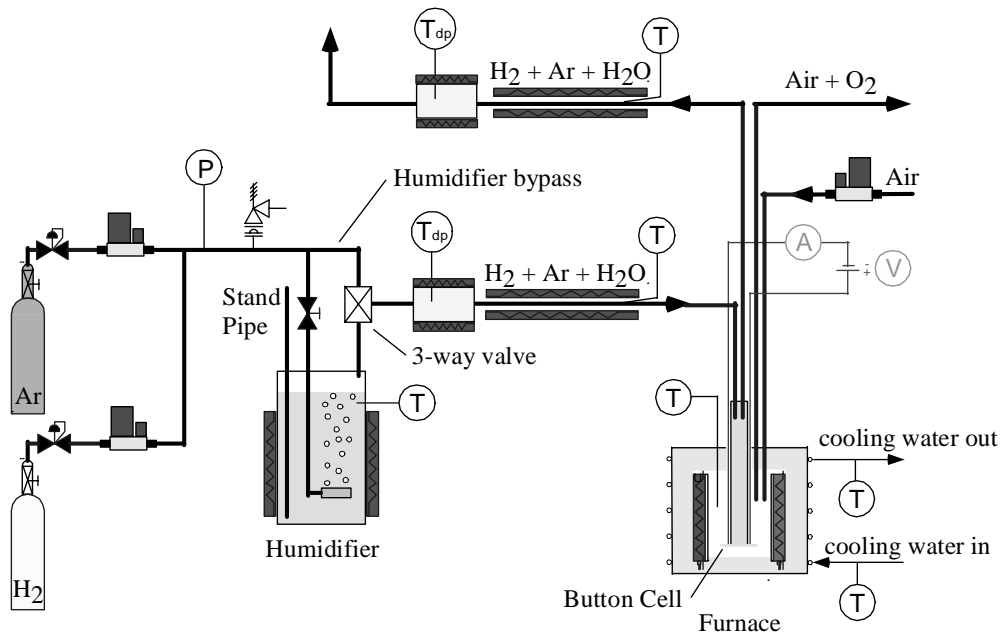


Figure 5. HTE test loop at INEEL



Experiment test loop

We are testing button cells manufactured by Ceramatec, Inc. in a test loop at the INEEL, shown schematically in Figure 5. Argon is being used as a carrier gas to control the steam-hydrogen ratio being fed to the button cell in the furnace in the lower right. The dew point temperatures of the feed stream and the exiting stream are directly measured to determine the amount of hydrogen produced by the button cell. As will be shown later, the dew point measurements correlate well with expected hydrogen production rates based on measurements of electrical current supplied to the cell. For safety reasons, the oxygen is diluted with air before being exhausted.

A close-up photo of a typical button cell is shown in Figure 6. The button cell is cemented to a zirconia tube and the apparatus is suspended in the furnace. The steam-hydrogen mixture is introduced into the interior of the zirconia tube and the air-oxygen mixture flows on the exterior of the tube. The overall electrode area is 3.2 cm^2 , with 2.5 cm^2 energised for hydrogen production and the remainder serving as a reference electrode. The button cell temperature is measured by the thermocouple (TC) shown. The cathode (in electrolysis mode) is a nickel zirconia cermet and the anode is strontium-doped lanthanum manganite. The electrolyte is yttria-stabilised zirconia with a thickness of $175 \text{ }\mu\text{m}$.

The test loop in its uninsulated condition is shown in Figure 7. The furnace is at the right and the humidifier is the steel cylinder in the centre. Dew point meters are shown on the heated horizontal inlet and outlet tubes leading to the furnace. We have found that good thermal instrumentation and heat tracing are very important in preventing condensation in the test loop.

Experimental results

Typical voltage-current characteristics for a button cell very similar to that shown in Figure 6 are shown in Figure 8. The button cell was operated in both electrolysis and fuel cell modes, using three different steam concentrations in the gas entering the cell. The sharp increase in the voltage for the 10% steam and 17% steam curves at about 0.3 and 0.7 A/cm^2 , respectively, is due to the cell completely electrolysing the available steam (steam starvation). Since the electrolyte is an ionic conductor, depletion of the available steam leads to a sharp limit on the current that can be conducted. The change in voltage and current that would occur as steam-hydrogen mixture flows along a channel in a planar electrolyser is indicated by the arrow. The L and R indicate flow from left to right in Figure 4. The steam-hydrogen mixture enters the channel at 56 volume percent and is progressively enriched in hydrogen and depleted in steam. Thus the states along the channel would lie along a horizontal arrow if the electrodes were much better conductors than the electrolyte (e.g. uniform voltage across the cell) and the arrow would be vertical if the electrodes were poorer conductors (e.g. uniform current density across the cell).

Figure 6. Button cell test configuration

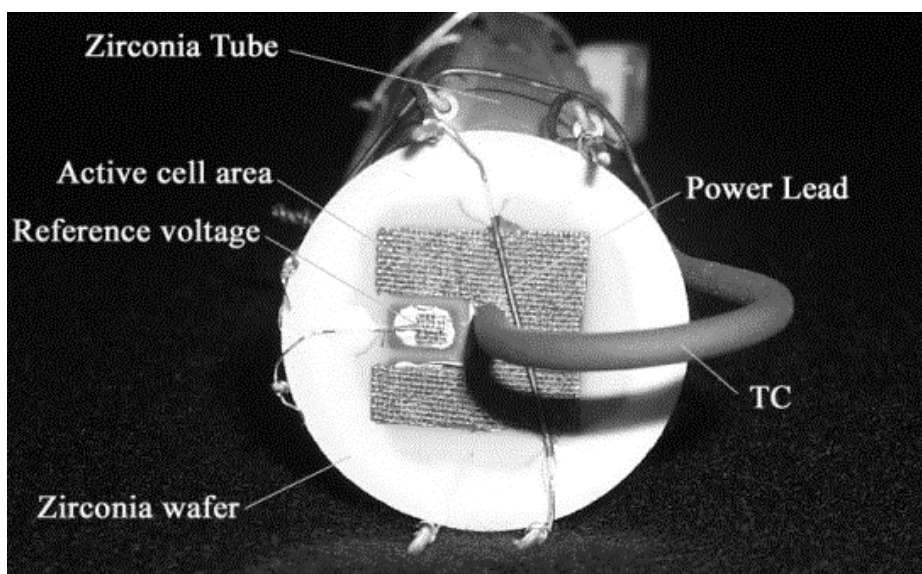


Figure 7. Photo of HTE test loop components

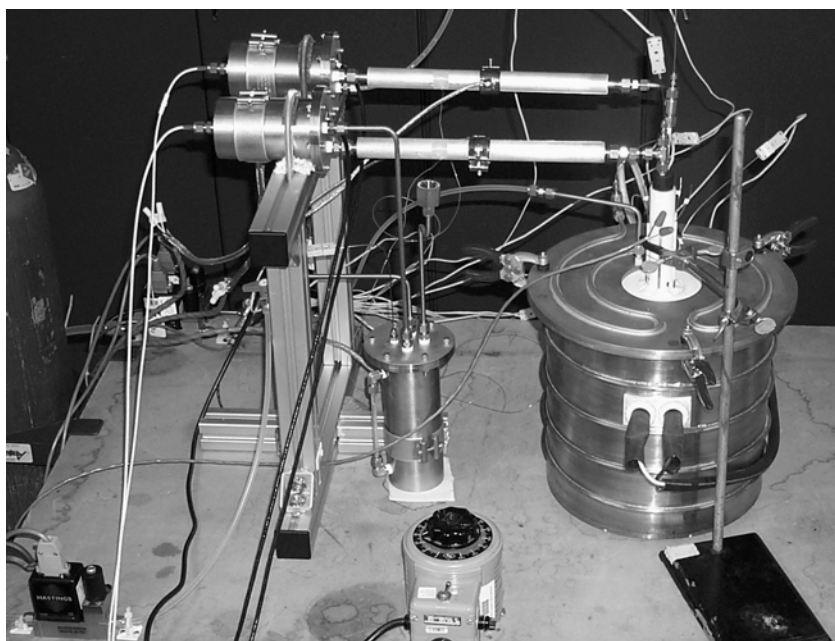
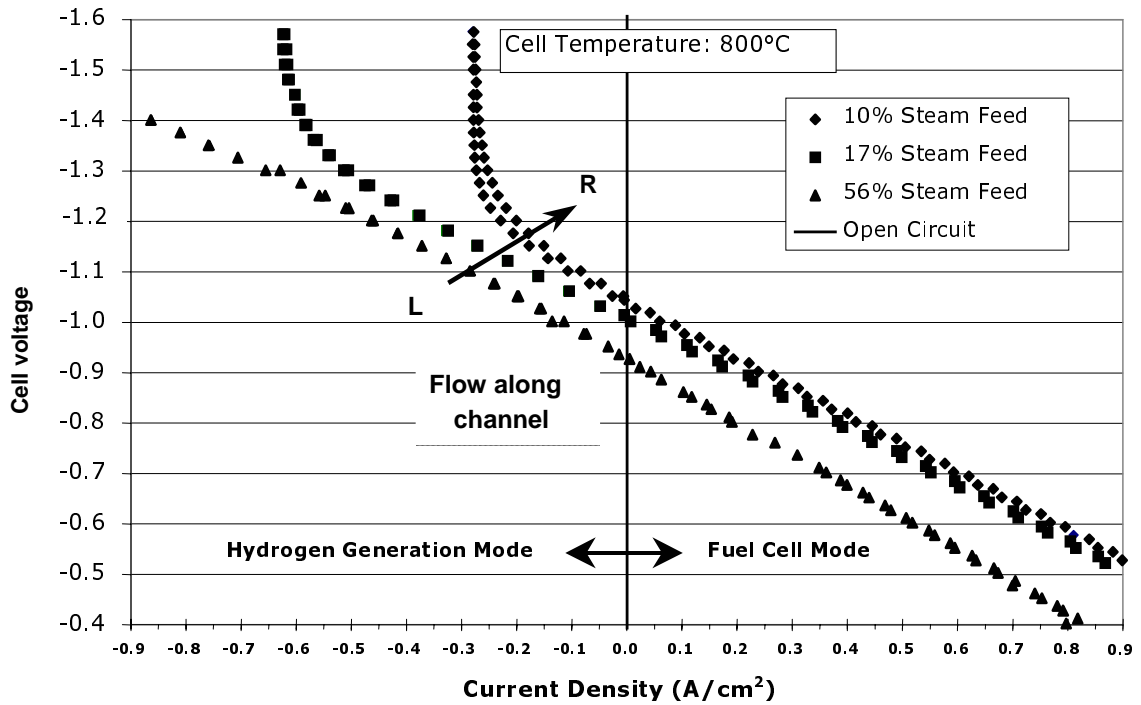
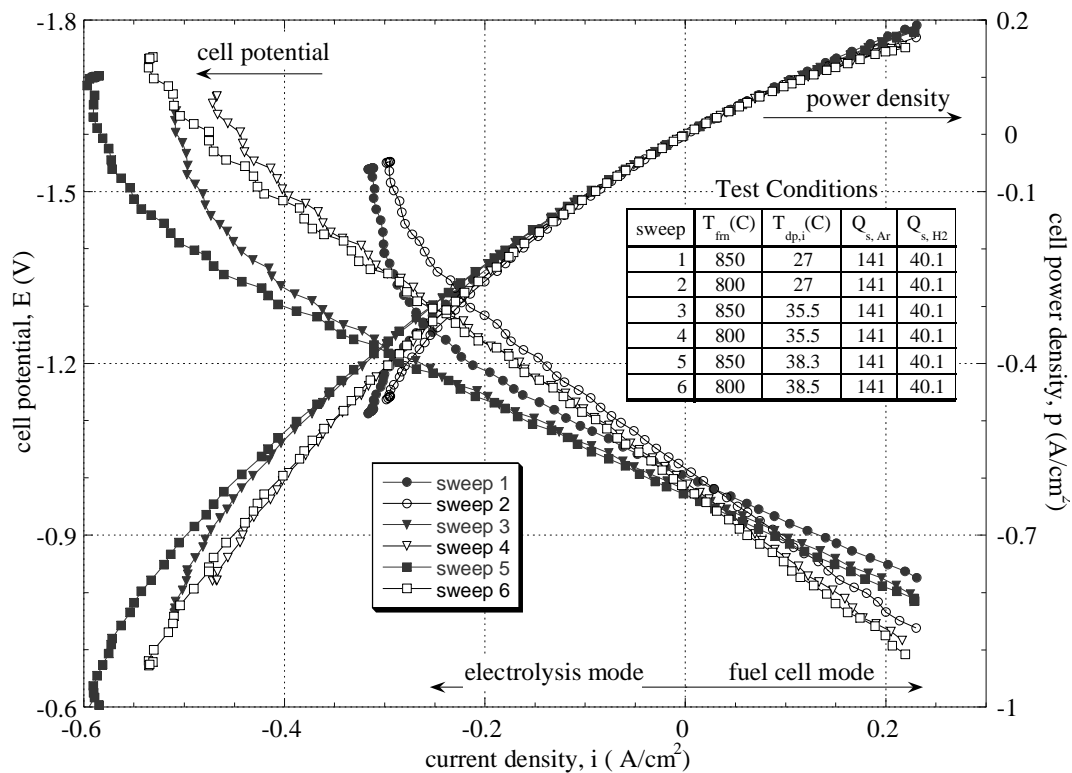


Figure 8. Voltage – current characteristic of LSGM cell



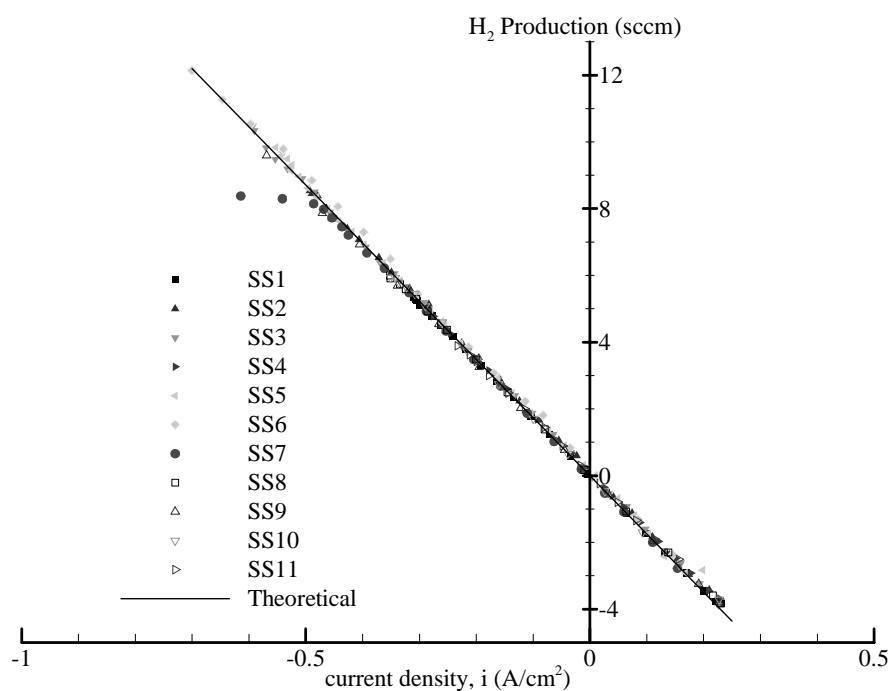
The cell potential and power density as functions of the current density for a wide range of operating conditions are shown in Figure 9. Each of the points on the graph represents equilibrium at a particular current and feed. The apparatus was operated for approximately ten minutes as each of the points in order for the gas flows and concentrations to stabilise. Three inlet steam concentrations are determined by inlet dew point temperatures of 27, 35.5 and 38.5°C.

Figure 9. Cell operating potential and power density as a function of current density



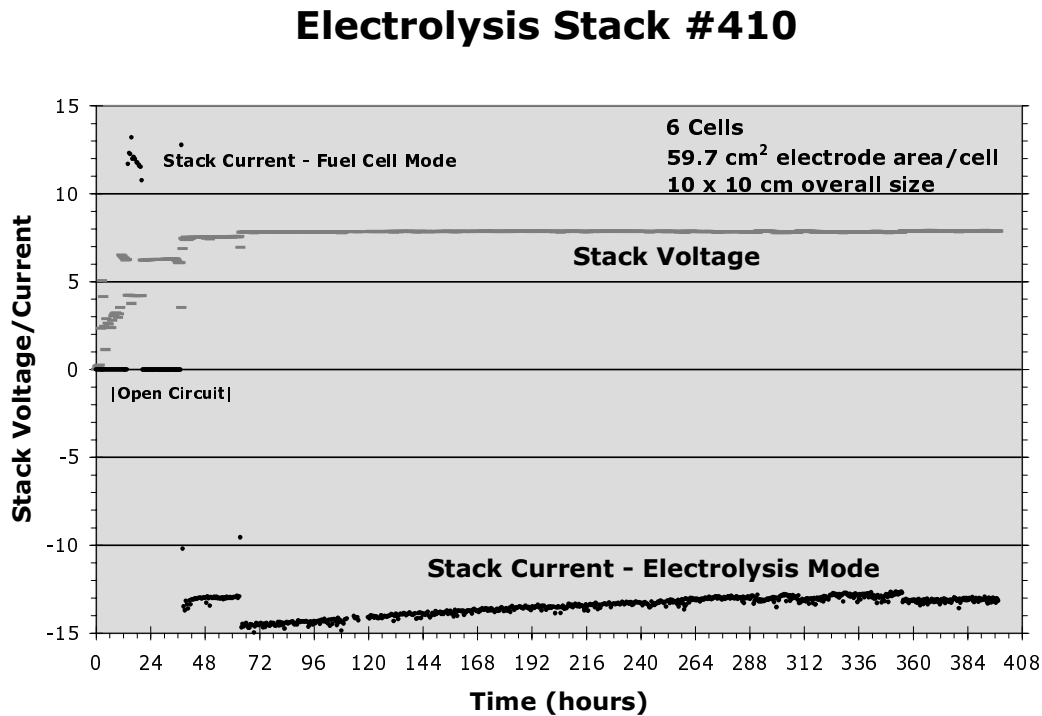
A comparison between the measured and theoretical amounts of hydrogen produced is shown in Figure 10. Note that the measured production is very close to the theoretical, except for a few cases at relatively high current density.

Figure 10. Hydrogen production as a function of current density, measured and predicted



Results of our most recent tests are shown in Figure 11. This test, being conducted at the Ceramatec facility in Salt Lake City, consists of six cells, each having an electrode area of 59.7 cm². In electrolysis mode, with a stack current of 13 A, the stack is producing about 32 normal liters of H₂ per hour. The current density is a relatively low 218 mA/cm². As shown in the figure, the test has been underway for about 360 hours in electrolysis mode and is continuing as of this writing.

Figure 11. Most recent results of the Ceramatec six-cell test



Conceptual HTE plant design

An HTGR conceptual design that could be used for simultaneous electrical power and hydrogen production was presented in Figure 1. In this design, the primary helium coolant is heated in the reactor to outlet temperatures in the range of 850 to 1 000°C. A portion of the hot helium outlet stream serves as the working fluid in a gas-turbine power cycle, and a separate helium stream flows through a high-temperature heat exchanger, providing process heat to a steam/hydrogen gas mixture. This gas mixture is then fed to a high-temperature steam electrolysis device, such as a solid-oxide cell, which produces one outlet stream of pure oxygen and another steam/hydrogen outlet stream that is significantly enriched in hydrogen. Both the steam/hydrogen stream and the oxygen stream are maintained at pressures of approximately 5 MPa.

High-pressure hydrogen production is desirable from a systems viewpoint, since, in any large-scale scheme, the hydrogen product will ultimately have to be compressed for storage and/or distribution. Significant plant energy savings could be achieved by compressing the water feedstock to the process operating pressure in the liquid phase. In addition, there are some potential advantages of high-pressure operation related to kinetic effects. In particular, the concentration overpotential, an

important irreversibility, should be reduced at high pressure. The steam/hydrogen mixture can be passed through a separator (e.g. steam condenser) to yield a high-purity hydrogen gas product.

Table 1. Conceptual plant parameters

High temperature electrolysis conceptual plant design		
Reactor power	600 MWth	
Hydrogen production	2.12 kg H ₂ /s	182.9 t/day 76.5 million scf/day
<hr/>		
Cell parameters		
Temperature	850°C	1 123 K
Pressure	5.0 MPa	702.5 psi
Current density	0.2 A/cm ²	
<hr/>		
Cell thickness		
Electrolyte	0.2 mm	
Anode	0.5 mm	
Cathode	1.0 mm	
Bipolar plate	2.5 mm	
Total cell thickness	4.2 mm	

As indicated in Figure 1, the focus of our research is the hydrogen-production process, including the development of reliable high-temperature solid-oxide fuel cells, and the development of an energy-efficient and cost-effective means for separation of hydrogen gas from the steam/hydrogen mixture.

This conceptual design will focus on the parameters for the gas supply to the electrolytic cells and on the number and configuration of the cells necessary to accommodate a reactor producing 600 MWth. At a nominal efficiency of 50% the HTE plant would produce about 2.5 kg of H₂ per second.

As indicated earlier, the input gas flow will be a 50:50 (volume) mixture of steam and hydrogen at 850°C. The input mixture is dictated by two considerations. First the gas must contain sufficient steam to provide steam for electrolysis across the entire width of the cell and secondly, some hydrogen (perhaps as little as 10%) must be present at the inlet to assure reducing conditions and to prevent electrode oxidation.

Table 2. Electrolyser size and water use

Electrolyser volume		
Stack volume	428.4 m ³	
Manifolding	75.0%	
Total hot volume	1 713.0 m ³	
Stack height	5.0 m	16.5 ft
Width	15.0 m	49.2 ft
Length	22.7 m	74.4 ft
Water use		
Input to hydrogen production	19.1 kg/s	302 gallons/minute 434 937 gallons/day
Cooling water evaporation	139.3 kg/s	2 208 gallons/minute 3 179 147 gallons/day

The gases have been approximated as ideal gases at these high temperatures. The volumetric flow on the steam/H₂ side of the cell remains constant, while the oxygen flow on the cathode side of the cell increases during its passage across the face of the cell. The output mixture on the steam/H₂ side has been found experimentally to be about 27 volume percent steam and 73 v/o H₂. Other steam/hydrogen ratios can be achieved with variation of flow rate, current density and cell size.

The current density adopted in this conceptual design is 0.2 A/cm² (2 000 A/m²) consistent with current densities that have yielded 40 000 hour-operation in solid-oxide fuel cells. Based on this current density a total active cell area of 120 000 m² would be necessary for the total hydrogen production rate indicated earlier.

For this conceptual design, the individual cells are assumed to have a 100 mm x 100 mm active area. The relatively small size is determined by the thermal expansion compatibility between the electrolyte and the electrodes in an electrolyte-supported configuration. Advanced in electrode materials to permit a more conforming bond between the electrolyte and electrodes could allow larger cell sizes. Alternatively, the use of an electrode-supported configuration, in which the electrolyte is of order 10-30 μm thick, would also allow for larger cell sizes.

In this design the electrolyte is assumed to be 50 μm thick. The anode is 500 μm, and the cathode is 1.0 mm. The bipolar plate, which provides passages for the steam-hydrogen mixture and separate passages for the produced oxygen, is 2.5 mm thick.

In estimating the total hot volume for the plant, we have assumed that the volume necessary for manifolding is three times the cell volume. Thus the total cell volume is 486 m³ and the overall hot volume is 1 994 m³.

The cells would be arranged in stacks of approximate 1 000 cells, with the current flowing vertically through the cells (electrically in series) while the two gas streams flow horizontally. A current of 20 A at a voltage of approximately 1 100 V would be supplied to each of the stacks. There would be 75 stacks in each row and about 155 rows in the overall plant. For manufacturing and maintenance reasons the stacks would probably be grouped in modules of 4 or 8 stacks. Each module would have common set of electrical, instrumentation and gas connections and would be installed and removed as a unit.

The channels in the bipolar plate are semicircular in cross-section, with a 1.0 mm diameter and a spacing of 2.0 mm. The preliminary gas-flow calculations indicate that the average flow velocity is about 0.043 m/s in the steam-hydrogen channels and about 0.005 m/s in the oxygen channels. Much more detailed modelling of the gas flow in individual cells is now being performed at Argonne National Laboratory in Chicago.

Nuclear hydrogen initiative research plans

The US Department of Energy, Office of Nuclear Energy (DOE-NE) is completing a plan for undertaking the R&D necessary to show that the nuclear production of hydrogen is technically and commercially feasible. The goal of the R&D plan, called the Nuclear Hydrogen Initiative, is to have demonstration facilities ready for use with the Next Generation Nuclear Plant (NGNP) a very high temperature helium-cooled reactor, in 2016. The Nuclear Hydrogen Initiative is considering the requirements of both the thermochemical cycles and high temperature electrolytic processes for hydrogen production.

The primary categories of nuclear-specific R&D for high temperature electrolysis are:

- System design studies to support cost and performance assessment for HTE nuclear plants,
- HTE cell and module optimisation to support technology demonstration.

System design and trade studies

The most pressing research need for HTE is the development of a conceptual design in order to identify the component needs specific to the nuclear production of hydrogen. The NHI design study will identify the changes in present SOFC materials, configurations and operating modes necessary for HTE. Today, the tubular SOFC design is the most developed of the SOFC designs. However, the tubular configuration requires approximately ten times more hot volume than a planar configuration for the same hydrogen production rate. Therefore a trade study is needed to determine the economic and engineering impacts of the cell configuration, arrangement of steam generator, the means for reheating the steam and the methods for steam-hydrogen separations. In addition, the trade study must consider the optimum operating pressure. The overall design of the HTE plant needs to be optimised within the context of electrical grid requirements, particularly with regard to peaking power, grid stability, and providing backup sources of electricity if the grid includes a substantial renewable energy (e.g. wind) component.

Models of HTE processes and systems performance are also required to support the conceptual design and assess performance potential. These analyses include cell and module thermal and structural models that address the behaviour of the electrodes, electrolyte, interconnection and seals in the face of thermal and chemical challenges and electrochemical models of materials flow through the individual cells. This will help determine the temperature and current distributions, particularly in response to changes in material properties. Thermal models of the HTE system and reactor interface, including heat exchangers, separators and flow-control devices are needed to optimise overall plant performance.

The costs of power electronics are an important output of these trade studies. Rectifiers for the conversion of AC to DC are a major cost in the overall HTE plant. Proper choices of stack voltage and current, and the use of standard components may substantially reduce the cost of power conditioning and control.

HTE cell/module optimisation

Although the development effort for solid oxide materials for high temperature fuel cells has been substantial, the engineering and optimisation of the solid oxide electrolyser cell (SOEC) is at an early stage. Several engineering issues must be addressed as part of the development of the cell/module for a HTE hydrogen production plant.

- *Interconnections* – The use of metallic interconnection between planar cells would result in lower ohmic losses, improved resistance to thermal and mechanical shock and reduced manufacturing costs. The choice of interconnection material is closely related to the choice of electrolyte, since the ionic resistivity of the electrolyte is very temperature dependent, dropping by a factor of two between 750 and 850°C. The use of metallic interconnections would require lower operating temperatures than present day ceramic interconnections.
- *Cell sealing* – Sealing between SOFC cells is a major issue in the choice of tubular versus planar configurations. The sealant must withstand both the oxidizing environment of the anode and the reducing conditions of the cathode. The tubular designs have avoided some of the sealing problems by closing the ends of the tubes and providing a plenum within the tube sheet to separate the oxidizing and reducing environments. Edge sealing in a planar configuration has more stringent requirements. Glass has been used as a bonding sealant since it can be tailored to match the expansion coefficients of the stack components. However, over long operating times at SOFC temperatures, glass tends to crystallize and to react with stack components. An alternative to bonding glass seals such as non-bonding compressive seals needs to be examined. Steam plenum design options, such as those patented by Siemens Westinghouse, may be applied to planar designs. Design studies and lab testing is needed to address these issues.
- *Electrolyte performance* – Research in the electrolyte material is seeking higher conductivity materials with comparable cost and chemical advantages. Advanced materials (e.g. scandium doped zirconia, lanthanum gallate with strontium doping) are being developed and will be examined for this application.
- *Cathode materials* – The use of nickel-nickel oxide or nickel zirconia cermets will be satisfactory as long as the steam-hydrogen mixture (rather than pure steam) is used to maintain reducing conditions. Cathode conditions are less challenging for HTE than for SOFC conditions, for which these cathode materials are being developed. Issues in the use of nickel with coal combustion gases pose more difficult problems due to the presence of sulphur and other contaminants.
- *Anode materials* – Lanthanum strontium manganite (LSM) has been the most frequently used material in SOFCs, both tubular and planar. Perovskite-structured ceramics have been developed for applications at lower temperatures. The consensus of experts is that initial demonstrations of HTE could rely on LSM.
- *Materials costs* – The operation of the SOECs at high temperatures requires the use of expensive alloys through the balance of plant. Therefore the development of materials for lower temperature operation may result in overall reduction in the hydrogen cost due to a reduced capital investment in the plant. The impact of reduced materials costs is a central consideration in the trade studies described above.

The R&D needed for the development of the nuclear HTE system is summarised in Table 3 below. In the column headed “Needed research”, those areas where DOE-NE should take the primary responsibility are indicated. In those areas where other offices within DOE are leading the research, an ongoing monitoring of such research is specified.

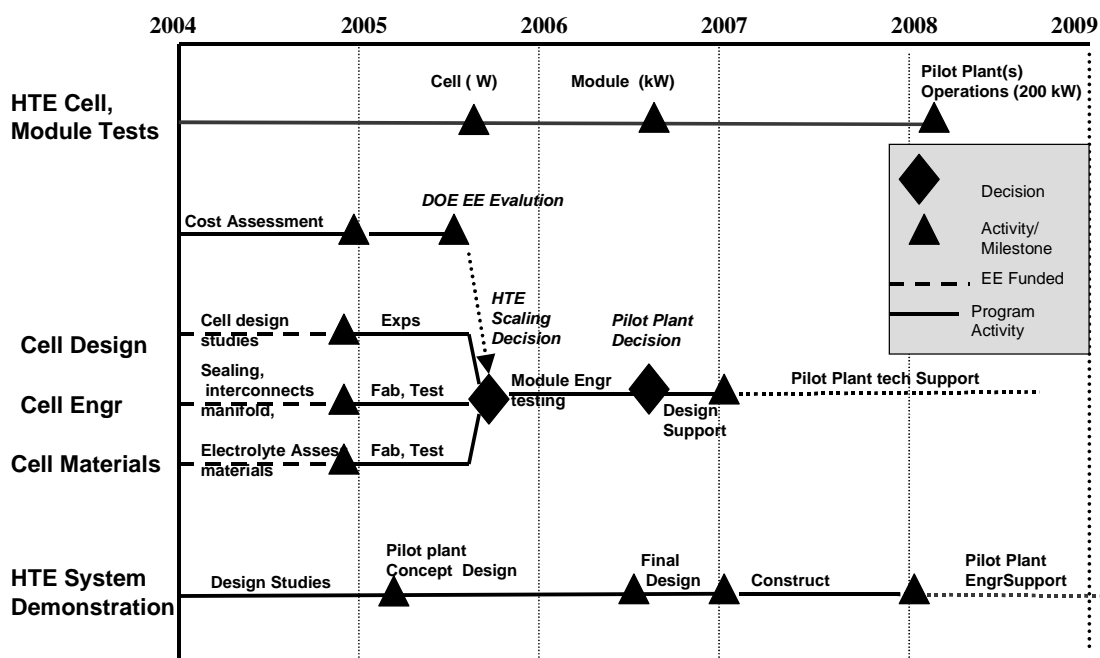
Table 3. Summary table of research needs

Technical issue	SOFC approach	HTE requirement	Ongoing research	Needed research
System configuration	15 kWe stack or tube bundle limit	100-300 MW hydrogen	None for electrolysis	Design and trade studies for materials and component selection. Include impact of pressurised operation. Need for NE lead
Interconnections	Lower temp – use of metallic interconnections	Less thermal cycling than SOFCs	FE, metallic interconnection	HTE may be less severe environment than combustion SOFCs. <i>Monitor FE research</i>
Cell sealing	Tubular – eliminate seals Planar – glass	Long duration compressive or steam sealing	FE, SECA	Incorporate current technology into trade studies. <i>Monitor FE research</i>
Modelling	Heat removal is the major issue	Reheat of steam necessary	None for electrolysis	Both cell-level and plant-level modelling necessary Need for NE lead
Electrolyte performance	YSZ	YSZ satisfactory if reactor can supply high temps	FE also working for lower temperatures	Assess impact of different/thinner electrolytes on reactor requirements
Cathode materials	Ni-Zr/NiO/ZrO ₂	HTE has less challenging environment	FE has lead.	<i>Monitor FE research</i>
Anode materials	LSM	Assess need for oxygen diluent	FE has lead	Incorporate consideration of O ₂ sales and requirements in trade study Need for NE lead
Power electronics	Inverters DC to AC	Rectifiers AC to DC	HTE has fundamentally different needs	Assess system operation in trade study
Material demands	Materials costs a smaller driver than performance	HTE will use large amounts of materials in cells and in BOP	Not as important to FE as to NE	Incorporate overall impact of materials choices in trade study. Need for NE Lead

The sequence and interaction of these major areas are summarised in Figure 12. The planning assumptions for this R&D plan include early testing of candidate cells (button) based on materials being developed in the DOE fuel cell programme. The NHI activities will focus on module testing to provide performance information for pilot plant decisions. The design and operation of a pilot plant at the nominal 200 kWe level could be initiated at a smaller power level and expanded as improved materials and electrolyser cells become available.

The highest priority for nuclear HTE development is developing a conceptual design that can be used to support cost and performance assessments in FY2004. With confirmation of performance and cost effectiveness, the NHI research effort will focus on the demonstration of HTE cell performance based on the most promising materials and technology available from the DOE FE programme. The cell engineering efforts will support the demonstration of SOEC modules in FY2006-2007. The NHI technology demonstrations will provide the basis for pilot plant decisions in FY2007. The DOE FE technology research and the NHI system design and cell demonstration activity will be closely coordinated to assure the most efficient use of R&D investments from both DOE Offices.

Figure 12. HTE Research plans in the nuclear hydrogen initiative



Conclusions

High temperature electrolysis using solid oxide technology appears to be a viable means for producing hydrogen using nuclear energy. Laboratory scale experiments over last year have shown that this technology can produce hydrogen at close to the theoretical parameters.

The needed R&D tasks have been identified in the Nuclear Hydrogen Initiative include determining the overall nuclear/hydrogen system parameters, as well as the development and long term testing of cell materials and components. Those long-term tests have begun and are continuing.

REFERENCES

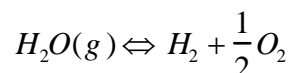
- [1] International Atomic Energy Agency (IAEA), *Hydrogen as an energy carrier and its production by nuclear power*, IAEA-TECDOC-1085, May 1999.
- [2] Hino, Ryutaro, Hideki Aita, Kenji Sekita, Katsuhiko Haga and Torno-o Iwata, *Study on Hydrogen Production by High Temperature Electrolysis of Steam*, JAERI-Research 97-064, Japan Atomic Energy Research Institute, September 1997.

HYDROGEN PRODUCTION BY WATER DISSOCIATION USING MIXED CONDUCTING MEMBRANES*

U. (Balu) Balachandran, T.H. Lee, S. Wang and S.E. Dorris
Energy Technology Division, Argonne National Laboratory
Argonne, IL 60439

Abstract

Water dissociates into oxygen and hydrogen at high temperatures:



The problem with exploiting this reaction is that very low concentrations of hydrogen and oxygen are generated even at relatively high temperatures (e.g., only 0.1 and 0.042% for hydrogen and oxygen, respectively, at 1 600°C), because the equilibrium constant for this reaction is small. However, significant amounts of hydrogen or oxygen can be generated at moderate temperatures if the equilibrium is shifted toward dissociation by either oxygen or hydrogen removal using a mixed-conducting (both electrons and ions) membrane. We have studied hydrogen production from water splitting at moderate temperatures (700-900°C) with novel mixed-conducting membranes. Hydrogen production rates were investigated as a function of temperature, water partial pressure, membrane thickness, and oxygen chemical potential gradient across the membranes. The hydrogen production rate increased with both increasing moisture concentration and oxygen chemical potential gradient. A hydrogen production rate of 6 cm³(STP)/min-cm² was measured with a 0.10 mm-thick membrane at 900°C using 50 vol.% water vapour on one side of the membrane and 80% hydrogen (balance helium) on the other side. The hydrogen production rate increased with decreasing membrane thickness, but surface kinetics played an important role as the membrane thickness decreased. In these experiments, hydrogen was used as a model gas to establish a high oxygen potential gradient; however, another reducing gas, such as methane, could be substituted to maintain the high oxygen potential gradient. With methane as a feed gas, hydrogen would be produced on one side of the membrane, while synthesis gas would be produced on the other side. Detailed results of hydrogen production from water splitting with mixed-conducting membranes will be presented in this talk.

* Work supported by US Department of Energy, Office of Fossil Energy, National Energy Technology Laboratory's Gasification Technologies Program, under Contract W-31-109-Eng-38.

A paper on this topic is accepted for publication in the International Journal of Hydrogen Energy, 2003.

COUPLING THE MODULAR HELIUM REACTOR TO HYDROGEN PRODUCTION PROCESSES

Matthew B. Richards, Arkal S. Shenoy and Kenneth R. Schultz*
General Atomics, P.O. Box 85608, San Diego, CA 92186

Abstract

Steam reforming of natural gas (methane) currently produces the bulk of hydrogen gas used in the world today. Because this process depletes natural gas resources and generates the greenhouse gas carbon dioxide as a by-product, there is a growing interest in using process heat and/or electricity generated by nuclear reactors to generate hydrogen by splitting water. Process heat from a high-temperature nuclear reactor can be used directly to drive a set of chemical reactions, with the net result of splitting water into hydrogen and oxygen. For example, process heat at temperatures in the range 850°C to 950°C can drive the sulphur-iodine (S-I) thermochemical process to produce hydrogen with high efficiency. The S-I process produces highly pure hydrogen and oxygen, with formation, decomposition, regeneration, and recycle of the intermediate chemical reagents. Electricity can also be used directly to split water, using conventional, low-temperature electrolysis (LTE). Hydrogen can also be produced with hybrid processes that use both process heat and electricity to generate hydrogen. An example of a hybrid process is high-temperature electrolysis (HTE), in which process heat is used to generate steam, which is then supplied to an electrolyser to generate hydrogen. This process is of interest because the efficiency of electrolysis increases with temperature. Because of its high-temperature capability, advanced stage of development relative to other high-temperature reactor concepts, and passive-safety features, the modular helium reactor (MHR) is well suited for producing hydrogen using nuclear energy. In this paper we investigate the coupling of the MHR to the S-I process, LTE, and HTE. These concepts are referred to as the H2-MHR.

* e-mail: Matt.Richards@gat.com, Arkal.shenoy@gat.com, Ken.Schultz@gat.com

I. Introduction

There is a large and growing demand for hydrogen in the United States and the rest of the world, with the bulk of the hydrogen being produced by steam reforming of methane with carbon dioxide as a by-product. Hydrogen and electricity are expected to dominate the world energy system in the long term. As the world transitions to a hydrogen economy, hydrogen will be used increasingly by the transportation, residential, industrial, and commercial sectors of the energy market. Eventually, the demand for natural gas may outpace its production. There may also be strong environmental and economic incentives in the future to produce hydrogen without generating carbon dioxide as a by-product. For these reasons, there is a growing interest in using nuclear energy to produce hydrogen.

Of the advanced reactor concepts currently being considered for future deployment, the modular helium reactor (MHR) is especially well suited for producing hydrogen, because of its high-temperature capability, advanced stage of development relative to other high-temperature reactor concepts, and passive-safety features [1]. Preliminary evaluations have shown the sulphur-iodine (S-I) process can produce hydrogen with high efficiency when driven by the 850°C to 1000°C process heat from a modular helium reactor (MHR), and economic assessments have shown an S-I-based H₂-MHR plant can be cost competitive with a steam-reforming plant, especially if the cost of natural gas increases because of increased demand. Hydrogen production efficiencies exceeding 50% may be possible using the SI process.

Hydrogen can also be produced using conventional low-temperature electrolysis (LTE) with electrolyzers that are commercially available today. The overall hydrogen production efficiency is the product of the heat-to-electricity conversion (thermal) efficiency and the electricity-to-hydrogen production (electrolysis) efficiency. When the MHR is coupled to a gas turbine operating with a Brayton cycle, the thermal efficiency is approximately 48%. If it is required to compress the hydrogen to pipeline pressures (~50 atm), the electrolyser efficiency is approximately 75%. Hence, the net efficiency of the process is about 36%. The efficiency of electrolysis can be improved by performing the process at higher temperatures, since the electrical energy required to split the water molecule decreases with increasing temperature. This concept is referred to as high-temperature electrolysis (HTE). With this concept, a portion of the heat from the MHR would be used to generate high temperature steam, and the remaining heat would be used to generate electricity. Both steam and electricity would be supplied to the electrolyser to produce hydrogen. Preliminary evaluations have shown that hydrogen production efficiencies on the order of 50% or higher can be achieved with this process.

II. The modular helium reactor

General Atomics (GA) has been developing high-temperature, helium-cooled nuclear reactors since the middle 1960s for electricity production and a variety of process-heat applications, including the production of hydrogen [2]. In more recent years, GA has been developing the passively-safe, modular-sized design referred to as the MHR. As shown in Figure 1, the MHR can be coupled directly to a Brayton-cycle power conversion system to generate electricity with high efficiency. This concept is referred to as the gas turbine modular helium reactor (GT-MHR). For applications that require process heat only (e.g. the SI process), the power conversion system is replaced with an intermediate heat exchanger (IHX). For hybrid applications that require both process heat and electricity, the power conversion system is supplemented with an IHX or a steam generator. Figure 2 shows a more detailed cross-sectional view of the MHR reactor system. The MHR operates at a thermal power level of 600 MW (t) with a core-outlet helium temperature in the range 850-1 000°C. For this design, the possibility of a core meltdown is precluded through the use of refractory, coated-particle fuel and

nuclear-grade graphite fuel elements with high heat capacity and thermal conductivity, combined with operation at a relatively low power density with an annular-core arrangement.

The MHR fuel element and its components are shown in Figure 3. The fuel kernels are manufactured using a sol-gel process and are coated with pyrolytic carbon and silicon carbide (SiC). The coating system consists of four layers and three materials; a low-density pyrolytic carbon layer (buffer), an inner high-density pyrolytic carbon layer (IPyC), a SiC layer, and an outer high-density pyrolytic carbon layer (OPyC). The coatings are deposited under conditions to produce isotropic material properties, and the layers are referred to collectively as a TRISO coating, which stands for TRI-material, ISOtropic. The coated particles are consolidated with a carbonaceous matrix into compacts which are loaded into graphite fuel elements. A standard fuel element has 210 blind fuel holes, 108 coolant holes, and contains 3 126 fuel compacts.

Figure 1. The gas turbine modular helium reactor

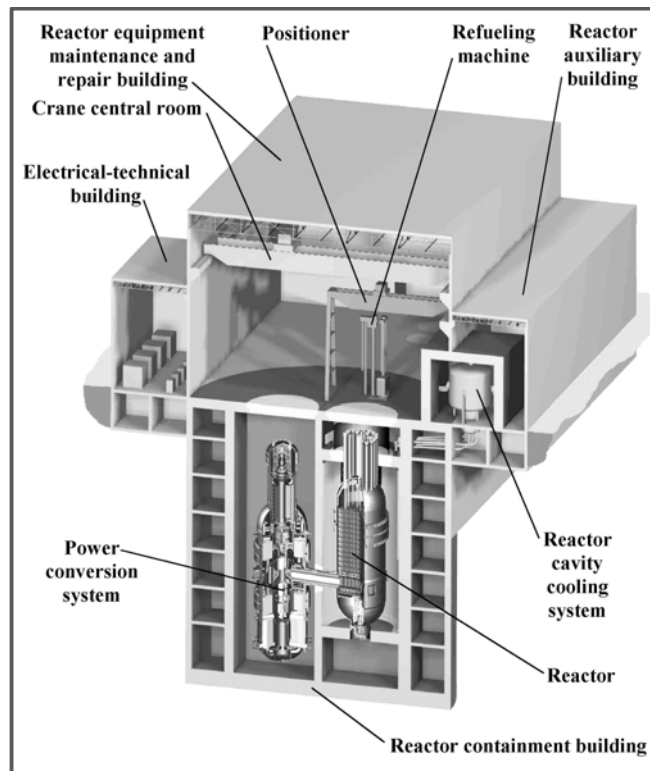


Figure 2. MHR internals

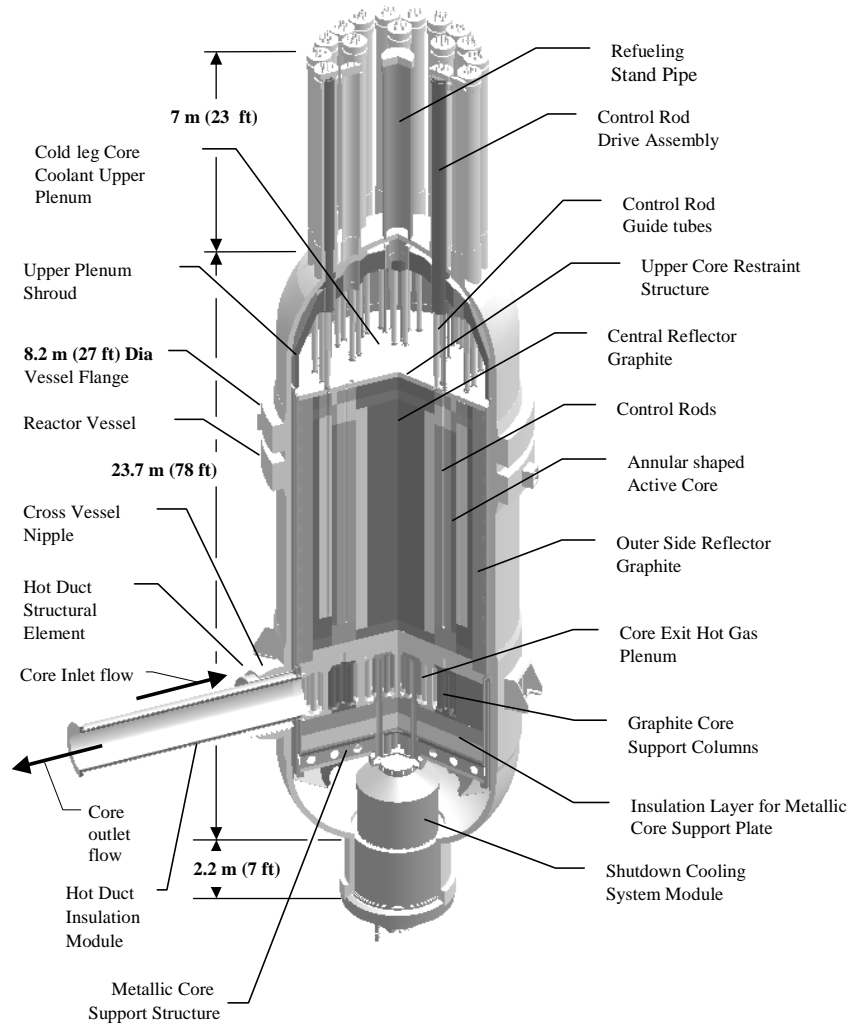
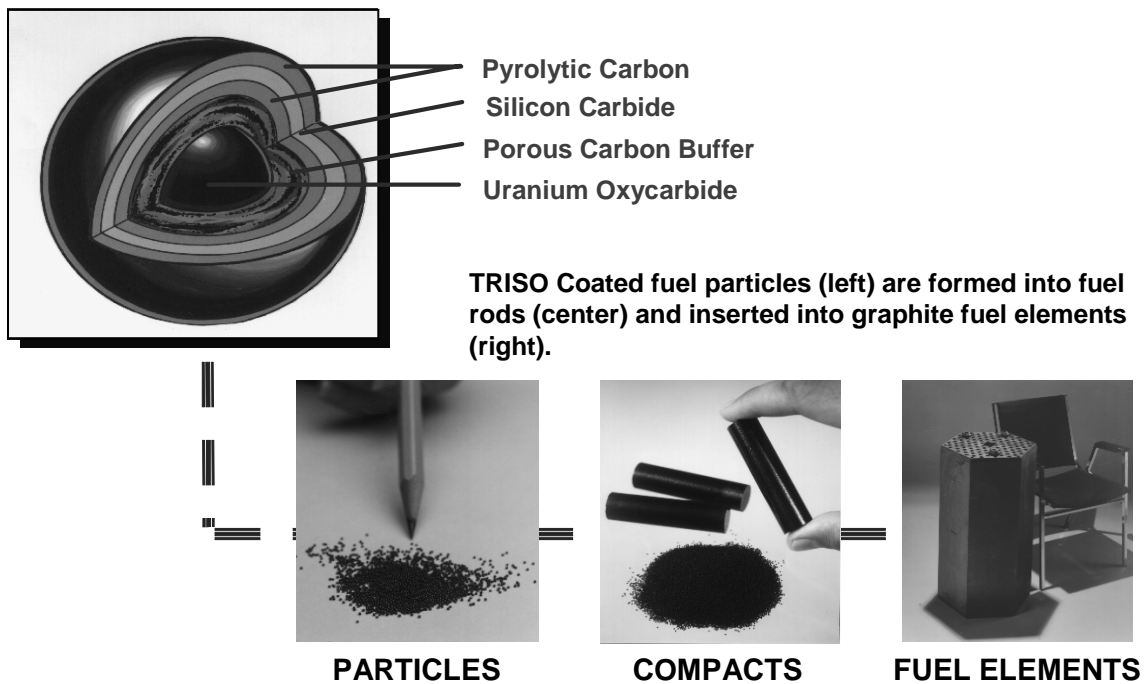


Figure 3. MHR fuel element components



III. Coupling the MHR to the S-I process

Water thermally dissociates into hydrogen and oxygen at temperatures approaching 4 000°C. As indicated in Figure 4, the S-I process consists of three primary chemical reactions that accomplish the same result at much lower temperatures. The process involves decomposition of sulphuric acid and hydrogen iodide, and regeneration of these reagents using the Bunsen reaction. Process heat is supplied at temperatures greater than 800°C to concentrate and decompose sulphuric acid. The exothermic Bunsen reaction is performed at temperatures below 120°C and releases waste heat to the environment. Hydrogen is generated during the decomposition of hydrogen iodide, using process heat at temperatures greater than 300°C. Figure 5 shows a simplified process flow diagram of the S-I cycle. Reference 3 provides a more detailed description of the S-I cycle, including thermodynamic analyses of flow sheets, equipment sizing, and cost estimates for the S-I cycle coupled to the MHR.

Figure 4. The sulphur-iodine thermochemical process

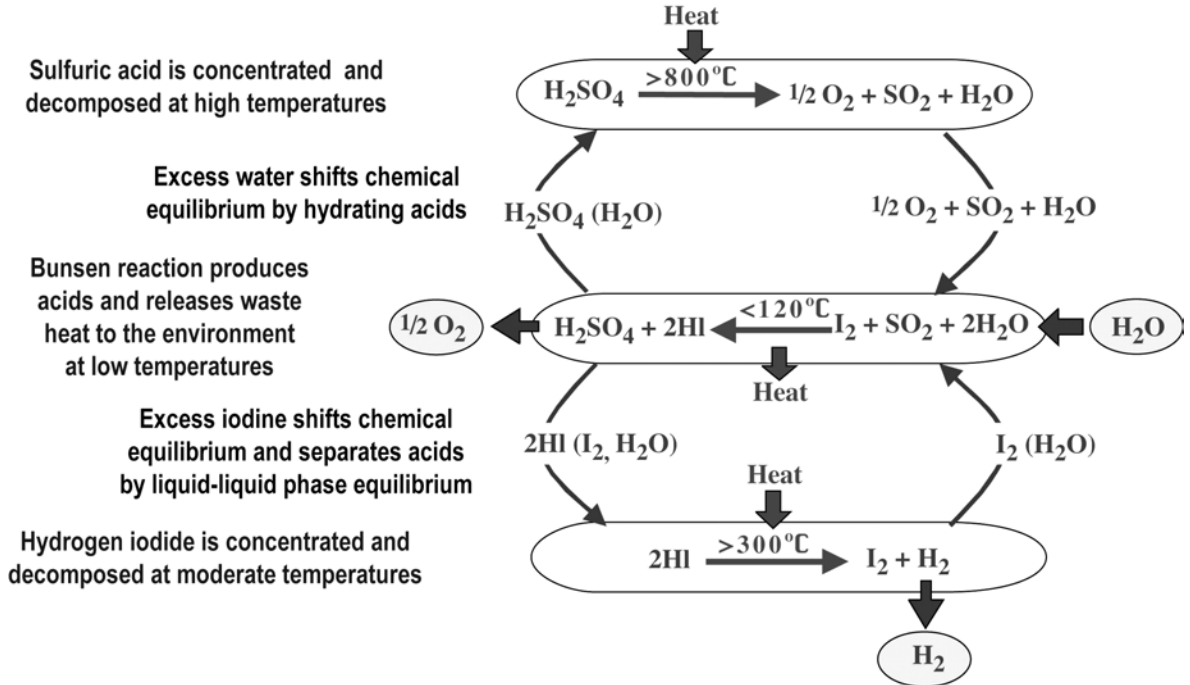


Figure 5. Simplified schematic of S-I process flow diagram

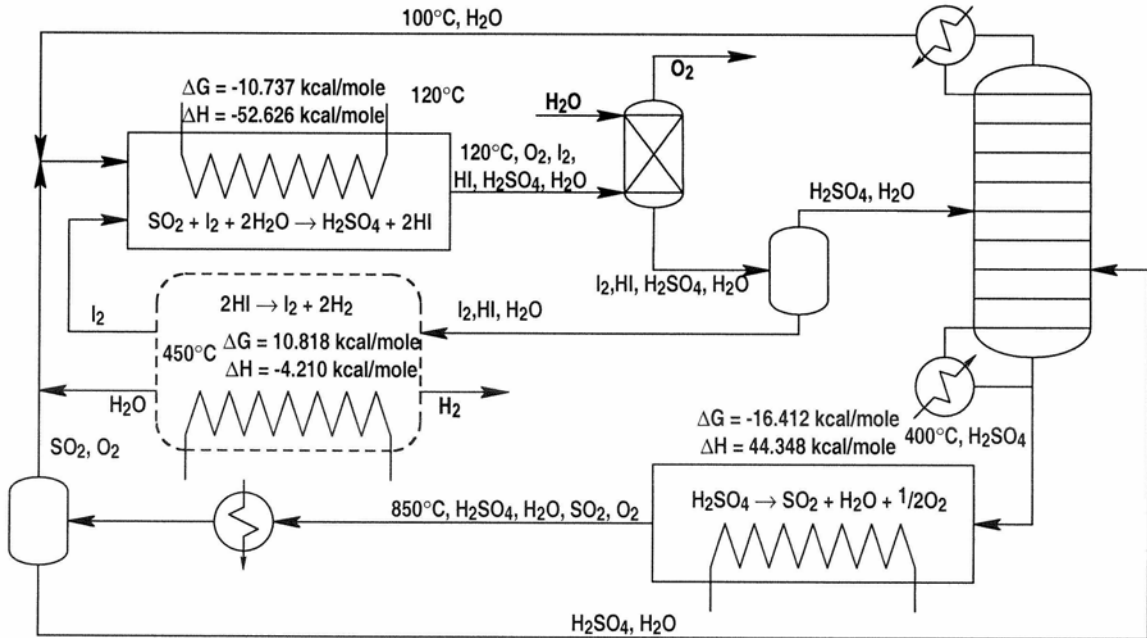
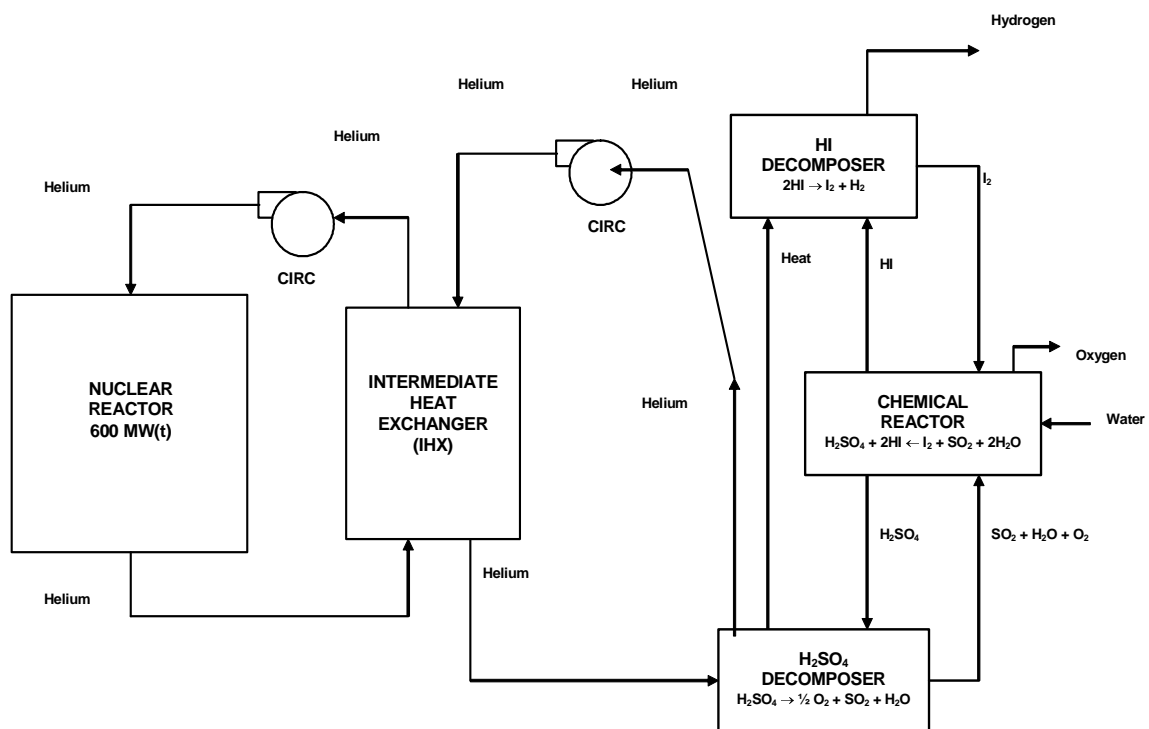


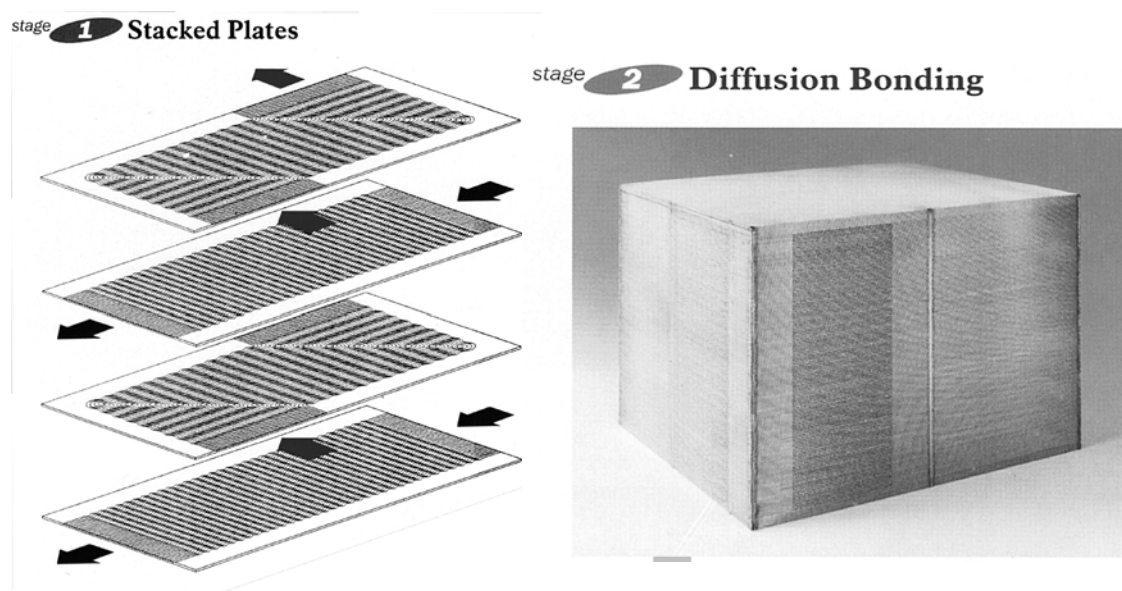
Figure 6 shows a simplified schematic of the S-I process coupled to the MHR. Heat from the primary cooling circuit is transferred to a secondary helium cooling circuit through the IHX. The highest temperature helium is utilized during decomposition of sulphuric acid. The overall efficiency of the S-I process will depend in large measure on how effectively the heat is utilized. Efficiency gains can be realised through effective recuperation of heat, minimisation of the quantity of water that must be vaporised (i.e., use more heat for decomposition of acids and less heat for concentration of acids), and minimisation of energy-intensive operations such as vapour recompression. Based on the Reference 3 assessments, the overall efficiency of the S-I process is 42% with a process-side temperature of 850°C and 52% with a process-side temperature of 950°C. This efficiency is defined as the ratio of the energy content of the hydrogen produced (using the higher heating value) to the thermal energy supplied to the process.

Figure 6. Simplified schematic of S-I-based H₂-MHR



The primary interface between the MHR and the hydrogen production plant is the IHX, which must be highly effective at transferring heat from the primary helium coolant to the process helium on the secondary side. The materials of construction must be compatible with the high process temperatures and the duty loads imposed by the plant, and should mitigate diffusion of plate out activity and tritium from the primary side to the secondary side. Maintenance requirements for the IHX must not be excessive, since plate out activity will build up on the primary side over time. A candidate concept for the IHX is the compact printed circuit heat exchanger (PCHE). These heat exchangers consist of metal plates that are diffusion bonded. Fluid-flow channels are chemically milled into the plates using a technique that is similar to that used for etching printed electrical circuits. With this technique, the PCHE design can be optimised for specific applications. Designs have been developed with thermal effectiveness greater than 98%. Figure 7 shows a PCHE manufactured by HEATRIC.

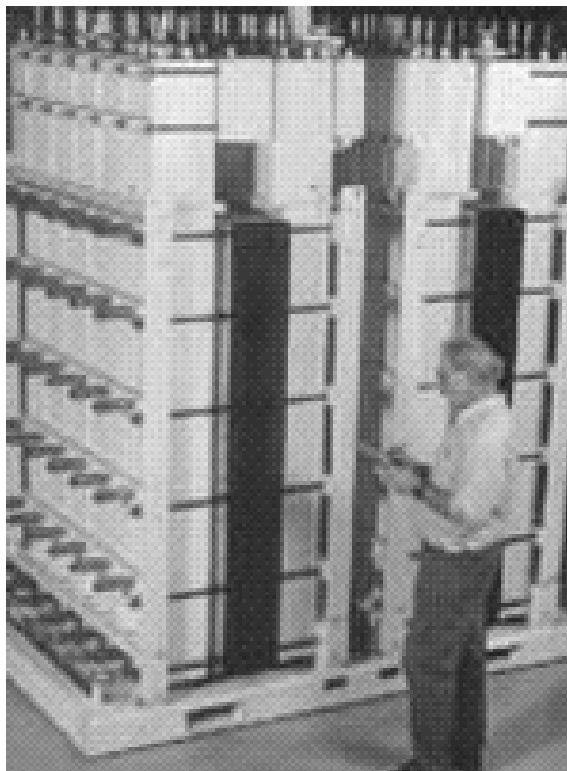
Figure 7. HEATRIC printed circuit heat exchanger



IV. Coupling the MHR to electrolysis

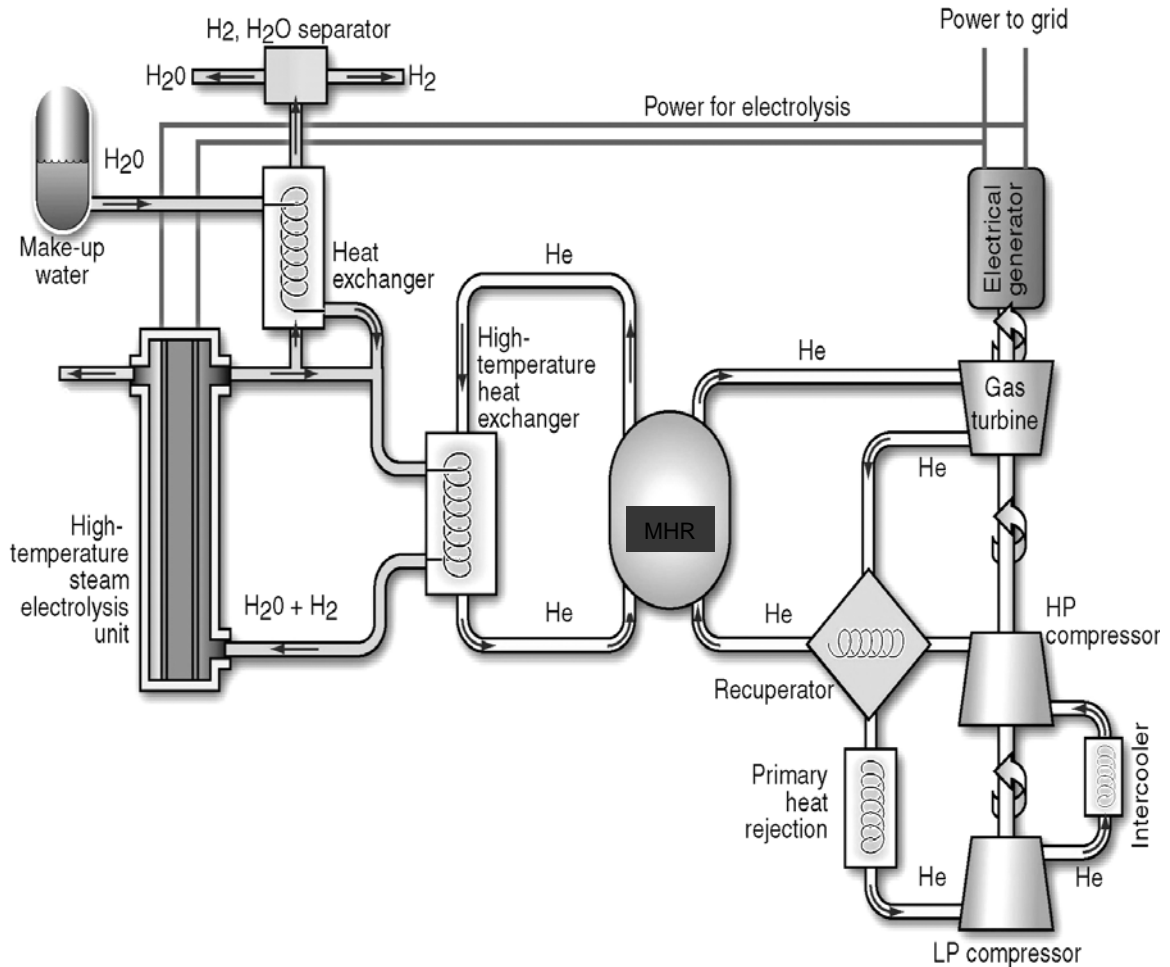
Coupling the GT-MHR to LTE is a straightforward process – the electricity generated by the GT-MHR is used to power conventional low-temperature electrolyzers. Commercial-scale electrolyzers could be co-located with MHRs. The hydrogen could then be compressed to approximately 50 atm and distributed via pipelines. Alternatively, the electricity could be distributed and used to make hydrogen at remote locations. Figure 8 shows a commercial-scale electrolyser manufactured by Stuart Energy. Economic evaluations of coupling nuclear energy with LTE have generally not been favourable when compared to the S-I process or steam reforming of methane [4]. It may be possible to lower the hydrogen production cost using LTE if efforts are made to maximise the use of lower-cost electricity available during off-peak periods.

Figure 8. Commercial-scale electrolyser manufactured by Stuart Energy



Coupling the MHR to HTE has been investigated by Idaho National Laboratory [5]. Figure 9 shows a simplified schematic of an MHR coupled to HTE. This concept involves operating a solid oxide fuel cell in reverse and using the MHR to supply both heat to generate steam and electricity to drive the electrolysis process. If the electrolyser is operated at about 800°C, approximately 75% of the energy is supplied to the electrolyser in the form of electricity and the remaining energy is supplied in the form of process heat to generate steam at 800°C. Theoretical hydrogen production efficiencies greater than 50% are predicted for MHR coolant outlet temperatures greater than 850°C.

Figure 9. Simplified schematic of HTE-based H₂-MHR
(figure courtesy of Idaho National Laboratory)



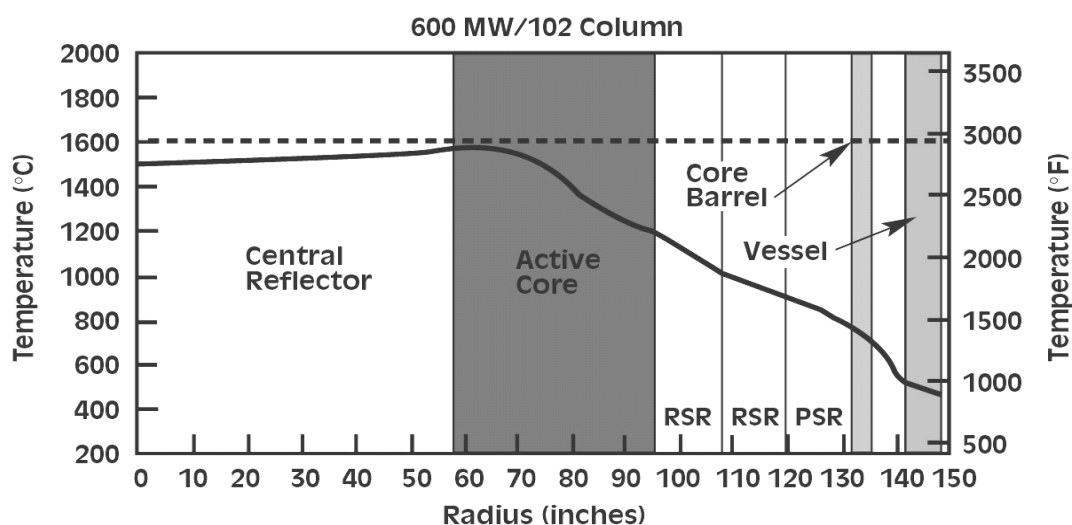
V. Safety considerations

The MHR's passive safety features include the high-temperature capability of coated particle fuel and the low power density and high heat capacity of the annular MHR core. During normal operation, the fuel temperature can be in the range 1 200°C to 1 300°C with end-of-life failure fractions below 10^{-4} . The fuel temperature can be as high as 1 600°C for shorter periods of time without any significant increase in the failure fraction. As shown in Figure 10, this temperature limit is not exceeded during hypothetical accidents, even for beyond design-basis events with conduction to the ground as the ultimate heat sink. The relatively small increase in fuel temperatures during accidents is a direct result of the MHR's high heat capacity and low power density. During normal operation and hypothetical accidents, the TRISO coating can be viewed as a miniature pressure vessel that provides containment of radionuclides. These coating materials are also highly resistant to oxidation and corrosion, and are excellent engineered barriers for retention of radionuclides in a repository environment.

A fundamental requirement for the H₂-MHR is that hydrogen production must not compromise the MHR's passive safety characteristics. This is accomplished by maintaining sufficient separation between the MHR and the hydrogen production process and ensuring that radioactivity levels in the hydrogen production plant are at sufficiently low levels to classify the hydrogen production process as a non-nuclear system. Radioactivity (including tritium) levels in the primary and secondary helium loops can be controlled to low levels using slipstream purification. Leakage from the primary to secondary side can be mitigated by operating the secondary side at higher pressure.

Figure 10. MHR temperature profile during a loss-of-coolant accident at the time when peak fuel temperatures occur

RSR = replaceable side reflector, PSR = permanent side reflector



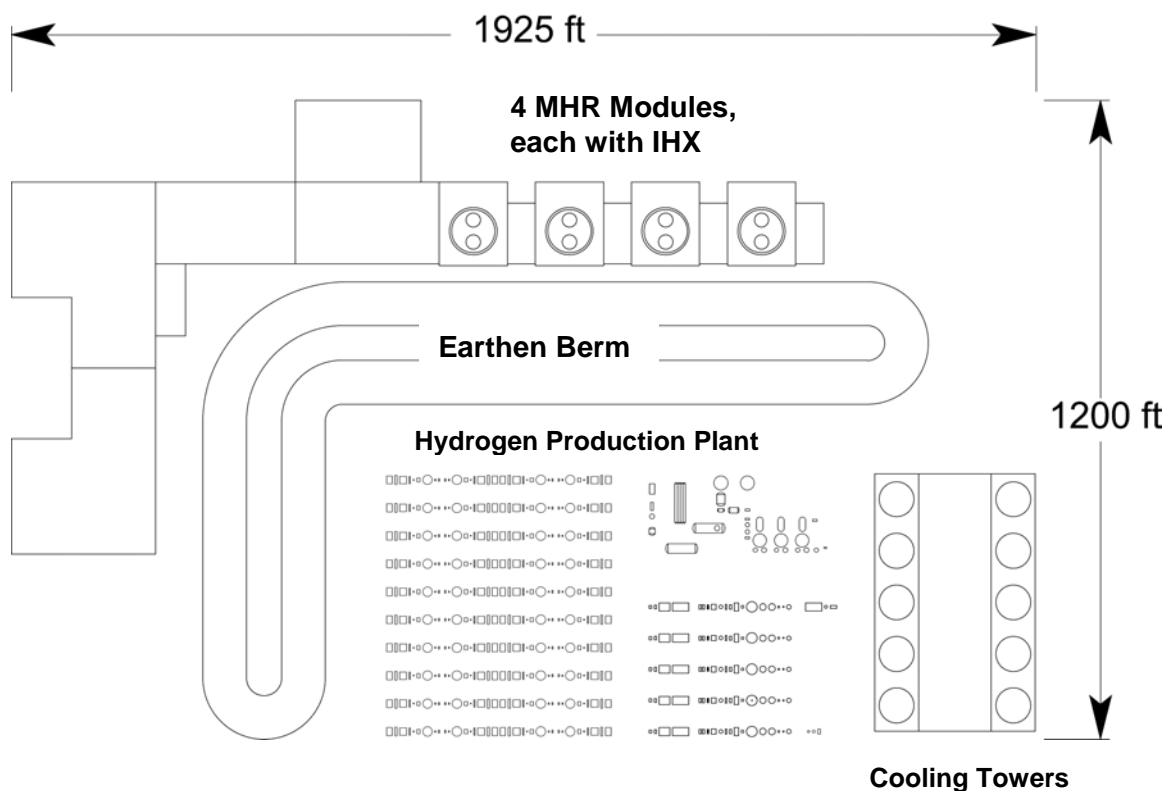
The impact of explosions and/or chemical spills in the hydrogen plant on reactor safety can be mitigated by physically separating the MHR from the hydrogen plant. One concept being evaluated is to use an earthen berm to provide protection while also minimising the separation distance (and lengths of piping runs) between the MHR and the hydrogen plant. If a chemical spill occurred, additional protection would be provided by the ventilation system for the MHR control room. Figure 11 shows a conceptual layout for an H₂-MHR plant consisting of four MHR modules. The equipment sizes and modular layout of the hydrogen plant are based on the studies described in Reference 3.

V. Economic considerations

A fundamental requirement for the H₂-MHR is to be economically competitive with hydrogen produced by steam reforming of methane. The Electric Power Research Institute (EPRI) has recently performed a comprehensive assessment of using high-temperature gas-cooled reactors to produce hydrogen, including economic evaluations of the MHR coupled to a variety of hydrogen production methods [4]. The EPRI assessment confirmed previous economic evaluations [3] for an S-I-based H₂-MHR plant, which concluded that hydrogen could be produced for about \$1.40/kg. If credit is taken for sale of the oxygen by-product, the cost could be as low as \$1.20/kg. These costs are competitive with hydrogen produced by steam reforming of methane at current natural gas costs of approximately \$5 per million BTU. If a carbon dioxide tax or carbon dioxide sequestration requirements were imposed, the S-I-based H₂-MHR plant would have a clear economic advantage over steam reforming of methane.

The EPRI study also confirmed the S-I process was the most economical process for coupling to the MHR and had a significant economic advantage over LTE. The EPRI study also evaluated an MHR coupled to HTE, but the concept evaluated by EPRI was different than that shown on Figure 9 and used a Rankine steam cycle to generate both electricity and high-temperature steam. For this concept, a portion of the steam exhausted from the high-pressure turbine is diverted through a reheater and then sent to the high temperature electrolyser. The cost estimate for hydrogen produced by this HTE-based H2-MHR is about 30% higher than that for the S-I-based H2-MHR. The cost-estimates for hydrogen produced by HTE are highly dependent on the cost and efficiency of solid oxide fuel cells.

Figure 11. Conceptual layout of S-I-based H2-MHR



VI. Conclusions

The MHR is well suited for coupling to the S-I process, LTE, and HTE for producing hydrogen. Hydrogen production will not compromise the passive safety features of the MHR. Economic evaluations have shown an S-I-based H2-MHR plant can produce hydrogen at costs that are competitive with a natural-gas fired steam-reforming plant, even if no cost penalties associated with carbon dioxide production are imposed on the steam-reforming plant. HTE is another promising concept for producing hydrogen with high efficiency. Although LTE does not appear to be economically competitive with other hydrogen-production processes, it is the most mature technology and could be a viable option under certain scenarios.

Work is continuing on developing the H2-MHR design, including optimisation of the reactor nuclear and thermal hydraulic design to increase the gas outlet temperature and improve efficiency,

while maintaining acceptable fuel and vessel temperatures during normal operation and accident conditions. Materials for the IHX are being evaluated and the IHX design is being developed to efficiently couple the MHR to the hydrogen plant. Flow sheets for the S-I-based hydrogen plant are being optimised to better utilize the heat supplied by the MHR and return helium to the IHX at acceptable temperatures. Work will also be performed to develop strategies for plant control and recovery from transients and off-normal conditions. In addition, the coupling of HTE to the MHR will be evaluated in more detail.

Acknowledgments

This work is funded by the US Department of Energy under NERI Grant DE-FG03-02SF22609/A000.

REFERENCES

- [1] Marshall, A.C., "An Assessment of Reactor Types for Thermochemical Hydrogen Production", SAND2002-0513, Sandia National Laboratories, Albuquerque, NM, February 2002.
- [2] Shenoy, A.S., "Modular Helium Reactor for Non-Electric Applications of Nuclear Energy", GA-A22701, General Atomics, San Diego, CA, November 1995.
- [3] Brown, L.C., G.E. Besenbruch, R.D. Lentsch, K.R. Schultz, J.F. Funk, P.S. Pickard, A.C. Marshall and S.K. Showalter, "High Efficiency Generation of Hydrogen Fuels Using Nuclear Power", GA-A24285, General Atomics, San Diego, CA, June 2003.
- [4] "High Temperature Gas-Cooled Reactors for the Production of Hydrogen: An Assessment in Support of the Hydrogen Economy", EPRI Report 10007802, Electric Power Research Institute, Palo Alto, CA, April 2003.
- [5] Herring, J., P. Lessing, J. O'Brien, C. Stoots, J. Hartvigsen and S. Elangovan, "Hydrogen Production Through High-Temperature Electrolysis in a Solid Oxide Cell", Proceedings of the Second Information Exchange Meeting on Nuclear Production of Hydrogen, Argonne National Laboratory, Argonne, IL., 2-3 October 2003.

SESSION IV

HYDROGEN PRODUCTION WITH FULLY INTEGRATED FUEL CYCLE GAS AND VAPOUR CORE REACTORS

Samim Anghaie and Blair Smith

Department of Nuclear & Radiological Engineering
University of Florida
Gainesville, FL 32611-8300

Abstract

This paper presents results of a conceptual design study involving gas and vapour core reactors (G/VCR) with a combined scheme to generate hydrogen and power. The hydrogen production schemes include high temperature electrolysis as well as two dominant thermochemical hydrogen production processes. Thermochemical hydrogen production processes considered in this study included the calcium-bromine process and the sulphur-iodine processes. G/VCR systems are externally reflected and moderated nuclear energy systems fuelled by stable uranium compounds in gaseous or vapour phase that are usually operated at temperatures above 1 500K. A gas core reactor with a condensable fuel such as uranium tetrafluoride (UF_4) or a mixture of UF_4 and other metallic fluorides (BeF_2 , LiF , KF , etc.) is commonly known as a vapour core reactor (VCR). The single most relevant and unique feature of gas/vapour core reactors is that the functions of fuel and coolant are combined into one. The reactor outlet temperature is not constrained by solid fuel-cladding temperature limits. The maximum fuel/working fluid temperature in G/VCR is only constrained by the reactor vessel material limits, which is far less restrictive than the fuel clad. Therefore, G/VCRs can potentially provide the highest reactor and cycle temperature among all existing or proposed fission reactor designs. Gas and vapour fuel reactors feature very low fuel inventory and fully integrated fuel cycle that provide for exceptional sustainability and safety characteristics. With respect to fuel utilisation, there is no fuel burn-up limit for gas core reactors due to continuous recycling of the fuel. Owing to the flexibility in nuclear design characteristics of cavity reactors, a wide range of conversion ratio from completely burner to breeder is achievable. The continuous recycling of fuel in G/VCR systems allow for complete burning of actinides without removing and reprocessing of the fuel. The only waste products at the backend of the gas core reactors' fuel cycle are fission fragments that are continuously separated from the fuel. As a result the G/VCR systems do not require spent fuel storage or reprocessing. Due to very low fuel inventory and continuous burning and transmutation of actinides, gas core reactors minimise the environmental impact and stewardship burden. G/VCR systems also feature outstanding proliferation resistance characteristics and minimum vulnerability to external threats. Even for comparable spectral characteristic, gas core reactors produce fissile plutonium two orders of magnitude less than light water reactors (LWRs). In addition, the continuous recycling and burning of actinides further reduces the quality of the fissile plutonium inventory. Results of the study indicate that due to high temperature operation of G/VCR systems an overall combined electricity and hydrogen production efficiencies of well over 50% are feasible. The high production efficiency is demonstrated for combined electric power generation and hydrogen production using all three schemes for wide range of output ratio.

1. Introduction

Gas and vapour core reactors (G/VCRs) are among the most revolutionary and promising energy production technologies for the 21st century. Perhaps the single most important and powerful feature of a gas core reactor is the fact that the fuel is in gaseous or vapour form, so that there is absolutely no threat of a core meltdown, the reactor is intrinsically safe and stable, and the energy released is transported directly by the circulating gas or vapour fuel. The gas core reactor nuclear energy system design is based on an externally moderated (cavity) reactor fuelled by stable uranium compounds in liquid and gaseous or vapour phase at peak operating temperatures that are usually above 1 500K. A condensable or non-condensable working fluid is added to enhance the heat transport property of the flowing core material. The primary fuel for these reactors is uranium tetrafluoride, which is one of the most stable uranium compounds in liquid and gaseous phases. Gas core reactors feature power generation, heat processing, and energy conversion at very high temperatures. The major competing technology to G/VCR systems are the high temperature gas cooled reactors (HTGRs), but HTGRs still use fuel in solid form, as do pebble bed reactors, liquid metal cooled reactors, and in fact all other nuclear reactors with the sole exceptions of molten salt core (MSR), molten metal (MMR), and aqueous core reactors. A brief introduction to gas and vapour core reactors follows, with emphasis on sustainability and fuel cycle aspects that motivate use of cleaner nuclear power for clean hydrogen production applications and/or cogeneration.

There are two distinct design options for G/VCRs.

(1) *A G/VCR-GT design (gas/vapour core reactor-gas turbine system)*. This is a near term two-stage power cycle system that uses a heat exchanger to heat a helium-xenon gas mixture that in turn drives a high temperature gas turbine, and rejects waste heat to further drive a conventional steam turbine cycle. The primary cycle would be a vapour core reactor with a fuel mixture of UF₄ and compatible molten salt such as an alkali metal halide such as BeF₂, LiF, KF, NaF, or a eutectic mix. Energy conversion efficiency close to 60% can be achieved in principle with such a combined cycle. Existing technology such as the industry standard Siemens-Westinghouse 501F and 501G systems that are widely used for natural gas burning power generation, would be adapted for the gas turbine cycle of this near term G/VCR system. The high temperature heat could also be transported to a separate part of the power plant for thermochemical hydrogen generation, for which peak temperatures around 1 200K are needed. In the G/VCR-GT cycle the reactor would operate at peak temperatures from 1 500K to 2 000K, and depending upon available material limits possibly up to 2 500K for peak electrical conversion efficiency (Carnot efficiency).

(2) *A G/VCR-MHD design (gas/vapour core reactor-magnetohydrodynamic system)*. This more advanced far-term deployment option would use a magnetohydrodynamic (MHD) power generator (a type of magnetic turbine) that can extract electrical power directly from the fissioning gas fuel, without any mechanical moving parts other than the flowing gas. The G/VCR-MHD concept is a longer term R&D project because of the severe temperatures that reactor vessel materials must withstand. This option will not be explicitly considered in this paper, but it should be noted that it's promise is considerable due to the high temperature operation that favours combined cycle options and/or cogeneration of heat for hydrogen production (at ~1 000°C).

Schematics for each of these proposed cycles are shown in Figure 1 and Figure 2 respectively. For the special purpose applications considered in this paper the bottoming heat recovery a thermochemical hydrogen production unit would replace the superheated steam Rankine cycle. The Brayton cycle would reject heat at approximately the same temperature ~800°C which would be used to split HBr in the calcium-bromine hydrogen production process (Ca-Br), or 900 to 1 000°C for the iodine-sulphur process (I-S).

A wealth of literature exists documenting the various design options and characteristics of gas core reactors. [1, 2, 3, 4] A complete review is beyond the scope of this paper. The main features are that G/VCR technology is thoroughly well proven. All of the theoretical challenges are understood and have been documented. The only unproven aspects of G/VCR technology development concern data uncertainties due to the lack of funding for basic experiments and materials research. The system described above would therefore be a viable system, but the estimates of efficiencies and performance of materials, particularly for the far-term G/VCR-MHD system, cannot be validated experimentally at this date. The primary challenges are material science R&D requirements. For example, the capabilities of the pressure vessels for high temperature are the limiting feature. The technical needs include development of ultra high temperature materials; determining the practicality of fission enhanced conductivity; nuclear design and control issues; and development of the nuclear MHD power conversion process.

The remainder of this paper looks in detail at electricity production and cogeneration options for G/VCRs, with emphasis on the fully integrated fuel cycle and high fuel utilisation and safety characteristics of G/VCRs in Section 2. Cogeneration of process heat for hydrogen production is the main other energy product considered. Section 3 discusses the literature on three promising methods for high temperature water splitting that would be suitable applications of G/VC process heat.

2. G/VCRs and electricity production

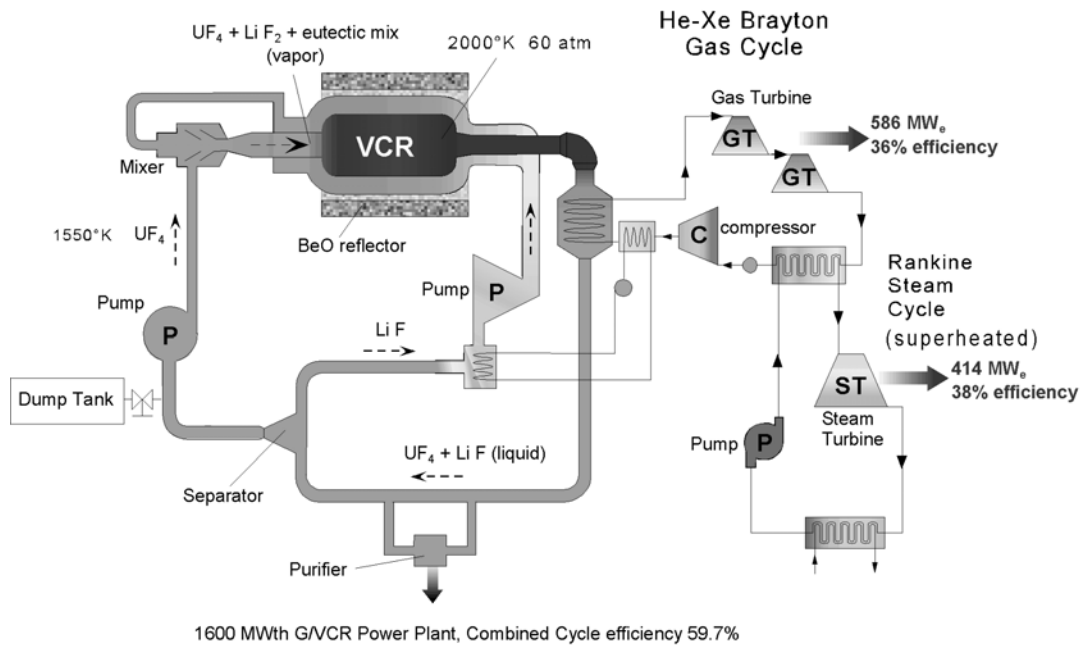
2.1 Highest energy conversion efficiency

Current LWRs use high quality nuclear energy to heat water. To make the best possible use of fission power requires a more direct energy conversion mechanism whereby the fissioning material itself is used to generate electricity without the need for an intermediate mechanism. The ultimate fission heat source would extract energy directly from the fissioning fuel. This is in fact possible with a gas/vapour core reactor.

However, even operating on a conventional gas turbine cycle a G/VCR can still produce electricity at higher efficiencies than most other high temperature advanced reactors. For example, the hot gaseous fuel from G/VCR can be used as a heat source for a conventional helium-xenon gas turbine, with enough heat left over in the gas turbine exhaust stream to allow a steam turbine cycle to extract further electrical power. In the advanced G/VCR-MHD design option an even greater efficiency is possible in principle due to direct or volumetric energy conversion.

The key features to note are the inherent safety of using a gaseous fuel that when heated expands and thus naturally shuts down the nuclear reaction. This is the complete opposite of most solid fuel reactors. Solid fuel reactors are always in danger of suffering fuel damage accidents and catastrophic meltdown because solid nuclear fuel can only give up heat to a surrounding coolant, and thus if coolant is restricted or stops flowing the fuel heats up and the nuclear chain reaction can go critical. Gas core reactors cannot suffer this fate, since the fuel is already gaseous, a coolant is not required, the gas just expands and the reaction shuts down when the pressure drops. A leak or other failing of the primary vessel would merely result in vapour condensing inside the secondary containment structure, which although expensive and undesirable this at least would not pose an environmental safety concern. The other key features that make gas core reactors more attractive than any other advanced nuclear fission energy system have already been mentioned above in the introduction.

Figure 1. Schematic of a near-term deployable gas or vapour core reactor (G/VCR) power system

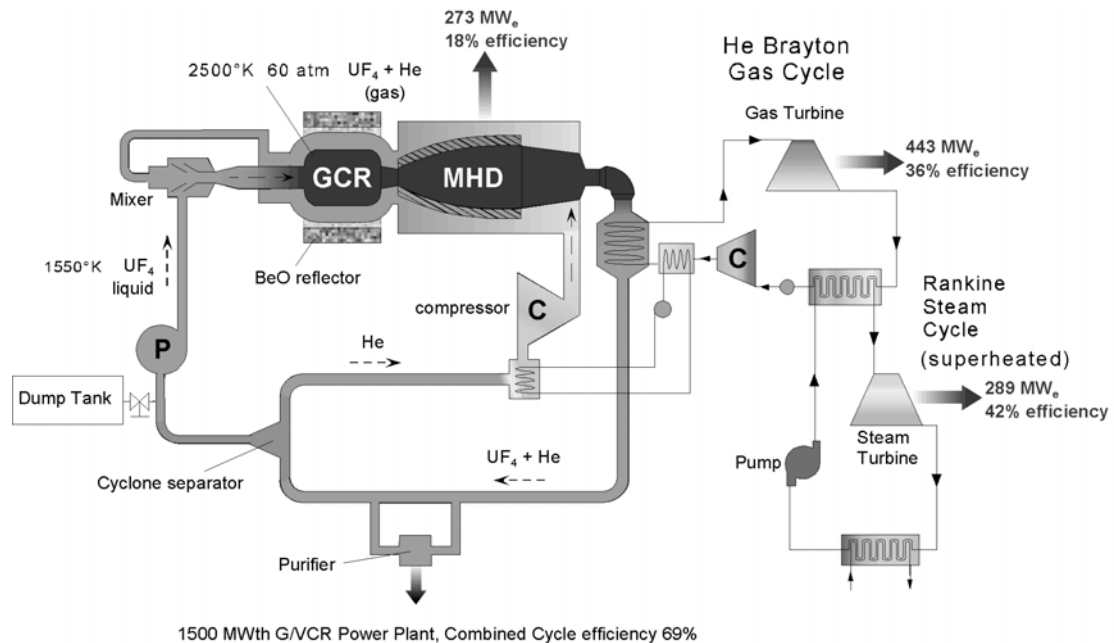


An ultra safe heat exchanger extracts heat from the high temperature G/VCR outlet stream and drives a closed cycle gas turbine. Modified Siemens-Westinghouse 501F GT series turbines could be used. The waste heat from the high temperature Brayton gas cycle would be recovered in a superheated steam Rankine cycle as illustrated.

The technology and engineering capabilities that exist at present would enable a small-scale prototype of the near-term deployable G/VCR-GT system to be built. The more advanced G/VCR-MHD system would not be capable of attaining the claimed efficiency of 70% net with present day technology. However, assuming that a gas core reactor could be fabricated, the entire system could in principle be built. Many modern coal-fired power stations for example use MHD generators (also see for example the Noyes Data Corporation review [5]) in combination with low ionisation potential seed materials (such as cesium) to enhance the electrical conductivity of the gas that must flow through the MHD generator fields. A gas core reactor built with current technology would probably not be robust enough to withstand the high temperature conditions, at least not over a long duration cycle, and hence the partial plasma properties of the fissioning gas would probably not be sufficiently enhanced for profitable MHD power conversion. Again some seed material could be added to enhance electrical conductivity but more R&D effort is required before this more advanced system can be considered for near-term deployment.

For thermochemical hydrogen production such extreme temperatures are not required. If process heat can be supplied at 850° to 1 100°C then water-splitting is possible. Thus for the remainder of this paper the gas/vapour core reactor system of choice is by default the near-term lower temperature G/VCR-GT type system in Figure 1.

Figure 2. Schematic layout for an advanced gas core reactor nuclear energy system



A high temperature magnetohydrodynamic turbine (MHD generator) extracts energy directly from the fissioning gas at the highest possible quality. A Brayton-Rankine combined cycle recovers the waste heat. This is one of the most efficient cycles imaginable with current technology.

2.2 A fully integrated fuel cycle

A closed fuel cycle implies that any useful fuel entering a system does not leave the system (without being used or safely disposed of in some way). Figures cited by the Uranium Institute [6] estimate that the total world recoverable resources of uranium are about 3 110 000 tons. Existing power plants operational worldwide require about 75 000 tons of uranium a year to produce roughly 17% of the total world power requirements. Thus the total natural resources will be sufficient to meet current and anticipated world demand for nuclear power for only about half a century. There are three solutions to the problem of finite non-renewable resources for nuclear power, (a) improve fuel utilisation by using nuclear reactors that recycle fuel, and (b) extract more energy per kilogram of fuel, (c) recycle previously spent fuel. The proposed gas core reactor systems described in this paper directly or indirectly can achieve all these goals.

A gas core reactor system can be designed to do more than simply close the fuel cycle, a G/VCR type system can employ a *fully integrated fuel cycle*, meaning that after mining of raw uranium, all subsequent movement of fissile and fertile nuclear material can be performed onsite, in-situ, at the gas core reactor facility itself. Firstly, the generic G/VCR system continuously circulates the fissioning fuel around a loop. By adding fresh fissionable isotopes and with continuous online removal of waste products the G/VCR is able to use all the available uranium fuel. No fissionable uranium is unused or wasted. Secondly, the fission energy released can be converted directly to electrical energy in a magnetohydrodynamic type of turbine, or indirectly, but still at high efficiency, by a combined power cycle. Thirdly, any fissionable spent fuel from old reactors can be fed into the circulating fuel of a G/VCR until the fuel is fully expended, leaving no waste fuel.

Fully integrated fuel cycles allow for complete burn up of fuel and actinides without the need for reprocessing, and moreover spent fuel from older decommissioned reactors can be reused, this is of

huge significance and should be factored in to any proposed solutions and analysis of future world energy needs. This is an especially acute observation knowing that fossil fuel reserves are dwindling and spent fuel from older reactors goes unused or stockpiles into an ever greater environmental burden.

To illustrate, consider for example the state of the art in modern light water reactor (LWR) technology considered to be the most robust and reliable current nuclear power generators, these reactors burn-up 150 to 200 metric tons of uranium fuel per Gigawatt of electricity per year, see also Table 1 which show other the fuel inventory requirements for selected conventional and advanced nuclear power plants. The G/VCR system is noticeably superior, with higher efficiency, fewer tones of uranium per gigawatt of power, and probably 10 times less fuel wasted, although in principle there should be *zero fuel waste* in a fully equipped, fully functioning G/VCR system. Indeed, in more than two dozen comparatives it is only in the areas of the capital cost, financial risk, and cost of deployment that are worse for G/VCR systems owing to the relative lower state of technological maturity of G/VCR systems. The important measurement is the low level of fuel waste attained by G/VCRs compared to all other competing solid fuel nuclear energy systems. Solid fuel systems cannot burn all their fuel without reprocessing spent fuel rods, whereas the G/VCR can recycle fuel online by continuous removal of impurities and can attain complete burn up of the fuel.

Table 1. Estimated comparative fuel use and efficiency measures for selected next generation nuclear power systems, (LWRs included for reference)

Generic system	Energy conversion efficiency	Fuel utilisation (MT per GW-year) of uranium	Fuel waste (MT per GW-year)
Gas/vapour core reactor	60 to 70%	<10	<5
Very high temperature gas cooled reactors	39%	100-150	5-10
Liquid metal cooled reactors	39%	<10	5-10
Light water reactor	33%	150-200	15-20

2.3 Nuclear waste minimisation

One of the most sensitive issues in the debate about future use of nuclear power is the problem of what to do with radioactive waste. Even fusion energy systems create large quantities of radioactive waste due to the high radiation levels and consequent massive doses of radiation imparted to the reactor materials (this is true even if the fusion process does not produce radiotoxic fuel products). The only permanent solution seems to be to radically reduce nuclear fuel waste by deploying new advanced reactor designs that utilise fuel more efficiently and produce less waste per megawatt of power produced by the system. A comparison of estimates of waste per megawatt is therefore most instructive. Table 1 shows that, by the level of long-term radioactive fuel waste produced, the gas/vapour core reactor is the more environmentally sound alternative. Similar estimates of other emissions and low level waste products also appear to favour gas core reactors over both light water reactors and the nearest comparable advanced high temperature concepts that use solid fuel (see for example the suite of Gen IV documents released recently by the DOE and the report by Anghaie & Lewis, 2002) [7].

Gas core reactors feature a fully burned and integrated fuel cycle. The only waste products at the backend of the gas core reactors' fuel cycle are fission fragments that are continuously separated from the fuel. It does not require spent fuel storage or reprocessing. Due to very low fuel inventory and continuous burning and transmutation of actinides, gas core reactors minimise the environmental impact and stewardship burden.

Low fuel inventory is a key design feature that distinguishes G/VCR systems as arguably the most proliferation resistant nuclear power systems and inherently safe with regard to physical protection. Lower fuel inventory (about two orders of magnitude lower than LWRs for the same power generation level) combined with continuous burning of actinides and separation of fission products significantly reduces the proliferation risk as well as the consequences of external or internal threats.

G/VCR systems also feature outstanding proliferation resistance characteristics and minimum vulnerability to external threats. Even for comparable energy characteristics on a par with LWRs, gas core reactors produce fissile plutonium two orders of magnitude less than LWRs. In addition, the continuous recycling and burning of actinides further reduces the quality of the fissile plutonium inventory, this is a highly *desirable* characteristic. In addition, the continuous recycling and burning of actinides further reduces the quality of the fissile plutonium inventory. The low fuel inventory (about two orders of magnitude lower than LWRs for the same power generation level) combined with continuous burning of actinides significantly reduces the need for emergency planning and vulnerability to external threats. Low fuel inventory, low fuel heat content, and online separation of fission fragments are among robust features that improve the safety performance and reliability of GVCR systems under normal operation and abnormal operational transients in compare with other fission power systems.

Due to circulation of fuel in gas core reactors, the entire operation is remote and robotically controlled. Continuous separation of fission products from fuel reduces the delayed source of radiation (after reactor shut down) to a bare minimum. These factors result in significant reduction in the probability of worker radiation overdose during normal operation. Any loss of system pressure, core damage, or fuel leakage results in loss of reactivity that is needed to keep the reactor critical. Because the fuel is in gaseous phase the core damage would be limited to pressure vessel and reflector damage that are not at the same level of severity with any other solid fuel reactor.

Clearly gas core reactors with their integrated fuel cycles and virtually complete fuel burn up (see the next section) characteristics stand out as unsurpassed in waste minimisation criteria.

2.4 Actinide burning

Many nuclear power systems produce high atomic mass with long-lived radioactive decay half-lives. These are considered contaminants and hazardous waste materials. A gas core reactor system is one of a number of new generation nuclear power systems that have been designed to burn these waste products. Only reactors that continuously circulate the fuel or somehow utilise neutrons to convert actinides into shorter-lived radioactive elements can get rid of actinides in this way. Gas core reactors may even take actinide waste from other power plants and convert or "burn" these actinides. Thus *G/VCRs can burn actinides from their own fuel as well as from the fuel waste of other "dirtier" nuclear power plants.*

Radionuclide generation and burn-up analysis was performed recently on a gaseous uranium-tetrafluoride fuelled reactor [8]. Data for the major actinides is shown in Figure 3 and Figure 4.

Figure 3. Masses of actinide radioisotopes in fuel versus burn up for 10% enriched fuel in a gaseous core reactor with UF₄ (10% mole fraction)-He (90% mole fraction) fuel

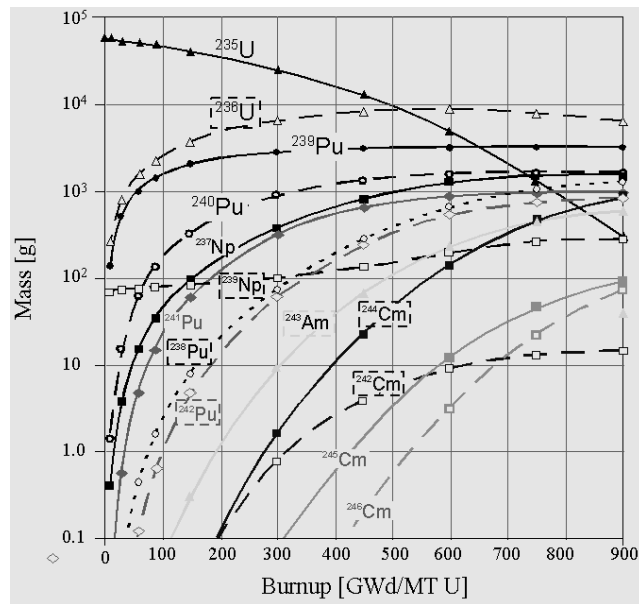
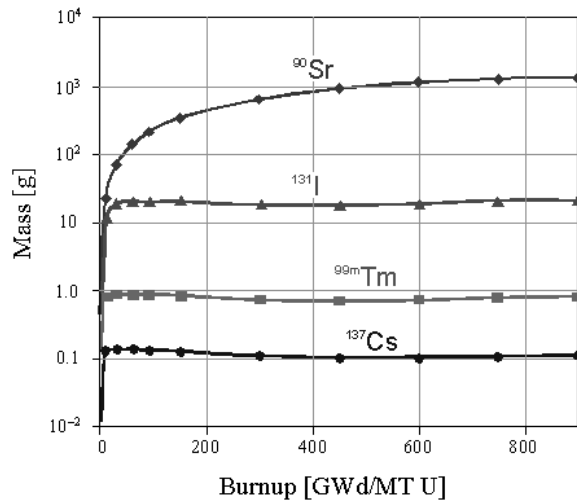


Figure 4. Masses of major source term radioisotopes versus burn up for 10% enriched fuel in a gaseous core reactor UF₄ (10% mole fraction)-He (90% mole fraction) fuel



Because actual experiments on nuclear systems are of course impractical the following modelling used the general purpose MCNP code using extrapolated fission cross sections for UF₄ at high temperatures. The gas core geometry corresponds to that of a 3m right circular cylinder operating under a pressure of 2 MPa, filled with He and UF₄ gas in a 9:1 molar ratio. At an enrichment of 10% this corresponds to ~60kg of ²³⁵U. Figure 3 shows uranium and plutonium concentrations in the 10% enriched G/VCR (600 kg ²³⁵U). Figure 4 shows the main radioisotope source terms (⁹⁰Sr, ^{99m}Tc, ¹³¹I, and ¹³⁷Cs) also in 10% enriched G/VCR fuel. The data clearly show that the concentrations of radioisotope sources generally build up rapidly then level off to between 0.1g (¹³⁷Cs) to 10³g (⁹⁰Sr).

Referring again to Table 1 we can see that other solid fuel reactors cannot approach the efficiency of burn up and fuel utilisation that circulating gaseous fuelled reactors can. This is an advantage inherent in the very *concept* of a gas core reactor. It would be difficult to design a gas core fuelled reactor that could *not* burn its fuel more efficiently and completely than any solid fuel reactor.

3. Nuclear assisted production of hydrogen

Hydrogen is primarily used to convert heavy crude oils into gasoline, diesel, and jet fuels. Hydrogen is particularly important for upgrading heavy crude oil from countries like Venezuela that have an abundance of oil but mainly in the form of low quality, low hydrogen to carbon ratio crude oil. Hydrogen is also used widely in fertilizer production, methanol production, conversion of iron ore to metallic iron, and production of many other chemical to numerous to list here. Such a combination of factors is rapidly increasing demands for H₂.

The benefits of using nuclear energy to produce hydrogen have been expounded upon in many reviews and will not be repeated here. [9] It suffices to note that generation IV nuclear power systems will perhaps be the best available means for thermochemically producing hydrogen because they will be inherently high-temperature reactors (most Gen IV systems achieve improved efficiency by going to higher temperatures) as well as cleaner more environmentally friendly systems. No other heat sources (solar, coal, natural gas) are as reliable or as clean as nuclear (solar energy is not dependable in all countries, and as far as collection is concerned is not as compact as a nuclear heat source).

Three approaches that are being considered in this paper for H₂ production using nuclear energy are (1) high-T steam electrolysis, (2) the Ca-Br cycle, and (3) the I-S cycle. There are two basic methods for producing hydrogen, one is electrolysis (using electricity to split water into hydrogen and oxygen), the other is thermochemical production of hydrogen. Electrolysis is itself reasonably efficient, but not when the cost of electricity production required for the electrolysis is included. Thermochemical production is more direct and does not require immediate electricity, but instead requires very high temperatures (750 to 1 000°C). Currently nearly all hydrogen is produced from natural gas and this creates carbon dioxide emissions. Two important alternative thermochemical hydrogen production processes are the calcium-bromine process and the sulphur-iodine process illustrated in Figure 5 and Figure 6 respectively.

Other methods for nuclear hydrogen production are possible, such as using nuclear heat for steam reforming of natural gas, but this is an energy-intensive process where a fraction of the natural gas is used to provide heat at temperatures of up to 900°C. Also steam reforming of methane has carbon dioxide as a by-product, which defeats the purpose of using cleaner nuclear power to produce hydrogen. Nevertheless, all these processes can potentially be driven with waste heat from a G/VCR electrical power plant because the waste heat temperature is very high and meets most requirements for high-T H₂ production.

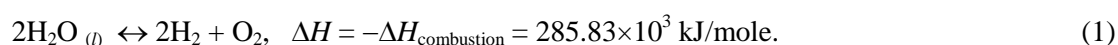
Thermochemical production of H₂ imposes certain requirements on the reactor chosen to supply the heat: Firstly the heat source must be high temperature. For the SI process temperatures of between 750 and 1 000°C are required. For the Ca-Br process steam needs to be provided at ~750°C. Secondly, the nuclear system must be sufficiently isolated from the chemical plant for safety reasons. The exact specifications for intermediate heat transport may vary depending upon the reactor type. A high pressure G/VCR may impose severe requirements on the isolation, but given that the Brayton cycle in the proposed G/VCR-H₂ system is already decoupled from the direct fission primary loop it is likely that the combined system can be engineered to meet stringent safety requirements without excessive penalties. (A low pressure coolant such as envisaged in Gen IV molten salt cooled reactors or liquid metal cooled fast reactors would also be compatible with thermochemical H₂ production and might be

considered more favourable due to the lower operating pressures in the reactors, but these other systems are not as flexible nor as fuel-efficient as the proposed G/VCRs.)

The attraction of water electrolysis and several of the thermochemical processes is that there is no associated production of carbon dioxide. These are now considered in turn.

3.1 High temperature electrolysis

Many direct methods [10] are possible for producing H₂ with the input of heat and water. In order to achieve reasonable production costs however, very high temperatures are required to ensure rapid chemical kinetics and high conversion efficiencies [11]. Nuclear heat sources therefore begin to be attractive for electrolysis applications. The theoretical energy requirement for electrolytic decomposition of water at 25°C is the negative of the heat of combustion of hydrogen in the reaction,



this is about 3.53 kW-hours per m³ of H₂. The decomposition voltage V , required is given by,

$$\Delta H = -nFV \quad (2)$$

where n = number of electrons transferred per mole of H₂O, F = Faraday's constant (96 000°C). The minimum actual voltage is therefore 1.48V at 298.15K. The theoretical minimum voltage is however determined by the Gibbs free energy of formation, which is $\Delta_f G = 237.53$ kJ/mole, or 1.23V. The difference between actual and theoretical electrolysis voltage is termed the over-potential.

Higher temperatures lower the electrolysis voltage according to the Gibbs-Helmholtz relation. However, as the temperature is increased the pressure increases as well which increases the electrolysis voltage, but only logarithmically by the Nernst relation, and the potential energy stored in the pressurised H₂ roughly balances this additional voltage. Overall, increased temperature and pressure lead to net gain in efficiency for the reaction of Equation (1). Process heat from a G/VCR-GT He-Xe Brayton gas turbine cycle can however be used to generate steam, which can then be electrolysed below the enthalpic voltage. This is the idea behind high-temperature steam electrolysis at $T > 1000^\circ\text{C}$. At this temperature thermal dissociation plays a significant role and 25% to 30% of the energy required for splitting H₂O is thermal, thereby reducing the electrical power demands considerably. Great potential exists for splitting water vapour because the theoretical energy requirements are less than those for conventional electrolytic cells by about 25%. Further, activation over-potential losses at higher temperatures are very low, which allows electrolysis operation at high current densities, and potentially ohmic heating due to the higher currents can supply (or make up for) some of the heating requirements. In Germany Dornier Systems evaluated possibilities for steam electrolysis using stabilised Zirconia as an oxygen ion conducting electrolyte [12]. Recent advances in high-temperature electrolysis have created renewed interest in this option, particularly for nuclear heat sources with very high temperature capability. [13]

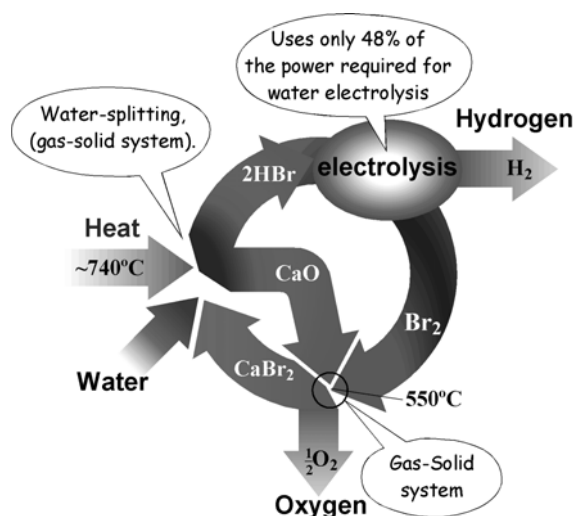
However, not very many nuclear reactors can deliver heat at the minimum of 1 000°C required for efficient high temperature electrolysis. G/VCRs perform best at around this range or upwards thereof, so they seem ideally suited for this application. For a combined electricity-hydrogen production facility the near-term G/VCR-GT would have to be tailored to reduce the gas-turbine power output in order for the highest temperature helium stream to be used for the electrolysis, or alternatively, the gas turbine could be by-passed entirely during hydrogen production mode and the waste heat from the electrolytic process used to drive a conventional steam turbine. Efficiencies for this combined power plant have yet to be determined. Problems with ceramic materials for the high-temperature cells and high contact resistances at interelectrodes have been partially overcome, and

operation of cells for 2 500 hours has been demonstrated [14] at voltages of 133 V and current densities of $0.33 \text{ A}\cdot\text{cm}^{-2}$.

3.2 Calcium-bromine processes

The Ca-Br process illustrated in Figure 5. One type of Ca-Br cycle that has received intense research and analysis is the so-called UT-3 cycle.

Figure 5. One of many possible thermochemical reaction systems for producing clean hydrogen fuel without greenhouse gas emission



Illustrated here is the calcium-bromine system. Its advantage is that electrolysis is performed on HBr rather than water (H_2O). Water is a very strongly bound molecule and therefore hard to split, so if hydrogen can be split from some weaker bound molecules then the potential for efficiency gains are considerable.

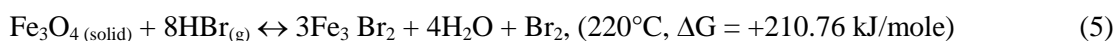
An idealised version of the UT-3 Ca-Br process consists of the following steps. Slow water splitting with HBR formation,



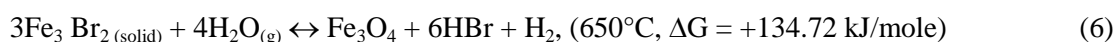
oxygen formation exothermically,



bromine regeneration



hydrogen formation from FeBr_2 ,



energetically this cycle is favourable and should lead to viable H_2 production, although the exact enthalpies of reaction would be required to know the theoretical efficiencies. An advantage of this process is that the primary reactions take place between a gas and a solid substrate making separation easier than thermochemical processes that have reactants and products entirely in a gas phase. The difficulties with this proposed process have to do with the significant physical change in dimension that cubic CaO must undergo to accommodate the orthorhombic CaBr_2 structure in the first step of the

process. There is a 76% increase in volume, and then this must be reversed in the second step. Unless the calcium is somehow physically dispersed then sintering will occur in the second stage. Thus some complicated mechanism for supporting CaO on a compatible substrate has to be considered.

Modifications to the basic UT-3 Ca-Br process have only recently been investigated, and the research is at too early a stage to report progress on here. To date most Ca-BR processes proposed have to deal with the size mismatch and sintering issue problem. If these technical challenges can be overcome without adversely affecting the energetics then ideal efficiencies on the order of 45% to 49% are in theory achievable with Ca-Br thermochemical H₂ production. There is promise and already small-scale tests of model UT-3 systems have been proven viable [15]. Tadakoro (1997) at JAERI reports on an actual bench-top model, while earlier Sakurai (1996) at U. Tokyo considered a simulated flow sheet, and these studies indicate that a Ca-Br H₂ production plant would require helium gas introduced at 850°C/1 125°C respectively, H₂ and O₂ production pressure would be 2.5MPa. Helium would return to a steam generator at 700°C, 4MPa. A HTGR or G/VCR nuclear reactor would be able to provide this heat source with no trouble. At this temperature a G/VCR would even be capable of cogeneration of electricity in a Brayton topping cycle with a single high-pressure turbine pass.

3.3 Iodine-sulphur processes

The sulphuric acid processes (hydrogen sulphide, iodine-sulphur, and sulphuric acid-methanol) are leading candidates for commercial thermochemical H₂ production. There are three idealised steps in the I-S process. The first is formation of sulphuric acid a hydriodic acid.



sulphuric acid decomposition,



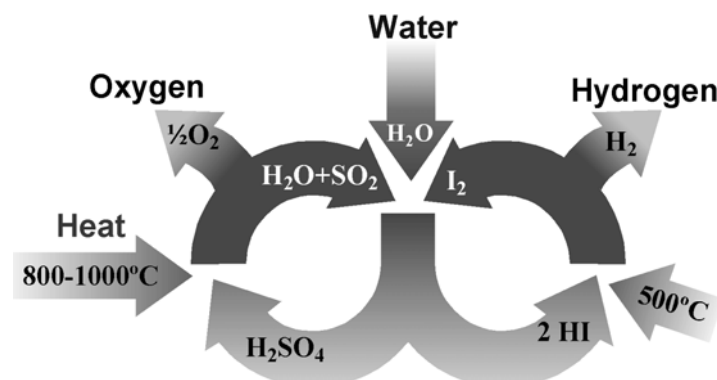
and the H₂-producing step



In each of these processes, the high-temperature, low-pressure endothermic (heat-absorbing) reaction is the thermal decomposition of sulphuric acid to produce oxygen: The difficulties in the sulphuric acid decomposition stem from the fact that the reaction kinetics are temperature limited, as the back reaction occurs at lower temperatures. Somehow the reaction products (which are gaseous) must be separated, but if allowed to cool the back-reaction would take place, and if cooled too rapidly (enough to prevent the back reaction) then the recuperation is limited.

The Japan Atomic Energy Research Institute is currently preparing to demonstrate the production of H₂ by steam reforming of natural gas with the heat-energy input provided by their high-temperature engineering test reactor (HTTR). The iodine-sulphur process is being developed with the ultimate goal to connect it to the HTTR. Research on this process is also under way in the United States. [16] Significant development work on H₂ thermochemical cycles is required, with the technology being applicable to both nuclear and solar-power tower heat sources.

Figure 6. Illustration of an alternative thermochemical hydrogen production process



This is the sulphur-iodine process. Its advantage is the high efficiency of the hydrogen forming step, but it requires the highly corrosive chemical, sulphuric acid. Concerns have been raised about the desirability of having such chemicals near reactor plants.

In summary, the economics of H₂ production strongly depends on the efficiency of the method used. Production efficiency can be defined as the energy content of the resulting H₂ divided by the energy expended to produce the H₂. Hydrogen production by electrolysis is relatively efficient (~80%). However, when this factor is combined with the electrical conversion efficiency, which ranges from approximately 34% (in current light-water reactors) to 50 % (for advanced systems), the overall efficiency would be approximately 25 to 40%. A significant capital investment in electrolytic cells is also required. For thermochemical approaches such as the iodine-sulphur process described previously, an overall efficiency of >50% has been projected. Combined-cycle (H₂ and electricity) plants may have efficiencies of ~60%. All of the efficient, potentially low-capital-cost thermochemical processes require high temperatures.

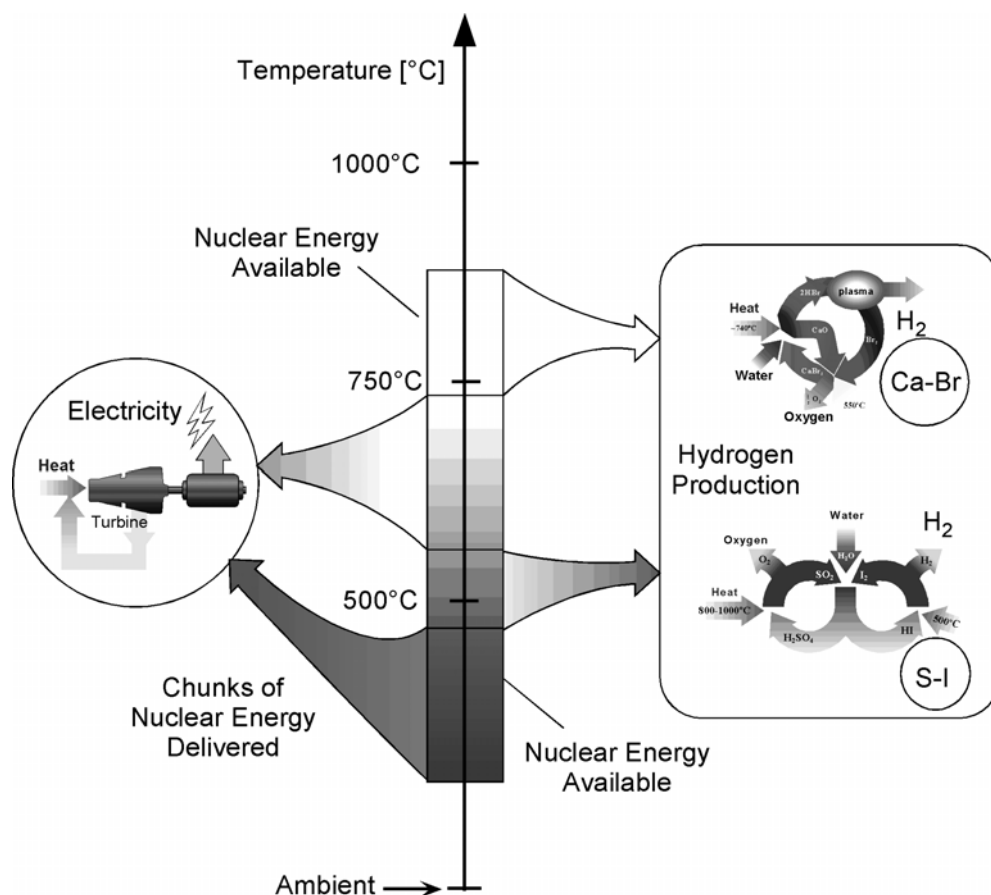
The proposed gas core reactor system would meet almost all the demands of an efficient and effective heat or electricity source for hydrogen production. Figure 7 illustrates conceptually the advantages of nuclear power for H₂ production using the highest temperatures available for solid or liquid fuelled reactors. Notably a G/VCR would be capable of providing additional heat at even higher temperatures than that shown in Figure 7, for example for single shaft gas turbine Brayton cycle operation. The combined cycle efficiency of the G/VCR-H₂ production facility can therefore be as high as 50% when operated at full capacity.

4. An integrated clean energy production concept

Gas core and vapour core reactors have sometimes been informally described as “the ultimate nuclear heat sources.” Unfortunately the scope of this paper does not allow a detailed technical comparison between gas core reactors and other fission or fusion power systems that would fully justify this claim. However we do know that light water reactors are unsuitable for intensive industrial chemical process requirements. We also know that advanced high temperature nuclear reactors are well suited for these applications and high temperature gas cooled reactors have often been proposed as suitable heat sources for coal and oil upgrading, co-processing and cogeneration.

A schematic illustration showing the logical flow and basic inputs and outputs of an integrated gas core nuclear power plant-coal/oil upgrading-hydrogen production facility is illustrated in Figure 8. This schematic combines many of the subsystems discussed as energy production systems in their own right in previous sections of this paper.

Figure 7. Conceptual illustration of availability of G/VCR nuclear heat and matching to cogeneration of electricity and process heat for thermochemical hydrogen production



Not drawn is the potential for even higher temperature Brayton gas turbine electricity production.

In principle gas core reactors might be prototyped and deployed for these exciting applications within a couple of decades. Realistically though, a considerable R&D effort needs to be expended before these ideas become a reality. Indeed, the R&D cost and likely cost of prototyping and testing of gas core and vapour core reactors is perhaps the only reason why these types of systems remain largely confined to designs on engineer's drawing boards.

5. Conclusions

In conclusion G/VCR based systems for electricity production and electrolytic or thermochemical hydrogen production and cogeneration are worth additional R&D development, not only as possible new generation technologies for the nuclear industry but also for the burgeoning future economy to be based upon diverse energy products such as syngas, hydrogen fuel, high quality liquid fuels, and cheap process heat for other important high temperature industrial processes. All these products may be produced with the aid of G/VCRs as heat sources without adverse environmental impact and more efficiently, safely, and thus in the long term, more economically than with any other nuclear or renewable energy source.

- [5] Grundy, Robert F. (ed.), "Magnetohydrodynamic Energy for Electric Power Generation", Noyes Data Corporation, Park Ridge, New Jersey. 1978.
- [6] Hore-Lacy, Ian. "Nuclear Electricity" (6th ed), Publ.: Uranium Information Centre Ltd and World Nuclear Association, ISBN 0-9593829-8-4.
- [7] Anghaie, S., Lewis, D., *et al.*, "GEN IV Nonclassical Concepts Technology Working Group-4 R&D Scope Report", **TWG-4 Summary Rpt ZR06-04**. Report prepared for the US Department of Energy. Edited by S. Anghaie and D. Lewis, 4 February 2003.
- [8] Anghaie, S., B.M. Smith, T.W. Knight, "Safe and sustainable nuclear power generation with gas core reactor systems", paper presented at the 11th International Conference on Emerging Nuclear Energy Systems, ICENES 2002, Albuquerque, NM, 29 Sept-4 Oct, 2002.
- [9] Forsberg, C.W. and K.L. Peddicord, "Hydrogen Production as a Major Nuclear Application", *Nuclear News*, **44** (10), p. 41-44, (2001).
- [10] OECD-NEA Nuclear Science Committee, 2-3 October 2000. *First International Exchange Meeting on Nuclear Production of Hydrogen*, Paris, France, 2000.
- [11] Miyamoto, Y. Shiozawa, S., *et al.*, "Overview of HTGR Heat Utilization System Development at JAERI", *Nuclear Heat Applications: Design Aspects and Operating Experience*, IAEA-TECDOC-1056, International Atomic Energy Agency, Vienna, Austria, 1998.
- [12] Donitz, W. and R. Schmidberger, *International Journal of Hydrogen Energy*, **7**, 321, 1982.
- [13] Donitz, W., Erdle, E., *International Journal of Hydrogen Energy*, **10**, 5, 291-295, 1985.
- [14] Donitz, W., Erdle, E., Schamm, R. and R. Streicher, *Proceedings of the 7th World Hydrogen Energy Conference*, Moscow, U.S.S.R., p. 65-73, 25-29 September, 1998.
- [15] Tadakoro, Y., Kajiyama, T., *et al.*, *Int. J. Hydrogen Energy*, **22**, 1, p. 49-56, 1997.
- [16] Brown, C.L., J.F. Funk and S.K. Showalter, *High Efficiency Generation of Hydrogen Fuels Using Nuclear Power*, GA-A23451, General Atomics Corp., San Diego, California, 2000.

MEETING THE NEAR-TERM DEMAND FOR HYDROGEN USING NUCLEAR ENERGY IN COMPETITIVE POWER MARKETS

A.I. Miller

Atomic Energy of Canada Limited, Canada

Romney B. Duffey

Atomic Energy of Canada Limited, Canada

Abstract

Hydrogen is becoming the reference fuel for future transportation and the timetable for its adoption is shortening. However, to deploy its full potential, hydrogen production either directly or indirectly needs to satisfy three criteria: no associated emissions, including CO₂; wide availability; and affordability. This creates a window of great opportunity within the next 15 years for nuclear energy to provide the backbone of hydrogen-based energy systems. But nuclear must establish its hydrogen-generating role long before the widespread deployment of Gen IV high-temperature reactors, with their possibility of producing hydrogen directly by heat rather than electricity. For Gen IV the major factors will be efficiency and economic cost, particularly if centralised storage is needed and/or credits for avoided emissions and/or oxygen sales. In the interim, despite its apparently lower overall efficiency, water electrolysis is the only available technology today able to meet the first and second criteria. The third criterion includes costs of electrolysis and electricity. The primary requirements for affordable electrolysis are low capital cost and high utilisation. Consequently, the electricity supply must enable high utilisation as well as being itself low-cost and emissions-free. Evolved Gen III+ nuclear technologies can produce electricity on large scales and at rates competitive with today's CO₂-emitting, fossil-fuelled technologies. As an example of electrolytic hydrogen's potential, we show competitive deployment in a typical competitive power market. Among the attractions of this approach are reactors supplying a base-loaded market – though permitting occasional, opportunistic diversion of electricity during price spikes on the power grid – and easy delivery of hydrogen to widely distributed users.

Gen IV systems with multiple product streams and higher efficiency (e.g., the SCWR) can also be envisaged which can use competitive energy markets to advantage and produce hydrogen both centrally (directly) and distributed (indirectly).

1. Introduction

In his presentation to the 2003 American Nuclear Society's Annual Meeting in San Diego, Magwood [1] provided an updated view of the US Department of Energy's (DOE) Hydrogen Energy Roadmap [2]. Within the context of Generation IV nuclear reactor systems, Magwood set out a timetable for high-temperature thermochemical production of hydrogen that envisages a start to construction of such systems in 2012. Given the challenging nature of the technologies (see, for example, Penfield) [3] and allowing time to gain experience from the first plants before large-scale deployment, even this ambitious timetable can hardly be expected to deliver significant amounts of hydrogen before about 2020.

Since AECL has previously suggested 2020 [4] as the appropriate year for emergence of large-scale demand for hydrogen as transportation fuel, the DOE's timing would be ideal. However, even assuming the DOE programme is then successful in delivering hydrogen at acceptable cost from high-temperature reactor heat, it does not address a vital issue of market preparation – the widely appreciated “chicken and egg” of needing extensive demand for hydrogen to justify deployment of an extensive hydrogen-distribution infrastructure. Supply of hydrogen into the developing market of hydrogen-fuelled transportation prior to 2020 is not addressed and yet it is just this build-up of this market that will be an essential precursor to deployment of new large-scale processes.

This paper focuses particularly on available technology, which could be deployed during the first two decades of the 21st century. It reviews that technology beside what the DOE programme may develop for subsequent deployment.

2. Hydrogen production technologies

Only two processes for hydrogen production are currently in use. Steam-methane reformers (SMRs) supply large-scale production; water electrolysis is the preferred method for small-scale production. SMRs require high-temperature heat input but, even if the heat comes from a non-chemical source, much of the energy in the hydrogen originates in chemical energy of the hydrocarbon (usually methane) feed. It is very important to appreciate that SMRs do not compete with electrolysis below about one million cubic feet per day (28 000 m³/d, 2.5 tonne/d, or 4 MW expressed as H₂ energy). For small quantities, electrolysis is the economic norm. (Various units are used to describe hydrogen production: for reference, they are compared in Table 1).

Table 1. Hydrogen scales in commonly-used units

Units	Small SMR	World-scale SMR
Million ft ³ /d	4	100
Thousand m ³ /d	113	2 830
Tonne/d	10.1	253
GJ/d (HHV)	1 440	35 900
GW (HHV)	0.0167	0.416

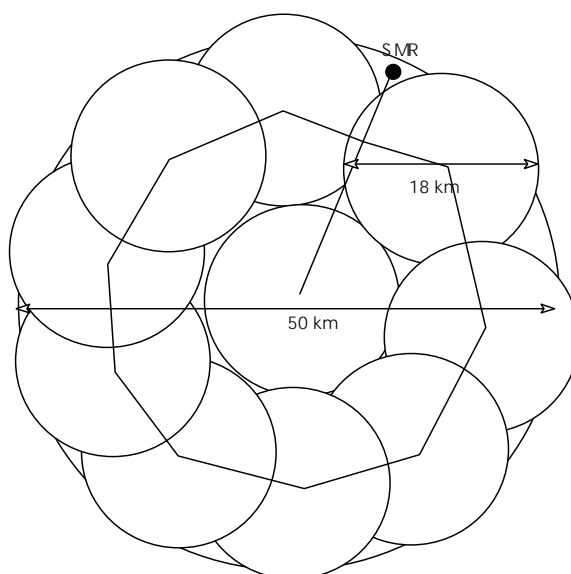
As the hydrogen economy begins to emerge over the next 15 years, it will mainly be applied to transportation. About half the transportation market is accounted for by light vehicles and, for these, hydrogen fuelling seems likely to be similar to today's fuelling for gasoline or diesel – i.e. at service stations. The cost of hydrogen at these local outlets will include three main cost elements covering (1) hydrogen production, (2) sequestration where CO₂ is also produced (or, less desirably, an equivalent carbon-emission charge), and (3) energy distribution either as hydrogen or as electricity for hydrogen production. Scale is a key consideration.

2.1 A hypothetical city case study

If one assumes that hydrogen-fuelled light vehicles will use fuel cells and have similar ranges to today's automobiles, a typical 40 litre gasoline or diesel fill-up (~ 28 kg) will be replaced by 3 kg of hydrogen (since the fuel cell has three times the efficiency and hydrogen has three times the energy density per unit of mass). So envisage a service station dispensing 340 fuelling per day – quite a high number – with the requirement for about 11 300 m³/d. (This choice fits the 11 000 m³ capacity of a typical tube trailer making one delivery a day.) Based purely on scale, this does not appear to be in the competitive range for SMRs to be sited at each service station. However, whether the demand of many service stations can be consolidated in one centralised SMR will be determined by distribution costs.

Envisage a hypothetical city of about 1 million light vehicles covering a diameter of 50 km. If one were to provide hydrogen-fuelling service to this city through ten service stations, it would require roughly the pattern of Figure 1 – a ring of nine stations each serving a 9 km radius plus one central station. Since 3 kg of hydrogen gives about 400 km of driving, based on the average annual driving distance of Canadian cars of 21 000 km, fill-ups are needed on once a week. Total cars served is 24 000 – so this is a level of significant penetration with one vehicle in forty is operating on hydrogen. Total demand for hydrogen is 10 t/d, the output of a small, but practicable SMR. Expressed in energy terms, hydrogen is being supplied with an energy content of 17 MW.

Figure 1. Distribution pattern for a hypothetical urban area



2.1.1 SMR production of hydrogen

There are three options for SMR production of hydrogen: (1) very small SMRs at every service station; (2) a single SMR supplying the city by pipeline distribution; and (3) a single SMR supplying the city by truck distribution.

For a pipeline option, the diagram shows a plausible arrangement of an SMR on the edge of the city, a supply pipeline to the central station and a ring-line linking the other stations. The total length is around 133 km. Alternatively, a trucking option must cover around 540 km (assuming straight-line

delivery and including return journeys). Two trucks operating 16 hours per day should be able to handle this distribution.

Padró and Putsche [5] have reviewed the costs of both distribution by pipeline or truck. The quote data from Oney *et al.* [6] are summarised in Table 2. For consistency with the rest of this paper, they are converted to the higher heating value (HHV). They may underestimate pipeline costs since Amos [7] gives pipeline costs that are approximately 50% higher.

Based on Oney *et al.*'s figure of 240 \$/t H₂ (2.04 \$/GJ) for transmission of 0.13 GW of hydrogen energy over 160 kilometres, Padró and Putsche conclude that pipelines give lower costs. But 0.13 GW (4.1 million GJ/a) is a quite prodigious scale, sufficient to fuel 180 000 cars or almost ten million refuelling annually. Further, Padró and Putsche's figures show that the cost of pipelines becomes virtually constant below 0.13 GW [8]. So the total cost for a 133 kilometre pipeline network of this minimum size can be calculated as:

$$133/160 \times 1.71 \text{ \$/GJ} \times 5 \times 10^6 \text{ GJ/a} = 7.06 \text{ M\$/a.}$$

Since the required delivery is only 1440 GJ/d (0.53 million GJ/a), the unit cost for pipeline delivery is 13.31 \$/GJ.

Table 2. Pipeline costs after Oney *et al.* and adjusted to HHV

Transmission Rate			Distance	Cost	
GW	GJ/d	Tonne/d	km	\$/GJ	\$/km tonne)
0.13	11 230	79	161	1.71	1.44
			805	7.49	6.33
			1 609	14.71	12.43
0.42	36 290	255	161	0.70	0.59
			805	2.43	2.05
			1 609	4.60	3.89
0.84	72 580	509	161	0.70	0.59
			805	2.43	2.05
			1 609	4.60	3.89
1.26	108 860	764	161	0.70	0.59
			805	2.43	2.05
			1 609	4.60	3.89

The truck transport alternative would likely operate with compressed gas, although hydride storage has also been proposed. Amos gives the cost of compressed gas transport by tube trailer in the 5 to 11 \$/GJ (LHV) range for distances of 16 and 160 km, respectively. (Because Amos used a tube trailer cost of \$140 000 rather than the actual current cost of \$400 000, it seems reasonable to raise the cost by 1 \$/GJ.) So, depending on the distribution distance, the delivery charge ranges from 700 to 1 400 \$/tonne H₂ (adjusting Amos's figures for the HHV of H₂). By simple proportion, for the average trucking distance of 13.3 km from a single SMR, the cost should be 5.9 \$/GJ. Trucking appears to be the better choice until the magnitude of the operation rises by a factor of three since hydrogen supply by pipeline could expand by an order of magnitude with no additional cost and so an inverse proportionate fall in unit cost.

2.1.1.1 Sequestration

The actual cost of sequestration will vary depending on accessibility of suitable underground storage opportunities but a reasonable, recent estimate of the likely cost of CO₂ sequestration is 135 \$/tonne C (30 \$/t CO₂). This is based on the UK Government's Department of Trade and Industry (DTI) position paper [9], which uses £84/tonne C for the typical cost for CO₂ sequestration, in a deep geological aquifer 300 km from the source. (Lower costs may occur where suitable disposal structures occur close-by but the DTI's estimate provides a plausible average cost of sequestration.). One tonne hydrogen by SMR produces 7.75 tonnes of CO₂ or 232 \$/tonne H₂. Expressed in energy terms, 1.6 \$/GJ.

One would expect that this cost is too low for smaller installations and that SMRs at every service station would incur a much higher cost. Releasing the CO₂ and assessing it a carbon-emission cost is probably what would be done in practice and so using the larger-scale cost of sequestration is somewhat plausible.

2.1.2 *Electrolytic production of hydrogen*

On small enough scales, water electrolysis is already the technology of choice even though there is great scope for the reduction of capital cost, mainly because the existing market for hydrogen in small quantities is minute beside its prospects for fuelling a hydrogen economy.

A service station [10] supplying hydrogen from electrolysis has three cost components associated with providing the fuel: (1) electricity; (2) hydrogen production equipment; and (3) hydrogen storage. The last element is important since it must both accommodate the daily cycle of customer demand and allow hydrogen production to be spread across almost the whole 24 hours. It can also be sized to allow avoidance of periods of exceptionally high electricity prices at times of peak demand to minimise electricity cost. On the other hand, nearly continuous production of hydrogen minimises the size and cost of the electrolysis installation [11]. Since fuelling demand will generally be low overnight, the storage requirement for the electrolytic system has to be at least 12 hours. Rejecting any solutions with less storage, one should optimise on a minimum cost for electricity, storage and cell installation for any electrical system.

2.1.2.1 Cell and storage costs

The complete electrolysis installation have been costed at 300 \$/kW. This is an installed cost that includes compression [12]. The cell requires 1.8 volts – and this is the basis for costing in dollars per kilowatt – but the associated compression is handled by raising the total voltage requirement to 2.1 volts. In a year, one kilowatt of cells produces 0.156 tonnes or 22.1 GJ/a so the capital cost component is 13.57 \$.

Storage has been costed at 400 000 \$/t H₂ – the same as for the delivery trailer.

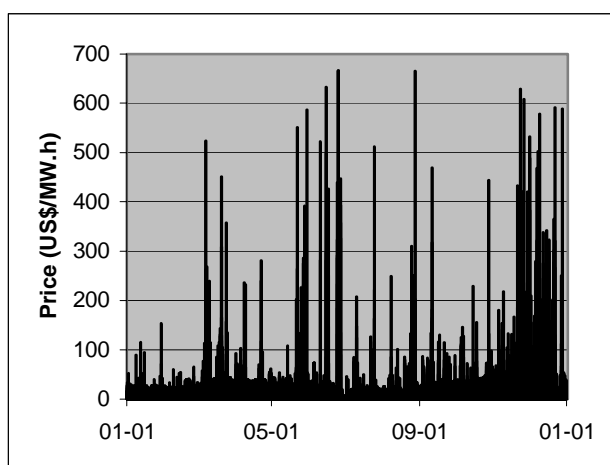
Capital has been amortised at 20%/a – approximately equivalent to a 15% ROI recovered over 10 years.

2.1.2.2 Electricity cost

Alberta operates an open market for electricity with suppliers bidding to supply in one-hour time blocks. We have analysed the Alberta data for 2002 (translating to US dollars at 1.5 C\$ = 1 US\$). Some idea of the way power prices fluctuated is conveyed by Figure 2 though the data in Figure 2 are

plotted too densely to reveal properly the sparsity of the actual peaks but it does show the amplitude. The average of 29.3 US\$/MWh is dragged up by the extreme price peaks. So, for example, for all power priced at 60 US\$/MWh or less, the average price was 22.4 US\$/MWh and prices above 60 US\$/MWh occupied only 5% of the year. An allowance of 10 US\$/MWh was added for distribution of the electricity to the actual Alberta producer prices. This is rather an arbitrary mark-up since confining electrolysis to off-peak periods should avoid any need to add to grid capacity.

Figure 2. Hourly Alberta power prices in 2002



Obviously, using a low price threshold to interrupt electrolysis will increase the required volume of storage while an increase in the installed electrolysis will decrease the volume of storage. Using the 2002 Alberta data, effects of these two parameters are shown in Table 3.

Table 3. Hours of hydrogen storage

% electrolysis	Hours of storage required for electricity threshold per MWh of					Total H ₂ cost (\$/t H ₂)				
	48 \$	50 \$	55 \$	60 \$	65 \$	48 \$	50 \$	55 \$	60 \$	65 \$
110	119	92	65	51	45	3 278	3 046	2 826	2 714	2 671
115	68	52	30	24	19	2 848	2 715	2 539	2 499	2 464
120	37	29	17	16	16	2 597	2 535	2 447	2 450	2 460
125	32	26	16	14	14	2 576	2 531	2 460	2 455	2 463
130	28	24	16	13	13	2 561	2 533	2 481	2 466	2 475
135	25	23	15	12	12	2 554	2 545	2 492	2 477	2 486
140	24	21	14	12	12	2 575	2 547	2 503	2 498	2 506

Table 3 shows a minimum cost for hydrogen of around 2 447 \$/t with a cut-off when the producer price exceeds 55 \$/MWh and 120% cell capacity. Storage of 17 hours of average demand is required. Of the 2 430 \$/t, 461 \$/t is for cell costs, 155 \$/t for storage costs, and 1 814 \$/t for electricity.

For comparison, a unit operating continuously would incur costs of, respectively, 384, 2212 and 109 (for a minimum storage of 12-hours capacity to meet diurnal fluctuation) for a total of 2 705 \$/t H₂. So flexible production of electrolytic hydrogen with the pattern of energy prices in Alberta in 2002 would have produced a reduction in production cost of about 275 US\$/t H₂. (The figure should be seen as conservative: since the price of power is set 24 hours in advance, a hydrogen producer could apply a more sophisticated approach to interruption of production than simply using a fixed price threshold.)

Note that a decrease in cell voltage of 0.28 volts would be needed to justify a 50% increase in cell capital cost. Emphasising low capital cost will usually give a superior return over efforts to lower cell voltage.

We also note the unfavourable economics of coupling low-availability electricity sources such as wind and solar to hydrogen generation as a way of utilising the electricity when grid demand is low. Using the electrolysis equipment for only a part of the 30% when wind or solar power is available would raise the cell cost to around 1 200 \$/tonne H₂.

2.1.3 SMR production

2.1.3.1 SMR capital

The capital cost of SMRs varies with size in proportion to about the 0.66 power. So a 250 tonne/d (world-scale) plant will cost about 75 M US\$, a 10 tonne/d will cost about 9 M US\$, and a 1 Mg/d will cost 2 M US\$. It is a reasonable first approximation to assign the same capital charge rates used for electrolysis – 20%/a.

2.1.3.2 SMR fuel

In recent years, the wholesale price of natural gas has been very volatile. Of course, as with electricity for electrolysis, the natural gas price should include distribution costs. Now natural gas can be converted to electricity at an efficiency of around 60% using a combined-cycle gas turbine, so it is at least reasonable to compare electrolysis and SMR hydrogen on that basis. Thus Alberta electricity at 39.29 \$/MWh, including distribution, is 10.91 \$/GJ. So natural gas would be worth converting at 6.55 \$/GJ. Though the SMRs are small, they should still come close to achieving 90% conversion efficiency on the basis of energy input to energy content of the output hydrogen so a fuel cost of 7.3 \$/GJ is appropriate on this basis.

2.1.3.3 SMR storage

For pipeline supply, there still has to be a matching of the continuous operation of the SMR with the diurnal variation in demand – 12 hours local storage is assumed, though the storage could be at the SMR since the pipeline has ample capacity for higher transmission rates. Local SMRs also need 12-hour storage. For truck supply, once-a-day delivery is assumed so 24-hour storage is needed.

2.1.4 Cost comparisons

The costs of the service station options can now be summarised in Table 4. SMRs can be presumed to run continuously at near full capacity since there is no rational basis for time-of-day natural gas prices and SMRs do not start-up and shut-down easily. The city-wide system is designed to dispense 1 440 GJ/d (10 tonnes/d).

Of course, water electrolysis only avoids CO₂ emission (and the cost of sequestration) where the new use of electricity for hydrogen production is supplied with essentially zero CO₂ emission. Since high reliability is also needed, the obvious source is nuclear power.

Table 4. Comparison of the supply options for hydrogen supply

	Remote SMR with pipeline distribution	Remote SMR with truck distribution	Local SMRs	Local electrolysis using off-peak power	Local electrolysis operating continuously
Unit production size (Mg/d)	10.0	10.0	1.0	1.0	1.0
SMR or electrolysis capital cost (M\$)	One at 9.0	One at 9.0	Ten at 2.0	Ten at 0.844	Ten at 0.703
Storage capital (M\$)	Ten at 0.2	Ten at 0.4	Ten at 0.2	Ten at 0.28	Ten at 0.2
Production and storage capital (M\$)	11.0	13.0	22.0	11.2	9.0
Capital charge for production + storage (M\$/a)	2.2	2.6	4.4	2.2	1.8
Capital charge (\$/GJ)	4.2	5.0	8.5	4.2	3.5
Energy cost (\$/GJ)	7.3	7.3	7.3	12.8	15.6
Distribution cost (\$/GJ)	13.3	5.9	0.0	0.0	0.0
Carbon charge (\$/GJ)	1.6	1.6	1.6	0.0	0.0
TOTAL (\$/GJ)	26.4	19.8	17.4	17.0	19.1

At the scale of this case, electrolysis using time-of-day pricing and local SMRs show close to equivalent costs. The obvious detraction from the local SMR is that actual sequestration of the CO₂ product is extremely unlikely both because a pipeline to a sequestration site would be expensive and separation on this scale disproportionately expensive. A single SMR with hydrogen distribution looks unattractive.

One other opportunity for electrolysis is the oxygen co-product. The market in the USA for oxygen exceed [13] 50 billion pounds per annum (23 million tonne/a) at about 1.25 ¢/lb or 27.5 \$/tonne. For each tonne of hydrogen, eight tonnes of oxygen are produced. Our hypothetical city produces 80 tonnes of oxygen a day and so 100 such cities (an order-of-magnitude approximation for the USA) would produce three million tonnes a year. This suggests that the oxygen market could likely absorb by-product oxygen commercially, giving a potential credit of 220 \$/tonne H₂ or 1.55 \$/GJ.

At any smaller scale, SMR unit cost would rise more rapidly than electrolysis cost.

2.2 Larger-scale production after 2020

The hypothetical case's 4% of light vehicles is no trivial level of conversion and might reasonably be projected to exist around 2020. However, this would only be a stepping stone to much larger scales of hydrogen use beyond 2020. By then, the advanced thermochemical processes now entering development could be contenders. Costing for these is particularly speculative but even the future capital costs of the conventional processes must be uncertain so far into the future, perhaps

excluding SMR technology, which could be considered fairly highly developed. The cost of conventional water electrolysis is projected to fall to close to 150 \$/kW with economies of scale and experience. Given the uncertainty over capital costs, we have attempted a limited assessment of the technologies based on non-capital costs. If it has reached 4% of the light-vehicle market (or its equivalent in a mix of transportation – around half of the total is light road vehicles), further fairly rapid penetration can be expected to follow so that 50% of *all* transport could be converted to hydrogen-fuelled, fuel-cell-powered vehicles by perhaps 2030. It is this scenario that is reviewed below.

2.2.1 Comparison of operating costs

A 50% conversion of *all* transport is roughly a 25-fold increase over the earlier case and supply to our hypothetical city is now consistent with a world-scale SMR of 4.2 million m³/d produces 0.73 GW of H₂ – or the output of a 1 GW(e) reactor if it were producing hydrogen via electricity by conventional electrolysis with 70% efficiency.

On this scale, pipeline delivery would be far superior to truck delivery and the cost of distribution would be far less important than for the earlier case. Service stations would now be only around three kilometres apart and the pipelines for a main network would no longer be oversized and built to minimum cost. Only the finest part of the network, the final connection laterals, would be small enough for their cost to have become independent of the flows handled but these would be short. If one thinks of repeated clusters within the city like the pattern of Figure 1, a reasonable pattern of distribution could repeat the original layout with a final, finer network superimposed and built for the 0.13 GW minimum size. This finer network would typically carry gas over only an average of about three kilometres to the individual stations. Final laterals would not need any booster compression.

From Table 2, based on 0.42 GW (handling half the flow), it seems reasonable to use 0.70 \$/GJ for the cost of the main grid plus 0.30 \$/GJ for the final lateral (in the absence of any need for further compression, the final three kilometres are simply prorated to 3 km from the 133-km cost in Table 2). The total of 1.0 \$/GJ is equivalent to 142 \$/t H₂.

To produce hydrogen, a wider range of processes could now be in the picture. As well as the existing processes, high-temperature nuclear reactors operating around 850°C could supply energy to (1) indirect thermochemical processes (such as sulphur-iodine (S-I) or the iron-calcium-bromine-based UT-3), (2) SMR's using nuclear rather than chemical heat, and (3) high-temperature electrolysis in which some of the energy would be supplied by heat. All of the processes under consideration use inputs of chemical, electrical or high-temperature thermal energy or combinations of these. As before, since the most versatile form of these three forms is electricity, they can be compared by converting the energy consumption of all of the processes to their electrical equivalents, using appropriate conversion efficiencies. Natural gas's chemical energy is assumed to convert to electricity at 60% efficiency. Heat at 850°C is assumed to convert to electricity with 55% efficiency. The value used for electricity is 3 ¢/kWh and is based on the expected generating cost from new reactors such as the ACR™ [14].

High-temperature electrolysis has been attributed an electrical usage of 1.4 volts and the S-I and UT-3 processes assumed to use heat with 50% efficiency. Heat and chemical energy for the nuclear-assisted SMR is distributed in the usual proportion for SMRs. The analysis (Table 5) considers energy, distribution and sequestration costs for this 0.70 GW scale.

In an electricity system with a much larger component of nuclear, the effect of time-of-day pricing would be expected to become even more pronounced than the 24% cost reduction for power

for 95% of the time shown in Alberta in 2002. Only the conventional, distributed electrolysis can take advantage of that.

Table 5. Comparison of processes beyond 2020

Process	Actual H ₂ energy	SMR	Electrolysis	Electrolysis with time-of-day pricing	SMR + nuclear	S-I or UT-3	High-temp Electrolysis
Electrical energy (GJ/t H ₂)			203 [15]	203			135
Chemical energy (GJ/t H ₂)	142	156			111		
Heat energy (GJ/t H ₂)					45	284	85
Electrical equivalent (GJ/t H ₂)		94	203	203	91	156	182
Electrical equivalent (MWh/t H ₂)		26	56	56	25	43	51
CO ₂ emission (t C/t H ₂)		2.11			1.50		
Electricity (\$/t H ₂)		780	1 692	1 284	761	1 302	1 515
Distribution (\$/t H ₂)		142	0 [16]	0 ^{vi}	142	142	142
Sequestration (\$/t H ₂)		285	0	0	203	0	0
TOTALS (\$/t H₂)		1 307	1 692	1 284	1 106	1 444	1 657

Costed for energy use, distribution and sequestration, Table 5 shows quite a fairly uncertain with all processes within about 20% of 1 400 \$/tonne. On this scale and provided CO₂ can be effectively and economically sequestered, the SMR routes look promising. Electrolysis can probably only compete if it can exploit its interruptibility and access low-cost off-peak power. Nuclear heat appears best deployed as a supplementary source of energy to SMRs though we note that it uses a significantly smaller nuclear source – perhaps not a real disadvantage since large centralised units will have to be located on a pipeline grid for security of supply. Conventional electrolysis using electricity at off-peak prices is comparably priced. The competitive positions of SI and UT-3 thermochemical processes and of high-temperature electrolysis suffer from far less efficient use of energy than SMRs.

Table 5 is very speculative. Though use of electricity as an energy currency eliminates the distortion introduced by relative fluctuations in the price of different energy sources, it does require judgment on an appropriate cost for electricity. While it is arguable that this should be increased to include distribution costs, so long as electrolysis does not use power at periods of peak load the incremental cost of distribution could be quite small. The competitive position of conventional electrolysis is highly dependent on low-cost electricity but, in an increasingly nuclear system, hydrogen from electrolysis has useful load-levelling attributes that could fully offset the cost of distribution. It also seems probable that massive experience with electrolysis in the early stages of hydrogen deployment – when we have shown that it is likely to be at a cost advantage – will have lowered the operating voltage.

Storage costs have not been considered here. Locally-produced hydrogen will obviously need storage but so will the larger systems based on centralised production and, since the distribution system has largely been sized to its average continuous capacity, local storage will be needed or the main pipeline system enlarged to accommodate the diurnal; variation in demand.

3. Discussion

But what prospect has hydrogen of ousting oil-based fuels? While one can simply argue that hydrogen is the only choice – barring an unforeseen breakthrough in electricity storage – because CO₂ emissions from vehicles are far too large to be acceptable, the economics for a hydrogen economy also look favourable.

Today's typical 21 000 km/a automobile uses about 2 400 L of gasoline costing close to \$1 000/a plus \$700/a for collateral CO₂ emissions (5.2 t CO₂/a). However, the competition by 2020 should probably be highly efficient diesel-electric hybrids and their fuel cost could be lower by a factor of three for a fuel cost of \$330/a plus \$240/a for collateral carbon emission (1.75 t CO₂/a). If powered by a fuel cell, the same automobile would need 161 kg/a of hydrogen. On that basis, the hybrid and the hydrogen-fuel cell break even if the base cost of hydrogen is just over 3500 \$/t or 24.65 \$/GJ. And provided the production process does not emit CO₂, the hydrogen route is pollution-free. The estimated costs of producing hydrogen in Table 3 strongly suggest that hydrogen will not require massive, sustained government support to displace oil-based fuels. Even the (low) taxes hidden in the North American cost of gasoline and diesel could be added and hydrogen would still be competitive with around 4% penetration of the light-vehicle market.

3.1 Scale of hydrogen supply

In Canada by 2030, total energy demand for all forms of transportation is projected to have increased by 30% from today's figure to reach around 2900 PJ/a. Allowing the superior efficiency of fuel cells, this would require about 1000 PJ/a expressed as hydrogen energy or 48 GW(e). So if the hydrogen were manufactured centrally, it would require around 23 reactors or world-scale SMRs to supply their fuel. In this context, distribution distances of 100 km are realistic.

4. Conclusions

Distributed, low-temperature electrolysis will be the production process of choice for the initial supply of hydrogen to the transport market provided an intermediate generation of nuclear reactors comes on-line between 2010 and 2020 and delivers electricity close to the target cost of 3 US¢/kWh. This will arise principally because local electrolysis can minimise any distribution costs by relying on off-peak electricity delivered over existing grids.

Consequently, a network of hydrogen fuelling for vehicles ought to be well-launched by the time that new processes based on high-temperature nuclear reactors are available around 2020. Distributed production is a nearly essential precursor to distribution networks that could utilise larger-scale production processes.

Whether competitive processes based on high-temperature nuclear heat will subsequently take over will depend on their capital costs and on what has happened to capital and operating costs for conventional electrolysis during its window of early opportunity. For large-scale production, suitable for a maturing hydrogen market, SMRs too will be strong competitors if both the cost of secure sequestration is in line with today's projected estimates and secure supplies of natural gas are available.

REFERENCES

- [1] W.D. Magwood., IV, “The Nuclear Energy Future”, 2003 American Nuclear Society Annual Meeting, San Diego, 2 June 2003.
http://nuclear.gov/briefings/Jun02_03%20ANS%20San%20Diego.pdf
- [2] “National Hydrogen Energy Roadmap”, United States Department of Energy, November, 2002
http://www.eere.energy.gov/hydrogenandfuelcells/pdfs/national_h2_roadmap.pdf
- [3] Penfield, S.R., “Gas Reactor Power Conversion Systems, Part 3: Hydrogen Production Concepts”, ANS Advanced Gas Reactor Technology Course, American Nuclear Society Annual Meeting, San Diego, 5-6 June 2003.
- [4] Miller, A.I. and R.B. Duffey, “Constraining Climate Change with Nuclear Electricity and Hydrogen (N + H₂)”, AECL-12142, Atomic Energy of Canada Limited, August 2003.
- [5] Padró, C.E.G. and V. Putsche, “Survey of the Economics of Hydrogen Technologies”, National Renewable Energy Laboratory (US DOE), Report NREL/TP-570-27079, September 1999.
- [6] Oney, F., T.N. Veziroglu and Z. Dulger, “Evaluation of Pipeline Transportation of Hydrogen and Natural Gas Mixtures”, *International Journal of Hydrogen Energy*, **19**, (10), pp. 813-822.
- [7] Amos, W. “Costs of Storing and Transporting Hydrogen”, National Renewable Energy Laboratory (US DOE), Report NREL/TP-570-25106, May 1998.
- [8] Since the cost of pipeline distribution systems will be dominated by the cost of the small-scale laterals, the service-station pattern of vehicle fuelling may endure at least until hydrogen penetrates widely into the energy market. For service stations, economies of scale obviously improve the economics of pipeline distribution but there are too many unknowns to predict whether that will ever become the norm. Yet finer distribution would seem to require extension of hydrogen as a fuel beyond transportation. This is certainly possible – hydrogen was the majority constituent of the town gas that preceded widespread use of natural gas.
- [9] “DTI Initial Contribution to the PIU Energy Policy Review”, United Kingdom Department of Trade and Industry (UK DTI) Working Paper, 2001 July.
<http://www.cabinet-office.gov.uk/innovation/2001/energy/EPQw.pdf>
- [10] With electrolytic hydrogen, there is no technical barrier to producing hydrogen in a consumer’s own garage – a single 120 V plug provides enough current for average fuel demand and prototype refuelling devices already exist. However, the conventional method of buying fuel at a service station will probably remain the norm and will likely be cheaper.
- [11] We note, in passing, the unfavourable economics of coupling low-availability electricity sources such as wind and solar to hydrogen generation as a way of utilising the electricity when grid

demand is low. Using the electrolysis equipment for only a part of the 30% when wind or solar power is available will occasion very large capital charges.

- [12] We have used 300 \$US/kW for the complete electrolysis installation, including compression. It is based on private communication with Stuart Energy Systems, a major producer of electrolysis equipment, and is the high end of their projection.
- [13] *Chemical and Engineering News*, 24 June 1996,
<http://pubs.acs.org/hotartcl/cenear/960624/prod.html>
- [14] ACR = Advanced CANDU™ Reactor.
- [15] Using total electricity input equivalent to 2.1 volts.
- [16] Electricity is likely to have a distribution cost too but it is hard to estimate. If it is utilised only when there is favourable time-of-day pricing, it could be low. Cost of input energy's distribution also has to be borne by processes using natural gas as fuel.

PRESENT STATUS AND FUTURE PLAN OF HTTR PROJECT

**Yoshiyuki Inagaki, Tetsuaki Takeda, Tetsuo Nishihara,
Kaoru Onuki, Masuro Ogawa and Shusaku Shiozawa**

Department of Advanced Nuclear Heat Technology
Oarai Research Establishment

Japan Atomic Energy Research Institute (JAERI)
Oarai-cho, Higashiibaraki-gun, Ibaraki-ken, 311-1394, Japan

Tel: +81-29-264-8725, Fax: +81-29-264-8608

Email: inagaki@spa.oarai.jaeri.go.jp

Abstract

The HTTR project aims at demonstrating inherent safety features of High temperature gas-cooled reactors (HTGRs) by safety demonstration tests, and establishing nuclear heat utilisation technology by a hydrogen production demonstration test. The safety demonstration tests are divided to the first phase and second phase tests. In the first phase tests, simulation tests of anticipated operational occurrences and anticipated transients without scram are conducted. The second phase tests will simulate accidents such as a depressurisation accident (loss of coolant accident). The first phase safety demonstration tests have been carried out during FY 2002-2005, and the second phase tests are planned to start in FY 2006. A hydrogen production facility will be connected to the HTTR for the hydrogen production demonstration test to establish the coupling technology such as well as the procedure on safety design and evaluation. The coupling technology consists of safety-related one such as countermeasures against explosion of combustible gas and tritium permeation from helium gas to process gas and so on, and control ones for preventing thermal mismatch between reactor and hydrogen production facility. This report describes the present status and the future plan of the HTTR project.

KEYWORDS: HTGR, HTTR, safety demonstration test, reactivity insertion test, flow reduction test, nuclear heat application, hydrogen production, coupling technology, control technology, safety-related technology, I-S process.

I. Introduction

Research and development (R&D) for clean, economical, stable, safe and abundant energy should be promoted from a viewpoint of technology as a potential measure to mitigate the global warming issue as well as for massive and stable energy supply and utilisation. We have various options as alternative energy for fossil fuels: solar, geothermal, hydropower and nuclear energy and so on. While available natural energy is limited due to its stability, quality, quantity and density, it is sure that nuclear energy by high-temperature gas-cooled reactors (HTGRs) has the potential to come up with a share as regards a satiable energy supply and utilisation. Nuclear energy has been exclusively utilised for electric power generation, but the direct utilisation of nuclear thermal energy is necessary and indispensable so that the energy efficiency can be increased and energy savings can be promoted in the near future. The hydrogen production is one of the key technologies for direct utilisation of nuclear thermal energy.

The high temperature engineering test reactor (HTTR), which is the first high temperature gas-cooled reactor (HTGR) in Japan with the thermal power of 30MW and the reactor outlet coolant temperature of 950°C maximum, was constructed at the Oarai Research Establishment of the Japan Atomic Energy Research Institute (JAERI) for the purpose of establishing and upgrading technologies of HTGRs as well as nuclear heat utilisation. [1]

The HTTR attained the first criticality on 10 November 1998. The rise to power test of the HTTR started in September 1999 and the HTTR reached the full power of 30MW and the reactor outlet coolant temperature of 850°C on 7 December 2001. Then, on 6 March 2002 JAERI received a certificate of the pre-operation test from the government, that is, an operation permit of the HTTR at the rated operation mode (operation at the reactor outlet coolant temperature of 850°C), completing the rise to power test at rated operation mode. The HTTR will accomplish the reactor outlet coolant temperature of 950°C at high temperature test operation mode in FY 2003 after accumulating operation experiences.

Various tests utilising the HTTR have been started. The HTTR tests can be categorised to three subjects:

- Safety demonstration test,
- Basic technological test, and
- Hydrogen production test.

In the safety demonstration test, inherent safety features of the HTGR are demonstrated. In the basic technological test, operational performance of the HTGR is to be quantified through operation and maintenance experiences of the HTTR. In the hydrogen production demonstration test, a hydrogen production facility is to be connected to the secondary helium cooling system. This paper describes an outline of the demonstration tests on safety and hydrogen production.

This research has been conducted as the contract research from the Ministry of Education, Culture, Sports, Science and Technology (MEXT) of Japan.

II. Outline of HTTR

1. *Reactor and cooling system*

The cross section views of the reactor are shown in Figure 1. The reactor consists of a reactor pressure vessel, fuel elements, replaceable and permanent reflector blocks, core support structures, control rods, etc. Thirty columns of fuel elements and seven columns of control rod guide blocks form the reactor core called fuel region, which is surrounded by replaceable reflector blocks and large-scale permanent reflector blocks. The fuel element of the HTTR is a so-called pin-in-block type. Sixteen pairs of control rods in the fuel and replaceable reflector regions of the core control reactivity of the HTTR. At a reactor scram, electromagnetic clutches of the control rod drive mechanisms are separated and the control rods fall into holes of the control rod guide blocks by gravity at a constant speed, shutting down the reactor safely. In an unlikely event that the control rods insertion fails, reserved shut down pellets made of B₄C/C are dropped into the core.

As shown in Figure 2, the cooling system of the HTTR consists of a main cooling system (MCS), which operates at normal operation, and an auxiliary cooling system (ACS) and a vessel cooling system (VCS), which operate to remove residual heat of the core after a reactor scram. The ACS and the VCS are engineered safety features. In commercialisation of economically competitive HTGR, it is necessary to eliminate the engineered safety features by establishing new safety evaluation philosophy making the most of results of the HTTR safety demonstration tests.

The main cooling system, which consists of a primary cooling system, a secondary helium cooling system, and a pressurised water cooling system, removes heat generated in the core and dissipates it to atmosphere by a pressurised water air cooler in the pressurised water cooling system.

The primary cooling system consists of an intermediate heat exchanger (IHX), a primary pressurised water cooler (PPWC), a primary concentric hot gas duct, etc. Primary coolant of helium gas from the reactor at 950°C maximum flows inside of an inner pipe of the primary concentric hot gas duct to the IHX and the PPWC. The primary coolant is cooled to about 400°C by the IHX and the PPWC and returns to the reactor flowing through an annulus between the inner and outer pipes of the primary concentric hot gas duct. The HTTR has two operation modes regarding use of heat exchangers for both of the rated operation mode and the high temperature test operation mode. At the single loaded operation mode only the PPWC is operated in the primary cooling system, whereas at the parallel loaded operation mode both the IHX and PPWC are operated, and the IHX and the PPWC remove heat of 10MW and 20MW, respectively.

The auxiliary cooling system, consisting of an auxiliary helium cooling system, an auxiliary water cooling system, a concentric hot gas duct, etc. is in standby during normal operation and starts up to remove residual heat after a reactor scram.

The vessel cooling system cools the biological concrete shield surrounding the reactor pressure vessel at normal operation, and removes heat of the core by natural convection and radiation outside of the reactor pressure vessel under accidents of no forced-cooling condition such as rupture of the primary concentric hot gas duct, when neither the main cooling system nor the auxiliary cooling system can cool the core effectively.

2. *Hydrogen production system*

There are three key technologies to commercialise HTGR H₂HTR, that is, a HTGR technology, a hydrogen production technology without CO₂ emission and a coupling technology to connect a

hydrogen production system to the HTGR. As for the HTGR technology, the research has been carried out with the HTTR [2], and the R&D on the thermochemical water splitting method by the IS process is underway for the hydrogen production technology without CO₂ emission [3].

The demonstration test of the HTTR hydrogen production system (HTTR-H2) aims at establishing the coupling technology which can be available to other hydrogen production systems such as IS process, coal gasification and so on as well as the first demonstration of hydrogen production directly using heat supplied from HTR in the world. Figure 3 shows a schematic flow diagram of the hydrogen production system downstream from the IHX. Main specifications of the HTTR-H2 are described in Table 1. The HTTR reactor supplies heat of 10MW with 950°C to an intermediate heat exchanger (IHX) in the primary helium loop, and then the heat is transferred from the IHX to the secondary helium loop to be utilised for the hydrogen production by the steam reforming of methane; $\text{CH}_4 + \text{H}_2\text{O} = 3\text{H}_2 + \text{CO}$. It is the reason that the technology of the steam reforming matured in fossil-fired plant enables the coupling to the HTTR in the early 2000's and technical solutions demonstrated can contribute to other hydrogen production systems

By a conceptual design, a steam generator (SG) is installed downstream from a steam reformer (SR) in the secondary cooling system to mitigate fluctuation of helium temperature at SR outlet as mentioned later. A steam superheater which needs high temperature heat, helium cooler to adjust helium temperature at inlet of the IHX and isolation valves were also installed in the secondary cooling system [4].

Natural gas supplied from an underground LNG tank is mixed with steam and transported into the SR after passing through a raw gas preheater. The product gas is burned by a flare stack after passing through the raw gas preheater, water preheater, process gas cooler, separator and water drum. A nitrogen supply system is installed to flow nitrogen in the SR instead of natural gas and steam at helium temperature below 700°C at SR inlet in normal start up and shut down operations. The process gas is controlled by a pressure valve installed downstream from the SR to keep the pressure difference of the reaction tube in the SR within an allowable value.

III. Safety demonstration test

1. Outline of test

In safety demonstration tests using the HTTR, anticipated operational occurrences (AOOs) and accidents are simulated mostly without scram, though most of the postulated AOOs and accidents for the HTTR safety evaluation initiate scrams. The postulated events were considered in the safety evaluation of the HTTR as AOOs and accidents [5]. The safety demonstration tests are conducted to demonstrate inherent safety features of the HTGRs as well as to obtain the core and plant transient data for validation of safety analysis codes and for establishment of safety design and evaluation technologies of the HTGRs.

The safety demonstration tests are divided into the first phase (phase I) and the second phase (phase II). In the phase I safety demonstration tests, AOO simulation tests without a reactor scram will be conducted. The phase I tests consist of the following subjects:

- i) Reactivity insertion test – control rod withdrawal test, and
- ii) Coolant flow reduction test.

In the “reactivity insertion test” a central pair of control rods is withdrawn and a reactivity insertion event is simulated. The “coolant flow reduction test” is composed of “partial loss of coolant flow test” and “gas circulators trip test”. In the “partial loss of coolant flow test”, the primary coolant flow rate is slightly reduced by the control system of the primary coolant flow rate with the reactor outlet coolant temperature control system being operated. In the “gas circulators trip test,” primary coolant flow rate is reduced to 67% and 33% of rated flow rate by running down one and two out of three gas circulators at the PPWC without a reactor scram, respectively. The phase I tests have already been licensed and are planned to be conducted from FY 2002 to 2005. Test methods and conditions as well as pre-test analysis and test results of the phase I tests are described in Sections 2 to 3.

In the phase II safety demonstration tests, accident simulation tests with or without scram will be mainly performed. The phase II tests, which are advanced tests of the phase I tests, will be conducted after confirming safety features of the HTTR by the phase I tests and obtaining new licenses. The phase II tests include:

- i) Loss of forced cooling test (all gas circulators trip test),
- ii) All black out test (vessel cooling system stop test), and
- iii) Depressurisation test [simulation of loss of coolant accident (LOCA)].

The schedule of the safety demonstration test is shown in Figure 4.

2. *Reactivity insertion test – control rod withdrawal test*

The reactivity insertion test demonstrates that rapid increase of reactor power by withdrawing the control rods is restrained by only the negative reactivity feedback of the core without operating the reactor power control system, and the transition of fuel temperatures is slow. The central pair of control rods out of 16 pairs in the core is withdrawn with the reactor power control system being disabled. The reactivity insertion tests at the initial reactor thermal power of 15MW (50%) was conducted in March 2003. Preliminary reactivity insertion tests at the initial power of 9MW (30%) had been conducted in June 2002.

As the result, the reactor power increased to about 56% from the initial reactor power of 51% and decreases afterward. The reactor power finally approached to about 52% in the test as the positive reactivity by control rod withdrawal compensates with the negative one by core temperature rise [2].

3. *Coolant flow reduction test*

The partial loss of coolant flow test demonstrates that the reactor becomes stable by inherent safety characteristics and control systems of HTGRs even when partial loss of coolant flow occurs. In the test, primary coolant flow rate is reduced to the level between 100 and 93% with all control systems operated normally. The HTTR scrams when the primary coolant flow rate reduces to 93% of rated flow rate.

The gas circulator trip test demonstrates that rapid decrease of coolant flow rate brings reactor power to stable level by negative reactivity feedback of the core without a reactor shut down, and the transition of fuel temperatures is slow. In the test, the primary coolant flow rate is reduced by running down one and two out of three gas circulators with the reactor power control system being disabled. All gas circulators trip test simulating loss of forced cooling will be conducted in the second phase

tests. One out of three gas circulators trip test at the initial reactor thermal power of 9MW (30%) was conducted in March 2003.

Figure 5 shows the transition of the primary coolant flow rate and reactor power. Because one gas circulator out of three is run down, the primary coolant flow rate decreases in accordance with the free coast down characteristics of the gas circulator. The primary coolant flow rate is finally controlled to 67% of initial flow rate because the rest gas circulators keep running with primary coolant flow control system operated. In this test, the core temperature increased due to reduction of primary flow, and the reactor power decreased to about 24% from the initial reactor power of 30% due to negative reactivity feedback effect. The saturated value of about 24% was in fairly good accordance with the pre-test analysis result of 22% [2].

IV. Hydrogen production demonstration test

1. Outline of test

The demonstration test aims at establishing the coupling technology as well as the procedure on safety design and evaluation. The coupling technology consists of safety-related and control ones. The safety-related technology includes countermeasures against explosion of combustible gas and tritium permeation from helium gas to process gas, and assurance of pressure boundary between the primary and the secondary helium gases. The control technology aims at preventing thermal mismatch between reactor and hydrogen production facility.

(1) Safety-related technology

i) Countermeasure against explosion of combustible gas

As for the countermeasure against explosion of combustible gas, the conceptual design has been carried out from a viewpoint of reduction of leakage amount by cut off valves and coaxial pipe in the raw gas supply and product gas combustion systems, mitigation of overpressure caused by explosion by separation of reactor and combustible gas components and so on. The coaxial pipe is composed of an inner pipe in which combustible gas flows and an outer pipe in which combustible gas flows. In the case of failure of the inner pipe, the outer pipe can protect leakage of combustible gas to atmosphere and the leakage can be easily detected.

ii) Countermeasure against tritium permeation

It is well known that hydrogen isotopes, hydrogen (H), deuterium (D), and tritium (T), permeate through solid metals. Therefore, tritium produced in the core tends to permeate through heat transfer tubes of the IHX and reaction tubes of a chemical reactor in the hydrogen production system. Further, it is probable that the tritium will mix with the product hydrogen. At the demonstration test, the permeation rate will be measured. As for the HTTR-H2, it is considered that the permeation rate will be enough small to assure the safety of the product hydrogen without the countermeasure at the pre-estimation by analysis and a component test using hydrogen and deuterium instead of tritium [6, 7].

iii) Assurance of pressure boundary between the primary and secondary helium

The heat exchanger tube in the IHX, pressure boundary between the primary and secondary helium, is designed considering the pressure difference between the primary and secondary helium by the same reason as the reaction tube in the SR. The isolation valve is key component to assure the structure of the heat exchanger tube at an accident of piping rupture of the secondary cooling system.

A high temperature isolation valve (HTIV) used in the helium condition over 900°C, however, has been not made for practical use yet. JAERI has been conducting design and a component test on the HTIV.

(2) *Control technology*

The reactor and hydrogen production systems are connected by the helium loop. A chemical reactor causes the temperature fluctuation of helium by the fluctuation of the reaction, which can be occurred at normal start up and shut down operation as well as malfunction or accident of a process gas line. The reactor operation would be stopped by the temperature fluctuation. The SG was installed downstream from the SR in the secondary helium loop to mitigate the temperature fluctuation within 10°C at the SG outlet, because the temperature rise above 15°C compared with the normal temperature at the reactor inlet causes the HTTR reactor scram. The temperature fluctuation changes a generation rate of steam, but saturation temperature of water is constant in the SG. As the result, the helium temperature can be kept near at the saturation temperature.

Prior to connection of the hydrogen production to the HTTR, a simulation test with a mockup model of the HTTR-H2 is in progress to investigate performance of the SG for mitigation of the temperature fluctuation and transient behavior of the hydrogen production system and to obtain experimental data for verification of a dynamic analysis code. The mock-up model test facility has an approximate hydrogen production capacity of 120Nm³/h and simulates key components downstream from the IHX. The SR has single full-scale reaction tube and an electric heater with 420kW is used as a heat source instead of the reactor in order to heat helium gas up to 880°C at the SR inlet which is the same temperature as the HTTR-H2. Design specifications and a schematic flow diagram of the test facility are shown in Table 1 and Figure 6, respectively [8, 9].

By the demonstration test, the following results can be obtained.

(a) *Safety*

i) Safety design and evaluation

The procedure on safety design and evaluation can be established by licensing, design and construction.

ii) Tritium permeation

The amount of tritium permeated from the primary helium to process gas can be estimated as described in Section 2.

(b) *Operability and controllability*

i) Mitigation of thermal disturbance

The technology with the SG can be established as described in Section 3.

ii) Operation and maintenance experience

The operation and maintenance experience can be accumulated.

(c) *Component*

i) Intermediate heat exchanger (IHX)

Operational data on temperatures, pressures and flow rates are obtained in steady and transient operations in order to verify the design and to establish the technology on high temperature heat exchanger as described in Section 4.

ii) High temperature isolation valve (HTIV)

The integrity of HTIV can be demonstrated as described in Section 5.

iii) Hot gas duct (HGD)

The integrity of the long HGD can be demonstrated focusing on thermal expansion as described in Section 6.

iv) Detection of combustible gas leakage

The detection technology of combustible gas leakage can be demonstrated as described in Section 7.

The schedule of the licensing, the manufacturing design, the construction and the hydrogen production demonstration test are shown in Figure 4. The target to connect the hydrogen production facility to the HTTR is around FY 2008. As for the IS process, hydrogen production by water splitting was successfully achieved with a bench test facility in 2003. A pilot test will be started from FY 2005.

2. *Tritium permeation*

In the HTGR hydrogen production system, tritium produced in the core is transported to the product hydrogen by permeating through tubes of the IHX and chemical reactor in high temperature environment. From the viewpoint of a safety design, tritium in the product hydrogen should be reduced within allowable concentration. The permeation quantities of tritium through the IHX and chemical reactor will be measured with the HTTR-H2 to establish estimation method of tritium permeation.

Quantities of tritium in the primary and secondary helium gas can be measured by helium purification systems, which are installed in both the primary and the secondary cooling systems. The tritium exists in helium gas in the form of T_2 and HT. Therefore, they are captured by the cold charcoal and molecular sieve traps after converted to T_2O and HTO in the copper oxide fixed bed, and T_2O and HTO are accumulated up to enough quantity to measure the dosage. By the measurement of the dosage, the quantities of tritium can be obtained.

On the other hand, permeated quantity of tritium in product gas must be measured by other way. In the IS process, the tritium permeation will be occurred at a SO_3 decomposition reactor which is used in the same temperature region as the steam reformer in the HTTR-H2. To simulate the tritium permeation in the IS process, nitrogen gas is flowed in the steam reformer. A part of nitrogen gas flowing through the steam reformer is sampled and T_2 and HT in the nitrogen gas are converted to T_2O and HTO to measure the dosage.

3. *Mitigation of thermal disturbance*

The technology on mitigation of thermal disturbance with the SG will be demonstrated by the operation of the HTTR-H2. The operation will be separated into three periods, that is, the first operation: normal start up and shut down, the second operation: fluctuation of chemical reaction, and the third operation: loss of chemical reaction.

(1) *First operation: normal start up and shut down*

The test on normal start up and shut down operation of the HTTR-H2 is performed aiming at demonstration on normal start up and shut down of the hydrogen production system giving no influence on operation of the nuclear reactor from the viewpoint of the feedback of the secondary helium temperature, that is, demonstration on function of the SG to mitigate fluctuation of the secondary helium temperature.

The normal start up and shut down will be carried out in the following method. According to the helium temperature at SR inlet, nitrogen, steam and natural gas are supplied to the SR step by step. At first, nitrogen is only supplied up to 700°C of helium temperature at SR inlet in normal start up operation. Steam and natural gas are gradually supplied with decrease of nitrogen feed over 700°C and feed of nitrogen is completely stopped in rated power operation. The normal shut down operation has reverse step of the normal start up operation.

(2) *Second operation: fluctuation of chemical reaction*

The test on fluctuation of chemical reaction is performed aiming at demonstration on operability and controllability, and function of the SG to mitigate fluctuation of the secondary helium temperature against the fluctuation of chemical reaction. From rated power condition, flow rates of natural gas and steam are changed by step input, and transient behavior of hydrogen production rate, temperatures, pressures, etc. are investigated.

(3) *Third operation: loss of chemical reaction*

The test on loss of chemical reaction is performed aiming at demonstration on operability and controllability, and demonstration on function of the SG to mitigate fluctuation of the secondary helium temperature against loss of chemical reaction.

Even if the process gas feed is stopped completely, we aim at shut down of the reactor by the normal operation procedure but not with the reactor scram. At this time, heat of the secondary helium gas cannot be removed at the SR because the chemical reaction is lost. It is required to cool the secondary helium gas at the SG instead of the SR. We aim at controlling the fluctuation of the secondary helium gas temperature within $\pm 10^\circ\text{C}$ at the SG outlet only to maintain the reactor operation. The cooling system of the secondary helium gas in case of the loss of chemical reaction has been designed using the SG and a condenser installed above the SG. Generation rate of steam in the SG increases more than twice compared with that in rated power operation. Steam produced in the SG is condensed into water at the condenser, and steam and condensed water circulated between the SG and condenser by natural circulation. In this system, there is no need to control the water feed to the SG in case of loss of chemical reaction

From rated power operation condition, feed of raw gas and steam is cut off and nitrogen is supplied instead of these gases to keep the pressure difference of the reforming tube in the SR within

allowable value. Steam is transported to the condenser and condensed water returns to the SG, that is, natural circulation of steam and condensed water occurs between the SG and condenser.

Figure 7 shows an experimental result of the simulation test at start up operation. In the test, natural gas and steam were supplied from time “0 hr”. The chemical reaction caused the helium temperature down of 85°C at outlet of the SR, however, the SG mitigated the temperature fluctuation within 2°C at outlet. The result can be applied for design of the SG of the HTTR-H2 and verification of the dynamic simulation code.

4. Intermediate heat exchanger (IHX)

In order to establish the technology on high temperature heat exchanger, operational data on temperature distributions of components in the IHX will be measured in steady and transient operations including shut down of the nuclear reactor and loss of chemical reaction.

The IHX is a vertical helically-coiled counter flow type heat exchanger in which the primary helium gas flows on the shell side and the secondary helium gas in the tube side as shown in Figure 8. The primary helium gas of 950°C and 4MPa enters into the IHX through the inner tube of the primary concentric hot gas duct. It is deflected under a hot heater and discharged around the heat transfer tubes to transfer the heat to the secondary helium cooling system. It flows to the primary circulator via the upper outlet nozzle and flows back to the annular space between the inner and outer shells. The secondary helium gas of 150°C and 4.1MPa flows downwards in the heat transfer tubes and upwards in the central hot gas duct through the hot heater. The inner insulation is installed inside the inner shell to maintain its temperature under the allowable one. The insulations outside and inside the central hot gas duct keep the heat transfer low so that high efficiency can be obtained, and also keep the temperature of the central duct under the allowable value. Primary helium gas is contained only in the primary cooling system because the pressure in the secondary helium cooling system is controlled higher than that in the primary cooling system.

5. High temperature isolation valve (HTIV)

The high temperature isolation valve (HTIV) used in the helium condition over 900°C, however, has been not made for practical use yet. JAERI has been conducting design and component tests on the HTIV. By the demonstration test of the HTTR-H2, the technology of the HTIV can be established and demonstrated.

The design of an angle-type HTIV was carried out from the viewpoints of reduction of thermal deformation and stress of seat and rod, and temperature fall at gland seal to prevent leakage. As for the reduction of thermal deformation and stress, structure of thermal insulator and seat focusing on the shape connected to the valve body was designed using the FEM analysis. A long bonnet was designed for the temperature fall at the gland seal. Figure 9 shows the cross section of the HTIV.

New coating material for seat and rod was developed based on stellite to increase hardness in high temperature condition. The tests on slide, welding, fatigue against thermal cycle and so on were performed to investigate durability of the coating material. As the result, it was confirmed that the material was available for the HTIV.

The test was carried out with a mockup model simulating the seat and rod on 1/5 scale to investigate effect of shape of the seat and rod using the new coating material, load on seat, etc. on seal performance. Moreover, the structural integrity of the seat and rod was investigated against thermal cycle and open/close cycle. The results were used for design of a mockup model on 1/2 scale.

The performance test with mockup model of the HTIV has been carried out until 2004. The mockup model simulates the seat, rod, valve body, thermal insulator and gland seal on 1/2 scale. The objective of the test is verification of the design from the following viewpoint,

- i) Structural integrity of the seat, rod, valve body and gland seal against thermal and open/close cycles especially focusing on thermal deformation,
- ii) Seal performance in high pressure and temperature condition, over 4.1MPa and 900°C,
- iii) Durability of the coating material, and
- iv) Performance of thermal insulator, etc.

In the demonstration test of the HTTR-H2, temperature distribution of the outer surface of the valve body is measured to investigate performance of the thermal insulator. At scram of the nuclear reactor, the HTIV is closed. After that, overhaul is carried out to investigate structural integrity of the seat, rod, gland seal and so on.

6. Hot gas duct (HGD)

In the HTTR-H2, the secondary helium gas at the IHX outlet temperature 905°C is transported to the steam reformer (SR) passing through inside of an inner pipe of a coaxial hot gas duct (CHGD) in an underground trench. The total length of the CHGD is approximately 64 m. In the underground trench, the form of the CHGD is straight and its length is approximately 30 m. Therefore, a countermeasure against the thermal expansion is very important to assure the structural integrity of the CHGD. As for the countermeasure, bellows will be installed at the inner pipe of the CHGD. The bellows will be used for a single hot gas duct (SHGD) of which total length is approximately 24 m. The advantage of the bellow is that the total lengths of the CHGD and SHGD become short because bends to absorb the thermal expansion are not necessary, that is, reduction of the construction cost.

In the demonstration test of the HTTR-H2, temperature distribution and displacement of the CHGD and SHGD and shrinkage of the bellows will be measured in steady and transient operations including shut down of the nuclear reactor and loss of chemical reaction.

7. Detection of combustible gas leakage

In the HTTR-H2, coaxial pipes will be used for the combustible gas line in the area near the HTTR to detect leakage of combustible gas as soon as possible. The coaxial pipe is composed of inner and outer pipes, suction and return pipes, a gas detector and a pressure gauge. The combustible gas such as methane and hydrogen flows in the inner pipe. The gas detector has a pump to circulate nitrogen between the gas detector and outer pipe passing through the suction and return pipes. The gas detector is used for small leakage and the pressure gauge detects large leakage such as rupture of the inner pipe. This detection system will be installed at an interval of 30 m, and number of the systems is five.

Leakage detection test will be carried out before operation of the HTTR-H2. The combustible gas, methane and hydrogen, is put into the outer pipe to investigate detection performance such as sensitivity and time delay.

V. Concluding remarks

The safety demonstration test results are applicable to demonstration of inherent safety features as well as upgrading of safety evaluation technologies of HTGRs, and provided for consideration of cost reduction of future HTGRs by eliminating engineered safety features such as the auxiliary cooling system and reactor containment vessel. Thus, it is expected that the obtained results contribute to commercialisation of HTGRs such as the very high temperature reactor system selected as one of the most promising Generation IV systems.

From a viewpoint of the global warming issue, technology to produce a great deal of hydrogen without CO₂ emission will be necessary in a near future. The hydrogen production with HTGRs can be considered as one of key technologies to solve the issue. The HTTR-H₂ is a very important milestone to commercialise the H₂HTTR from a viewpoint of demonstration of coupling of reactor and hydrogen production plant, and hydrogen production directly using thermal energy supplied from reactor.

JAERI would like to contribute the solution of the environmental issue of CO₂ emission as well as a possible energy crisis, which might happen in future.

References

- [1] Saito, S. *et al.*, “Design of High Temperature Engineering Test Reactor (HTTR)”, Report of the Japan Atomic Energy Research Institute, JAERI 1332 (1994).
- [2] Tachibana, Y. *et al.*, “Safety Demonstration Tests using High Temperature Engineering Test Reactor”, to be published in GENES4/ANP2003, Kyoto, Japan, 15-19 Sept. (2003).
- [3] Onuki, K. *et al.*, “Thermochemical Hydrogen Production by Iodine-Sulfur Cycle”, Proc. 14th World hydrogen Energy Conf., Montreal, Canada (2002).
- [4] Nishihara T. *et al.*, “A Conceptual Design Study on the Hydrogen Production Plant Coupled With the HTTR”, Proc. 11th Int. Conf. on Nucl. Eng., Tokyo, Japan, 20-23 April 2003 ICONE-36319 (2003).
- [5] Nakagawa, S. *et al.*, “Methods and Results of Safety Evaluation of the High Temperature Engineering Test Reactor”, Nuclear Technology, Vol. 115, pp. 266-280 (1996).
- [6] Takeda, T. *et al.*, “Permeability of hydrogen and deuterium of Hastelloy XR”, to be published in Journal of Nuclear Materials.
- [7] Takeda, T. *et al.*, “Counter permeation of deuterium and hydrogen through Inconel 600”, to be published in Nuclear Technology.
- [8] Inagaki, Y. *et al.*, “Out-of-Pile Demonstration Test of Hydrogen Production System Coupling with HTTR”, Proc. 7th Int. Conf. on Nucl. Eng., Tokyo, Japan, 19-23 April 1999, ICONE-7101 (1999).
- [9] Ohashi, H., *et al.*, “Performance Test Results of Mock-up Test Facility of HTTR Hydrogen Production System”, Proc. 11th Int. Conf. on Nucl. Eng., Tokyo, Japan, 20-23 April 2003, ICONE-36059 (2003).

Table 1. Main design specifications of HTTR hydrogen production system and mock up model

Items	HTTR-H2	Mock-up
Pressure Process gas/helium	4.5/4.1 MPa	4.3/4.0 MPa
Inlet temperature at steam reformer Process gas/helium gas	450 / 880°C	
Outlet temperature at steam reformer Process gas/helium	580/585°C	600/650°C
Natural gas feed	1 400kg/h	43.2kg/h
Helium feed	9 070kg/h	328kg/h
Steam-carbon ratio (S/C)	3.5	3.5
Hydrogen product	4 200Nm ³ /h	120Nm ³ /h
Heat source	Reactor (10MW)	Electric heater (420kW)

Figure 1. Cutaway and cross-section views of the reactor

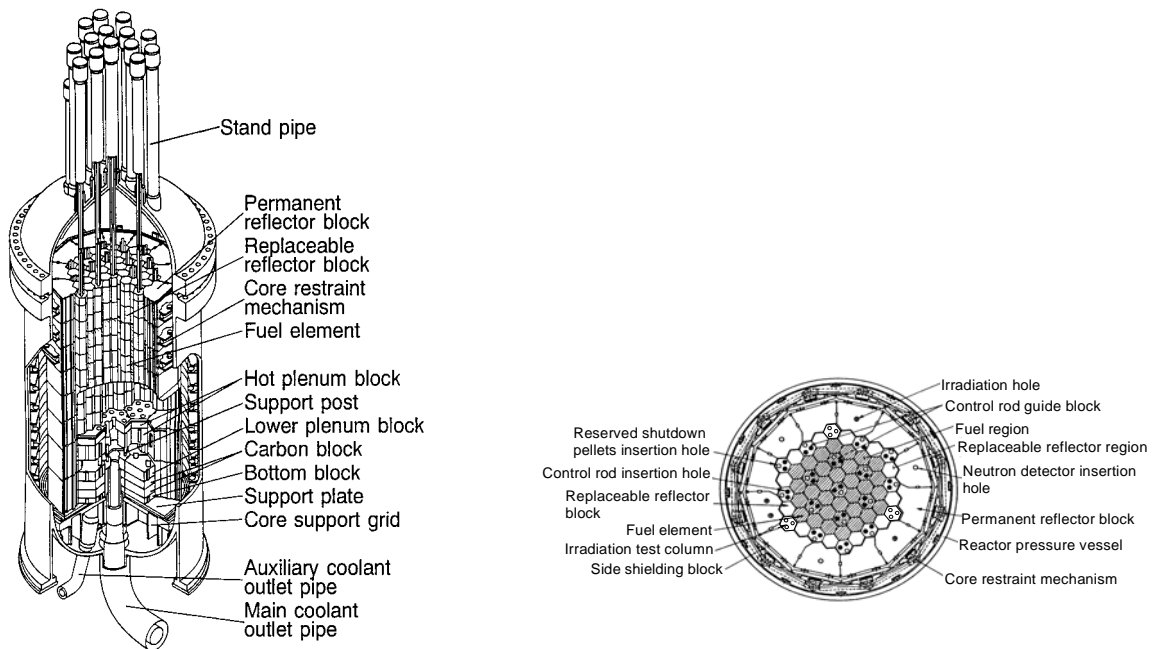
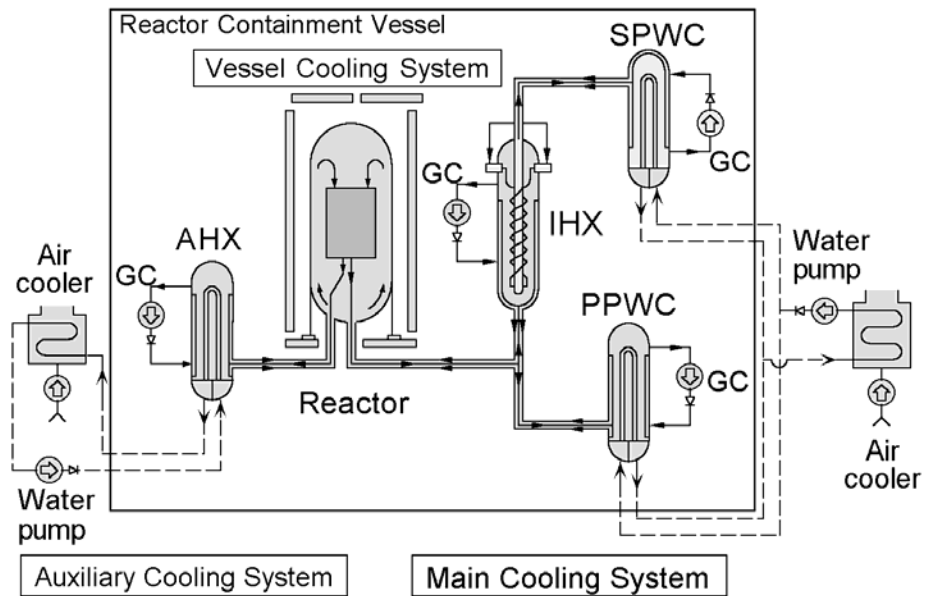


Figure 2. Cooling system of HTTR



AHX: Auxiliary heat exchanger
 GC: Gas circulator
 IHX: Intermediate heat exchanger
 PPWC: Primary pressurized water cooler
 SPWC: Secondary pressurized water cooler

Figure 3. Flow diagram of hydrogen production facility downstream from IHX

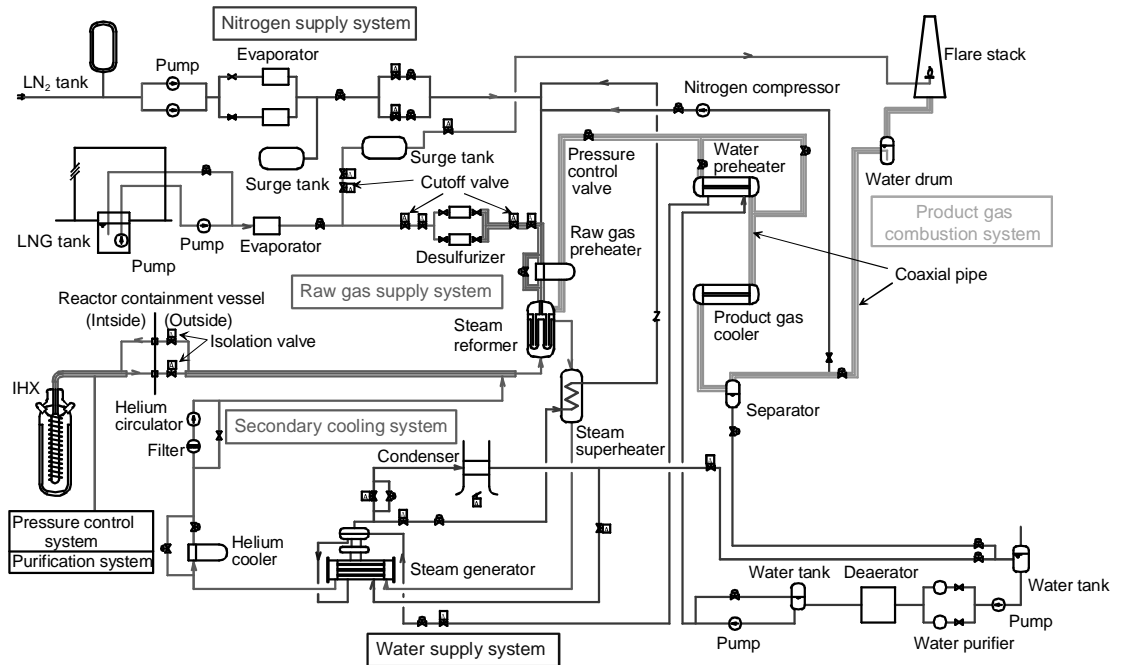


Figure 4. Schedule of HTTR project

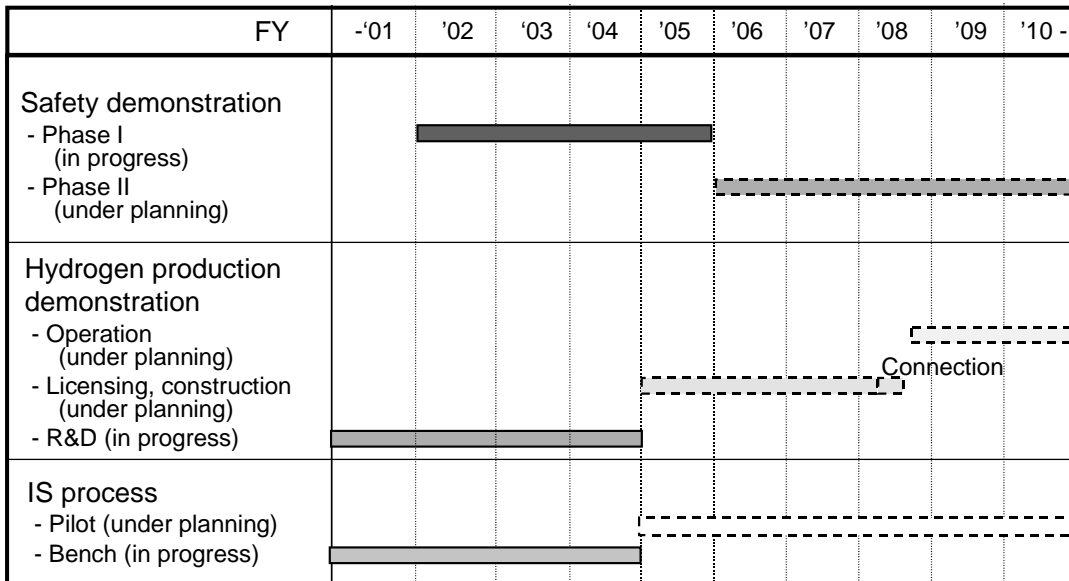


Figure 5. Pre-test analysis and test results of the gas circulators trip test

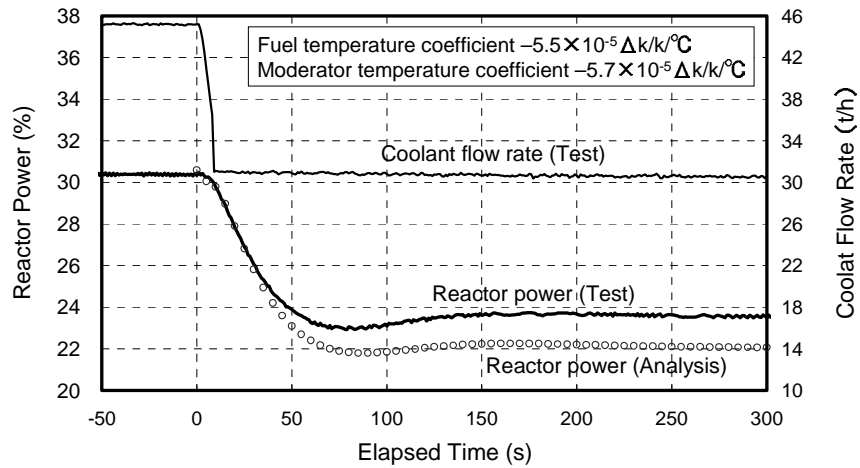


Figure 6. Schematic flow diagram of mock up model test facility

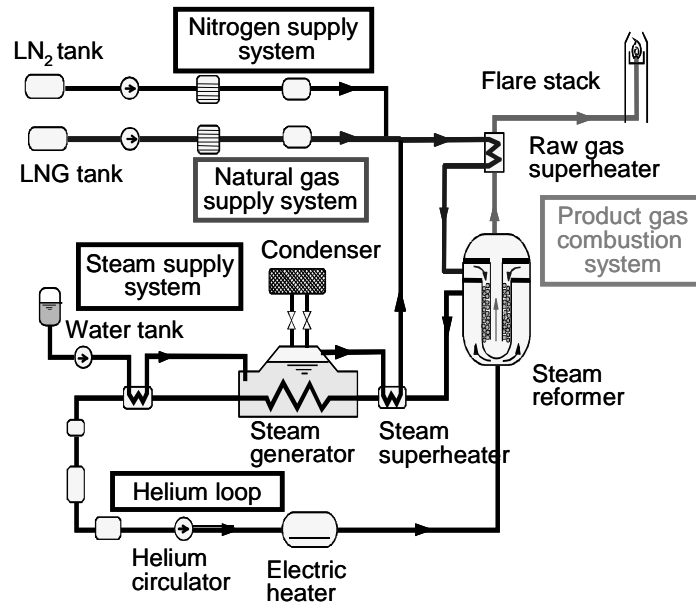


Figure 7. Experimental result of simulation test at start up operation

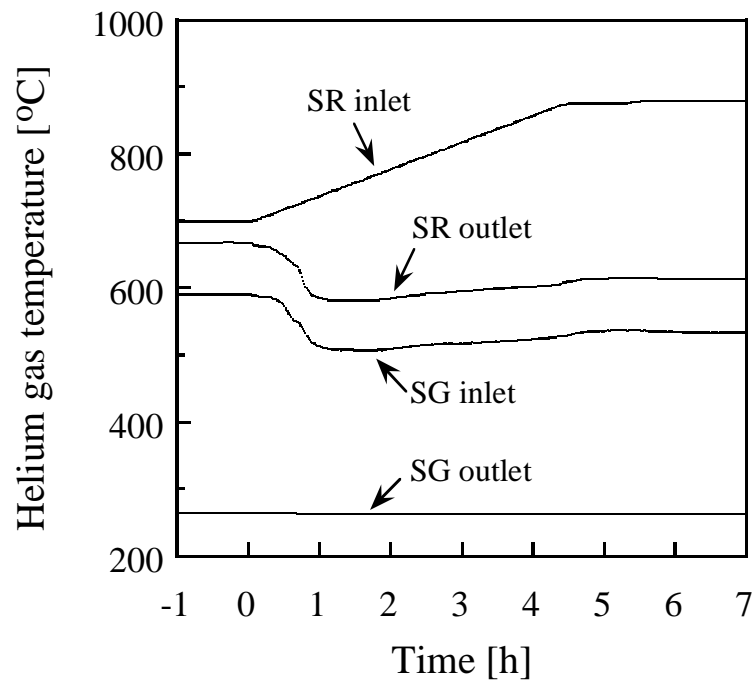


Figure 8. Isometric view of IHX

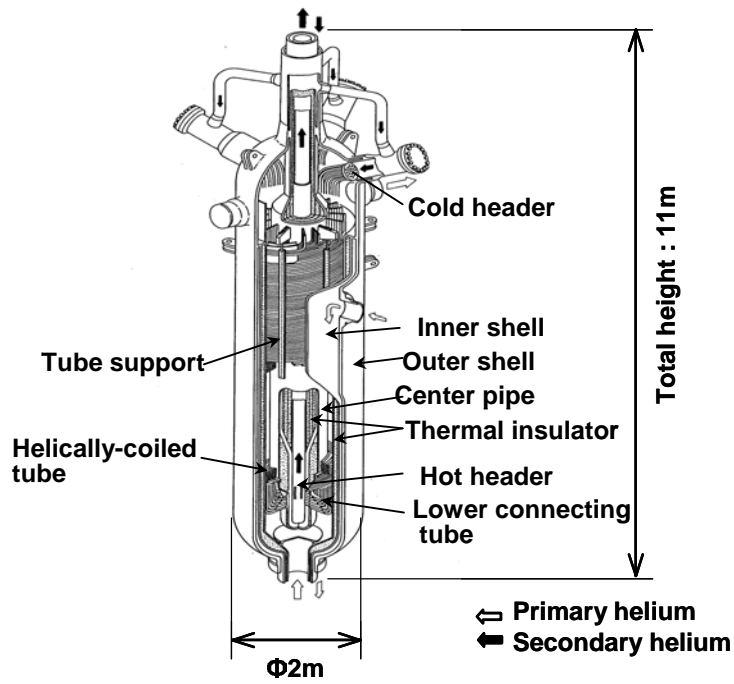
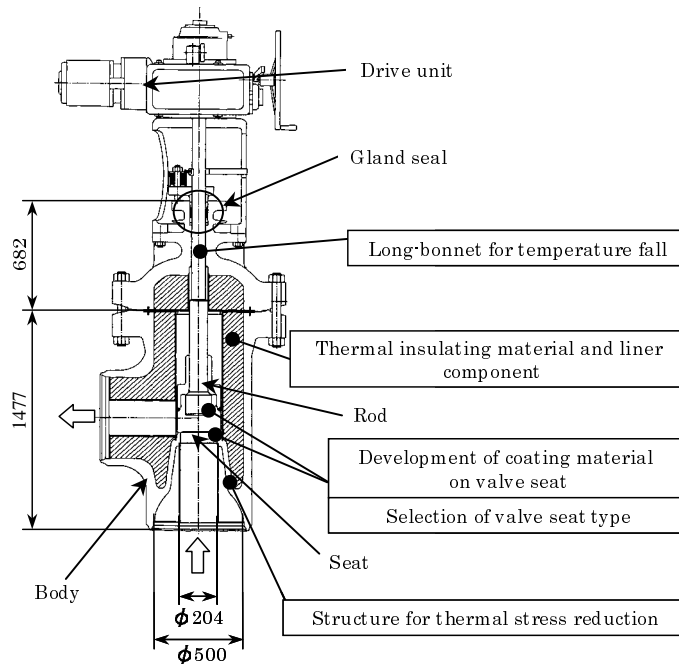


Figure 9. Cross-section of HTIV



ADVANCED DESIGN OF FAST REACTOR-MEMBRANE REFORMER (FR-MR)

Masanori Tashimo

Advanced Reactor Technology Co., Ltd.

Masao Hori

Nuclear Systems Association

Isamu Yasuda

Tokyo Gas Co., Ltd.

Yoshinori Shirasaki

Tokyo Gas Co., Ltd.

Kazuto Kobayashi

Mitsubishi Heavy Industries, Ltd.

Abstract

A new plant concept of nuclear-produced hydrogen is being studied using a Fast Reactor-Membrane Reformer (FR-MR).

The conventional steam methane reforming (SMR) system is a three-stage process. The first stage includes the reforming, the second contains a shift reaction and the third is the separation process. The reforming process requires high temperatures of 800~900 °C. The shift process generates heat and is performed at around 200°C. The membrane reforming has only one process stage under a non-equilibrium condition by removing H₂ selectively through a membrane tube. The steam reforming temperature can be decreased from 800 °C to 550 °C, which is a remarkable benefit offered by the non-equilibrium condition. With this new technology, the reactor type can be changed from a High Temperature Gas-cooled Reactor (HTGR) to a Fast Reactor (FR).

A Fast Reactor-Membrane Reformer (FR-MR) is composed of a nuclear plant and a hydrogen plant. The nuclear plant is a sodium-cooled Fast Reactor with mixed oxide fuel and with a power of 240 MWt. The heat transport system contains two circuits, the primary circuit and the secondary circuit. The membrane reformer units are set in the secondary circuit. The heat, supplied by the sodium, can produce 200 000 Nm³/h by 2 units. There are two types of membranes. One is made of Pd another one (advanced) is made of , for example V, or Nb. The technology for the Pd membrane is already established in a small scale. The non-Pd type is expected to improve the performance.

Introduction

Nuclear energy has been used mainly for electricity generation for the past 50 years since the EBR-I generated electric power. Now about 18% of world electricity is supplied by nuclear power.

The major issues in the 21st century are a sustainable growth, energy supply and environment. Upon these prospects, nuclear production of hydrogen is expected to be one of the promising concepts.

A new concept for nuclear-production of hydrogen is studied, which utilises the fast reactor and the membrane reformer (FR-MR) technology. This concept is simpler and provides more compact system than the combination of the high temperature gas reactor and the steam methane reforming (HTGR-SMR) technology.

1. Advantage of the FR-MR method

There are two important advantages in this FR-MR method. [1]

- 1) **Reduction of methane consumption and consequently CO₂ emission** – Full conversion of the C-H bonding force of methane to the production of hydrogen is achieved by use of the nuclear heat and membrane reformer.
- 2) **Separation of CO₂ within the process** – Separation of the reaction product CO₂ is achieved within the process easier than that of CO₂ in the combustion gas. This would be advantageous for sequestration of CO₂ in case it is necessary in a future.

These two points will be important in the coming future for sustainable energy supply with conserving fossil resources and environment.

2. Steam methane reforming

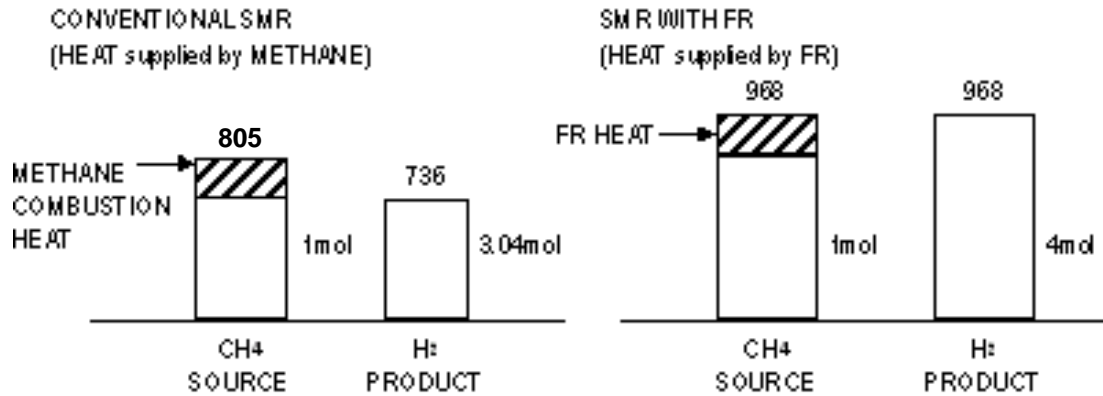
Methane can produce 805 kJ/mol when it is burned. By the chemical reaction of methane with steam and additional heat (SMR), 1 mol of methane is transformed into 1 mol of CO and 3 mol of H₂, theoretically [CH₄+H₂O <=> CO+3H₂]. The equilibrium processed gas composition, which links to H₂ yield, is strongly dependent on temperature; the higher yield at higher temperatures.

Usually a temperature 750~900°C is selected for industry use. A yield improvement is achieved by shift reaction [CO+H₂O <=> CO₂+H₂]. This chemical reaction is exothermic process at around 200°C. The overall theoretical H₂ yield from 1 mol of methane is 4 mol of H₂, which could generate 968 kJ by combustion.

Practically, yield of the produced H₂ by the conventional SMR is 2.5~3 mol even in a larger plant, because heat must be supplied by combustion of methane itself and heat loss and H₂ loss occur in the plant.

In case of FR-MR, as the heat required for endothermic SMR reaction is supplied by nuclear energy and the efficient production by combined reforming and shift reactions of the membrane reformer, the yield of process can be increased almost to the theoretical value of 4 mol of H₂ per 1 mol of methane (Figure 1).

Figure 1. Specific rate of hydrogen production

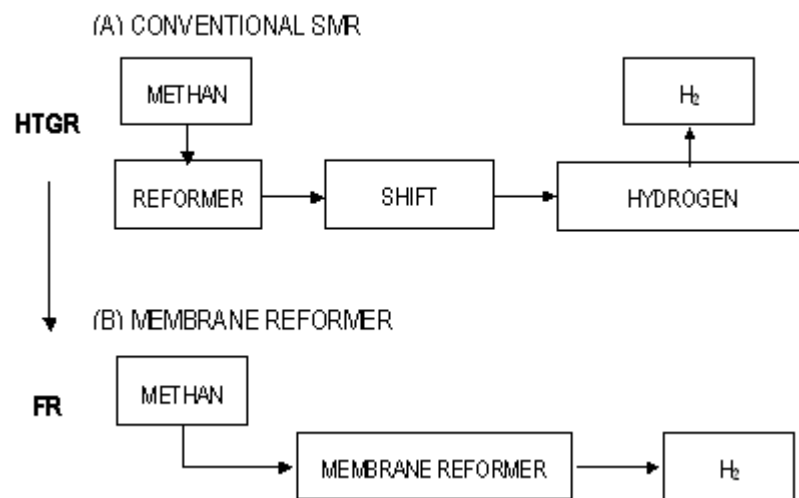


3. Membrane reformer

A comparison of the conventional SMR process and membrane reformer process is shown in Figure 2.

The conventional SMR has three-stage process. The first stage is reforming, the 2nd is shift reaction and the 3rd is separation process. The reforming process requires high temperature of 750~900°C. The shift process generates heat and is performed at around 200°C.

Figure 2. Membrane reformer

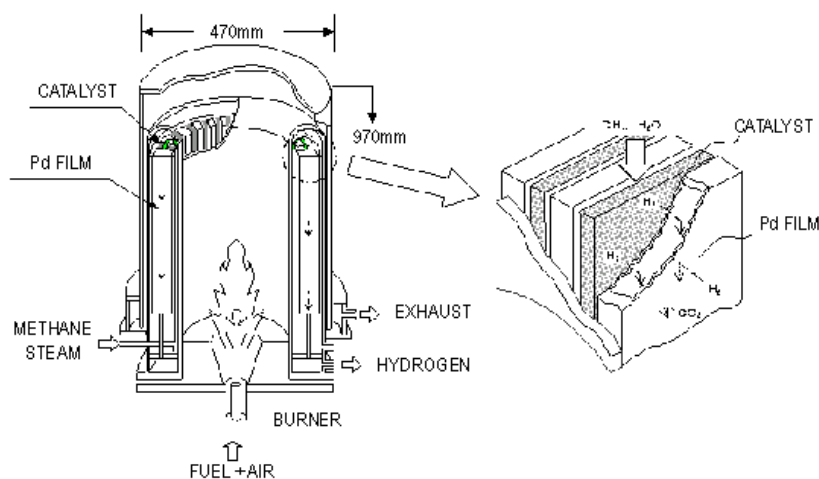


The membrane reforming has only one stage of process, in which the reforming and the shift reaction and selective removal of H₂ through membrane tubes take place concurrently. The steam

reforming temperature can be decreased from 750~900°C to 550°C, which is a remarkable benefit offered by the non-equilibrium condition.

With this new technology, the reactor type can be changed from a gas-cooled reactor such as HTGR to a sodium-cooled reactor such as FR. Figure 3 shows a small-scale test membrane reformer with the capacity 4 Nm³/h, the concept and its technical feasibility was already demonstrated experimentally in 1996.

Figure 3. Structure of membrane reformer (15 Nm³/h)



A 15 Nm³/h pilot module for the hydrogen supply stations has been tested by the Tokyo Gas Company for 1 100 hours using city gas as the fuel. [2, 3]

4. General requirements for a nuclear hydrogen production plant

The general requirements for a nuclear hydrogen plant are:

- **Scale** – FR with 240 MWt can supply heat to produce 200 000 Nm³/hr of hydrogen. With this hydrogen, we could supply fuel to 1.8 million fuel cell vehicles in Japan. An average oil refinery plant in Japan supplies the gas to 1.8 million cars.
- **Site** – The plant will be located in industrialised areas (LNG receiving sites and refinery plant sites).
- **Safety** – Special attention should be paid to safety for both the nuclear plant accident and chemical plant accident.
- **Operability** – The inspection and maintenance interval of chemical plants is usually 2 years in Japan. Then, the nuclear plant's refuelling and maintenance interval should be 2 years.

- **Code and standards** – There are two-candidate code and standard structures for the nuclear produced hydrogen plant, the one is nuclear plant and the other is chemical plant. It is very important to limit systems because of hydrogen cost reduction applied nuclear plant code and standard.

5. Plant design

A FR-MR plant concept is shown in Figure 4. The hydrogen plant is built on the ground and the nuclear plant is built under the ground to make sure the nuclear plant safety. The principal concerns to ensure safety of the plant are “open-and-diffuse” for the hydrogen plant and “close-and-contain” for the nuclear. The system diagram and performance is shown in Figure 5. The major difference in the system design between the hydrogen production and electric generation is the core outlet temperature and the temperature rise in the core. The temperature 580°C is selected to supply heat to maintain the temperature of the membrane reformer at 565°C. The temperature rise in the core is 80°C according to the heat balance of methane reforming and preheat.

The reformer design and specifications are shown in Figure 6. The hydrogen production by this reformer is 100 000 Nm³/h by one unit. The material of the vessel and the tube is stainless steel and ferritic alloy. The membrane tubes are made of Palladium (Pd).

Figure 4. Bird view of FR-MR

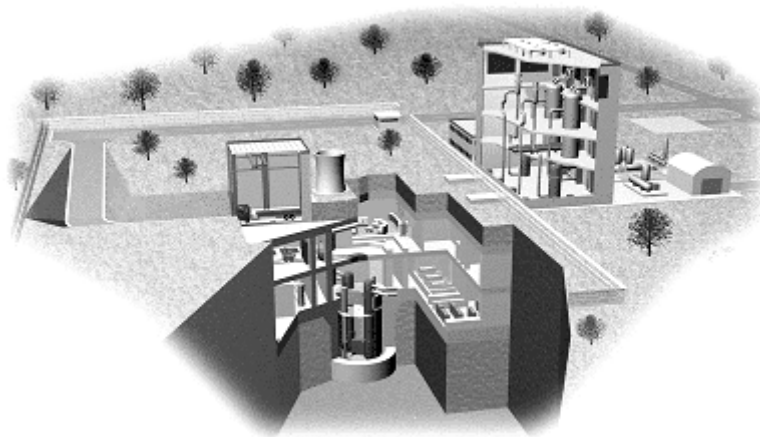


Figure 5. System diagram and performance

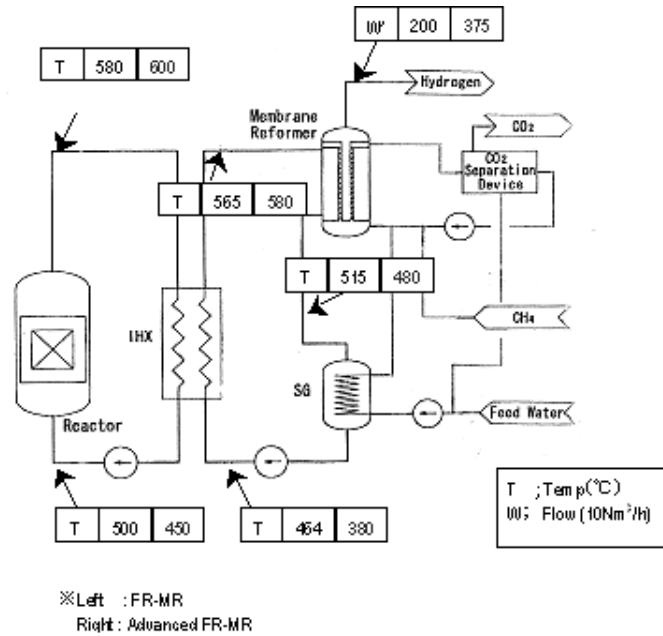
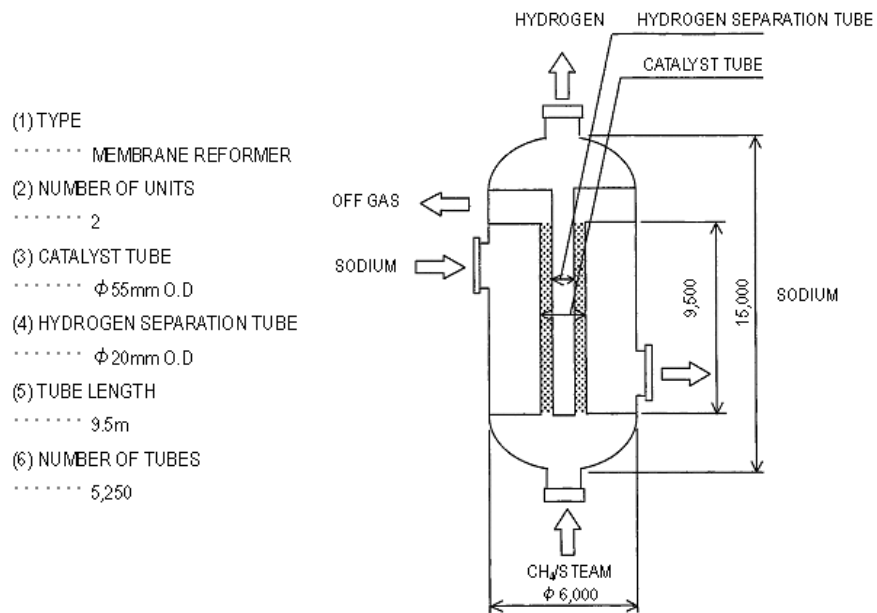


Figure 6. 100 000 Nm³/h-class membrane reformer design in FR-MR plant



6. Advanced FR-MR

1) Membrane performance

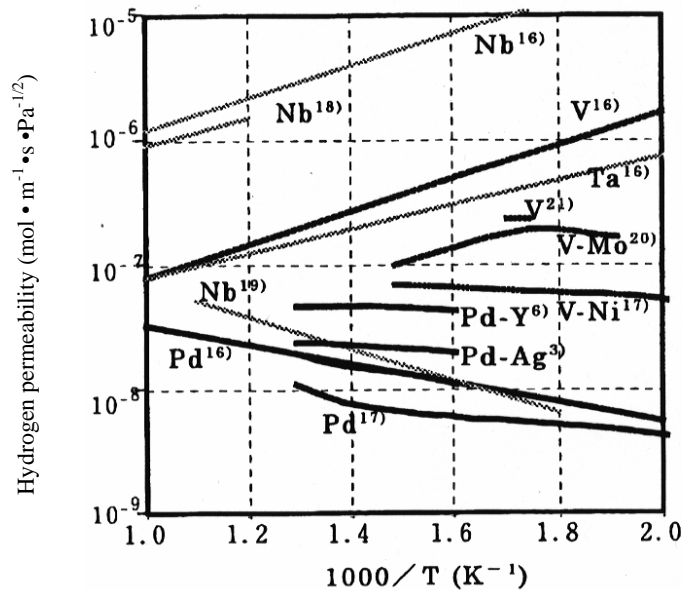
Advanced FR-MR plant concept is basically same as FR-MR. The separation performance of the membrane by non-Pd film is expected to be much better than by Pd film. (Figure 7)

The system diagram and performance is shown in Figure 5. In this case, the separation performance of the membrane is assumed 5 times of Pd film. The reactor outlet temperature is 600°C and the core temperature rise is 150°C. The reactor heat generation is 480 MWt, almost 2 times of FR-MR. The reformer size is expected to be same as FR-MR unit shown in Figure 6, but the hydrogen production by this is almost 200 000 Nm³/h by one unit, almost 2 times of FR-MR.

2) Advanced core design method

Conventional approach

Figure 7. Hydrogen permeability of 5a group alloys compared with PD alloys



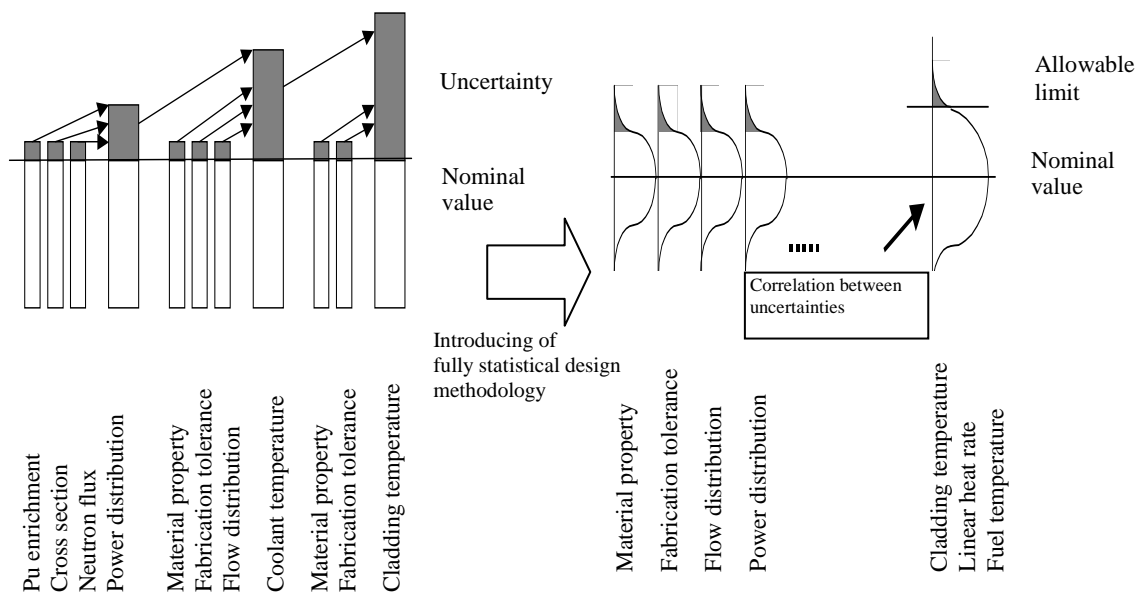
The design approaches adopted in the conventional FBR's had excess margins due to the lack of operating experiences.

In the thermal-hydraulic design semi-statistical method was commonly used where systematic uncertainties are treated cumulatively and statistical uncertainties are treated statistically. The sum of uncertainties has to be divided into two groups: statistical and non-statistical sub-factors because not all parameters are postulated to be actually statistical in nature. In the fuel design, uncertainties such as the fabrication tolerances and the temperature uncertainties were accumulated in the manner to evaluate the worst material damage.

Introducing fully statistical design methodology

The fully statistical design assumes that all uncertainties have statistical distributions and they are treated statistically introducing correlations between factors. The concept of the statistical method is illustrated in Figure 8 with comparison of the conventional method.

Figure 8. Illustration of the concept of statistical design method

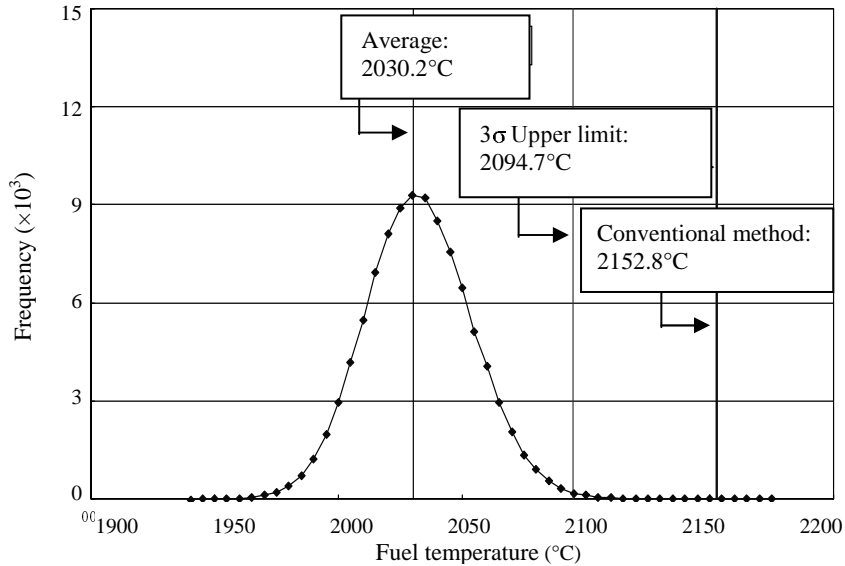


Examples of statistical analyses – Fuel temperature evaluation

The maximum fuel temperature of the highest heat rate fuel pin is evaluated statistically with the normal distributions of the fabrications (diameters of cladding and fuel pellet, density of the fuel, enrichment of plutonium, oxide to metal ratio).

The fuel temperature is expressed in Figure 8. The maximum temperature is evaluated to be 60°C less than the conventional approach.

Figure 9. Statistical evaluation of the maximum fuel temperature



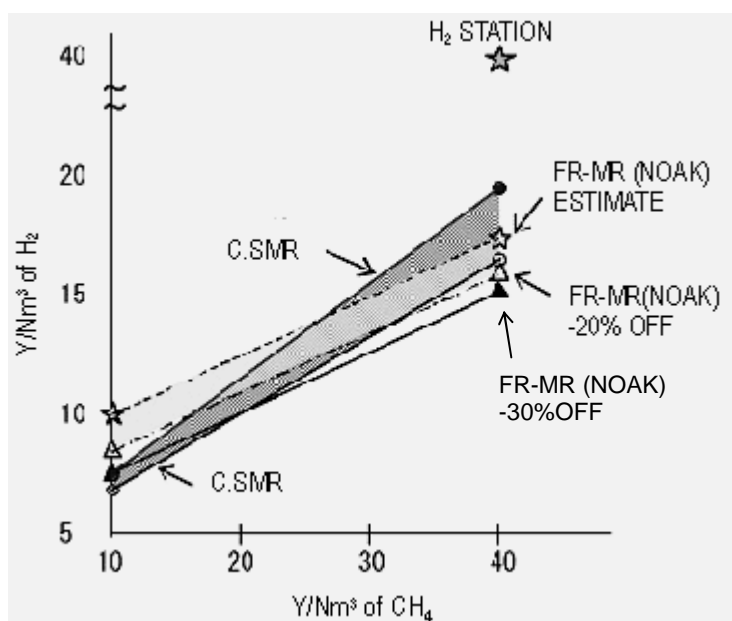
7. Preliminary economical assessment

The assumptions in this study are as follows:

- 1) The capital cost of the large-scale conventional SMR plant is extrapolated from a small-scale station.
- 2) The cost estimation is limited only to main facilities, not including the receiving facilities of CH₄ and the delivery facility of H₂.
- 3) The hydrogen cost is expected to decrease by improvement of performance of membrane and the NOAK.

The result is shown in Figure 10. In general, the hydrogen production cost strongly depends on the natural gas cost. In case of FR-MR, the high capital cost and the low running cost (better H₂ productivity) makes less sensitivity to the natural gas cost than the conventional SMR. And the Advanced FR-MR is a promising method to be competitive to the conventional SMR method.

Figure 10. Evaluation of H₂ cost vs. CH₄ cost



REFERENCES

- [1] Tashimo, M., M. Hori, K. Kobayashi "Concept of FR-MR", ICON-11-36321, 20-23 April 2003.
- [2] Yasuda, I., Y. Shirasaki, *et al.* "Development of Membrane Reformer for Hydrogen Production from Natural Gas", 22nd Hydrogen Energy System Society Symposium. 2002.12
- [3] Yasuda, I. *et al.*, "Development of Membrane Reformer for Hydrogen Production from Natural Gas", 14th World Hydrogen Energy Conference, 9-13 June 2002.

INTEGRATED HEAT BALANCE OF STAR-H2 SYSTEM FOR HYDROGEN PRODUCTION*

Anton Moiseyev
Texas A&M University

Diana T. Matonis
Argonne National Laboratory
9700 S. Cass Avenue
Argonne, Illinois 60532, USA

Abstract

The secure transportable autonomous reactor (STAR) hydrogen project is part of the US Department of Energy's (DOE's) Nuclear Energy Research Initiative (NERI) to develop Generation IV nuclear reactors that will supply high-temperature heat at over 800°C. The goal of NERI is to develop an economical, proliferation-resistant, sustainable, nuclear-based energy supply system based on a modular-sized fast reactor that is passively safe and cooled with heavy liquid metal. STAR-H2 consists of:

- a 400 MW_{Thermal} reactor with Pb as the primary coolant;
- exchange of primary Pb coolant against a salt heat transfer pipe;
- exchange of salt against steam;
- a combined thermochemical water-splitting cycle to generate hydrogen;
- a CO₂ Brayton cycle to generate electricity ($\eta = 44.4\%$); and
- an optional capability to produce potable water from brackish or salt water.

STAR-H2 is a hydrogen production plant which uses a STAR lead-cooled fast reactor with natural circulation for supplying the energy needed in a Ca-Br thermochemical cycle splitting water to produce hydrogen. The supercritical carbon dioxide Brayton cycle is used to produce electricity for running the pumps of the hydrogen production plant and water desalination plant. The excess heat at the bottom of the Brayton cycle is available for desalination of seawater to produce the fresh water for the Ca-Br cycle. We calculate the whole system heat balance, including calculated temperature and pressure distribution of the working fluids inside the reactor, the intermediate molten salt loop, the hydrogen production plant, the Brayton cycle, and the desalination plant. Our results show that 7 100 kg/hr of hydrogen can be produced with the integrated plant and a 400 MW_{Thermal} reactor.

* This manuscript has been created by the University of Chicago as Operator of Argonne National Laboratory ("Argonne") under Contract No. W-31-109-Eng-38 with the US Department of Energy. The US Government retains for itself, and others acting on behalf, a paid-up, nonexclusive, irrevocable worldwide license and said article to reproduce, prepare derivative works, distribute copies to the public, and perform publicly and display publicly, by or on behalf of the Government.

1. The integrated plant

The work was done as a joint effort between the authors, so that the heat inputs and outputs would be correct in all stages of the plant. Figure 1 illustrates the overall final integrated STAR-H2 plant scheme. It shows the relationships between all stages in the plant. The reactor produces heat from a nuclear reaction. A portion of this heat (about 1%) is removed by the RVACS; the other portion is delivered to the intermediate loop through the reactor heat exchanger. This heat is used to superheat the reagent steam and to maintain the required temperature at the hydrogen production plant reactors (beds R1-B3). Any excess heat from the reactor is also delivered to the S-CO₂ Brayton cycle, in addition to the heat released from beds R4-R5. The heat delivered to the Brayton cycle is divided into turbine work (which gives generator output with some losses), heat rejected and cooled, and the heat delivered to the desalination plant. In the desalination plant, the heat is divided between the brine boiler and the steam heater. Reagent steam from the steam heater at the bottom of the Brayton cycle, is additionally heated by the heat available from oxygen cooling (hydrogen production plant). A desalination bottoming cycle is used for the production of potable water for feedstock to hydrogen production and for revenue from potable water sales.

2. The nuclear reactor

As was previously described, the reactor is a secure transportable autonomous reactor (STAR). It is designed to operate for about 15 years at 400 MW_{Thermal}. [1] The lead-cooled fast reactor operates at low power density and achieves 100% natural circulation cooling; passive load following; passive safety performance; and a 15-year cassette reloading interval. The selected fuel is TRU-nitride – known to be compatible with Pb and expected to be pyro-recycleable and vibropac-remote-fabricable. Silicon carbide was selected as the cladding material, because of the high operational temperatures. This material is said to work with lead under temperatures up to 900°C [2]. Therefore, as a safety limit for the core integrity, the peak cladding temperature should not exceed 900°C under normal operations, either on full or reduced power level, or under accident conditions.

3. The hydrogen production plant

A chemical process simulation code, ASPEN[®], was used to evaluate the overall Ca-Br thermochemical water-splitting cycle. The corresponding process flow diagrams are shown in Figures 2 and 3. The ASPEN[®] chemical process simulation code is currently under license from AspenTech. Simulation efforts refined and optimised the hydrogen production cycle in the integrated process design. Information required for the simulation included the heat source temperature, pressure, and duty requirements, the heat carrier medium, the conditions and purity of the heat transfer medium to the reactor, as well as the data describing the fluid dynamics and reaction kinetics.

The primary Pb coolant from the Gen IV reactor transfers heat to the molten salt heat carrier at 800°C, which heats and maintains the 1 024 K temperature of the Ca-Br cycle first-stage reactors as shown in Figure 2. In the first stage reactors of the thermochemical cycle, the reagent steam feed reacts with CaBr₂ to form HBr gas. To dissociate the HBr gas to H₂ and Br₂, a “plasmatron” system is being investigated, as shown in Figure 3. This system employs plasma-chemical reactions and operates at low temperatures and pressures. The practical efficiency is 48% for the integrated STAR-H2 Ca-Br cycle as calculated from the detailed process flow diagrams. The heat and mass balance for the thermochemical cycle is the subject of a companion paper by Doctor, Matonis, and Wade that explores the Ca-Br system heat and material balance. [3]

4. Intermediate molten salt loop

Figure 4 illustrates the integrated plant with heat and mass balances. The intermediate loop serves to deliver the heat from the reactor to the hydrogen plant and to the Brayton cycle. The loop uses molten salt (Li_2BeF_4 -Flibe) as a working fluid. The intermediate loop consists of the reactor heat exchanger (RHX), where the heat is transferred from the reactor coolant to the molten salt; beds R1-B3 of the hydrogen production plant, where the heat is supplied to the reactors; steam superheater (SS), in which the reagent steam is heated up to required temperature; molten-salt-to- CO_2 heat exchanger to use remaining heat in the Brayton cycle; and pump to compensate the pressure losses in the loop. Since the beds R1-B3 and steam superheater both require high-temperature heat, the Flibe flow is divided into two sub-flows, one for the beds and one for the steam superheater. These flows merge together before MS- CO_2 heat exchanger.

For this RHX design, the average coolant temperature at the core outlet was calculated to be 793°C with an 826°C maximum value for the hot channel. The peak cladding temperatures are 836°C and 878°C for the average and hot channel, respectively. Figures 5 and 6 show that these peak cladding temperatures are both below the set safety limit of 900°C^2 for all included operation variations.

5. Supercritical carbon dioxide Brayton cycle

The Brayton cycle is used to convert the heat available from the intermediate loop and from the last stage of the hydrogen plant (beds R4-R5) into electricity [4, 5, 6]. Carbon dioxide is heated in the beds R4-R5 in the thermochemical cycle and in the MS- CO_2 heat exchanger as shown in Figure 4. It is then expanded in a turbine to produce electricity after the (high-temperature and low-temperature recuperators – HTR and LTR, respectively), and enters the desalination plant.

In the desalination plant, the CO_2 is divided into two flows; one goes to the brine boiler, where the brine is boiled and steam is produced, the other flow goes through a steam superheater, where the steam produced in the brine boiler is superheated as much as possible. At this point, the two flows merge. After the desalination plant, the CO_2 flow is divided again, as follows:

- 1) One flow goes to the cooler, where the CO_2 is cooled down to almost the critical pressure and temperature. This heats the seawater at compressor #1 up to about boiling temperature. From there, the flow returns to the low-temperature recuperator.
- 2) The other CO_2 flow goes through the compressor #2 and rejoins the first flow after the low-temperature recuperator.
- 3) The process is now repeated with the CO_2 flow being heated up in the high-temperature recuperator and returning to beds R4-R5 for additional heating.

The Brayton cycle operates in the pressure and temperature range from about the critical point ($p_{\text{crit.}}=7.377\text{ MPa}$, $T_{\text{crit.}}=30.98^\circ\text{C}$) to 20 MPa and 650°C . The cycle efficiency is about 44%. The system is designed to generate enough electricity to run the plasmatron and pumps in the hydrogen production plant, intermediate loop, and desalination plant.

6. Desalination plant

As mentioned above, the desalination plant for reagent steam production shown in Figure 3 consists of a brine boiler and steam superheater. The seawater is heated in the cooler of the Brayton

cycle before entering the brine boiler. All heat exchangers use the heat from the bottom of the Brayton cycle.

The Brayton cycle was optimised to assure that the desalination plant produces enough steam for the hydrogen production plant.

7. Detailed system heat balance

The detailed heat and mass balance diagram is shown in Figure 4. It begins with the primary Pb coolant from the Gen-4 reactor transferring heat to a Salt heat carrier. The molten salt mass flow rate and its maximum temperature are selected to simultaneously satisfy the heat removal requirements for maintaining reactor temperatures constant, reactors R1 through R4, and heating carbon dioxide in the Brayton cycle and the inlet steam in Ca-Br cycle. The CO₂ temperature and mass flow rate are calculated after heat exchange with reactors R4 and R5. Then the salt-CO₂ heat exchanger calculations are performed and outlet temperatures for both fluids are calculated. If the outlet temperature of the molten salt differs from the optimum temperature, 700.7°C, a new value for CO₂ mass flow rate is selected to satisfy the remainder of the Brayton Cycle. This ensures the CO₂ mass flow rate is uniquely defined by this temperature.

At the same time, the CO₂ temperature, after heat exchange with beds R4 and R5, cannot exceed the temperature at which the heat is supplied. Table 1 reveals how much heat can be supplied if the bromination stage of the thermochemical is upset by turnaround or some other unforeseen plant incident. The CO₂ mass flow rate through beds R4 and R5 is adjusted accordingly, and if the mass flow rate is increased, any excess CO₂ flow would bypass the molten salt-CO₂ heat exchanger to maintain the final optimum temperature of the salt.

Note that heat needed by hydrolysis was also varied in Table 2, by decreasing the amount of water vapour available for reaction, thus reducing the amount of heat recovered in the bromination stage of the hydrogen plant cycle. The CO₂ temperature after the molten salt-CO₂ heat exchanger (after mixing with bypass flow, if any) defines the maximum temperature for the Brayton cycle. The Brayton cycle calculations give the CO₂ temperature before beds R4 and R5. On the bottom of the Brayton cycle, the CO₂ temperature is adjusted by selecting the size of the low-temperature (and high-temperature, if needed) recuperator. The flow split between the brine boiler and steam heater is proportional to the heat required for those components.

A FORTRAN code was developed to perform these heat balance calculations. It consists of three big modules – for reactor, intermediate loop, and Brayton cycle. The calculations include temperature and pressure changes, as well as a heat balance inside each subsystem, and the two smaller modules – for RHX and MS-CO₂ heat exchanger – which serve to connect the subsystems.

The intermediate loop module calculates the Flibe temperatures and mass flow rate for given reactor power, heat requirements from the hydrogen production plant, reagent steam mass flow rate, its inlet and required outlet temperature, and minimum temperature at which beds should be maintained. The heat duty for the beds itself, together with the amount of heat available from beds R4-R5, is calculated using ASPEN software for a given steam mass flow rate. The reactor module calculates the temperatures inside the reactor such that the Flibe temperatures at RHX inlet and outlet match those calculated by the intermediate loop module.

The Brayton cycle module calculates the net amount of electricity produced by the Brayton cycle and the amount of steam produced at the desalination plant at the bottom of the cycle. The net

electricity is the total electricity produced minus the requirements for the compressors and Flibe circulating pump, i.e. the amount available for the hydrogen production plant and desalination plant.

The reagent steam mass flow rate, and therefore the hydrogen production rate, is selected such that the amount of net electricity produced by the Brayton cycle would be enough to run the plasmatron and pumps for the hydrogen production plant. It is estimated that the plasmatron requires about $0.47\text{MW}_{\text{Electrical}}$ for every $1\text{MW}_{\text{Thermal}}$ supplied to the beds R1-B3, and the pumps for the hydrogen production plant require about 10% of the electricity needed for plasmatron. The excess electricity is used to run pumps for the desalination plant.

8. Conclusion

We calculated the heat system balance for the STAR-H2 system, which includes a lead-cooled fast reactor with natural circulation, an intermediate molten salt loop, a hydrogen production plant, a supercritical carbon dioxide Brayton cycle for electricity production, and a water desalination plant.

The hydrogen production rate was selected such that the electricity produced by the Brayton cycle is just enough to run the plasmatron and pumps for the hydrogen production plant. For the $400\text{MW}_{\text{Thermal}}$ reactor power, the hydrogen production rate is 7 100 kg/hr. The temperatures of working fluids, reactor coolant, cladding, and fuel were also calculated. We have shown that these temperatures are below the safety limits.

Acknowledgments

This effort was sponsored by the US Department of Energy's (DOE's) Nuclear Energy Research Initiative at Argonne National Laboratory under Contract No. W-31-109-Eng-38 with DOE.

References

- [1] Wade, David C., *et al.*, "STAR-H2: A 400 MWth Lead-Cooled, Long Refueling Interval Reactor for Hydrogen Production", ICONE11, *Proceedings of ICONE 11, Eleventh International Conference on Nuclear Engineering*, Tokyo, 20-23 April 2003.
- [2] Zinkle, S.J. and N.M. Ghoniem, "Operating temperature windows for fusion reactor structural materials", *Fusion Engineering and Design* **51–52**, 55–71 (2000).
- [3] Doctor, R., D. Matonis and D. Wade, "Hydrogen Generation Using a Calcium-Bromine Thermochemical Water-Splitting Cycle", OECD meeting, Argonne, 2-3 Oct. 2003.
- [4] Moisseytsev, A.V., J.J. Sienicki and D.C. Wade, "Cycle Analysis of Supercritical CO₂ Gas Turbine Brayton Cycle Power Conversion System for Liquid Metal-Cooled Fast Reactors", ICONE11-36023, *Proceedings of ICONE 11, Eleventh International Conference on Nuclear Engineering*, Tokyo, 20-23 April 2003.
- [5] Dostal, V., P. Hejzlar, M.J. Driscoll and N.E. Todreas, "A Supercritical CO₂ Brayton Cycle for Advanced Reactor Applications", *Trans. Am. Nucl. Soc.*, **85** (2001).
- [6] Dostal, V., M.J. Driscoll, P. Hejzlar and N.E. Todreas, "A Supercritical CO₂ Gas Turbine Power Cycle for Next-Generation Nuclear Reactors", ICONE10-22192, *Proceedings of ICONE 10, Tenth International Conference on Nuclear Engineering*, Arlington, 14-18 April, 2002.

Figure 1. STAR-H2 heat and electricity balance

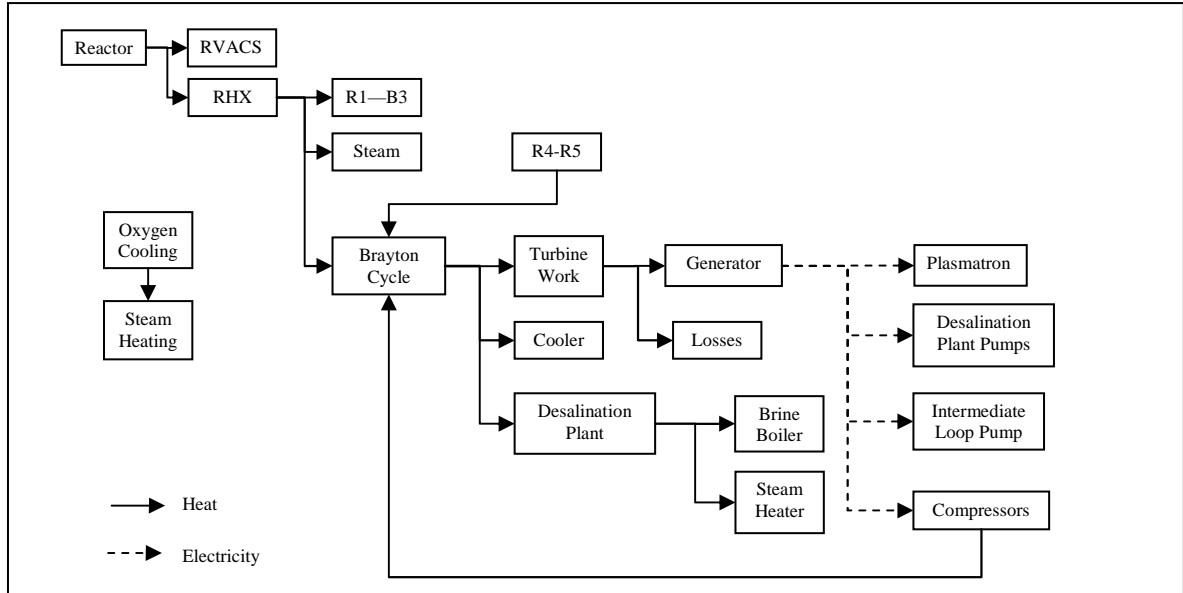


Figure 2. Process flow diagram of stage 1 – steam to HBr and stage 3 – oxygen liberation

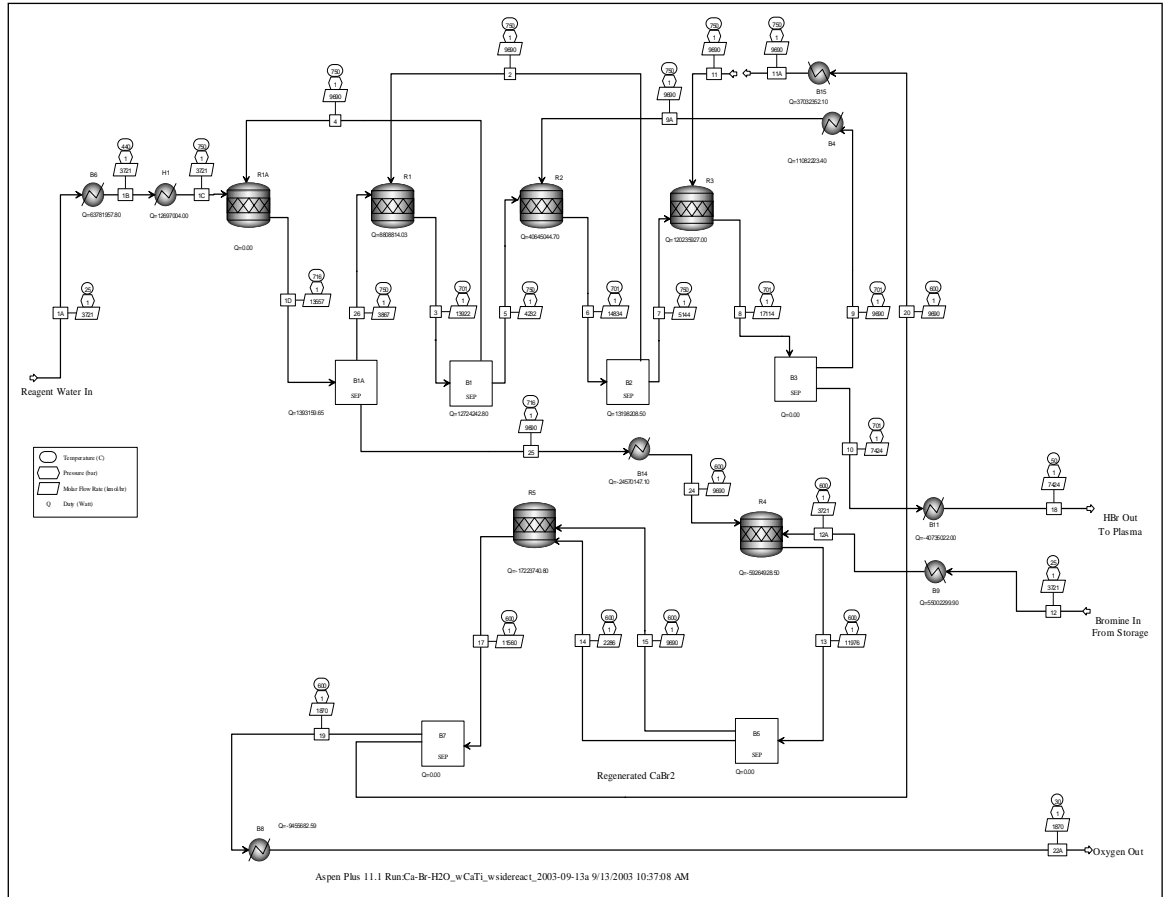


Figure 3. Process flow diagram of stage 2 – Plasmatron production of H₂ with pressure swing adsorption

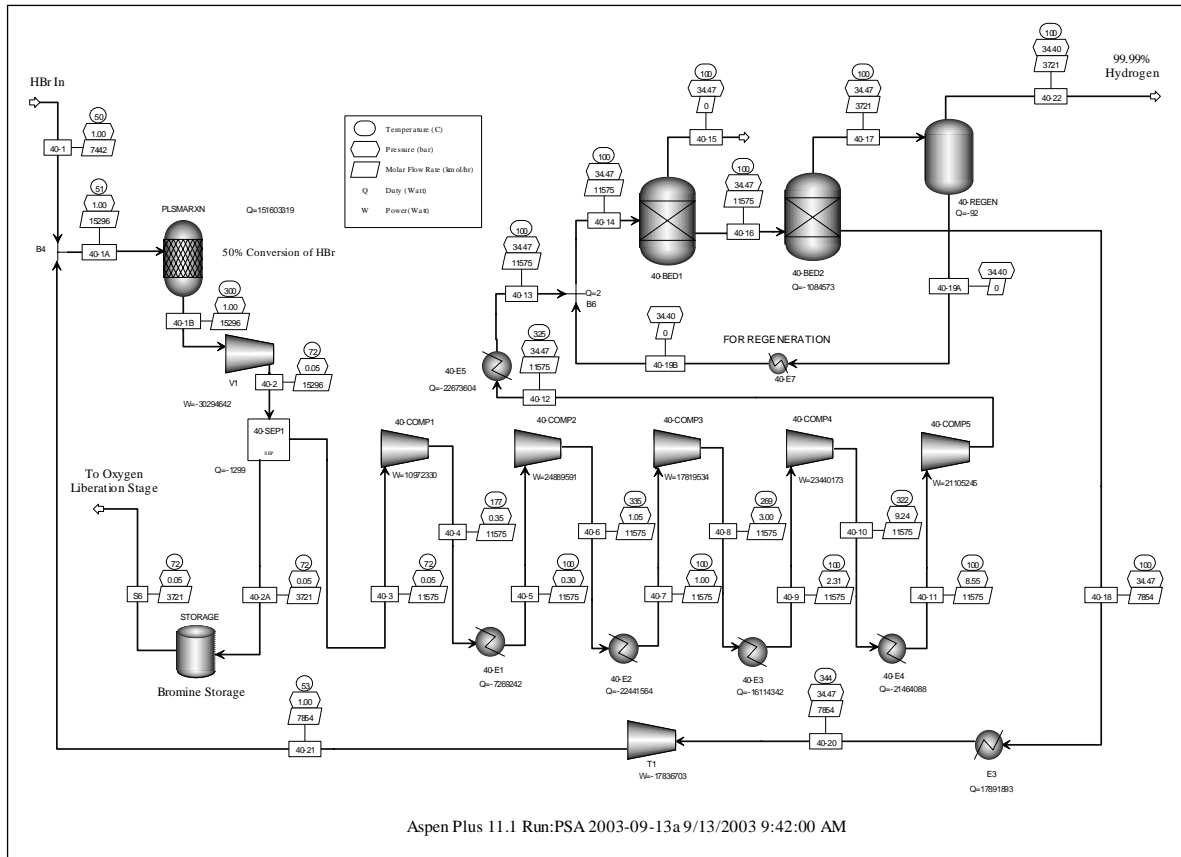


Figure 4. Heat balance of STAR-H2 system

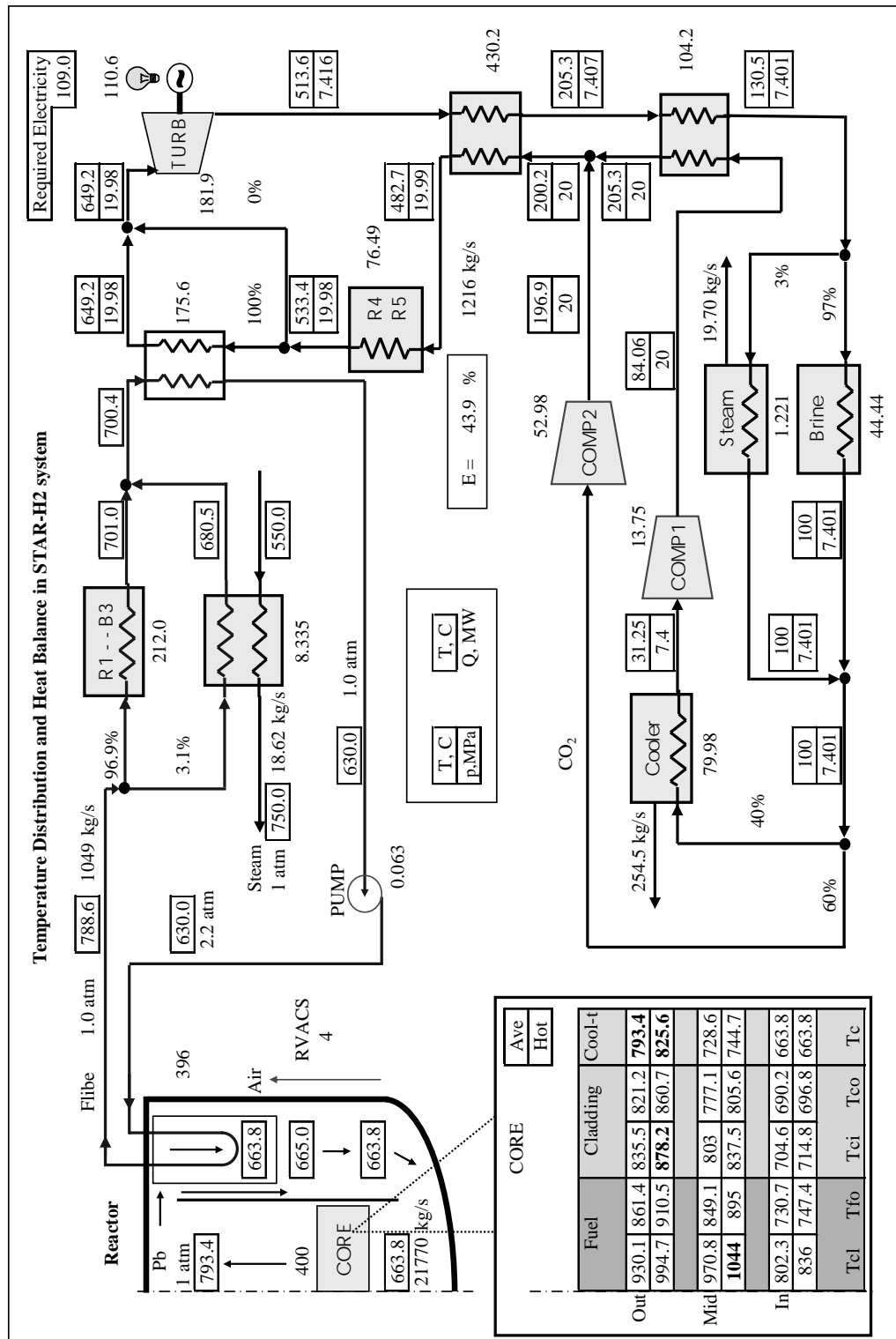


Figure 5. STAR-H2 load follow inlet steam flow variation

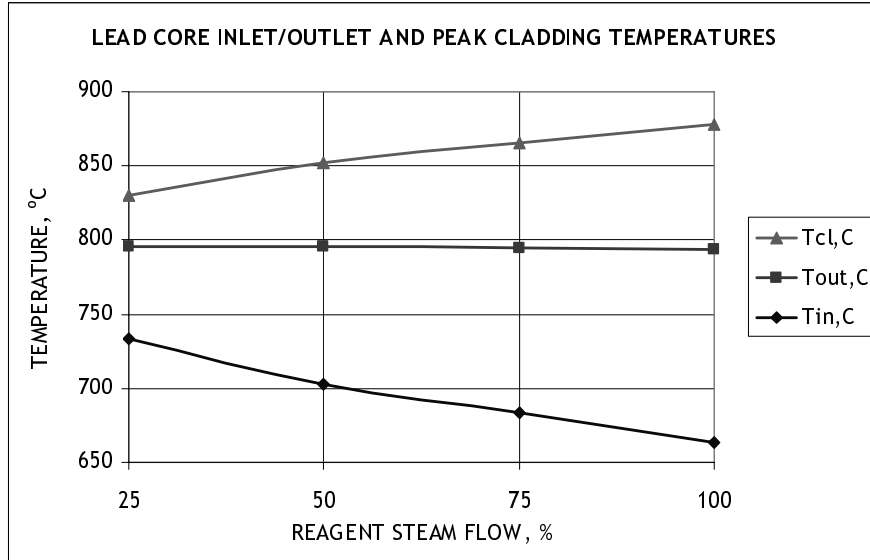


Figure 6. STAR-H2 load follow with reduced bromine flow

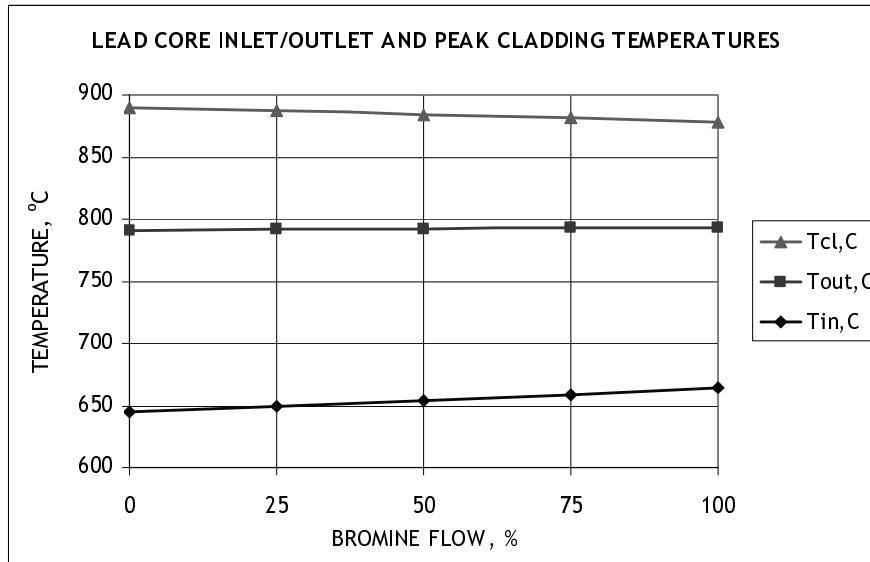


Table 1. Thermal energy analysis of Ca-Br cycle if the inlet bromine amount is varied

Inlet water molar flowrate, kmol/hr:	3 721	3 721	3 721	3 721
Inlet bromine molar flowrate, kmol/hr:	3 721	2 790.75	1 860	930.25
Process/reactor	Energy, MW*	Energy, MW	Energy, MW	Energy, MW
Heat water to 750°C	76.5	76.5	76.5	76.5
Bed preheat	37.0	37.0	37.0	37.0
R1A	0.0	0.0	0.0	0.0
R1	8.8	8.8	8.8	8.8
B1A+B1	14.9	14.9	14.9	14.9
R2	40.6	40.6	40.6	40.6
B2	13.2	13.2	13.2	13.2
R3	120.0	120.0	120.0	120.0
B3	0.2	0.2	0.2	0.2
B4	11.1	11.1	11.1	11.1
Heat input for hydrolysis without integration	322.3	322.3	322.3	322.3
Subtract steam generation – Brayton	-76.5	-76.5	-76.5	-76.5
Total heat with integration	245.8	245.8	245.8	245.8
Heat bromine	55.0	41.3	27.5	13.8
Heat bromine with B11 reject	-40.4	-40.4	-40.4	-40.4
Heat bromine with B4 reject	-24.6	-24.6	-24.6	-24.6
Excess heat	-9.9	-23.7	-37.5	-51.2
Heat rejection				
R4	-59.3	-57.6	-38.4	-19.2
R5	-17.2	0.0	0.0	0.0
Total heat rejection => Brayton cycle	-76.5	-57.6	-38.4	-19.2
Compression for PSA	139.5	139.5	139.5	139.5
Thermal energy required for plasmatron	135.2	135.2	135.2	135.2
Thermal energy form Brayton cycle	-160.23	-160.23	-160.23	-160.23
Total thermal heat input for entire process without subtracting thermal energy from Brayton cycle	520.5			
Cycle efficiency taken at lower hydrogen heating valve of 250 MMW	48%			

Table 2. Thermal energy analysis of Ca-Br cycle if the reagent steam flow is varied

Inlet water molar flowrate, kmol/hr:	3 721	2 790.75	1 860	930.25
Inlet bromine molar flowrate, kmol/hr:	3 721	3721	3 721	3 721
	Energy, MW*	Energy, MW	Energy, MW	Energy, MW
Process/reactor				
Heat water to 750°C	76.5	57.4	38.2	19.1
Bed preheat	37.0	37.0	37.0	37.0
R1A	0.0	76.5	96.9	42.4
R1	8.8	61.4	0.0	0.0
B1A+B1	14.9	16.1	15.4	13.8
R2	40.6	0.0	0.0	0.0
B2	13.2	14.6	13.8	13.0
R3	120.0	0.0	0.0	0.0
B3	0.2	0.2	0.2	0.2
B4	11.1	11.1	11.1	11.1
Heat input for hydrolysis without integration	322.3	168.7	126.3	69.4
Subtract steam generation – Brayton	-76.5	-54.4	-38.2	-19.1
Total heat with integration	245.8	111.4	88.1	50.2
Heat bromine	55.0	55.0	55.0	55.0
Heat bromine with B11 reject	-40.4	-32.21	-18.1	-7.83
Heat bromine with B4 reject	-24.6	-24.57	-24.57	-24.57
Excess heat	-9.9	-1.78	12.34	22.60
Heat rejection				
R4	-59.3	-46.1	-32.6	-19.2
R5	-17.2	-13.4	-9.5	-5.6
Total heat rejection => Brayton cycle	-76.5	-59.5	-42.1	-24.7
Compression for PSA	139.5	104.6	69.8	34.9
Thermal energy required for plasmatron	135.2	101.4	67.6	33.8
Thermal energy form Brayton cycle	-160.23	-120.1725	-80.115	-40.0575
Total thermal heat input for entire process without subtracting thermal energy from Brayton cycle	520.5			
Cycle efficiency taken at lower hydrogen heating valve of 250 MMW	48%			

**ADVANCED CSiC COMPOSITES FOR HIGH-TEMPERATURE NUCLEAR HEAT
TRANSPORT WITH HELIUM, MOLTEN SALTS, AND SULPHUR-IODINE
THERMOCHEMICAL HYDROGEN PROCESS FLUIDS**

Per F. Peterson

University of California, Berkeley
4153 Etcheverry, Berkeley, CA 94720-1730

Charles W. Forsberg

Oak Ridge National Laboratory
P.O. Box 2008; Oak Ridge, TN 37830-6179

Paul S. Pickard

Sandia National Laboratories
P.O. Box 5800, Albuquerque, NM 87185

Abstract

This paper discusses the use of liquid-silicon-impregnated (LSI) carbon-carbon composites for the development of compact and inexpensive heat exchangers, piping, vessels and pumps capable of operating in the temperature range of 800 to 1 100°C with high-pressure helium, molten fluoride salts, and process fluids for sulfur-iodine thermochemical hydrogen production. LSI composites have several potentially attractive features, including ability to maintain nearly full mechanical strength to temperatures approaching 1 400°C, inexpensive and commercially available fabrication materials, and the capability for simple forming, machining and joining of carbon-carbon performs, which permits the fabrication of highly complex component geometries. In the near term, these materials may prove to be attractive for use with a molten-salt intermediate loop for the demonstration of hydrogen production with a gas-cooled high temperature reactor. In the longer term, these materials could be attractive for use with the molten-salt cooled advanced high temperature reactor, molten salt reactors, and fusion power plants.

1. LSI composites introduction

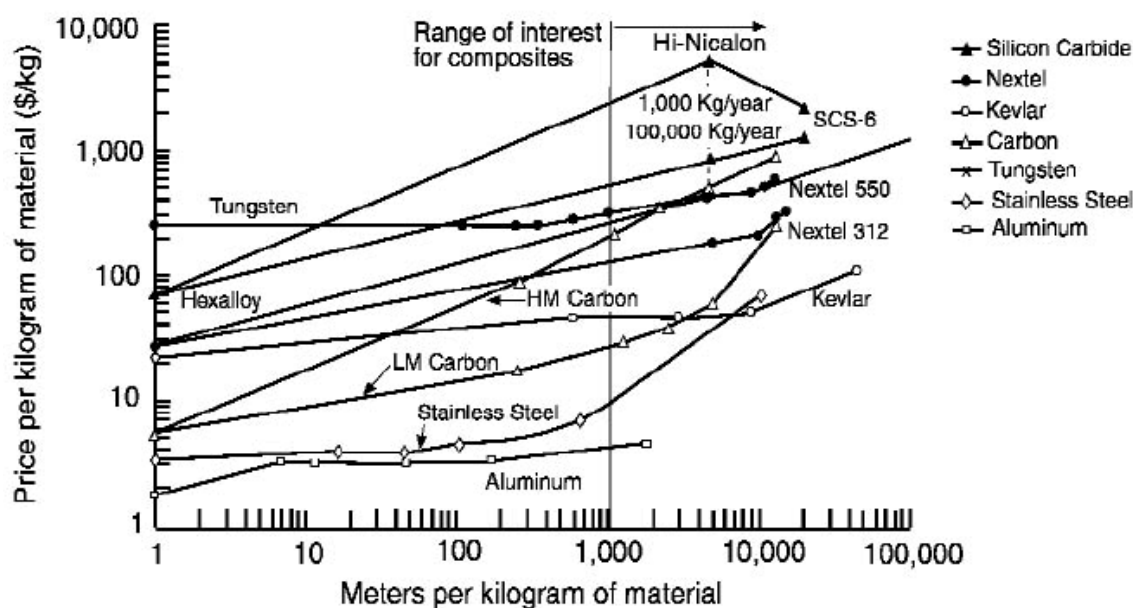
Liquid silicon infiltrated (LSI) carbon-carbon composites provide a potentially attractive construction material for high-temperature heat exchangers, piping, pumps, and vessels for nuclear applications, due to their ability to maintain nearly full mechanical strength to high temperatures (up to 1 400°C), the simplicity of their fabrication, their low residual porosity, and their low cost. LSI composites are fabricated from low-modulus carbon fiber that can be purchased in bulk at around \$20 per kilogram, and at lower costs for chopped carbon fibers (Figure 1). The typical steps in fabricating LSI composites include:

- Green manufacturing of C/C fiber/phenolic resin performs by die pressing, including formation of flow channels in plates if desired;
- Vacuum carbonization and graphitization (900 to 2 100°C);
- Greenbody milling (conventional machine tools);
- Vacuum plasma spray (VPS) application of SiC, corderite, or other surface coating if desired;
- Joining of multiple parts using phenolic adhesives;
- Chemical vapour infiltration (CVI) coating of flow channel surfaces with carbon if desired;
- Liquid silicon capillary infiltration (1600°C vacuum or inert atmosphere);
- Chemical vapour deposition (CVD) coating of flow channel surfaces with carbon if desired;
- Net shape part results with very small dimensional changes from green part (<1%).

LSI C/C-SiC materials have desirable high-temperature properties [8]:

- Composition SiC: Si: C 30-79%: 1-30%: 10-40%;
- Low specific density (2.6-2.7 g/cm³);
- Tunable stiffness (240-260 GPa) and strength (50-210 MPa);
- Low coefficient of thermal expansion (20°C-1 000°C: 1.8-4.1x10⁻⁶ K⁻¹);
- High thermal conductivity and diffusion (~ 20-135 W/mK);
- High temperature resistance (~ 2 100°C, Air).

Figure 1. Cost of bulk fibre materials as a function of fibre length [1]



Better properties, particularly fracture toughness, can be obtained with carbon or SiC fiber composites with chemical vapour infiltration and other methods of fabrication. LSI composites also are not expected to perform well under neutron irradiation. However, the low cost and simple fabrication and joining methods that can be performed with LSI C/C-SiC composites, combined with the excellent high temperature properties, make them interesting candidates for heat exchanger, centrifugal pump, and other flow-loop components.

Chopped carbon fibre with phenolic resin matrix material can be readily formed by pressing with dies, and can be machined using standard milling tools and then assembled into complex parts, with examples of typical LSI parts now being manufactured shown in Figure 2. In the United States, centrifugal pump impellers and casings are now routinely machined from carbon-fiber reinforced phenolic resin preforms, as shown in Figure 3, a machining process that could be extended to the machining of carbon/carbon preform materials prior to LSI processing for use at high temperatures.

The German Aerospace Research Establishment DLR is currently working to develop high-temperature LSI composite heat exchangers for use for indirect gas power cycles with heat from high temperature (950°C to 1 200°C) moist flue gases, under the HITHEX project funded by the European Union. This work has successfully developed coating methods capable of resisting oxidation damage in moist air in this temperature range, and is developing methods to reduce gas permeation for high-pressure gas contained inside the heat exchanger. Figure 4 shows a heat exchanger developed under the HITHEX project.

Figure 2. Typical C/C-SiC parts (disc brakes, rocket nozzles, telescope mirrors, etc.) fabricated by the LSI process using random oriented chopped C/C felt (BPM/IABG)

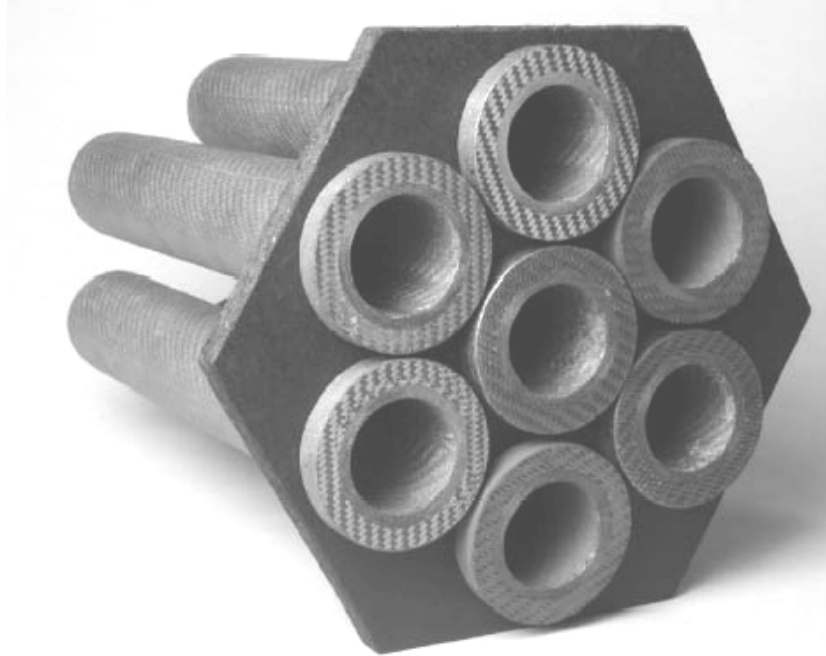


Figure 3. Centrifugal pump components fabricated by numerically controlled machining of carbon-fibre reinforced phenolic resin matrix perform material



www.simsite.com

Figure 4. LSI composite heat exchanger with 0.3-m long tubes being developed for high-temperature (950-1 200°C) heat recovery from moist flue gas to indirect high-pressure gas power cycles under the EU HITHEX project [2]



2. Approaches to LSI heat exchanger fabrication

Several applications, shown in Table 1, would benefit from improved high temperature heat exchangers with compatibility with high-pressure helium, molten fluoride salts, and sulfur-iodine thermochemical hydrogen process fluids. This section outlines potential approaches to the fabrication of compact LSI C/C-SiC composite heat exchangers capable of operating with these fluids, that could have great value for thermochemical production of nuclear hydrogen with the sulfur-iodine process, for molten salt reactors for waste transmutation, and for use for components in fusion blanket systems using molten salts as coolants and neutron shielding media (e.g. heat exchangers to transfer heat from molten salts to power-cycle helium).

Compact plate-type heat exchangers, like the example shown in Figure 5, provide very high surface area to volume ratios and very small fluid inventories. Methods currently exist that could permit the fabrication of similar high-temperature heat exchangers using green carbon/carbon plates a few to several millimetres thick, fabricated from chopped carbon fibre preform material. The flow channels of the resulting LSI C/C-SiC heat exchangers would look like those shown in Figure 6.

Table 1. Applications of interest for LSI C/C-SiC heat exchangers

Application	Compatibility requirements		
	Molten salt	High-pressure helium	S-I process fluids
Intermediate molten salt loop for near-term nuclear hydrogen	×	×	×
AHTR (hydrogen production)	×		×
AHTR (electricity production)	×	×	
Molten salt reactor	×	×	
Fusion chamber coolant (electricity production)	×	×	

Each of the individual processes required to fabricate compact LSI C/C-SiC heat exchangers has been demonstrated, although, as yet, such heat exchangers have not been fabricated. The first operation involves fabrication of the green plate material. One side of each plate is die embossed, or milled, to provide appropriate flow channels, leaving behind fins or ribs that would provide enhanced heat transfer, as well as the mechanical connection to the smooth side of the next plate. Offset strip fins are shown in Figure 6. Offset fins provide high mechanical strength as well as heat transfer enhancement.

For the green carbon-carbon material, milling can be performed readily with standard numerically controlled milling machines, as shown in Figure 7. Alternatively, plates can be molded with the flow channels, as has been demonstrated for carbon-carbon composite plates fabricated at Oak Ridge National Laboratory for fuel cells, shown in Figure 8.

Processes for joining LSI materials are well established. Phenolic resin glues are used to join green parts, as shown in Figure 9. Subsequently, when LSI is performed the joint is reaction bonded, with the joint strength being roughly equal to the bulk strength [5].

For assembly, the ends of the fins and other remaining unmachined surfaces of around the machined flow channels would be coated with phenolic adhesive, the plate stack assembled, header pipes bonded and reinforced, and the resulting monolith pyrolysed under compression. Then liquid silicon would be infiltrated to reaction-bond the plates and headers together, forming a compact heat exchanger monolith.

Figure 5. Typical flow configuration for a compact brazed plate heat exchanger

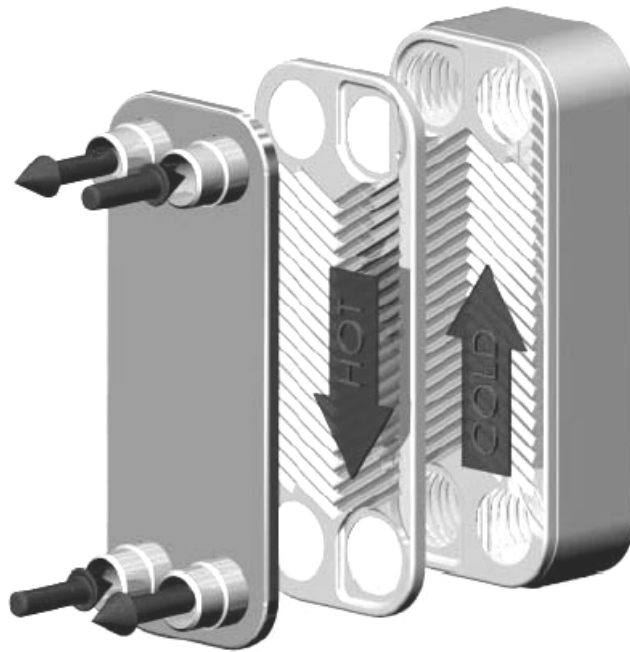
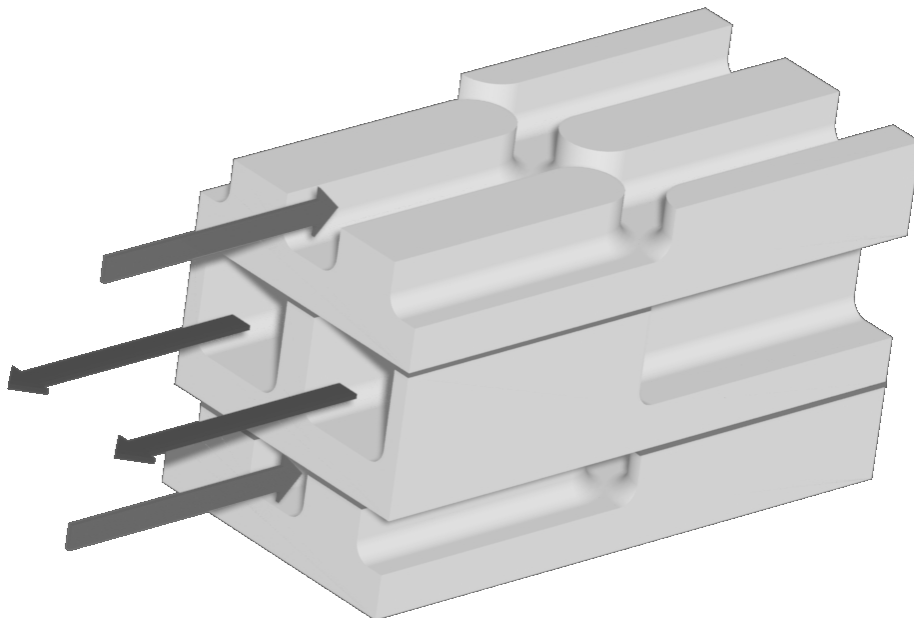


Figure 6. Cut-away through a plate showing alternating molten salt (red) and helium (blue) flow channels. Dark bands at the top of each fin indicate the location of reaction-bonded joints between each plate

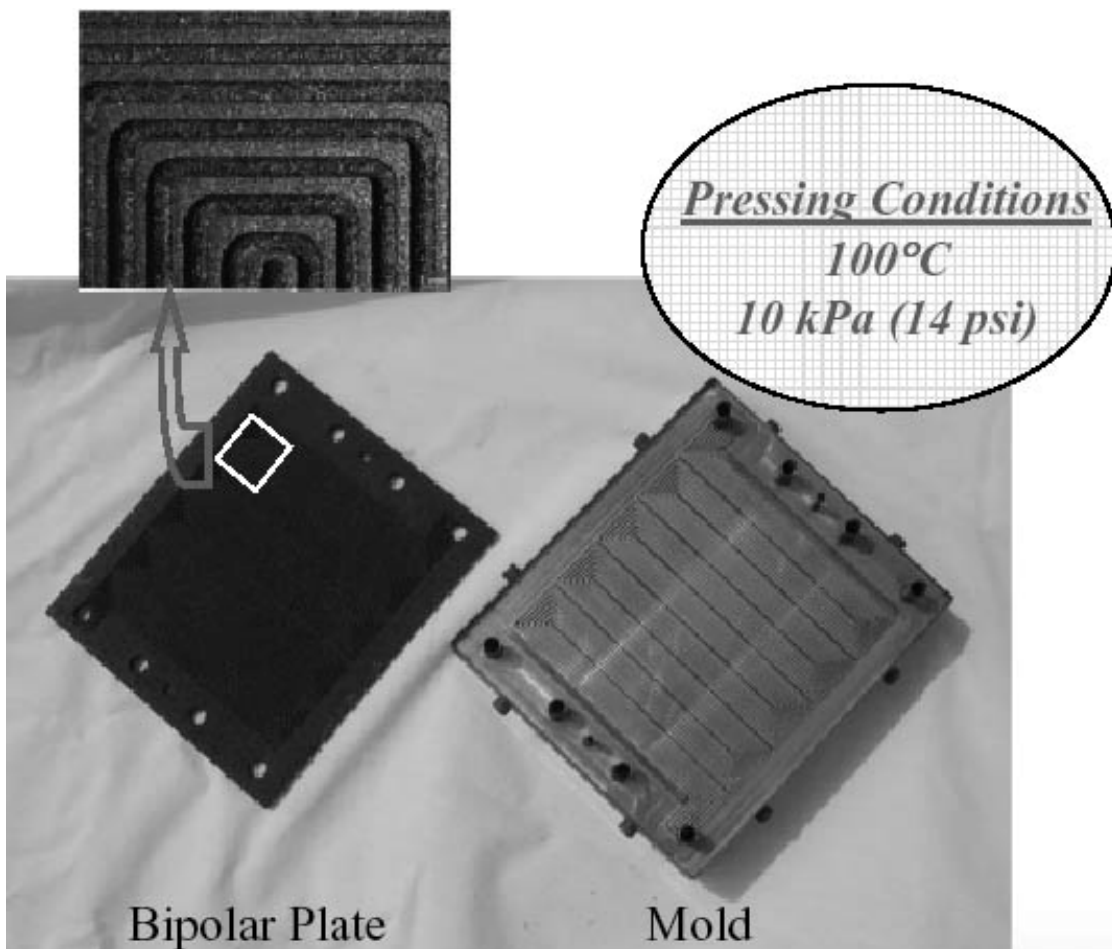


(Credit: R. Abbott, LLNL)

Figure 7. Photos of numerically-controlled milling being performed on carbon-carbon green-body material [5]



Figure 8. Pressed plate of short-fibre carbon-carbon composites showing the fabrication of flow channels using molds, for application to fuel cells [6]



(see also: <http://www.pnl.gov/microcats/ottreview/ottmeeting/14-Besman.pdf>)

Figure 9. An example of a C/C-SiC joint before and after LSI [5]

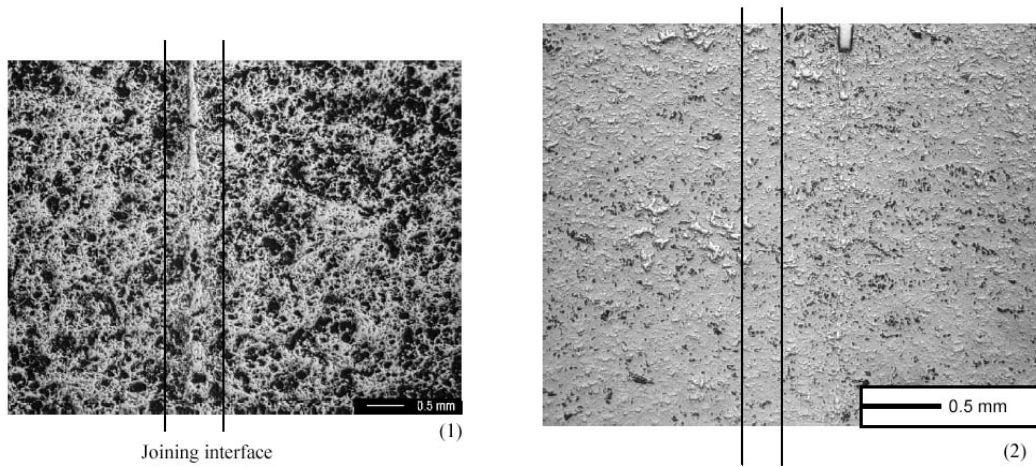
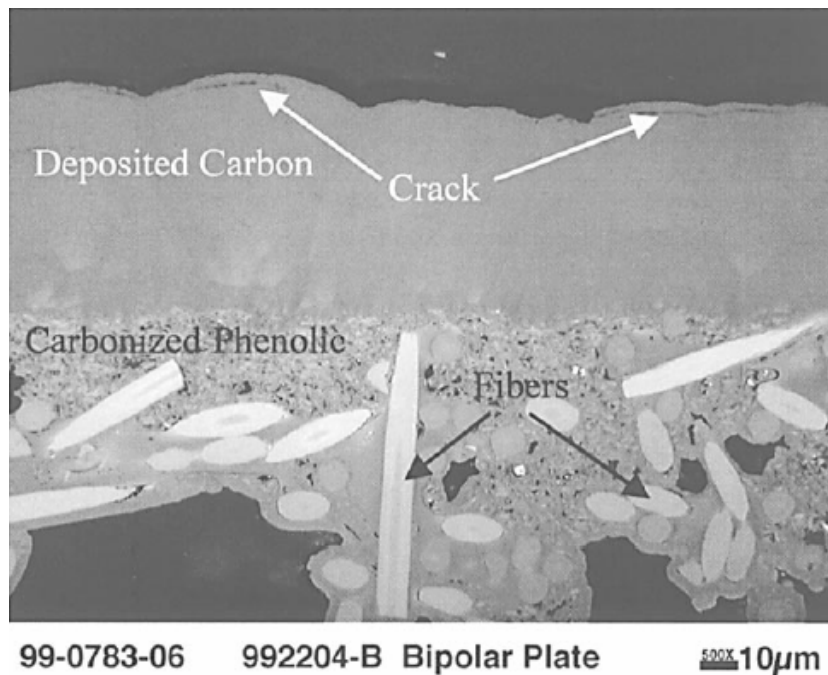


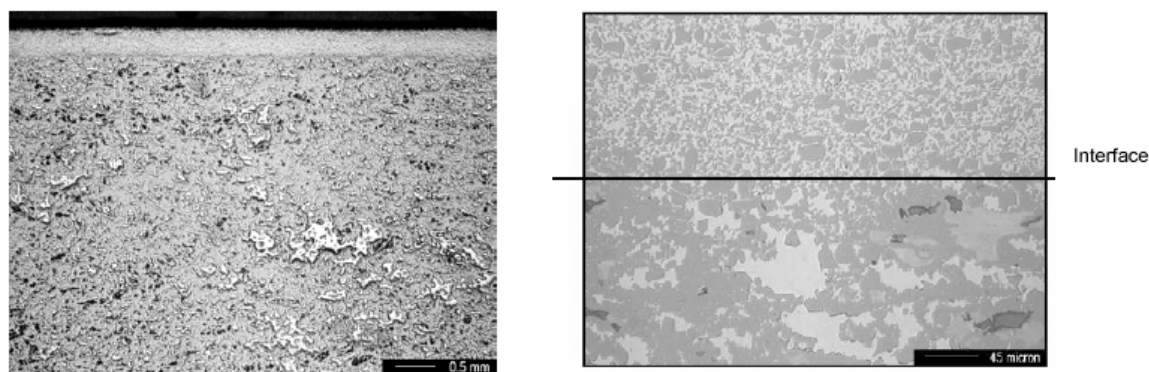
Figure 10. Photo of CVI-deposited carbon layer on a carbon-carbon composite plate [6]



Optionally, surfaces to be exposed to molten salts could be coated with carbon using chemical vapor infiltration (CVI) or chemical vapor deposition (CVD). Such methods have been developed at ORNL for coating carbon/carbon composite plates for fuel cells [6]. Figure 10 shows a carbon-carbon composite plate coated at ORNL using the CVI method. Methane, potentially with a carrier gas like argon, flows at low pressure (~8 kPa) between the plates at temperatures around 1 500°C and deposits a graphitic carbon layer with a preferred crystallographic orientation with the *c* direction of the hexagonal structure normal to the deposition surface. The basal planes then lie parallel to the surface, so that cracks are more likely directed along the surface rather than through the thickness.

From the perspective of protecting the substrate material from the molten salt, some porosity of the carbon layer could be acceptable, as is found for nuclear graphites, where DeVan et al. [7] have noted, “Completely sealing these pores [in graphite] is impractical, the material will simply ‘blow-up’ due to internal pressure developed during heat treatment”. However, because the molten salts are non-wetting to graphite and possess a high surface tension, it is only necessary to reduce the entrance pore diameter to ≤ 1 micron to prevent salt intrusion.

Figure 12. Cross-section through a silicon carbide cladding system developed for optical mirror surfaces on LSI composites [5]



ORNL also subjected samples treated by CVI of carbon to 100 MPa stresses in bi-directional bending of plates [6]. These samples were then tested for hermeticity by pressurizing one side with 206 kPa of hydrogen and measuring the through-thickness gas leakage rate, and it was found that excellent permeation resistance could be achieved. Figure 8 shows schematically how the CVI coating system configuration used by Besmann et al. [6] could be adapted to coating the internal flow channels of a small test article for studying LSI heat exchanger helium leakage resistance under prototypical pressure loading and thermal conditions.

To further reduce helium permeation through the plates, and to control tritium permeation as well, the flat side of each plate could receive an additional coating or cladding. One possible coating system would use a slurry consisting of primarily of small silicon carbide particles to form a surface layer. Figure 12 shows a 0.3-mm thick example of this type of silicon-carbide coating that has been developed to provide high-precision (<2 nm RMS) polished surfaces on LSI composites for use in mirrors. In the case shown in Figure 11, the coating system is applied after the substrate structure has been infiltrated with liquid silicon and rough ground.

Figure 13. Schematic of potential compact C/C-SiC heat exchanger channels and fins, showing key dimensions. For the figure shown, the fins occupy 25% of the cross-sectional area of the plate

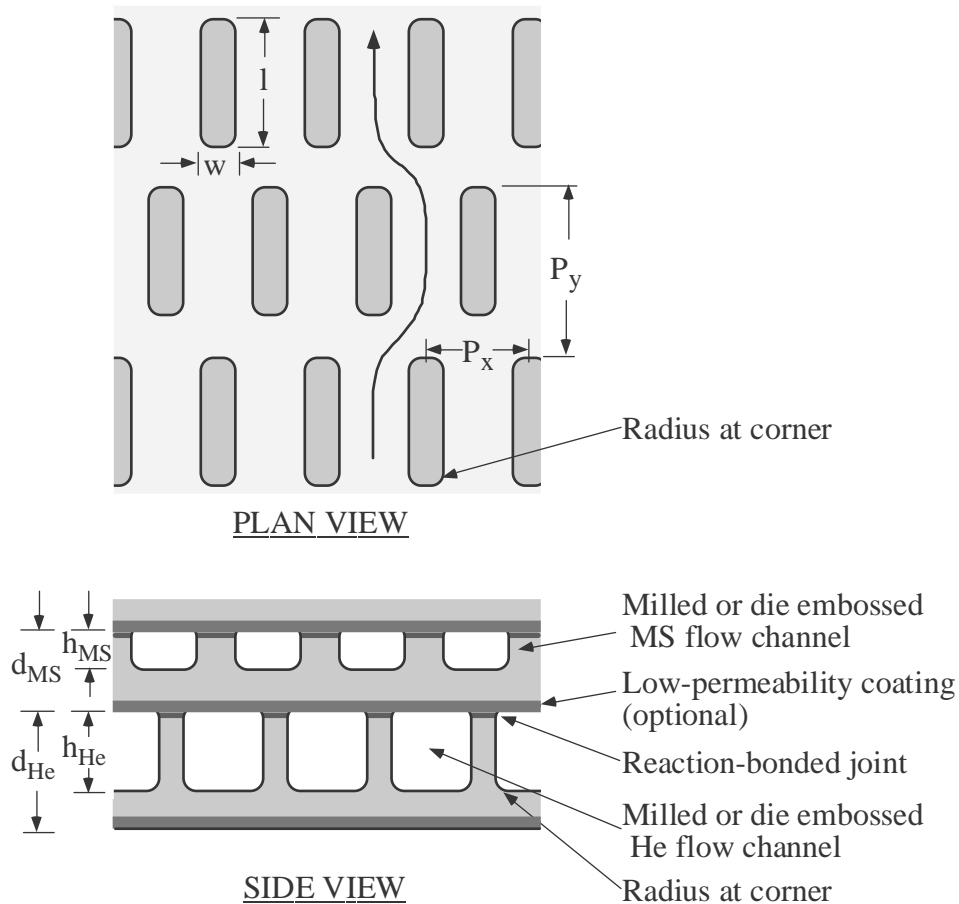
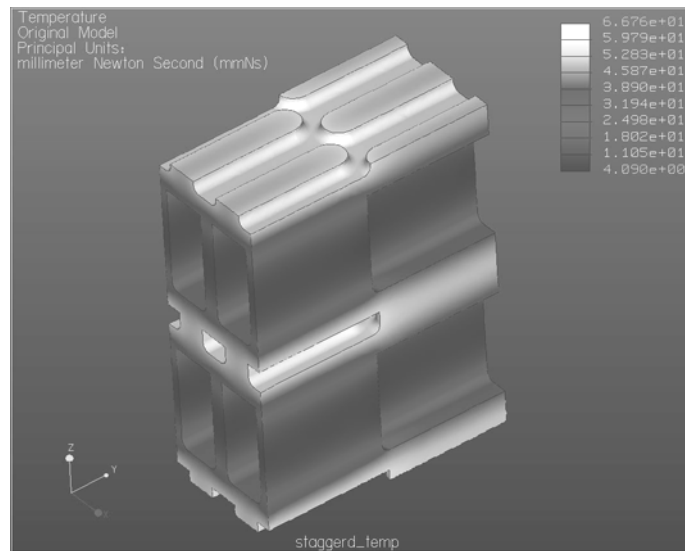


Figure 13 illustrates the offset strip fin geometry for the compact heat exchanger in greater detail. The cross-sectional area of the fins, and the thickness of the remaining plate below the machined channels, can be adjusted to provide sufficient strength against thermal and mechanical stresses. By making the fins discontinuous, as shown in Figure 13, a fracture in one fin will not propagate to other fins, assuming that the overall strength was sufficient so that the neighbouring fins could carry the loads of the broken fin. The largest mechanical stresses occur when the heat exchanger is used with high-pressure helium. In this case, it is expected that the heat exchangers will be immersed in the high pressure helium environment, so that the principal stresses induced are compressive.

Temperature and stress analysis was performed for representative unit cells of an LSI heat exchanger. Figure 14 shows an example calculation for a case with relatively long fins for the helium channel, where it is seen that the effectiveness of the fin heat transfer is poor. Subsequent analysis has focused on fins with shorter aspect ratios, like the fins shown in Figure 6. With appropriate design, with 10 MPa helium and 0.2 MPa molten salt, tensile stresses in can be maintained below 10 MPa. Furthermore, it is found that thermal stresses create a very small effect, relative to the mechanical stresses due to the fluid pressure.

Figure 14. Temperature distribution in an example LSI C/C-SiC heat exchanger with 5-mm high helium fins and 1-mm high molten salt fins



(Credit: R. Abbott, LLNL).

The major questions for the development of compact LSI C/C-SiC heat exchangers center on functionality with the three candidate fluids.

Helium performance

For the helium (the primary heat source for nuclear hydrogen production, and Brayton power-cycle working fluid for molten-salt fusion blankets) the operating pressure will be around 7 to 10 MPa and temperatures in the range of 800 to 1000°C. Because helium that leaks can be recovered from the molten salt, small leakage rates through the heat exchangers would be considered acceptable. The other major issue for high-pressure helium relate to controlling mechanical stresses in heat exchanger and ducting components due to the high helium pressure.

Molten-salt performance

For the molten salt, there exist several candidate combinations of fluorides for different applications. For baseline testing, a 50% ZrF₄, 50% NaF salt mixture (melting temperature of ~500°C) is currently being used in a Hastelloy natural circulation test loop at Oak Ridge National Laboratory, that operates at around 750°C [4]. Graphite is essentially completely inert, while SiC and residual silicon have low, but significantly larger, solubility in molten salts. UCB thermodynamics calculations indicate that, with proper control of the salt fluorine potential, that the rate of dissolution of the silicon may be acceptably low. CVI or CVD coating of the channel surfaces with carbon would result in a negligibly low corrosion rate, as long as the carbon layer remains mechanically intact. Carbon coatings may have another, substantial benefit, due to the fact that most noble metals that might contaminate the salt do not wet carbon, and thus are not likely to foul LSI heat exchangers as has been observed to occur in nickel-alloy heat exchangers for molten salts.

Sulphur-iodine process fluids performance

For sulphuric acid thermal decomposition, the decomposition products are SO_3 , SO_2 , O_2 , and H_2O , which create an aggressively oxidizing environment. Heat exchanger surfaces exposed to this process stream must be capable of protecting the carbon-fiber matrix from oxidation using coatings, matrix additives, or other approaches, as is being done in the HITHEX project to protect exchanger tubes from high-temperature moist combustion flue gases [2]. For the compact plate heat exchanger geometry envisioned here, processes for applying coatings must be compatible with the limited physical access to the heat exchanger surfaces that exists after assembly of the heat exchanger monolith, or be compatible with final assembly following coating.

The German Aerospace Center HITHEX project is currently obtaining good results with a vacuum plasma sprayed (VPS) cordierite coating on top of chemical vapor deposited (CVD) SiC and CVD-BoraSiC ($\text{SiC-B}_4\text{C-SiC}$), which has been shown to provide good results in oxidation and hot gas corrosion. Cordierite has an exceptionally low coefficient of thermal expansion ($1-2 \times 10^{-6} \text{ 1/K}$). When cooling down from coating temperature Cordierite is stressed under compression, so most cracks are stopped at the interface SiC-B₄C-Cordierite. This results in a clear reduction of crack density. Furthermore Cordierite is chemically stable against typical flue gases (Cordierite-honeycombs are used as substrates for noble metal catalyst converter in diesel engines of trucks, vessels and heavy power sets). Therefore researchers in the HITHEX project are convinced that BoraSiC-Cordierite will be a good environmental barrier coating for C/C-SiC under oxidizing environments like those generated by S-I process fluids.

3. Conclusions

LSI C/C-SiC composites are a potentially promising material for high-temperature heat exchangers and other flow-loop components. Potentially inexpensive and simple fabrication methods exist for compact plate-type heat exchangers. Carbon coating by CVI or CVD provides a route toward very low corrosion rates with molten fluoride salts, and because carbon is not wetted by noble metals, precipitation and fouling performance may also be good with molten salts. Extensive work has examined approaches to make carbon-carbon composites resistant to oxidation at high temperatures. Some of these approaches may provide acceptable barriers for use with process fluids for sulfur-iodine thermochemical production of hydrogen, making LSI C/C-SiC composites an interesting candidate material for the nuclear thermochemical production of hydrogen.

REFERENCES

- [1] “Ceramic Fibers and Coatings: Advanced Materials for the Twenty-First Century”, Committee on Advanced Fibers for High-Temperature Ceramic Composites, National Academy Press, NMAB 494, Washington, D.C., pg. 77, 1998.
(<http://books.nap.edu/books/0309059968/html/77.html#pagetop>)
- [2] Schmidt, J., M. Scheiffele and W. Krenkel, “Engineering of CMC Tubular Components”, Int. Conf. High Temperature Ceramic Matrix Composites, Munich, 2001.
- [3] Steckert, H.H. K.P. Norton and C.P.C. Wong, “Hermetic SiC Composite Tubes”, *American Ceramic Bull.*, **75**, No. 12 (December 1996).
- [4] Williams, D.F., D.F. Wilson, L.M. Toth, J. Caja and J.R. Keiser , “Research on Molten Fluorides as High Temperature Heat Transfer Agents”, to appear, Global 2003, New Orleans, Louisiana, 16-20 November 2003.
- [5] Krödel, M., G.S. Kutter, M. Deyerler and N. Pailer, “Short carbon-fibre reinforced ceramic – Cescic – for optomechanical applications”, SPIE Optomechanical Design and Engineering, Seattle, Washington, 7-9 July 2002.
- [6] Besmann, T.M., J.W. Klett, J.J. Henry, Jr. and E. Lara-Curzio, “Carbon/Carbon Composite Bipolar Plate for Proton Exchange Membrane Fuel Cells”, *Journal of The Electrochemical Society*, 147 (11) 4083-4086 (2000).
- [7] DeVan, D.H., *et al.*, “Materials Considerations for Molten Salt Accelerator-Based Plutonium Conversion Systems”, AIP Conference, International Conference on Accelerator-Driven Transmutation Technologies and Applications, LANL Report LA-UR-95-1792, Las Vegas, NV, pp. 476-487, July 1994.
- [8] Papenburg, Ulrich, Michael Deyerler, Wilhelm Pfrang, G. Siegfried Kutter, “Carbon Fibre-Reinforced Silicon Carbide (C/SiC) Technology”, BDM/IABG and Dornier Satellite Systems (DSS) (<http://ngst.gsfc.nasa.gov/cgi-bin/pubdownload?Id=170>).

LIST OF PARTICIPANTS

BELGIUM

RAHIER, Andre
Project Leader R&D
SCK•CEN
200, Boeretang, B-2400 Mol

Tel: +32 14 33 22 79
Fax: +32 14 32 15 29
Eml: arahier@sckcen.be

CANADA

DUFFEY, Romney
Research and Product Development
Atomic Energy of Canada Ltd.
Mail Station 99, Bldg. 600
Chalk River Laboratories
Ontario, KOJ 1J0

Tel: +1 613 584 8811 +6272
Eml: duffeyr@aecl.ca

FORTIN, Leo
Bruce Power
P.O. Box 1540
Tiverton, Ontario, N0G 2T0

Tel: +1 519 361 2673, Ext. 3318
Fax: +1 519 361 7017
Eml: leo.fortin@brucepower.com

MILLER, Alistair I.
Manager, Heavy Water Technology Branch
Atomic Energy of Canada Ltd.
Chalk River Laboratories
K0J 1J0 Chalk River

Tel: +1 613 584 8811, Ext. 3207
Fax: +1 613 584 4445
Eml: millera@aecl.ca

SCOTT, David
Evenstar Inc.
1601 Hollywood Place
Victoria, BC, V8S 1J6

Tel: +1 250-598-7755
Fax: +1 250-598-7799
Eml: davidsanbornscott@scottpoint.c

FRANCE

BORGARD, J.M.
CEA/DEN/DPC/SCP
CEN Saclay
F-911191 Gif-sur-Yvette Cedex

Tel: +33 1 69 08 80 86
Fax: +33 1 69 08 92 21
Eml: borgard@carnac.cea.fr

GOLDSTEIN, Stephen
CEA/DEN/DPC
CEN Saclay
F-911191 Gif-sur-Yvette Cedex

Tel: +33 1 69 08 64 10
Fax: +33 1 69 08 68 02
Eml: stephen.goldstein@cea.fr

LECOMTE, Michel
Direction Technique
FRAMATOME
Tour Fiat, Cedex 16
F-92084 Paris-La-Défense

Tel: +33 0(1) 47 96 56 73
Fax: +33 0(1) 47 96 15 09
Eml: michel.lecomte@framatome-anp.c

MAISSEU, André
Président
World Council of Nuclear Workers (WONUC)
49, rue Lauriston
F-75116 Paris

Tel: +33 0(1) 39 48 52 87
Fax: +33 0(1) 39 48 51 64
Eml: wonuc@wanadoo.fr

VITART, Xavier
Head, Physico-Chemistry Department
Direction of Nuclear Energy
DPC, Bât. 450
F-911191 Gif-sur-Yvette Cedex

Tel: +33 0(1) 69 08 37 05
Fax: +33 0(1) 69 08 51 31
Eml: xavier.vitart@cea.fr

ITALY

FURRER, Gianfilippo
Direzione Centrale Sicurezza Nucleare e
Protezione Sanitaria (DISP)
Agenzia Nazionale per la Protezione dell
Ambiente per I Servizi Tecnici (APAT)
Via Vitaliano Brancati, 48, I-00144 Roma

Tel: +39 0(6) 50 07 21 46
Fax: +39 0(6) 50 07 20 44
Eml: furrer@apat.it

LANCHI, Michela
SOLTERM-SVIL Department
Research Centre Casaccia
Via Anguillarese, 301
I-00060 S. Maria di Galeria, Roma

Tel: +39 0(6) 30 48 32 92
Fax: +39 0(6) 30 48 67 79
Eml: michela.lanchi@casaccia.enea.i

JAPAN

AOTO, Kazumi
Sodium and Safety Engineering Division
O-arai Engineering Center
Japan Nuclear Cycle Development Institute
4002 Narita-cho, O-arai-machi
Ibaraki-ken 311-1393

Tel: +81 29 267 41 41
Fax: +81 29 267 08 02
Eml: aoto@oec.jnc.go.jp

HORI, Masao
Nuclear Systems Association
1-7-6 Toranomom, Minato-ku
Tokyo 105-0001

Tel: +81 3 35 06 90 71
Fax: +81 3 35 06 90 75
Eml: mhorii@mx.mesh.ne.jp

NAKAGIRI, Toshio
Japan Nuclear Cycle Development Institute
O-arai, Higashi-Ibaraki
Ibaraki-ken 311-1393

Tel:
Fax:
Eml: naka@oec.jnc.go.jp

ONUKEI, Kaoru
Dept. of Advanced Nuclear Heat Technology
JAERI
Naritamachi Niihori 3607
Oarai-machi, Ibaraki-ken 311-1394

Tel: +81 29 264 8738
Fax: +81 29 264 8741
Eml: onuki@spa.oarai.jaeri.go.jp

OSHIRO, Shuji
SUMITOMO Corporation
1-8-11, Harumi, Chuo-ku
Tokyo 104-8610

Tel: +81 35 166 4326
Eml: shuji.oshiro@sumitonecorp.co.jp

TAKEDA, Tetsuaki
Dept. of Advanced Nuclear Heat Technology
Japan Atomic Energy Research Institute
Ibaraki-ken, 311-1394

Tel: +81 29 264 8707
Eml: takeda@popsvr.tokai.jaeri.go.jp

TASHIMO, Masanori
Advanced Reactor Technology Co.
16-5 Konan 2-choume Minato-ku
Tokyo 108-0075

Tel: +81 3 6716 5312
Fax: +81 3 6716 5912
Eml: tashimo@artech.co.jp

TSUCHIE, Yasuo
The Japan Atomic Power Company
Mitoshiro Bldg.
1-1 Kanda Mitoshiro-cho, Chiyoda-ku
Tokyo, 101-0053

Tel: +81 3 4415 6605
Fax: +81 3 4415 6690
Eml: yasuo-tsuchie@japc.co.jp

THE NETHERLANDS

OFFEREIN, Jelmer
NRG Arnhem
P.O. Box 9035
6800 ET Arnhem

Tel: +31 26 356 38 29
Fax: +31 26 445 90 35
Eml: offerein@nrg-nl.com

UNITED STATES OF AMERICA

ALLEN, Todd
University of Wisconsin
1500 Engineering Drive
Madison, WI 53706

Tel: +1 608 265 4083
Fax: +1 608 263 7451
Eml: allen@engr.wisc.edu

ANDERSON, Raymond
INEEL, Engineering Research Office
2525 Fremont Avenue
P.O. Box 1625, Idaho Falls, ID 83415

Tel: +1 208 526 1623
Eml: anderp@inel.gov

ANGHAIE, Samim
Director, Innovative Nuclear Space Power
and Propulsion Institute (INSPI)
University of Florida, 202 NSC
Gainesville, FL 32611-8300

Tel: +1 352 392 8656
Fax: +1 352 392 8656
Eml: anghaie@ufl.edu

BALACHANDRAN, U.
Argonne National Laboratory
Energy Technology Division
9700 S. Cass Avenue, Bldg. 212
Argonne, IL 60439

Tel: +1 630 252 4250
Fax: +1 630 252 3604
Eml: balu@anl.gov

BLISS, Henry E.
Argonne National Laboratory
Nuclear Engineering Division
9700 S. Cass Avenue, Bldg. 208
Argonne, IL 60439-4842

Tel: +1 630 252 1076
Fax: +1 630 252 6302
Eml: hankbliss@anl.gov

BROWN, Russell A.
Argonne National Laboratory
Special Term Appointment
162 East 22nd Street
Idaho Falls, ID 83404

Tel: +1 208 524 4409
Eml: rbrown@anl.gov

BUCKNER, M.R.
Westinghouse Savannah
River Company
Savannah River Site, Bldg. 773-42A
Aiken, SC 29808

Tel: +1 803 725 0596
Fax: +1 803 725 8829
Eml: mel.buckner@srs.gov

CASPERSSON, Sten
Westinghouse Electric
2000 Day Hill Road
Windsor, CT 06095

Tel: +1 860 731 6568
Eml: sten.a.caspersson@us.westinghouse.com

CHALK, Steven G.
EE-2H Forrestal Building
US Department of Energy
1000 Independence Ave. S.W.
Washington, DC 20585

Tel: +1 202 586 3388
Fax: +1 202 586 9811
Eml: steven.chalk@hq.doe.gov

DITMARS, Jack
Argonne National Laboratory – East
9700 S. Cass Avenue
Argonne, IL 60439

Tel: +1 630 252 5953
Fax: +1 630 252 4611
Eml: jditmars@cmt.gov

DOCTOR, Richard
Argonne Partnerships Hydrogen Program
Hydrogen and Greenhouse Gas Engineering
Energy Systems Division, Bldg. 362/C357
Argonne National Laboratory
9700 S. Cass Avenue
Argonne, IL 60439-4815

Tel: +1 630 252 5913
Fax: +1 630 252 9281
Eml: rdoctor@anl.gov

FAIBISH, Ron
Argonne National Laboratory – East
9700 S. Cass Avenue
Argonne, IL 60439

Tel: +1 630 252 8355
Fax: +1 630 252 4500
Eml: rfaibish@anl.gov

FORSBERG, Charles Winfield
Oak Ridge National Laboratory
P.O. Box 2008
37831-6180, Oak Ridge, TN

Tel: +1 865 574 6783
Fax: +1 865 574 9512
Eml: forsbergcw@ornl.gov

GAINES, Linda
Argonne National Laboratory – East
9700 S. Cass Avenue
Argonne, IL 60439

Tel: +1 630 252 4919
Fax: +1 630 252 3443
Eml: lgaines@anl.gov

GILLETTE, Jerry
Program Manager
Argonne National Laboratory
9700 S. Cass Avenue
Argonne, IL 60439

Tel: +1 630 252 7475
Fax: +1 630 252 6073
Eml: jgillette@anl.gov

HABEGGER, Loren
Argonne National Laboratory – East
9700 S. Cass Avenue
Argonne, IL 60439

Tel: +1 630 252 3761
Fax: +1 630 252 4611
Eml: lhabegger@anl.gov

HENDERSON, David
Office of Nuclear Energy, Science &
Technology
US Department of Energy
Washington, DC 20585

Tel: +1 301 903 3097
Fax: +1 301 903 5057
Eml: David.Henderson@hq.doe.gov

HERRING, J. Stephen
Idaho National Engineering Laboratory
Environmental Laboratory
Bechtel BWXT Idaho, LLC
P.O. Box 1625 MS 3860

Tel: +1 208 526 9497
Fax: +1 208 526 2930
Eml: sth@inel.gov

KEUTER, Dan R.
Entergy Nuclear
Vice President
1340 Echelon Parkway
Jackson, MS 39213

Tel: +1 601 368 5744
Fax: +1 601 368 5323
Eml: dkeuter@entergy.com

KOCHENDARFER, Richard
FRAMATOME ANP
3315 Old Forest Road
Lynchburg, VA 24501

Tel: +1 434 832 2990
Eml: richard.kochendarfer@frametome

KOLTS, John H.
Defense Threat Reduction Agency
8725 John J. Kingman Road, Stop 6201
Fort Belvoir, VA 22060-6201

Tel: +1 703 325 7801
Fax: +1 703 325 0493
Eml: john.kolts@dtra.mil

KOTEK, John
INEEL
Willow Creek Building
1955 N. Fremont Avenue, Mailstop 1203
P.O. Box 1625
Idaho Falls, ID 83415

Tel: +1 208 526 2497
Fax: +1 208 526 0542
Eml: kotekjf@inel.gov

LEWIS, David
Argonne National Laboratory – East
9700 S. Cass Avenue
Chemical Engineering Division
Argonne, IL 60439

Tel: +1 630 252 4383
Fax: +1 630 252 5528
Eml: lewisd@cmt.anl.gov

LEWIS, Michele
Argonne National Laboratory – East
9700 S. Cass Avenue
Chemical Engineering Division
Argonne, IL 60439

Tel: +1 630 252 6603
Fax: +1 630 252 5246
Eml: lewism@cmt.anl.gov

LI, Jie
Argonne National Laboratory – East
9700 S. Cass Avenue
Argonne, IL 60439

Tel: +1 630 252 4764
Eml: jieli@anl.gov

LYCZKOWSKI, Robert W.
Argonne National Laboratory – East
9700 S. Cass Avenue
Argonne, IL 60439

Tel: +1 630 252 5923
Fax: +1 630 252 5210
Eml: rlyczkowski@anl.gov

MACDONELL, Margaret
Argonne National Laboratory
Environmental Health Risk Section
Environmental Assessment Division
9700 S. Cass Avenue, Bldg. 900
Argonne, IL 60439-4832

Tel: +1 630 252 3243
Fax: +1 630 252 4336
Eml: macdonell@anl.gov

MARSHALL, Christopher L.
Argonne National Laboratory
9700 S. Cass Avenue
CMT/205, Argonne, IL 60439-4837

Tel: +1 630 252 4310
Fax: +1 630 972 4408
Eml: clmarshall@anl.gov

MASIN, Joseph G.
Argonne National Laboratory – East
9700 S. Cass Avenue
Argonne, IL 60439

Tel: +1 630 252 8316
Eml: masin@cmt.anl.gov

MATONIS, Diana T.
Argonne National Laboratory – East
9700 S. Cass Avenue
Argonne, IL 60439

Tel: +1 630 252 4680
Fax: +1 630 252 9281
Eml: dmatonis@anl.gov

MELANCON, Stephen P.
Entergy Nuclear, Inc.
1340 Echelon Parkway
Jackson, MS 39213

Tel: +1 504 576 3518
Fax: +1 601 368 5323
Eml: smelanc@entergy.com

MILLER, James F.
Argonne National Laboratory – East
9700 S. Cass Avenue
Argonne, IL 60439

Tel: +1 630 252 4537
Fax: +1 630 252 4537
Eml: millerj@cmt.anl.gov

MINTZ, Marianne
Argonne National Laboratory – East
9700 S. Cass Avenue
Argonne, IL 60439

Tel: +1 630 252 5627
Fax: +1 630 252 3443
Eml: mmintz@anl.gov

MOISSEYTEV, Anton
Texas A&M University
129 Zachry Engineering Center/Mail Code 3133
College Station, TX 77843-3133

Tel: +1 979 847 8791
Eml: amoissei@cedar.tamu.edu

PARK, Charles
INEEL
Engineering Research Office Building (EROB)
2525 Fremont Avenue
P.O. Box 1625
Idaho Falls, ID 83415

Tel: +1 208 526 1091
Eml: park@ineel.gov

PASTER, Mark D.
Department of Energy
Hydrogen and Fuel Cells Program
1000 Independence Ave.
Washington, DC 20585

Tel: +1 202 586 2821
Fax: +1 202 486 9234
Eml: mark.paster@ee.doe.gov

PETERSON, Per F.
Department of Nuclear Engineering
University of California, Berkeley
Berkeley, CA 94720-1730

Tel: +1 510 643 7749
Fax: +1 510 643 9685
Eml: peterson@nuc.berkeley.edu

PETRI, Mark C.
Argonne National Laboratory – East
9700 S. Cass Avenue
Argonne, IL 60439

Tel: +1 630 252 3719
Fax: +1 630 252 1932
Eml: mcpetri@anl.gov

PICKARD, Paul
Sandia National Laboratories
P.O. Box 5800
Albuquerque, NM 87185-1136

Tel: +1 505 845 3046
Fax: +1 505 284 4276
Eml: PSPICKA@sandia.gov

PLANCHON, Pete
Argonne National Laboratory – West
P.O. Box 2528
Idaho Falls, ID 83403-2528

Tel: +1 208 533 7691
Fax: +1 208 533 7340
Eml: pete.planchon@anl.gov

RICHARDS, Matt
General Atomics/Los Alamos Office
2237-S Trinity Drive
Bldg. 2/Floor 3
Los Alamos, NM 87544

Tel: +1 505 661 4433
Fax: +1 505 661 2525
Eml: matt.richards@gat.com

ROGLANS, Jordi
Reactor Analysis Division
Argonne National Laboratory
9700 S. Cass Avenue, Bldg. 208
Argonne, IL 60439

Tel: +1 630 252 3283
Fax: +1 630 252 4500
Eml: roglans@anl.gov

ROMANCO, Mike
Gas Technology Institute
1700 South Mount Prospect Road
Des Plaines, IL 60018-1804

Tel: +1 847 768 0819
Eml: michael.romanco@gastechnology

SANDELL, Layla
Manager, Advanced Nuclear Plants Systems
EPRI
3412 Hillview Avenue
Palo Alto, CA 94303

Tel: +1 650 855 2756
Fax: +1 650 855 2002
Eml: Lsandell@epri.com

SANDO, Kiyooki
Sumitomo Corporation of America
5000 USX Tower
600 Grant Street, Suite 5000
Pittsburgh, PA 15219-2702

Tel: +1 412 391 9680
Eml: kiyooki.sando@sumitomoep.co.jp

SCHMITZ, Mark A.
Westinghouse Safety Management Solutions
Nuclear Fuel
5801 Bluff Road
Columbia, SC 29250

Tel: : +1 803 502 9705
Eml: mark.schmitz@wxsms.com

SCHWARTZ, Elmer George
University of South Carolina
Mechanical Engineering
Columbia, SC 29208

Tel: +1 803 777 4875
Fax: +1 803 777 0106
Eml: schwartz@enr.sc.edu

SERBAN, Manuela
Argonne National Laboratory – East
9700 S. Cass Avenue
Argonne, IL 60439

Tel: : +1 630 252 0584
Eml: serban@cmt.anl.gov

SHERMAN, Steven
Argonne National Laboratory
P.O. Box 2528
Idaho Falls, ID 83403

Tel: +1 208 533 7327
Fax: +1 208 533 7735
Eml: steven.sherman@anlw.anl.gov

SIMONSON, Scott
Lockheed Martin Corp.
2401 River Road
Scherectudy, NY 1265

Tel: +1 518 395 7202
Fax: +1 518 395 6136
Eml: simonso@kapl.gov

SIMPSON, Michael
Argonne National Laboratory
P.O. Box 2528
Idaho Falls, ID 83403

Tel: +1 208 528 0672
Eml: michael.simpson@anl.gov

STOLLE, Alison Mary
215 Washington Avenue
Scotia, NY 12302

Tel: +1 518 395 4551
Fax: +1 518 395 4422
Eml: stolle@kapl.gov

SUMMERS, William
Savannah River Technology Center
Westinghouse Savannah River Co.
Savannah River Site
Aiken, SC 29808

Tel: +1 803 725 7766
Eml: william.summers@srs.gov

TAIWO, Temitope
Nuclear Engineering Division
Argonne National Laboratory – East
9700 S. Cass Avenue, Bldg. 208
Argonne, IL 60439-4842

Tel: +1 630 252 1387
Fax: +1 630 252 4500
Eml: Taiwo@anl.gov

TAYLOR, Amy
NE-40
US Department of Energy
1000 Independence Ave., SW
Washington, DC 20585-1290

Tel: +1 301 903 7722
Eml: amy.taylor@hq.doe.gov

TETENBAUM, Marvin
Argonne National Laboratory – East
9700 S. Cass Avenue
Argonne, IL 60439

Tel: +1 630 252 4540
Fax: +1 630 252 9373
Eml: tetenbaum@cmt.anl.gov

VAN ERP, Jan
Argonne National Laboratory – East
9700 S. Cass Avenue
Argonne, Illinois 60439

Tel: +1 630 325 7938
Fax: +1 630 252 6500
Eml: vanerp@aol.com

VILIM, Richard
Argonne National Laboratory – East
9700 S. Cass Avenue
Argonne, Illinois 60439

Tel: +1 630 252 6998
Fax: +1 630 252 4620
Eml: rvilim@anl.gov

VYAS, Anant
Argonne National Laboratory – East
9700 S. Cass Avenue
Argonne, Illinois 60439

Tel: +1 630 252 7598
Fax: +1 630 252 3443
Eml: avyas@anl.gov

WADE, David C.
Senior Technical Adviser
Engineering Research Directorate
Argonne National Laboratory
9700 S. Cass Avenue, Bldg. 208
Argonne, IL 60439

Tel: +1 630 252 4858
Fax: +1 630 252 4500
Eml: dcwade@anl.gov

WANG, Michael
Argonne National Laboratory – East
9700 S. Cass Avenue
Argonne, Illinois 60439

Tel: +1 630 252 2819
Fax: +1 630 252 3443
Eml: mqwang@anl.gov

WU, Ye
Argonne National Laboratory – East
9700 S. Cass Avenue
Argonne, Illinois 60439

Tel: 1 630 252 2533
Fax: 1 630 252 9681
Eml: ywu@anl.gov

YILDIZ, Bilge
MIT-CANES
77 Massachusetts Avenue, Bldg. 24
Cambridge, MA 02139

Tel: +1 617 253 7404
Eml: byildiz@mit.edu

INTERNATIONAL ORGANISATIONS

METHNANI, Mabrouk
International Atomic Energy Agency
Wagramer Strasse 5
Box 100
A-1400 Vienna

Tel: +43 1 2600 22810
Fax: +43 1 2600 29598
Eml: M.Methnani@iaea.org

NORDBORG, Claes
OECD Nuclear Energy Agency
Le Seine Saint-Germain
12 boulevard des Iles
F-92130 Issy-les-Moulineaux

Tel: +33 (1) 45 24 10 90
Fax: +33 (1) 45 24 11 10
Eml: claes.nordborg@oecd.org

ALSO AVAILABLE

NEA Publications of General Interest

NEA News

ISSN 1605-9581

Yearly subscription: € 43 US\$ 48 GBP 28 ¥ 5 500

Nuclear Energy Today

ISSN 9264-10328-7

Price : € 21 US\$ 24 GBP 14 ¥ 2 700

Nuclear Science

Advanced Reactors with Innovative Fuels

Workshop Proceedings, Chester, UK, 22-24 October 2001 (2002)

ISBN 92-64-19847-4

Price: € 130 US\$ 113 GBP 79 ¥ 15 000

Advanced Reactors with Innovative Fuels

Workshop Proceedings, Chester, UK, 22-24 October 2001 (2002)

ISBN 92-64-19847-4

Price: € 130 US\$ 113 GBP 79 ¥ 15 000

Basic Studies in the Field of High-temperature Engineering (2002)

Second Information Exchange Meeting, Paris, France, 10-12 October 2001

ISBN 92-64-19796-6

Price: € 75 US\$ 66 GBP 46 ¥ 8 600

Physics of Plutonium Recycling

Volume VII – BWR MOX Benchmark – Specification and Results (2003)

ISBN 92-64-19905-5

Price: € 45 US\$ 45 GBP 29 ¥ 5 500

Volume VI – Multiple Pu Recycling in Advanced PWRs (2002)

ISBN 92-64-19957-8

Price: € 45 US\$ 45 GBP 28 ¥ 5 250

Utilisation and Reliability of High Power Proton Accelerators (2003)

Workshop Proceedings, Santa Fe, New Mexico, USA, 12-16 May 2002

ISBN 92-64-10211-6

Price: € 90 US\$ 90 GBP 60 ¥ 11 500

Accelerator-driven Systems (ADS) and Fast Reactors (FR) in Advanced Nuclear Fuel Cycles (2002)

ISBN 92-64-18482-1

Free: paper or web.

Actinide and Fission Product Partitioning and Transmutation (2003)

Proceedings of the Seventh Information Exchange Meeting, Jeju, Republic of Korea, 14-16 October 2002

ISBN 92-64-02125-6

Free: paper or web.

Benchmark on Beam Interruptions in an Accelerator-driven System (2003)

Final Report on Phase I Calculations

ISBN 92-64-02138-8

Free: paper or web.

Benchmark on Deterministic Transport Calculations Without Spatial Homogenisation (2003)

A 2-D/3-D MOX Fuel Assembly Benchmark

ISBN 92-64-02139-6

Free: paper or web.

Burn-up Credit Criticality Benchmark (2003)

Phase IV-A: Reactivity Prediction Calculations for Infinite Arrays of PWR MOX Fuel Pin Cells

ISBN 92-64-02123-X

Phase IV-B: Results and Analysis of MOX Fuel Depletion Calculations

ISBN 92-64-02124-8

Free: paper or web.

CD-ROM Complete Collection of Published Reports (as of May 2003)

Free on request.

Plutonium Management in the Medium Term (2003)

ISBN 92-64-02151-5

Free: paper or web.

Pressurised Water Reactor Main Steam Line Break (MSLB) Benchmark

Volume IV: Results of Phase III on Coupled Core-plant Transient Modelling (2003)

ISBN 92-64-02152-3

Free: paper or web.

VVER-1000 Coolant Transient Benchmark (2003)

Phase I (V1000CT-1) – Vol. I: Main Coolant Pump (MCP) Switching On – Final Specifications

ISBN 92-64-18496-1

Free: paper or web.

Order form on reverse side.

ORDER FORM

OECD Nuclear Energy Agency, 12 boulevard des Iles, F-92130 Issy-les-Moulineaux, France
Tel. 33 (0)1 45 24 10 15, Fax 33 (0)1 45 24 11 10, E-mail: neapub@nea.fr, Internet: www.nea.fr

Qty	Title	ISBN	Price	Amount
Total*				

* Prices include postage fees.

Payment enclosed (cheque payable to OECD Publications).

Charge my credit card VISA Mastercard American Express

Card No.	Expiration date	Signature
Name		
Address		Country
Telephone	Fax	
E-mail		

Questionnaire on the quality of OECD publications

We would like to ensure that our publications meet your requirements in terms of presentation and editorial content. We would welcome your feedback and any comments you may have for improvement. Please take a few minutes to complete the following questionnaire. Answers should be given on a scale of 1 to 5 (1 = poor, 5 = excellent).

Fax or post your answer before 31 December 2004, and you will automatically be entered into the prize draw to win a year's subscription to *OECD's Observer magazine*.*

A. Presentation and layout

1. What do you think about the presentation and layout in terms of the following:

	Poor	Adequate		Excellent	
Readability (font, typeface)	1	2	3	4	5
Organisation of the book	1	2	3	4	5
Statistical tables	1	2	3	4	5
Graphs	1	2	3	4	5

B. Printing and binding

2. What do you think about the quality of the printed edition in terms of the following:

Quality of the printing	1	2	3	4	5
Quality of the paper	1	2	3	4	5
Type of binding	1	2	3	4	5
Not relevant, I am using the e-book	<input type="checkbox"/>				

3. Which delivery format do you prefer for publications in general?

Print CD E-book (PDF) via Internet Combination of formats

C. Content

4. How accurate and up to date do you consider the content of this publication to be?

1 2 3 4 5

5. Are the chapter titles, headings and subheadings...

Clear Yes No
Meaningful Yes No

6. How do you rate the written style of the publication (e.g. language, syntax, grammar)?

1 2 3 4 5

D. General

7. Do you have any additional comments you would like to add about the publication?

.....
.....
.....

Tell us who you are:

Name: E-mail:

Fax:

Which of the following describes you?

IGO NGO Self-employed Student
Academic Government official Politician Private sector

Thank you for completing the questionnaire. Please fax your answers to:

(33-1) 49 10 42 81 or mail it to the following address:

Questionnaire qualité PAC/PROD, Division des publications de l'OCDE
23, rue du Dôme – 92100 Boulogne Billancourt – France.

Title: NUCLEAR PRODUCTION OF HYDROGEN

ISBN: 9264107703 OECD Code (printed version): 662004021P1

* Please note: This offer is not open to OECD staff.

OECD PUBLICATIONS, 2, rue André-Pascal, 75775 PARIS CEDEX 16
PRINTED IN FRANCE
(66 2004 02 1P) – No. 53491 2004